

---

*VACUUM  
TECHNOLOGY  
PRACTICE COURSE  
(SUPPORT MATERIAL)*

---

## CONTENT

INTRODUCTION.....	3
1. CONCEPT OF VACUUM.....	4
1.1. Gas laws.....	4
1.2. Kinetic theory of gases.....	5
1.3. Gas flow.....	10
1.4. Pressure of gas, levels of vacuum, vacuum units.....	12
2. VACUUM SYSTEMS CALCULATION.....	15
3. VACUUM SYSTEMS PROJECTION.....	16
3.1. Materials for vacuum systems.....	16
3.2. Gas load sources.....	22
3.3. Absorption, diffusion, and outgassing.....	23
3.4. Elements of vacuum systems.....	26
3.5. Throughput capacity of vacuum systems elements.....	26
4. CLEANING.....	35
5. VACUUM PUMPS.....	43
5.1. Mechanical pumps.....	43
5.2. Condensers.....	47
5.3. Jet and diffusion pumps.....	47
5.4. Molecular and turbomolecular pumps.....	52
5.5. Sorption pumps.....	57
5.6. Cryotechnology and cryopumps.....	67
6. VACUUM MEASUREMENT.....	78
6.1. Mechanical vacuum gauges.....	78
6.2. Spinning rotor gauges.....	84
6.3. Direct electric pressure measuring transducers.....	85
6.4. Thermal conductivity vacuum gauges.....	85
6.5. Thermal mass flowmeters.....	89
6.6. Ionization gauges.....	91
6.7. Combined vacuum gauges.....	100
7. VACUUM COMPONENTS, SEALS, AND JOINTS.....	104
7.1. Vacuum hygiene.....	104
7.2. Joining technologies in vacuum technology.....	106
7.3. Components.....	114
7.4. Vacuum sealing technology.....	119
8. LEAK DETECTION.....	129
8.1. Basic principals.....	129
8.2. Mass spectrometers and residual gas analysis.....	131
8.3. Leak detection with tracer gases.....	136
8.4. Application notes.....	140
9. VACUUM SYSTEM OPERATING.....	143
9.1. Electronic integration of vacuum system.....	143
9.2. Pressure control.....	145
9.3. Technic for operating low-vacuum system.....	146
9.4. Technic for operating fine-vacuum system.....	147
9.5. Technic for operating high-vacuum system.....	148
9.6. Technic for operating ultrahigh-vacuum system.....	149
REFERENCES .....	154

## INTRODUCTION

Historically, vacuum technology has been of major importance in the evolution of electronics ever since the first vacuum tube was constructed. Means for obtaining and measuring vacuums have proven indispensable in the development of nearly all electronic devices. Likewise, such means are basic to the understanding of surface physics and surface chemistry.

For many experiments and purposes, pressures of the order of  $10^{-6}$  Torr ( $10^{-6}$  mm Hg or about  $10^{-9}$  atmosphere) are low enough, even though surface phenomena studies show that at  $10^{-6}$  torr a surface becomes covered with adsorbed gas in only a few seconds. Other experiments, however, require the use of ultrahigh vacuum. At lower pressures the number of collisions of gas phase atoms and molecules with a surface is so small that a clean surface remains free of contamination long enough to do experiments on the surface itself. Recent surface studies have required pressures of  $10^{-9}$  torr or lower. At this pressure no significant surface contamination occurs for a several-hour period. Pressures of  $10^{-9}$  torr and below are generally called the ultrahigh vacuum range. Ultrahigh vacuum is a requisite for many experiments that involve either the reaction between a surface and a gas or the properties of the surface itself.

Currently, the understanding and application of techniques of ultrahigh vacuum are somewhat restricted to specialists who of necessity are familiar with meeting reports, subject literature that appears in scientific journals, and parts of textbooks. From this material these men have gained a working knowledge of the inherently simple techniques needed in ultrahigh vacuum experiments. It has been clear for some time that a book devoted to the study of ultrahigh vacuum was needed.

The main idea of the book is to cover all aspects of vacuum science and technology in order to enable engineers, technicians, and scientists to develop and work successfully with the equipment and "environment" of vacuum. Beginners in the field of vacuum shall be able to start and experts shall be able to deepen their knowledge and find the necessary information and data to continue their work.

# 1. CONCEPT OF VACUUM

## 1.1. Gas laws

For a proper understanding of phenomena in gases, more especially at low pressures, it is essential to consider those phenomena from the point of view of the kinetic theory of gases. This theory rests essentially upon two fundamental assumptions. The first of these postulates is that matter is made up of extremely small particles or molecules, and that the molecules of the same chemical substance are exactly alike as regards size, shape, mass, and so forth. The second postulate is that the molecules of a gas are in constant motion, and this motion is intimately related to the temperature. In fact, the temperature of a gas is a manifestation of the amount or intensity of molecular motion.

In the case of monatomic molecules (such as those of the rare gases and vapors of most metals) the effect of increased temperature is evidenced by increased translational (kinetic) energy of the molecules. In the case of diatomic and polyatomic molecules increase in temperature also increases rotational energy of the molecule about one or more axes, as well as, vibrational energy of the constituent atoms with respect to mean positions of equilibrium. However, in the following discussion only the effect on translational energy will be considered.

According to the kinetic theory a gas exerts pressure on the enclosing walls because of the impact of molecules on these walls. Since the gas suffers no loss of energy through exerting pressure on the solid wall of its enclosure, it follows that each molecule is thrown back from the wall with the same speed as that with which it impinges, but in the reverse direction; that is, the impacts are perfectly elastic.

Suppose a molecule of mass  $m$  to approach the wall with velocity  $v$ . Since the molecule rebounds with the same speed, the change of momentum per impact is  $2mv$ . If  $v$  molecules strike unit area in unit time with an average velocity  $v$ , the total impulse exerted on the unit area per unit time is  $2mvv$ . But the pressure is defined as the rate at which momentum is imparted to a unit area of surface. Hence,

$$2mvv = P \quad (1.1)$$

It now remains to calculate  $v$ . Let  $n$  denote the number of molecules per unit volume. It is evident that at any instant we can consider the molecules as moving; in six directions corresponding to the six faces of a cube. Since the velocity of the molecules is  $v$ , it follows that, on the average,  $(n/6)v$  molecules will cross unit area in unit time.

Equation (1) therefore becomes

$$P = \frac{1}{3} mnv^2 \quad (1.2)$$

Since

$$mn = \rho \quad (1.3)$$

where  $\rho$  denotes the density, equation (2) can be expressed in the form

$$P = \frac{1}{3} \rho v^2 \quad (1.4)$$

which shows that, at constant temperature, the pressure varies directly as the density, or inversely as the volume. This is known as Boyle's law.

Also, from equation (2) it follows that the total kinetic energy of the molecules in volume  $V$  is

$$\frac{1}{2} mnv^2 V = \frac{3}{2} PV \quad (1.5)$$

Now it is a fact that no change in temperature occurs if two different gases, originally at the same temperature, are mixed. This result is valid independently of the relative volumes. Consequently, the average kinetic energy of the molecules must be the same for all gases at any given temperature and the rate of increase with temperature must be the same for all gases. We may therefore define temperature in terms of the average kinetic energy of the molecules, and this

suggestion leads to the relation

$$\frac{1}{2}mv^2 = \frac{3}{2}kT \quad (1.6)$$

where  $T$  is the absolute temperature (degrees Kelvin), defined by the relation  $T = 273.16 + t$  ( $t =$  degrees Centigrade), and  $k$  is a universal constant, known as the Boltzmann constant ( $k = 1.380649 \times 10^{-23} \text{ J/K}$ ). Combining equation 6 with 5, it follows that

$$P = nkT \quad (1.7)$$

This is an extremely useful relation, as will be shown subsequently, for the determination of  $n$  for given values of  $P$  and  $T$ . Also, from equation 3 and the last equation, it follows that

$$P = \frac{k}{m}\rho T \quad (1.8)$$

that is,

$$\frac{P}{\rho} = \frac{k}{m}T \quad (1.9)$$

which is known as Charles' law.

Lastly, let us consider equal volumes of any two different gases at the same values of  $P$  and  $T$ . Since  $P$  and  $V$  are respectively the same for each gas, and  $\frac{1}{2}mv^2$  is constant at constant value of  $T$ , it follows from equations 5 and 7 that  $n$  must be the same for both gases. That is, equal volumes of all gases at any given values of temperature and pressure contain an equal number of molecules. This was enunciated as a fundamental principle by Avogadro in 1811, but it required about 50 years for chemists to understand its full significance.

On the basis of Avogadro's law, the molecular mass,  $M$ , of any gas or vapor is defined as that mass in grams, calculated for an ideal gas which occupies, at  $0^\circ \text{C}$  and one atmosphere, a volume

$$V_0 = 22,414.6 \text{ cm}^3 = 22.4146 \text{ l}$$

This is therefore designated the molar volume, and the equation of state for an ideal gas can be written in the form

$$PV = \frac{W}{M}R_0T \quad (1.10)$$

where  $W =$  mass in grams.

$M =$  molecular mass in grams.

$R_0 = 8.131462618 \text{ J} \cdot \text{K}^{-1} \cdot \text{mol}^{-1}$  a universal constant.

$V =$  volume of  $W$  grams at pressure  $P$  and absolute temperature  $T$ .

It is convenient to express the last equation in the form

$$PV = n_M R_0 T \quad (1.11)$$

where  $n_M$  denotes the number of moles (corresponding to  $M$  in grams) in the volume  $V$  under the given conditions of temperature and pressure.

Obviously, the exact value to be used for  $R_0$  must depend upon the units in which  $P$ ,  $V$ ,  $T$ , and  $W$  are expressed.

## 1.2. Kinetic theory of gases

A gas completely fills an available volume and shows a number of macroscopic properties: it has a temperature and exerts a temperature-dependent pressure to the walls. An equation of state, equations (1.7) – (1.10), connects the state quantities pressure, volume, and temperature. Additionally, a gas is capable of conducting frictional force between surfaces in motion (viscosity), transferring thermal energy between surfaces with unequal temperatures (thermal conductivity), and can influence spreading of molecular particles (diffusion).

These different properties of a gas can be explained easily by considering the microscopic behavior of individual gas particles (atoms, molecules), by means of the kinetic theory of gases. This theory is based on the conception that a gas consists of a very large number of tiny particles that move thermally (kinetics). The moving particles hit the walls of the container and one another. All collisions

are assumed elastic, that is, the total energy is conserved. During a collision, however, velocities of the colliding particles change with respect to value and direction, following the mechanical laws of collisions. The kinetic theory of gases derives the macroscopic properties of a gas from the microscopic motion of individual particles.

Krönig developed the kinetic theory of gases as a model in Berlin during the mid-nineteenth century. Later, it was verified in experiments and has proven very successful. Using the model, the pressure on a wall can be calculated from the molecular impacts of many individual particles. It therefore permits developing the equation of state of a gas. Furthermore, the transport properties viscosity, thermal conductivity, and diffusion can be derived easily. This is briefly discussed in the following sections.

In its simplest form, the kinetic theory of gases assumes that gas particles are small, hard spheres with a fixed diameter, and which remain practically unaltered during a collision, such as billiard balls. This conception often already yields good understanding of reality and is used in this chapter. When further developing the model, soft spheres can be assumed that deform like rubber balls during a collision and additionally attract one another mutually when they come close.

The hard-sphere model of gas particles is used to calculate wall pressure. In the calculation,  $n$  gas particles, each having the mass  $m_p$ , being in a volume  $V$ , that is, a cube with an edge length  $d$ , are considered (Figure 1.1). To simplify matters, the particle size is assumed to be negligibly small. The particles are evenly (homogeneously) distributed in the volume and move about randomly (kinetic motion). The directions of motion are distributed isotropically in three dimensions.

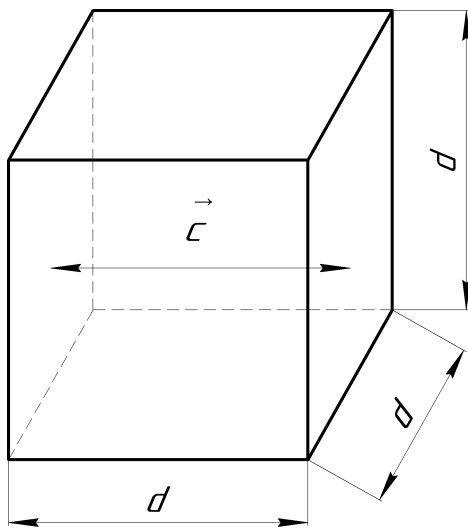


Figure 1.1 Particle motion in a cube and resulting wall pressure.

Of all gas particles, one third,  $\frac{1}{3}n$ , each move along or reversely to the  $x$ -,  $y$ -, or  $z$ -axis. The movement is described by the terms velocity  $c$  (vector  $c$  or vector component  $c_x$ ) or speed  $c$  (absolute value). We will now consider an individual particle moving back and forth horizontally between the confining walls of the cube in the  $x$ -direction. The velocity  $c_x$  of the particle is constant. Before impacting a wall, the momentum of the particle is  $m_p c_x$ ; after colliding, it leaves the wall with a momentum  $-m_p c_x$ . The value of the momentum therefore changes by  $2m_p c_x$  during the collision.

If the particle moves at constant velocity  $c_x$ , it hits the walls periodically. The collision frequency, that is, the number of collisions per time interval, is the ratio of velocity  $c_x$  and traveling distance ( $2d$  for back and forth distance), that is,  $c_x/2d$ .

According to the laws of mechanics, the force that is exerted to the wall is the product of the change in momentum

per collision and the collision frequency:

Wall force caused by particle:

$$2m_p c_x \frac{c_x}{2d} = \frac{m_p c_x^2}{d} \quad (1.11)$$

The pressure is calculated from the force by dividing the wall force by the wall 's surface area ( $d^2$ ):

Wall pressure caused by particle:

$$\frac{m_p c_x^2}{d} \frac{1}{d^2} = \frac{m_p c_x^2}{d^3} \quad (1.12)$$

$d^3$  can be written as volume  $V$ . The pressure applied to the wall by the total gas is obtained by multiplying the wall pressure caused by a single particle with the number of particles hitting the wall ( $\frac{1}{3}N$ ):

$$p = \frac{m_p c_x^2 N}{d^3} \frac{1}{3} = \frac{N m_p c_x^2}{3 V} \quad (1.13)$$

Rearranging the equation finally yields

$$pV = N \frac{m_p c_x^2}{3} \quad (1.14)$$

When comparing equation (1.14), obtained from the kinetic theory of gases, with the experimentally found equation of state (1.9- 1.10), the two equations correspond, if the velocity  $c_x$  complies with the following relation:

$$c_x = \sqrt{\frac{3kT}{m_p}} \quad (1.15)$$

In our simple model, the speed  $c$  of a particle is just the absolute value of its velocity  $c_x$ . Then, by rewriting using specific gas constant ( $R = \frac{R_0}{M} = \frac{k}{m_p}$ ):

$$c = \sqrt{\frac{3RT}{M}} = \sqrt{3R_0 T} \quad (1.16)$$

Additionally, equation yields that the speed of gas particles rises when the temperature increases and that heavy gas particles are slower than lighter particles.

Previously, we assumed that all gas particles travel with the same velocity  $c_x$ . Collisions between particles were neglected.

In fact, however, particles do collide mutually due to their finite particle size. Depending on the type of collision between two particles (head-on or rather grazing), velocity values and directions change. Similar considerations apply to collisions with a wall. A real vessel wall is not a static, flat surface but shows microscopic roughness and vibrates thermally. Thus, the collision with a wall is not a simple reflection.

Overall, a large number of collisions occur within a gas, and the sheer number makes it impossible to consider them individually. This may initially create the impression that quantitative relations of gas properties cannot be derived from microscopic behavior. However, this is not the case. On closer inspection, we find that just the large number of particles allows deriving accurate mean values of motion quantities.

To begin with particle velocity, general symmetry considerations suggest that all directions of motion (arbitrary orientation in three dimensions) appear equally often. Considering the component velocity of all gas particles in any given direction, for example, the  $x$ -direction, particles possess different values that can be positive (along the considered direction) or negative (opposite to the considered direction). This behavior can be expressed mathematically using a distribution function, for example, the function  $F_1$  for the normalized  $x$ -component velocity  $c_x$ . Normalization is performed by dividing by the most probable velocity  $c_{mp}$ .

$$F_1 \left( \frac{c_x}{c_{mp}} \right) = \frac{1}{N} \frac{dN}{d \left( \frac{c_x}{c_{mp}} \right)} \quad (1.17)$$

Here,  $dN$  is the fraction of particles from the total number  $N$  with a velocity component in the  $x$ -direction in the interval from  $c_x = c_{mp}$  to  $(c_x + dc_x)/c_{mp}$  when the components in the  $y$ - and  $z$ -directions are of arbitrary values. As all particles are considered, the normalizing condition reads

$$\int_{-\infty}^{\infty} F_1 \left( \frac{c_x}{c_{mp}} \right) d \left( \frac{c_x}{c_{mp}} \right) = 1 \quad (1.18)$$

Now what does the velocity distribution  $F_1$  look like? Around 1860, Maxwell presumed a Gaussian bell-like distribution curve. Boltzmann determined the absolute value of the velocity about one decade later. The velocity distribution is therefore referred to as the Maxwell–Boltzmann velocity distribution. Later, it was derived precisely from statistical mechanics [5]. Modern computer simulations that calculate the motion and collisions of large numbers of particles, as well as many

experiments, have verified this distribution. It reads

$$F_1\left(\frac{c_x}{c_{mp}}\right) = \frac{1}{\sqrt{\pi}} \exp\left(-\frac{c_x^2}{c_{mp}^2}\right) \quad (1.19)$$

This one-dimensional velocity distribution is symmetric to the axis of the ordinate because positive and negative velocity values appear equally often.

The distribution  $F_0$  of speed values  $c$ , that is, the absolute value of the velocity vector, can be obtained by integration over the  $F_1$  distributions of the three directions with boundary condition of fixed  $c$ . Calculation leads to the function given below,

$$F_0\left(\frac{c_x}{c_{mp}}\right) = \frac{4}{\sqrt{\pi}} \frac{c_x^2}{c_{mp}^2} \exp\left(-\frac{c_x^2}{c_{mp}^2}\right) \quad (1.20)$$

For normalization, the most probable speed  $c_{mp}$ , that is, the peak speed, has already been used, indicating the speed value at the peak of the distribution function  $F_0$ . In order to describe macroscopic phenomena, it can be advantageous to use other speed values. The mean speed  $\bar{c}$  is obtained by calculating the weighted average of the gas particles' speed values. The effective speed  $c_{eff}$  is determined by calculating the square root of the weighted average of the gas particles' squared speed values. Calculation yields the following values:

Most probable speed  $c_{mp} =$  argument value where  $F_0$  obtains its maximum

$$\sqrt{\frac{2kT}{m_p}} = \sqrt{\frac{2RT}{M}} = \sqrt{2R_0T} = \sqrt{\frac{2p}{\rho}} \quad (1.21)$$

Arithmetic mean thermal speed

$$\bar{c} = \int_0^{\infty} c F_0\left(\frac{c}{c_{mp}}\right) dc = \sqrt{\frac{8kT}{\pi m_p}} = \sqrt{\frac{8RT}{\pi M}} = \sqrt{\frac{8}{\pi} R_0T} = \sqrt{\frac{8p}{\pi\rho}} \quad (1.22)$$

Effective speed = root-mean-square speed

$$c_{rms} = \sqrt{\int_0^{\infty} c^2 F_0\left(\frac{c}{c_{mp}}\right) dc} = \sqrt{\frac{3kT}{m_p}} = \sqrt{\frac{3RT}{M}} = \sqrt{3R_0T} = \sqrt{\frac{3p}{\rho}} \quad (1.23)$$

Many macroscopic properties of a gas, for example, pressure, are determined by the impingement rate at which gas particles collide with a surface. Here, the term collision rate  $j_N$  is introduced, also referred to as the rate of incidence. It is defined as the number of collisions with a surface per unit area and time. The kinetic theory of gases allows calculating the collision rate, when assuming a Maxwell–Boltzmann velocity distribution:

$$\text{Collision rate } j_N = \frac{\text{Number of collision with wall}}{\text{Area of wall} \times \text{time}} = \frac{N}{At} = \frac{n\bar{c}}{4} = \frac{p\bar{c}}{4kT} \quad (1.24)$$

An application example for using the collision rate is a gas flow through an opening in a wall, referred to as effusion (gas escape) (Figure 1.2). A thin wall that has a small hole with the area  $A$  separates one vessel from the other. If the pressure in vessel 1, to the left of the wall, is  $p_1$ , the temperature is  $T_1$ , and the pressure in vessel 2 is negligible, the particle flow (= number of particles per unit time) leaving the vessel 1 is

$$\begin{aligned} \text{Effusion - particle flow } q_N &= \frac{\text{Number of emanating particles}}{\text{Time}} = \\ &= j_n A = \frac{p\bar{c}}{4kT} A = \frac{n\bar{c}}{4} A \end{aligned} \quad (1.24)$$

A precondition for this equation is that the pressure is small enough so that disturbing collisions between gas particles do not occur in the area of the opening (molecular flow). For the volumetric flow of the escaping gas, the above equation yields

$$\text{Effusion - volumetric flow } q_V = \frac{\text{Emanating gas volume}}{\text{Time}} = \frac{\Delta V}{\Delta t} = \frac{\Delta N/n}{\Delta t} = \frac{\bar{c}}{4} A \quad (1.24)$$

So far, the size of the gas particles remained unconsidered. Their sizes play a crucial role for

transport phenomena. Different methods are available to determine the size, as shall be discussed next.

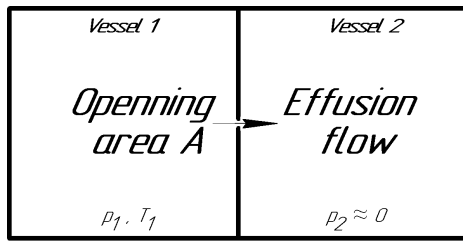


Figure 1.2 Effusion from a vessel.

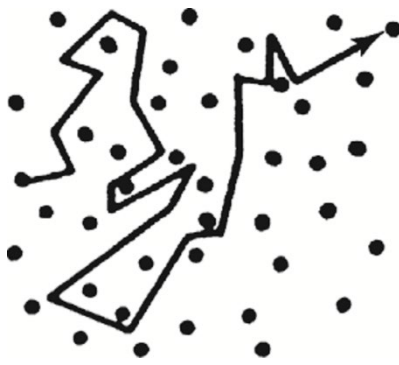


Figure 1.3 Zigzag path of a gas particle.

individual particle follows a zigzag route (Figure 1.3).

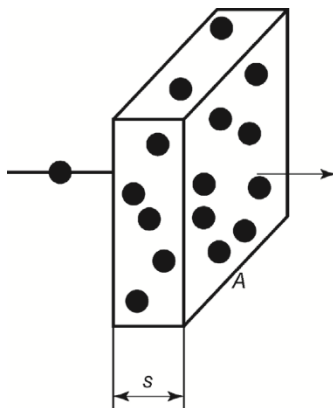


Figure 1.4 A gas particle traveling through a volume of gas.

multiplied by the individual areas with the number  $N$  of atoms in the volume:

Total collision area

$$N\pi d^2 = nV\pi d^2 = nA s \pi d^2 \quad (1.25)$$

The larger the thickness  $s$  of the layer, the more probable a collision. In the case of a statistical (irregular) arrangement of the stationary gas particles in the volume, the thickness of the layer amounts to the mean free path, thus  $s = \bar{l}$ , if the total effective collision area (1.25) is equal to the geometrical area  $A$ . This leads to the condition

$$\bar{l} = \frac{1}{\pi d^2 n} \quad (\text{gas particles in the volume assumed stationary}) \quad (1.26)$$

Due to the statistical arrangement of the gas particles in the volume, an incoming particle

When a gas is cooled far enough, it initially liquefies and finally freezes. A certain amount of gas then forms a liquid or solid with a certain volume. The assumption is plausible that the individual atoms and molecules in a solid are arranged as small, closely packed spheres. Using this model, the volume filled by an individual particle can be calculated by dividing the particle mass by the density of the solid. Based on the used volume, the diameter of the sphere is obtained after specifying the structure in which the spheres are arranged in the solid.

Modern experimental methods, such as structure analysis by X-ray diffraction or surface scanning with an atomic force microscope, allow direct measurement of the distance between two particles, and therefore, of their size. Results reveal that the diameter of simple gas particles (i.e., individual gas atoms) amounts to approximately  $3 \times 10^{-10} \text{ m} = 0.3 \text{ nm}$ , quite independent of the gas species. As gas particles, in fact, are not hard spheres, their size is not well defined but depends on the type of phenomenon observed.

During their kinetic motion, gas particles come into contact when the distance between their centers drops below their diameter. The collision changes the particles' directions and speeds. Due to multiple particle collisions, the path of an

The path lengths that a particle travels between two successive collisions vary due to the statistical motion of the particles. An average value of this path length can be defined, referred to as the mean free path  $\bar{l}$ .

We will now calculate this mean free path, while assuming that the gas particles are small hard spheres with diameter  $d$ . Furthermore, we shall presume that no force is transferred between particles except during elastic collisions. First, we will consider a simplified case in which a gas particle travels through a virtual gas volume  $V$  (cross-sectional area  $A$ , thickness  $s$ ), containing static particles of the same species (Figure 1.4).

A moving gas particle collides with a stationary gas particle inside the volume if the distance between their centers drops below the particle diameter  $d$ . Thus, the effective collision area (perpendicular to the particle's trajectory) for this collision amounts to  $\pi d^2$ . The total effective collision area for all possible collisions is obtained by

passes the distance  $s = \bar{l}$  without collisions with a probability of 37%, and passes the distance  $s = 4\bar{l}$  with a probability of just under 2%.

In reality, all gas particles travel with a statistic velocity distribution according to Maxwell–Boltzmann. Therefore, more collisions occur and the mean free path drops. Maxwell investigated this problem in 1860 and added a factor of  $1/\sqrt{2}$  to equation (1.26):

$$\bar{l} = \frac{1}{\sqrt{2}\pi d^2 n} \quad (\text{all gas particles in motion}) \quad (1.27)$$

This formula is valid when the mean free path is defined as the total distance traveled by molecules in a time period divided by the total number of their collisions in this period. Other definitions of the mean free path may be used, for example, the mean distance moved by a molecule between a given instant and its next collision. These definitions lead to slightly different numerical values, see [5]. Nearly all literature uses equation (1.27) and so will we.

By replacing the number density of particles  $n$  with the term  $p/kT$  in equation (1.27), and by moving  $p$  to the left-hand side, we find

$$\bar{l}p = \frac{kT}{\sqrt{2}\pi d^2} \quad (1.28)$$

Thus, for a particular gas (with particles of diameter  $d$ ), the product of mean free path and pressure depends only on the temperature.

### 1.3. Gas flow

Gas flow patterns play an important role in vacuum technology. When a vessel is evacuated, the gas that initially filled the vessel flows to the pump through tubes. During operation of the vessel, gas released by components (desorption) or supplied to the process flows from high-pressure to low-pressure regions. Knowledge of flow patterns is vital for designing vacuum systems intelligently and understanding their performance characteristics.

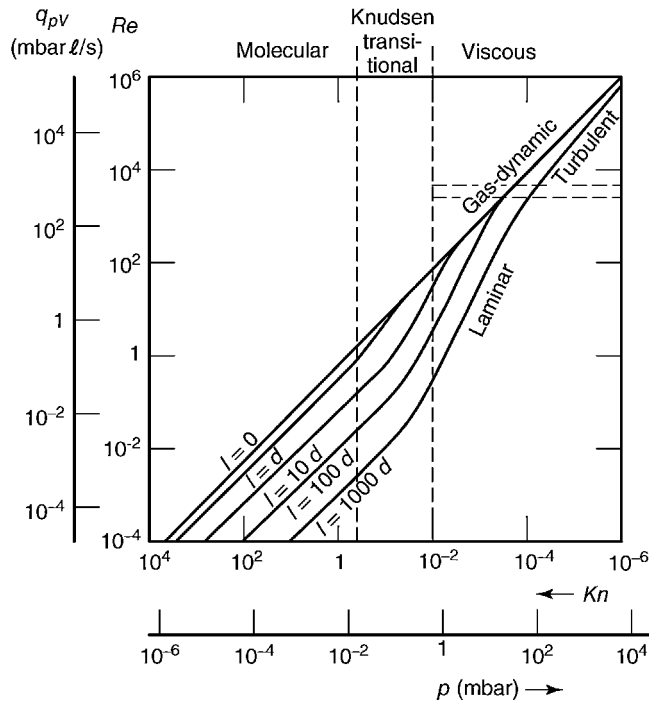


Figure 1.5 Flow types in tubes with circular cross section, diameter  $d = 1\text{cm}$ , and length  $l$  as indicated taken as an example. The gas is air at  $20^\circ\text{C}$ . Inlet pressure is taken as abscissa and the outlet pressure is assumed negligible.

compared with the cross dimensions of the tube. Any mutual particle collision hardly occurs. Each

gas particle travels through the tube due to its thermal motion, independent of other particles. However, frequent collisions with the tube walls cause a zigzag route. On average, the paths of many individual particles combine to form the macroscopic flow behavior. This situation is referred to as single-particle motion or molecular flow.

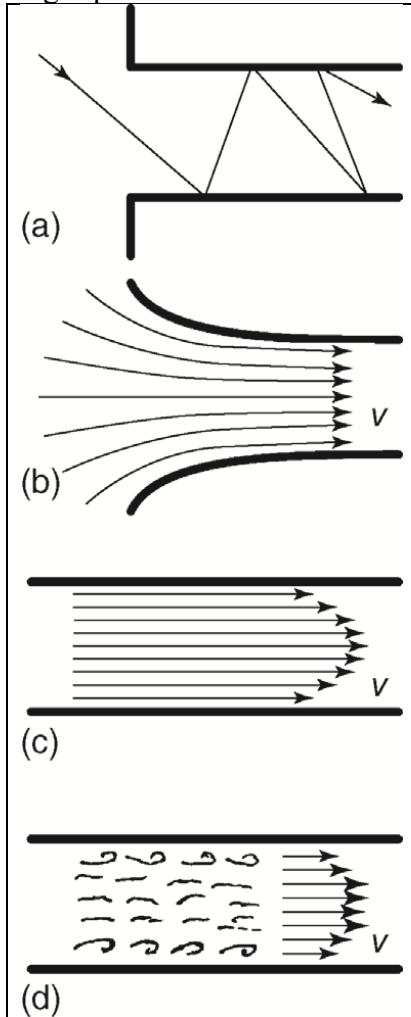


Figure 1.6 Different types of gas flows. (a) Molecular flow. (b–d) Different types of viscous flows: gas-dynamic (intake flow), laminar, and turbulent.

2) Under high pressure, the mean free path of gas particles is much lower than the cross dimensions of the tube. The particles experience frequent mutual collisions, thereby exchanging momentum and energy continuously. Even a small volume contains many frequently colliding particles. Thus, the gas behaves as a continuum. A flow is the result of local pressure gradients. This situation is referred to as continuum flow or viscous flow.

3) The medium-pressure range is characterized by a transition between molecular and viscous flows. In this transition, collisions of gas particles with the wall occur just about as often as mutual collisions among gas particles. This situation is referred to as transitional flow or Knudsen flow.

Thus, for a particular type of flow to occur, two main criteria can be identified: one criterion is the mean free path of gas particles in relation to the cross dimensions of the tube (for circular cross sections, the diameter). The second criterion is the velocity of flow for given cross dimensions of the tube and internal friction of the gas. Thus, two dimensionless characteristic numbers may be defined to describe these criteria quantitatively.

The Knudsen number  $K_n$  is the ratio of the mean free path  $\bar{l}$  of the gas particles between two particle–particle collisions and the characteristic geometrical dimension  $d$  of the tube’s cross section (for circular tube cross sections, the diameter):

$$K_n = \frac{\bar{l}p}{d} \quad (1.29)$$

As known, the mean free path can be obtained from viscosity  $\eta$ . Thus, for practical reasons, equation (1.29) can be rewritten as

$$K_n = \frac{\pi \bar{c}\eta}{4pd} \quad (1.30)$$

denoting that the Knudsen number is inversely proportional to the pressure. A high Knudsen number indicates low pressure, and thus molecular flow, whereas a low value of the Knudsen number suggests viscous flow. Transition between the two types of

flows is smooth and leads to a change in gas flow through the tube. The limiting cases of molecular or viscous flow are approximately reached when roughly 90% of this change in flow has established. The quantitative investigations described below show that this assumption leads to the following conditions:

$$\begin{array}{ll} K_n > 0.5, & \text{molecular flow,} \\ 0.5 > K_n > 0.01, & \text{transitional flow,} \\ K_n < 0.01, & \text{viscous flow.} \end{array}$$

We will now investigate the second criterion for the type of flow: the velocity of flow. The velocity  $v$  of a gas flow is the mean velocity component of the gas particles in the direction of the tube. Usually, the velocity’s mean value is given as an average across the tube’s cross section.

In the case of molecular flow, the individual gas particles travel back and forth between the walls of the tube with thermal velocity. A particle’s direction after hitting the wall is (nearly)

independent of its direction prior to the collision. Thus, a zigzag route develops (Figure 1.6, a). The geometry of the tube determines the resulting velocity of flow.

The situation is different in the case of viscous flow. Here, three types of flows in a tube are differentiated. The length of the tube determines the type of flow (Figure 1.6, b–d).

1) Initially, the gas has to leave a reservoir (vessel) to reach the entrance of the tube. Subsequently, it streams into the tube (Figure 1.6, b). Here, the gas accelerates from a quiescent state (velocity of flow equals zero) to a finite velocity of flow. This process requires acceleration energy that is taken from pressure energy (pressure drops) and thermal energy (temperature drops).

Thus, as a volume element of gas travels along a path, velocity rises, and simultaneously temperature and pressure drop. For short distances, wall friction is usually negligible. This so-called intake flow is a particular type of gas-dynamic flow.

2) Now, the gas flows through the tube. The velocity of flow at the inlet is approximately constant across the complete cross section. As the gas continues its way through the tube, the gas layers near the walls decelerate, and the velocity of flow drops to zero in the boundary layer at the wall. The thickness of the boundary layer increases along the way. The velocity of flow, the friction behavior of the gas, and the dimensions of the cross section determine the type of flow that develops after a certain intake stretch. For low velocities, all individual volume elements move in the direction of the tube. Now, the volume elements in the center of the tube move quicker than the volume elements at the boundary of the tube. Thus, a velocity profile develops across the cross section of the tube (Figure 1.6, c). This type of flow is referred to as laminar flow.

3) If, however, flow velocity is high, frictional forces are high as well because they are determined by flow velocity. A volume element, traveling at higher velocity and some distance from the wall of the tube, is deflected toward the wall by the decelerating action of the slower moving layers near the wall. The deflecting effects increase with friction and thus velocity, whereas the inertia of mass, which tends to preserve the direction of flow, remains unchanged by a change in velocity. Thus, for sufficiently high velocities, deflecting forces dominate and the flow shows turbulences and eddies (Figure 1.6, d). The criterion for turbulences to develop is the ratio of frictional force (proportional to gas viscosity  $\eta$ ) and inertia of mass (proportional to gas density  $\rho$ ) for a specified velocity of flow  $v$  (cross-section average) and specified cross section. Typically, the Reynolds number  $Re$  is used to describe this criterion:

$$Re = \frac{\rho}{\eta} vd \quad (1.30)$$

The quantity  $d$  characterizes the cross section of the tube. For a downpipe, this corresponds to the diameter  $d$ .

$$\begin{array}{ll} Re > 2300, & \text{laminar flow,} \\ Re > 4000, & \text{turbulent flow,} \end{array}$$

#### 1.4. Pressure of gas, levels of vacuum, vacuum units

The Latin word vacuum means "empty". The term "vacuum" refers to a given space filled with gas at pressures below atmospheric (American Vacuum Society [6]).

According to the kinetic theory a gas exerts pressure on the enclosing walls because of the elastic impact of molecules on these walls. Thus, the pressure is the force applied by the gas per unit area of real wall surface or imaginary surface located inside the gas. The pressure units used in vacuum measurements are expressed as force per unit area (e.g. Newtons per square meter, dynes per square centimeter, pounds per square inch, kilograms per square meter, etc.) or as height of a column of liquid balanced by the gas at the given pressure (e.g. centimeter or inch of water; inch, millimeter or micron of mercury, etc.). The pressure unit recommended by the American Vacuum Society [6] to be used in vacuum technology is the torr (millimeter of mercury) defined as  $1/760$  of a standard atmosphere or  $1,013,250/760 \text{ dyne/cm}^2$ .

Factors for the conversion of the various pressure units used in vacuum techniques are listed

in table 1.3

In a gas the molecules travel in straight line until they collide with other molecules or with the walls of the vacuum system. The average distance travelled by a gas molecule between two successive collisions is known as its mean free path. The mean free path  $\bar{l}$ , is inversely proportional to the number of molecules per unit volume, thus at a given temperature it is inversely proportional to the pressure:

$$\bar{l} = \frac{k}{p(\mu)} \quad (1.31)$$

Table 1.1 lists the values of the constant  $k$  for various gases. These values are in fact the mean free paths (expressed in cm) at a pressure of  $10^{-3}$  torr (1 micron).

Table 1.1. Values of  $k$  (cm.micron) at 20 °C

<i>Gas</i>	<i>k</i>		<i>Gas</i>	<i>k</i>
Xenon	3.00		Nitrogen	5.1
Water vapour	3.40		Air	5.1
Carbon dioxide	3.34		Oxygen	5.4
Chloride	3.47		Mercury vapour	6.3
Krypton	4.05		Hydrogen	9.3
Argon	5.07		Neon	10.4
			Helium	14.6

The lowest pressure to be obtained, measured and maintained in a vacuum chamber or system determines the main characteristics of the system, the pumps to be used, the gauges and the seals. According to the lowest pressure and the corresponding mean free path vacuum ranges were established.

The low vacuum range includes pressures less than atmospheric and greater than 25 torr. The lower limit of this range was set at that pressure (about one inch of mercury) corresponding to approximately the vapor pressure of water at 25 °C.

Medium vacuum is considered to be in the range of 25 to  $10^{-3}$  torr. Another classification divides the same range ( $760$  to  $10^{-3}$ ) into rough vacuum ( $760$  to 1 torr) and fine vacuum (1 to  $10^{-3}$  torr).

In any case the low vacuum is the range of water vapors and the medium or fine vacuum the range of other vapors (mercury, hydrocarbons, etc.). High vacuum is defined as the condition in a gas-filled space at pressures less than  $10^{-3}$  torr. This range is used to be divided into high, very high and ultra-high vacuum (table 1.2). The high and very high vacuum range is limited to use materials having corresponding low vapor pressures at room temperature. This is the range of elastomer gasket seals. The ultra-high vacuum requires baking. This practically restricts the list of materials to a few metals, glasses and ceramics, and the gaskets to metallic ones.

Table 1.2. Vacuum ranges

Pres sure (torr)	Mean free path	Vacuum range		Pumps	Gauges	Materials	Seals*
760	0.06 $\mu$	Rough	Low	Piston Rotary	Diaphragm Liquid Level	Any	
25	2 $\mu$						
1	50 $\mu$	Fine	Me- dium	Rotary	McLeod Tesla coil Pirani gauge Alphatron	Waxes, glasses, ceramics metals and elastomers  Porous and high vapor pressure materials excluded	Any elastomer seals, waxes seals, soldered seals, greased ground seals, liquid seals.

Pressure (torr)	Mean free path	Vacuum range	Pumps	Gauges	Materials	Seals*
$10^{-3}$	5 cm	High	Molecular Diffusion	McLeod Penning Ionization	Only glass, metal, ceramics and low vapor pressure elastomers	
$10^{-6}$	50 m					
$10^{-9}$	50 km	Very high	Molecular Diffusion Ion Pump	Ionization Bayard-Alpert	Preferably clean bakeable materials (glass, copper, stainless steel, ceramics, Viton)	Elastomer, greaseless ground, glass-glass, glass-metal, guard vacuum, ethoxyline, silver chloride
		Ultra-high	Ion Pump Cryopump	Bayard-Alpert Magnetron	Only bakeable materials and with low permeability for glasses	Welded and brazed glass-metal, glass-ceramic and ceramic metal, metal gasket

*Connected to this chapter the author has made use of the following treatises. The abbreviations used for the references in this volume are indicated in parentheses.*

1. E. H. Kennard, *Kinetic Theory of Gases with an Introduction to Statistical Mechanics*, McGraw-Hill Book Company, New York, 1938 (ERK).

2. L. B. Loeb, *Kinetic Theory of Gases*, McGraw-Hill Book Company, New York, 2nd ed., 1934 (LBL).

3. J. H. Jeans, *An Introduction to the Kinetic Theory of Gases*, The Macmillan Company, New York, 1940 (JHJ).

4. S. Chapman and T. G. Cowling, *The Mathematical Theory of Non-Uniform Gases*, Cambridge, England, The University Press, 1939 (CC).

5. Chapman, S. and Cowling, T.G. (1970) *The Mathematical Theory of Non-Uniform Gases*, 3rd edn, Cambridge University Press, Cambridge, UK.

6. American Vacuum Soc., *Glossary of Terms Used in Vacuum Technology*, Pergamon Press, London, 1958.

## 2. VACUUM SYSTEMS CALCULATION

Ultrahigh vacuum technology requires consideration of many factors that would be considered trivial in routine high vacuum work. Not only must a system be sealed off completely from the atmosphere, but every component must be made of such material and construction that it does not contribute gas to the vacuum. Indeed, the permeation of the envelope by the atmosphere can limit the ultimate pressure attained. In this chapter, the components required for the production, measurement, and use of ultrahigh vacuum are described. Before discussing the various components, it is well to consider the fundamentals of vacuum production.

Fundamental Vacuum System Considerations.

The pumping speed,  $S_p$ , of any pump is defined by the expression

$$Q_p = \frac{S_p}{P} \quad (2.1)$$

where  $Q_p$  is the quantity of gas removed from a given volume per unit time and  $P$  is the pressure at the pump. If the pump is separated from the system by a constriction of conductance,  $C$ , the effective speed,  $S$ , of the pump is given by

$$\frac{1}{S} = \frac{1}{S_p} + \frac{1}{C} \quad (2.2)$$

The rate of reduction of pressure in a system of volume  $V$  is given by

$$\frac{dP}{dt} = -\frac{S}{V}P \quad (2.3)$$

If gas is backstreaming from the pump at a constant rate,  $Q$ , then the rate of reduction of pressure is given by the following expression

$$\frac{dP}{dt} = -\frac{S}{V}P + \frac{Q}{V} \quad (2.4)$$

This expression may be rewritten as

$$\frac{dP}{dt} = -\frac{S}{V}(P - P_u) \quad (2.5)$$

where  $P_u$  is the ultimate pressure attainable with the given pump. The equilibrium pressure of the system,  $P_e$ , may be written as

$$P_e = \frac{Q_T}{S} \quad (2.6)$$

where  $Q_T$  is the total influx rate into the system. The production of ultrahigh vacuum is a matter of reducing the ratio of gas influx to pumping speed.

Gas influx to the vacuum system can be decreased by high temperature bakeout, cooling of the walls, and by adequate trapping of the pump. These procedures preclude the use of ordinary vacuum components such as rubber O-rings, stopcocks, wax, etc. The gas influx to the system is due to backstreaming from the pumps, desorption from the walls and internal parts of the vacuum system, leaks in the system, and permeation of gases through the walls of the system. Alpert and Buritz have demonstrated that the ultimate limit to the achievement of low pressures in glass systems is due to the diffusion of atmospheric helium through the walls of the system.

One must also consider not only the vapor pressure of the construction materials but also the vapor pressure of the electron emitting sources in the pressure measuring equipment. At 2300°K the vapor pressure of tungsten is  $10^{-12}$  torr. This is the equilibrium vapor pressure. In practice, however, the important phenomenon is the evaporation rate of the atoms from the filament since the large majority of atoms which leave the surface of the filament never return to the filament. At any given time, one can calculate the number of tungsten atoms within the grid volume of the ionization gauge. Furthermore, measurements and calculations have demonstrated that the vapor pressure of tungsten presents no difficulty down to pressures of  $10^{-12}$  torr. Other filament materials may also be used.

1. For an excellent discussion of vacuum system calculations, see J. Delafos.se and G. Mongodin, "Les Calculs de la Technique du Vide," *Le Vide* 16, #92, 1 (1961).

### 3. VACUUM SYSTEMS PROJECTION

#### 3.1. Materials for vacuum systems

Materials to be used in the construction of ultrahigh vacuum systems must satisfy several basic requirements. In order to keep the influx of gas into the vacuum system low, materials must have a low vapor pressure and be impervious to the diffusion of gases through them. These criteria must be satisfied at temperatures up to 450°C or 500°C as well as at the system operating temperature. Since it generally is necessary to bake the vacuum system at 450°C for long periods of time to remove adsorbed layers of gas from the walls, the materials used must maintain their physical strength while evacuated at this temperature. These criteria in general preclude the use of rubber O-rings, waxes, greases, glass stopcocks, glass joints, brass, and soft solder found in many ordinary laboratory vacuum systems. The vapor pressures of the elements and common gases encountered in ultrahigh vacuum technology are thus of considerable practical importance both in the design of the vacuum system and in the experiment to be carried out. Honig et al. have recently compiled vapor pressure data for the more common elements and for some of the common gases.

Depending on the particular type of usage, requirements for materials of vacuum technology are manifold. For example, materials used to build vacuum vessels must be absolutely gas tight, that is, ambient air must be held back from the vacuum. Vessel material has to be strong enough not to deform when evacuating produces a pressure differential of 100 kPa (1 bar), corresponding to the force exerted by a weight of 10 t per 1 m<sup>2</sup>. At the same time, gas emissions from the material into the vacuum are an issue. The desired vacuum pressure determines the maximum tolerable gas emission rates. For built-in components surrounded by vacuum, in contrast, tightness is of less or no concern at all. Rotor blades of turbomolecular pumps are subject to extreme accelerations. Significant warming of such blades due to gas friction is not tolerable. Materials for helium bath cryostats have to withstand temperature variations down to only a few K; materials for high-bakeable ultrahigh-vacuum equipment are exposed to up to 450 °C.

Thus, the main requirements specific to materials for vacuum technology are as follows:

- sufficient mechanical strength;
- corrosion resistance;
- high gas tightness (leak rates, e.g.,  $< 10^{-9} \text{ mbar } \ell \text{ s}^{-1}$  ( $10^{-7} \text{ Pa } \ell \text{ s}^{-1}$ ));
- low intrinsic vapor pressure;
- low foreign-gas content;
- favorable degassing properties;
- high melting and boiling points;
- clean surfaces;
- adopted thermal expansion behavior;
- high thermal fatigue resistance.

Additionally, materials must provide sufficiently high chemical resistance against gases and vapors developing in the processes.

Requirements in terms of gas emissions and tightness increase when approaching the ultrahigh-vacuum range. Table 3.1 provides an overview of materials used in vacuum technology.

Metals and metal alloys in the solid state are made up of atoms arranged regularly in characteristic lattice structures. Only in special cases does this lattice structure fill the complete metal part. Components are rather composed of numerous small crystal grains, so-called crystallites with sizes ranging from several cubic micrometers to several cubic millimeters. Such materials are thus termed polycrystalline materials.

The grains are separated by grain boundaries with at times considerably different chemical and mechanical properties than the crystallites. The shape and size of the crystallites determine mechanical properties. They are influenced by the processing techniques chosen for manufacturing, also including heat treatments. Fine, stretched crystallites make the material hard and brittle. The strength of the material is high. Such materials are cold-rolled, work-hardened, and cold-worked.

When material is heated beyond its recrystallization temperature  $T_R$  for longer periods, large crystallites form, making the material soft and ductile (annealing). Usually, this recrystallization temperature is given by  $T_R \approx 0.4 T_E$ , with  $T_E$  denoting the melting point, both temperatures given in K.

Table 3.2 lists processing techniques as well as their corresponding advantages and disadvantages for applications in vacuum technology.

Table 3.1 Overview of commonly used materials for vessels and seals as well as corresponding vacuum ranges

Pressure and vacuum ranges		Application examples	Materials
$10^2$ mbar ( $10^4$ Pa)	Rough or low vacuum	Drying	Structural steel
1 mbar ( $10^2$ Pa)		Degassing Distillation	Stainless steel Ceramics Aluminum Elastomer seals
1 mbar ( $10^2$ Pa)	Medium or fine vacuum	Vacuum process technology	Aluminum
$10^{-3}$ mbar ( $10^{-1}$ Pa)			Stainless steel Ceramics Elastomer seals
$10^{-3}$ mbar ( $10^{-1}$ Pa)	High vacuum	Coating technology Molecular beam epitaxy	Stainless steel Aluminum
$10^{-7}$ mbar ( $10^{-5}$ Pa)			Al <sub>2</sub> O <sub>3</sub> ceramic Elastomer seals Tantalum Molybdenum
$10^{-8}$ mbar ( $10^{-6}$ Pa)	Ultra-high vacuum	Deposition of high-purity coatings Materials analysis	Stainless steel Aluminum Al <sub>2</sub> O <sub>3</sub> ceramic
$10^{-12}$ mbar ( $10^{-10}$ Pa)		Accelerator technology	Copper seals Special seals Gold, silver, tantalum, molybdenum

#### Mild Steel/General Structural Steel

General structural steels are known as S235 and S355. Usually, they are contaminated with carbon, phosphorous, and sulfur. They are used for high-vacuum applications down to  $10^{-4}$  Pa ( $10^{-6}$  mbar) if corrosion resistance is not required. Due to processing technology, such steels emit CO gas continuously.

Grades must be picked carefully. Generally, an operating experiment is conducted in order to investigate the behavior of selected sample components in terms of weld ability and helium tightness. Transfer of working techniques from boiler making and tank construction to vacuum-tank construction is limited. For example, multiple welding beads and machining down into segregation zones (agglomerations of undesired chemical elements in the metal) should be avoided. Tools should be held separate from tools used for stainless-steel processing in order to prevent microscopic residue of mild steel from contaminating stainless-steel parts. Selection has to take into account material characteristics, for example, in terms of weld ability.

Starting materials include sheets, rods, and tubes. Cast parts (e.g., pumps and valve housings) are restricted to low- and fine-vacuum applications.

Mild steel is also of interest for certain special applications, for example, for providing a particular magnetic shielding effect. If such applications call for corrosion resistance, the steel surface has to be coated.

Table 3.2 Processing technologies for metals and corresponding characteristics

Processing technologies	Characteristics
Casting of molten metal into casting molds	Series production possible Volume shrinkage during solidification Possible inclusions and shrinkage cavities (exhalation sources, leakage) Applicable to components in fore- and low-vacuum range or for low requirements
Drawing and rolling	Compression of materials Applicable to any components down to UHV
Special melting (electroslag remelting, ESR) and additional forging or rolling	Production of high-purity and homogeneous materials Additional materials compression during forging Expensive Required for special applications
Vacuum melting	Production of materials with low contents of foreign gases Expensive Required for special materials (e.g., titanium)
Extruding	Special geometries producible, not feasible with any other technique Restricted to appropriate materials (aluminum)

### Stainless Steel

Stainless steel is common to vacuum technology. The reason is that stainless-steel surfaces, due to their surface microstructure, show sufficient passivation, and thus, are protected adequately against corrosion during baking and vacuum processing. At the same time, the group of stainless-steel materials also includes grades providing sufficient strength for flange joints exposed to baking procedures (typically, 200–300 °C in the UHV range).

A wide range of stainless steels is available (see also Table A.24): nonstabilized (high-carbon) grades such as 1.4301 (DIN, AISI: 304), low-carbon grades such as 1.4306 (304 L), as well as stabilized grades such as 1.4541 and 1.4571 (316 Ti). The latter include alloying elements that react with carbon during welding and thus prevent a drop in corrosion resistance usually caused by this element. For welding, stainless steels with low carbon contents or stabilized grades are recommended.

Analyzer and accelerator technologies mostly use low-magnetic permeability stainless steels such as 1.4429 (316LN), 1.4404 (316 L), and 1.4435 (316 L).

### Steel – Special Alloys

Special alloys are used for glass–metal joints or for joints to premetallized ceramics. This is because the differences in coefficients of thermal expansion between commercial stainless steel and glass or ceramics are so high that manufactured joints, if produced at all, suffer cracks or offsets.

In terms of thermal expansion, employed special alloys are adopted to glass and ceramics. Such alloys mainly comprise binary iron–nickel alloys or ternary iron–nickel–cobalt alloys known as Kovar, Fernico, Nilo-K, or Vacon. Note that these materials are highly magnetic, which might cause problems in certain physical applications.

### Titanium

The material is highly gas binding. Therefore, titanium is produced in vacuum-melting processes. Commercial grades show low carbon contents and high ductility. Titanium's density lies between those of iron and aluminum. Above approximately 150 °C, titanium reacts easily with atmospheric gases such as oxygen and nitrogen. This behavior is disadvantageous in certain situations (e.g., when welding without shielding). On the other hand, it is just this reactivity that paves a way for applications of titanium in vacuum technology: titanium hydride is used for premetallization

of ceramics providing reliable bonds between the ceramic and subsequent metal coatings (e.g., nickel). Applying pure titanium coatings onto appropriate ceramics allows active brazing without separate metal-lization procedures. Titanium is also used as getter material in pump technology (Sections 11.3.3 and 11.4). Titanium evaporates very easily even below its melt-ing point of 1670 °C; thus, it is evaporated from solid phase in titanium evapora-tion pumps (evaporation at approximately 1350 °C), heated by an electrical current passing through. Typical coatings reach thicknesses of 5 μm after one hour of evaporation. Ion getter pumps feature titanium plates as cathodes sput-tered by ion bombardment.

#### Aluminum

Aluminum is used mainly in fore and high vacuum. Small-flange components are often made from aluminum bulk material. Furthermore, aluminum is used for seals operating at temperatures up to 100 °C. Alloys used should be free of ele-ments with high vapor pressures such as lead or zinc. Mostly, alloys are com-posed of aluminum and silicon. Vapor pressure is low and reaches approximately  $10^{-6}$  Pa ( $10^{-8}$  mbar) at the melting point of 660 °C. Disadvantages include high thermal expansion, a porous aluminum-oxide surface layer, and high thermal conduction. This causes particular susceptibility to porosity and cracking in welding processes, and high distortion due to preheating required for welding. New applications utilize aluminum-UHV components [2]. Such applications call for special processing techniques in order to overcome some of the negative properties of aluminum, for example, surface porosity or low hardness.

#### Copper

Predominant features of copper include high thermal and electrical conductivity. These properties are required in cryotechnology and for heat sinks (e.g., radiation absorbers in particle accelerators) as well as for high-performance electrical conduc-tors. Such components are used frequently in many fields of vacuum technology.

A negative property of copper is associated with hydrogen embrittlement. Hydrogen appearing in heat treatments reacts chemically with the oxygen con-tained in copper. Developing water fissures the copper's microstructure. Thus, UHV applications use so-called OFHC copper (oxygen-free, high conductivity) or copper with reduced oxygen content.

Materials selection should pay particular attention to avoid alloy constituents with high vapor pressure. Alloys such as tombac and brass contain tin or zinc as alloying elements that easily evaporate at higher temperatures under vacuum and thus degrade the vacuum.

On a large scale, UHV technology uses metal seals made of copper, bakeable to approximately 450 °C. Grades used here provide controllable hardness (CF-flange seals) and good cold weld ability (for COF-flange seals). Filler metals for high-temperature brazing include Cu/Au and Cu/Au/Pd alloys.

#### Gold and Silver

Vapor pressures of gold and silver are sufficiently low for the metals to be used in ultrahigh vacuum.

Gold is used for seals in appropriately manufactured flange connections, for sealing valve faces in all-metal valves, or as coatings for high-performance electrical conductors and connectors. Similar to copper, gold is used in high-temperature brazing filler metals made of Cu/Au and Cu/Au/Pd alloys. Silver-plated stainless-steel screws yield prolonged service lives and show reduced tendency to cold welding. Also the copper CF-sealings are silver plated for some applications.

#### Indium

Indium is used for metal seals in high-vacuum applications, as solid sealing material between flanges, and to provide high heat transmission between differ-ent materials.

Its vapor pressure is low even though the melting point is quite low (156 °C). Special applications (e.g., cryotechnology) call for the material in cases where other sealing materials are inappropriate. Indium is soft, and thus, required seal-ing forces are low.

#### Materials for Special Vacuum Processes

Many vacuum processes require materials that differ from standard materials. Examples of such processes include measuring processes, heating, and cooling, all of which depend on special

materials and components.

Special materials such as tungsten, tantalum, or molybdenum are employed for measuring systems, in high-temperature applications (shielding, evaporator crucibles), in accelerator technology (radiation absorbers), as well as in low-temperature applications.

### Glasses

Glasses are categorized according to their mean coefficients of linear thermal expansion  $\alpha$  as follows:

- soft glass ( $60 \times 10^{-7} - 120 \times 10^{-7} \text{ K}^{-1}$ );
- hard glass ( $< 50 \times 10^{-7} \text{ K}^{-1}$ );
- quartz glass ( $\approx 5 \times 10^{-7} \text{ K}^{-1}$ ).

Additionally, we differentiate

- sintered glass;
- crystallized glass.

They differ significantly in terms of physical and chemical properties, thus qualifying for appropriate applications:

#### Soft Glass

SiO<sub>2</sub> content in soft glass is comparably low, whereas the content of alkali elements is relatively high. Typical amounts of substance are, for example, 65–70%SiO<sub>2</sub>, 2.5–15% Na<sub>2</sub>O, and 5–15% CaO. Typical soft glasses include Rührglas AG AR Glass in Germany and Dow Corning Glass Works 0010 in the United States, with coefficients of thermal expansion of  $90 \times 10^{-7} \text{ K}^{-1}$ . Usually, the lower cooling temperature is in the range 370–450 °C.

Soft glasses are used mainly because of their good electrical insulation properties and low permeabilities for H<sub>2</sub> and He. The permeability of lead glass, a particular type of soft glass, is only 1/10 000 of the permeability of common hard glasses.

Soft glasses show certain characteristics limiting utilization and processing. Their resistance to thermal shocks is poor, that is, cooling and heating have to be performed very slowly. Thus, after processing, intense stress relief in the transformation range is required, followed by slow cooling.

Thus, their use in high-vacuum technology is limited because softening occurs even at low temperatures. Therefore, they cannot be baked out completely.

#### Hard Glasses

SiO<sub>2</sub> contents in hard glasses usually exceed 70%. Hardness generally increases with boron content; thus, so-called borosilicate glass is hard glass. Other brand names are Pyrex and Duran. Their coefficients of expansion are approximately  $30 \times 10^{-7} \text{ K}^{-1}$ . One glass of this group, Corning 7056, is particularly popular in vacuum technology.

Their resistance to thermal shocks is good because lower cooling temperatures are above 500 °C. Likewise, the transition range is at relatively high temperature. Thus, hard glasses are better suitable than soft glasses for the high-and ultrahigh-vacuum range.

#### Quartz Glass

Quartz glass is pure SiO<sub>2</sub> glass. Its resistance to thermal shocks is very high because the coefficient of expansion is only  $5 \times 10^{-7} \text{ K}^{-1}$ .

Temperatures for processing and transition ranges are the highest of all known glasses. It devitrifies at temperatures above 1100 °C and can be used continuously up to approximately 1050 °C. Thus, quartz glass is used in vacuum furnaces (muffle furnaces) for high temperatures.

Comparably low amounts of alkali vapors lower the temperature for devitrification considerably. Therefore, quartz glass has to be processed carefully (separate from other types of glass).

Due to its optical properties, quartz glass is also used for sophisticated windows.

#### Sintered Glass and Crystallized Glass

Sintered glass is finely ground glass, sintered after being pressed, and thus, is easily formed into any desired shape. Appropriate powder selection allows adjusting the coefficient of thermal expansion to any value obtainable with glass.

Crystallized glasses are produced by adding crystallizing agents. After shaping at relatively

low temperatures as with standard glasses, further heating initiates crystallization. Materials produced show beneficial thermal (and usually also electrical) behavior compared to the starting material.

### **Ceramic Materials**

Ceramics are nonmetal inorganic materials (more than 30% crystalline) used in vacuum technology mainly for insulation purposes. This section provides an overview of their most prominent properties.

Burning of ceramics for vacuum applications must provide high tightness. Appropriate burning temperatures and durations have to be chosen. Often, the exhalation material is dried, preferably under vacuum. Ceramics are frequently glazed to provide proper tightness. Hard glazing (enamel) is applied to dried or preburnt pieces, and soft glazing to ready-burnt parts. Shrinking should always be expected when baking ceramics. Usually, ready-baked ceramic parts are cut with diamond saws and finished by grinding. Utilizing ceramics requires employment of appropriate custom molds.

Ceramics are categorized according to their chemical compositions:

- silicate ceramics;
- pure-oxide ceramics;
- special ceramics, for example, glass ceramics.

Their properties differ, thus determining individual fields of applications in vacuum technology.

Silicate ceramics are mixtures of inorganic crystalline substances with glassy fluxing or binding agents. Typical are porcelain (mass fractions approximately 6–8% undissolved quartz fragments, approximately 26% mullite, and approximately 66% feldspar silicic acid), steatite, forrestite, and ceramics with high  $\text{Al}_2\text{O}_3$  contents.

They do not show fixed melting points and most of their properties are similar to those of hard glasses. However, their thermal resistance is higher and mechanical as well as electrical properties are better. Baking temperatures are between 1300 °C and 1500 °C. Nearly any porcelain, steatite, and forrestite can be used up to approximately 1000 °C, and high- $\text{Al}_2\text{O}_3$  ceramics up to approximately 1350 °C.

Pure-oxide ceramics are made of crystalline aluminum-, beryllium-, zirconium-, or magnesium oxides. Their melting point is well defined. Baking temperatures are in the range of 1800–2000 °C. Vacuum technology mostly uses alumina ( $\text{Al}_2\text{O}_3$ ). In contrast to silicate ceramics, they are more temperature resistant (maximum working temperature 1800 °C) and show better resistance to thermal shocks. Additionally, their mechanical and electrical properties are better. Zirconium oxide is used in cases where required thermal resistance is even higher than provided by  $\text{Al}_2\text{O}_3$ . Due to its toxicity, beryllium oxide is used far less, and magnesium oxide is limited to lower temperature applications.

Glass ceramics are crystalline ceramics modified from the standard amorphous condition using crystallizing agents and heat treatment. The baked material can be machined with standard tools [3]. It is available under the brand name Macor and Corning no. 9658. The mean coefficient of linear thermal expansion is equal to expansion coefficients of standard technical soft glasses (see Table 16.3). Maximum operating temperature is 1000 °C. Macor can be metallized and is used for electrical leadthroughs, for electrical insulators, and vacuum-tight ceramic molds. Applications should be picked carefully because Macor softens at high temperatures.

Vacuum technology predominantly employs ceramics based mainly on  $\text{Al}_2\text{O}_3$  (amount of substance > 92%). This is due to the above-mentioned advantages of  $\text{Al}_2\text{O}_3$  ceramics and their low costs.  $\text{Al}_2\text{O}_3$  ceramics are used for heavy-duty thermal and electrical components (transmitting tubes), for vacuum vessels in accelerators, and electrical leadthroughs.  $\text{Al}_2\text{O}_3$  ceramics are particularly widespread as electrical insulators for high-bakeable electrical leadthroughs (more than 300 °C).

Sapphire is a special kind of monocrystalline  $\text{Al}_2\text{O}_3$ . Its radiation transparency (for infrared and UV) is high. Sapphire disks are used for bakeable windows.

### **Zeolite**

Zeolites are highly porous alumina silicates with alkali metals. Industrial applications use them as drying agents. Artificially produced zeolites show homogeneous porosity. In vacuum

technology, they are utilized for adsorbing water, oil vapors, and a number of other gases. Adsorption is increased by liquid-nitrogen cooling. Vice versa, zeolites can be regenerated nearly completely by heating.

### Plastics

Vacuum technology employs plastics mainly for sealing purposes. Plastics are made of more or less cross-linked organic macromolecules. Specific properties are created by additives, for example, softening agents for reducing chemical linkage forces between molecules, or fillers.

The main groups of plastics used in vacuum technology are elastomers, thermoplastics, and duroplastics.

The filamentous macromolecules in elastomers are cross-linked with more or less strong chemical bonds. Showing rubbery behavior, the materials are easily deformed by tension as well as compression and return to their initial shape after load relief thereby maintaining their total volume. This behavior makes the materials particularly suitable for seals. Typical examples are Perbunan (NBR), Viton, Kalrez, Chemraz, and silicone. Natural rubber is rarely used due to its sensitivity toward oil and wear [4,5].

Thermoplastics feature filamentous macromolecules as well. At room temperature, the materials show more or less moderate hardness. They can be soft gluey when dominated by short macromolecules, or when containing long macromolecules, tough-hard, elastic, or rubbery, depending on type and amount of softeners. At higher temperatures (approximately 100 °C), the mobility of macromolecules increases, making the materials ductile.

Duroplastics feature a network of spatially cross-linked macromolecules. They retain their hardness even at higher temperatures. Vacuum technology uses epoxy resins (e.g., araldite), thermally irreversible fillers made from resin solution and hardening agent. The constituents are stored separately and mixed just before joining. Cold-hardening grades operate at temperatures up to 100 °C, and warm-hardening types at up to approximately 180 °C. Their adhesion to metals, glass, and ceramics is high. Carefully processed parts (fully hardened, dried) show gas emissions comparable to those of Teflon or Hostafion.

### 3.2. Gas load sources

The most fundamental problems with vacuum systems are leaks and outgassing. Leaks can be categorised as either real leaks where gas enters the vacuum system from outside of the vessel or leaks from trapped voids which is in effect an internal leak. Trapped voids can contain gas that will continue to outgas for long periods reducing the ultimate vacuum that can be reached in a vessel. (Fig. 3.1).

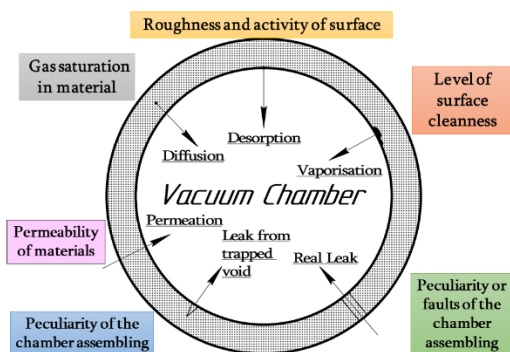


Figure 3.1 Gas load sources

Real leaks can be found with the aid of a helium leak detector whereas internal leaks from trapped voids may never be found. Outgassing can be minimised through careful selection of materials used within the vacuum space. The appendices have helpful tables to estimate outgassing rates. Outgassing may be in the form of desorption, diffusion or vaporisation. Permeation is not outgassing as the source of gas originates from outside of the vacuum space.

Examples commonly used substances in the accelerator systems that outgas,:

- Teflon, PVC, Ertalyte
- Viton, neoprene

- Copper, aluminium, stainless steel, brass, tantalum, rubidium, caesium, lithium, zinc
- Vacuum pump oil, vacuum greases, vacuum epoxies

These are just a few but it demonstrates that all materials will outgas at some point when the temperature and vacuum pressure reach their individual vapour pressure. Neither of the problems is

resolved by increasing the pumping speed (capacity) of the vacuum pump. There will be a point where the rate of gas entering the system will equalise with the pumping speed of the pump. The rate may vary depending on the vapour pressure of the substance outgassing and the temperature of that substance.

### 3.3. Absorption, diffusion, and outgassing

Vacuum chambers must be clean in order to reach the desired pressure as quickly as possible when they are pumped down. Typical contaminants include oil and grease on screws and seals, process reaction products or condensed vapours, particularly water that is adsorbed on the walls of the vessel. Consequently, it is necessary to ensure that the components are clean when installing vacuum equipment. All components attached in the vacuum chamber must be clean and grease-free.

All seals must also be installed dry. If high or ultra-high vacuum is to be generated, clean gloves must be worn during the assembly process.

Examples of common contaminants in accelerator vacuum systems

- Rotary pump oil
- Water
- Plasticisers from various plastics
- General airborne dust
- Machining oil
- Residual gases from stripper gases, venting gases, ion source gases
- Sample breakdown

#### Condensation and vaporisation

All substances can occur in a liquid, solid or gaseous state. Their aggregate status is a function of pressure and temperature. Liquids are transformed into their gaseous state through vaporisation, solids through sublimation. The separation of liquids or solids out of the gaseous phase is termed condensation. Since normal room air contains approximately 10g of water vapour per m<sup>3</sup>, condensed water vapour is always present on all surfaces.

Adsorption on surfaces is especially pronounced due to the strong polarity of the water molecules.

Natural fibres, in particular, such as paper, contain large quantities of water that escape during drying processes under vacuum. Cooled condensers are used to separate the water vapour in this connection. Even some metals (Cd, Zn, Mg) can vaporise in noticeable quantity at temperatures of several 100 °C. Consequently, use of these metals is avoided in plant construction.

#### Desorption

In addition to water, other substances (oil) can be adsorbed on surfaces (Figure 3.2). Substances can also diffuse out of the metal walls, which can be evidenced in the residual gas. In the case of particularly rigorous requirements, stainless steel vessels can be baked out under vacuum, thus driving the majority of the volatile components out of the metal walls.

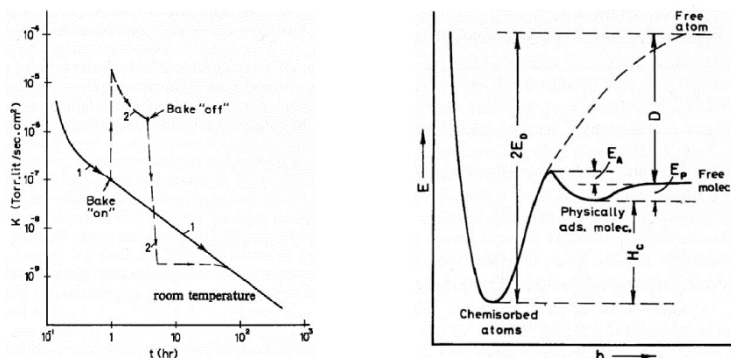


Figure 3.2 Desorption and adsorption curves

Gas molecules, (primarily water) are bound to the interior surfaces of the vacuum chamber through adsorption and absorption, and gradually desorb again under vacuum. The desorption rate of the metal and glass surfaces in the vacuum system produces a gas yield that is a function of time, however. A good approximation can be obtained by assuming that after a given point in time  $t > t_0$  to the reduction will occur on a

linear basis over time.  $t_0$  is typically assumed to be one hour.

### Diffusion with desorption

At operation below  $10^{-4}$  kPa, desorption of plastic surfaces, particularly the seals, assumes greater significance. Plastics mainly give off the gases that are dissolved in these plastics, which first must diffuse on the surface.

Following extended pump downtimes, desorption from plastics can therefore dominate the metal surfaces. Although the surface areas of the seals are relatively small; the decrease in desorption rate over time occurs more slowly in the case of metal surfaces. As an approximation it can be assumed that the reduction over time will occur at the square root of the time.

The gas produced from plastic surfaces can thus be described as:

Desorption from plastic material

$$Q_{diff} = q_{diff}A \cdot \sqrt{\frac{t_0}{t}} \quad (3.1)$$

Where  $A$  denotes the surface area of the plastics in the vacuum chamber and  $q_{diff}$  denotes the surface area-specific desorption rate for the respective plastic. At even lower pressures, similar effects also occur with metals, from which hydrogen and carbon escape in the form of CO and CO<sub>2</sub> and can be seen in the residual gas spectrum.

### Permeation and leaks

For a gas passing through small holes in a thin wall in the Knudsen Flow regime, the number of molecules that pass through a hole is proportional to the pressure of the gas and inversely proportional to its molecular weight (Table 3.3).

Table 3.3. Conversation table for leak rates

To Convert to Leakage Rate of:	Multiply Helium Leak Rate by:	
	Laminar Flow	Molecular Flow
Argon	0.88	0.316
Air	1.08	0.374
Nitrogen	1.12	0.374
Water vapor	2.09	0.469
Hydrogen	2.23	1.410

Seals, and even metal walls, can be penetrated by small gas molecules, such as helium, through diffusion. Since this process is not a function of time, it results in a sustained increase in the desired ultimate pressure. The permeation gas flow is proportional to the pressure gradient  $p_0/d$  ( $d$  = wall thickness,  $p_0$  = atmospheric pressure = ambient pressure) and to the permeation constants for the various materials  $k_{perm}$ .

Permeation

$$k_{perm} Q_{perm} = k_{perm} A \cdot \frac{p_0}{d} \quad (3.2)$$

Permeation (fig. 3.3) first manifests itself at pressures below  $10^{-6}$  kPa.

$Q_l$ , denotes the leakage rate, i.e. a gas flow that enters the vacuum system through leaks at a volume of  $V$ . The leakage rate is defined as the pressure rise  $\Delta p$  over time  $\Delta t$ :

Leakage rate

$$Q_l = \frac{(\Delta p V)}{\Delta t} \quad (3.3)$$

If a vessel is continuously pumped out at a volume flow rate  $S$ , an equilibrium pressure  $p_{gl}$  will be produced. Throughput is equal to the leakage rate  $Q_l = S \cdot p_{gl}$ . A system is considered to be adequately tight if the equilibrium pressure  $p_{gl}$  is approximately 10 % of the working pressure. If, for example, a working pressure of  $10^{-4}$  kPa is attained and the vacuum pump that is being used has a pumping speed of 100 L/s, the leakage rate should not be more than  $10^{-3}$  kPa L/s. This corresponds to a leak of approximately  $20.20 \mu\text{m}^2$  in size. Leakage rates  $Q_l$  of less than  $10^{-6}$  kPa L/s can usually be easily attained in clean stainless steel vessels. The ultimate pressure achievable after a given period of time  $t$  primarily depends upon all of the effects described above and upon the pumping speed of the vacuum pump. The prerequisite is naturally that the ultimate pressure will be high relative to the base pressure of the vacuum pump.

## Leaks

The source of leaks is as wide and varied as can be imagined. There is no such thing as a common leak however there are several types generally seen. The following lists types in rough order of prevalence:

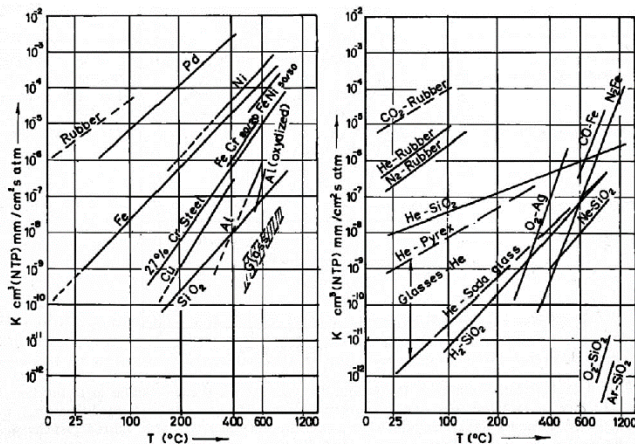


Figure 3.3 Permeation of Different Gases

of prevalence:

- Dirty seals – elastomer type seals with traces of dust, dirt and fibres on the surface
- Jarred seals – ill fitted flanges where the seal lays across the sealing surface
- Vacuum pumping tubes – where a fitting has been fitted without care and the pump cannot reach its full capability
- Distortion – over tightened or misaligned flanges and fittings that “lift” seals off the sealing surface
- Stress cracks – usually in places around flanges and fittings that have been incorrectly tightened

- Pressure dependant – mostly related to accelerator tubes that develop leaky seals allowing insulation gas to enter when the pressure is greater than atmospheric pressure.

## Bake-out

The following prerequisites must be satisfied in order to achieve lower pressures ( $<10^{-6}$  kPa):

- The base pressure of the vacuum pump should be a factor of 10 lower than the required ultimate pressure
- Stainless steel vacuum recipients and components must be used
- Metallic seals (CF flange connections) are required
- Leaks must be avoided and eliminated prior to activating the heater (use helium leak detectors!)
- Clean work is a must, i.e. all parts must be thoroughly cleaned and must be installed with grease-free gloves
- Pump and equipment must be baked out

Bake-out significantly increases desorption and diffusion rates, and this produces significantly shorter pumping times. Bake-out temperatures of up to  $300^{\circ}\text{C}$  are used. The instructions of the pump manufacturers relating to maximum bake-out temperatures and maximum permissible radiation levels in the pump flange must be observed.

Following installation the equipment is switched on, and after reaching a pressure of  $P < 10^{-3}$  kPa the heater is then switched on. During the heating process, all gauge heads must be operated and degassed at intervals of 10 hours. In the case of stainless steel vessels and the use of metallic seals, bake-out temperatures of  $120^{\circ}\text{C}$  and heating times of approximately 48 hours are sufficient for advancing into the pressure range of  $10^{-8}$  kPa. Bake-out should be continued until 100 times the expected ultimate pressure is attained. The heaters for the pump and vacuum chamber are then switched off. After cool-down, the desired ultimate pressure will probably be achieved. In connection with pressures  $P < 5 \times 10^{-8}$  kPa and large interior surface areas, it will be advantageous to use a titanium sublimation pump that pumps the hydrogen escaping from the metals at a high volume flow rate.

## Residual gas spectrum

When leaks have been solved in a vacuum system and poor vacuum persists than a residual gas analysis (RGA) measurement should be made to determine the composition of the gas load. This will give vital information on where the vacuum problem may be. Interpreting the information will be trial and error as users will have to think about all possible sources of gases (and outgassing) that may be present. Also, relative ratios of gases should be considered to make sense of the measurement. Care should be taken especially if making a measurement near a source such as a cryopump. Some gases that have been trapped on the cryopump may be liberating from the cold surface and will make

up a part of the gas spectrum. Other places to take care are near the accelerator tubes and ion sources.

If developing an ultra-high vacuum system, it is important to know all sources of gas otherwise moving lower than  $1 \times 10^{-6}$  Pa will be an unnecessary challenge. For all other systems it is nice to know but not essential unless residual gases affect ion beam measurements.

### 3.4. Elements of vacuum systems

When designing or operating a vacuum system, it is critical to understand the function of the vacuum pumps. We will review the most common types of vacuum pumps, their principles of operation and where in the system they are used. In the coming months we will focus on each of these pumps in more detail.

Vacuum pumps are categorized by their operating pressure range and as such are classified as: primary pumps, booster pumps or secondary pumps. Within each pressure range are several different pump types, each employing a different technology, and each with some unique advantages in regard to pressure capacity, flow rate, cost and maintenance requirements.

Regardless of their design, the basic principle of operation is the same. The vacuum pump functions by removing the molecules of air and other gases from the vacuum chamber (or from the outlet side of a higher vacuum pump if connected in series). While the pressure in the chamber is reduced, removing additional molecules becomes exponentially harder to remove. As a result, an industrial vacuum system (Figure 3.4) must be able to operate over a portion of an extraordinarily large pressure range, typically varying from 1 to  $10^{-6}$  Torr of pressure. In research and scientific applications this is extended to  $10^{-9}$  Torr or lower. In order to accomplish this, several different styles of pumps are used in a typical system, each covering a portion of the pressure range, and operating in series at times.

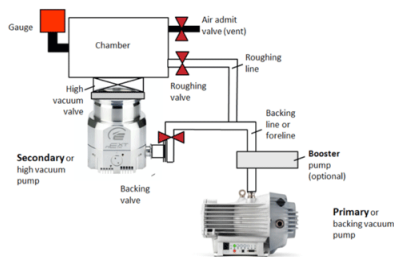


Figure 3.4 – Typical industrial vacuum system

Vacuum systems are placed into the following broad-based grouping of pressure ranges:

- Rough/Low Vacuum:  $>$  Atmosphere to 1 Torr
- Medium Vacuum: 1 Torr to  $10^{-3}$  Torr
- High Vacuum:  $10^{-3}$  Torr to  $10^{-7}$  Torr
- Ultra-High Vacuum:  $10^{-7}$  Torr to  $10^{-11}$  Torr
- Extreme High Vacuum:  $<$   $10^{-11}$  Torr

The different types of pumps for these vacuum ranges can then be divided into the following:

- Primary (Backing) Pumps: Rough and low vacuum pressure ranges.
- Booster Pumps: Rough and low vacuum pressure ranges.
- Secondary (High Vacuum) Pumps: High, very high and ultra-high vacuum pressure ranges.

### 3.5. Throughput capacity of vacuum systems elements

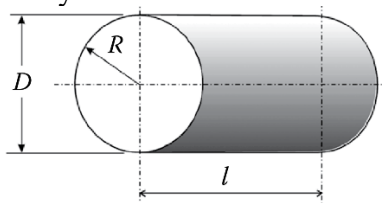
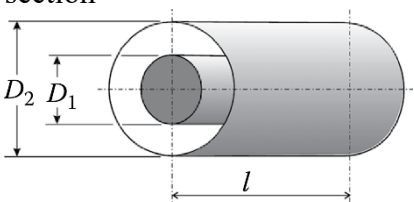
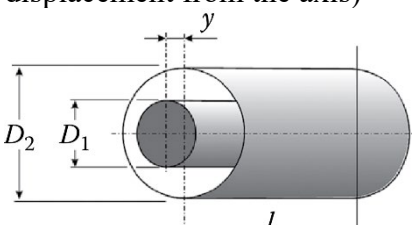
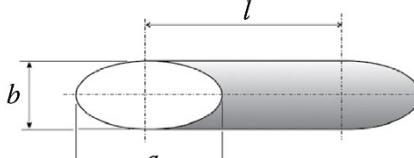
The viscous laminar flow conditions are satisfied when Reynolds number  $Re < 1100$  and inverse Knudsen number  $Kr = D/L > 110$ . The flow is characteristic with parallel streamlines, a parabolic velocity profile across the duct cross section, and zero velocity at the duct wall. This velocity profile is invariable along the entire tube length, which is

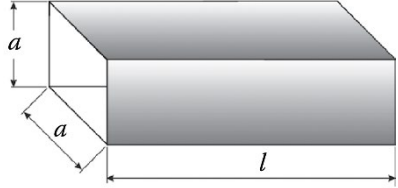
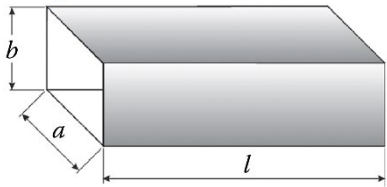
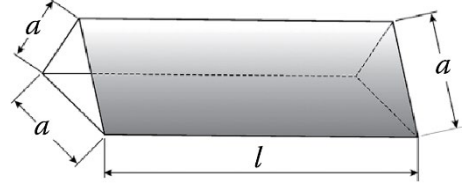
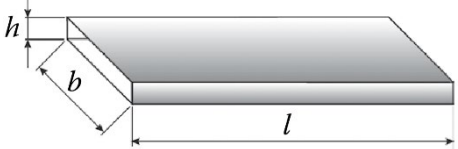
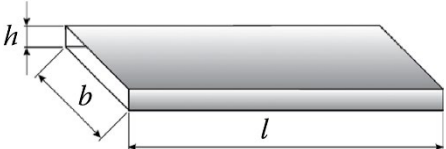
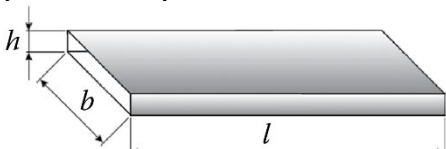
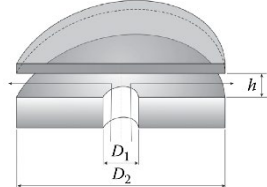
maintained in long ducts. The statement on well-developed stream parallel lines excludes turbulent gas behavior. Invariable streamlines also indicate that the gas stream is considered to be incompressible (isochoric). This means that the gas mass density is taken as constant. Gases are generally compressible, but they may behave as incompressible at low flow velocities when a half of the square Mach number is significantly smaller than one ( $M_n^2/2 \ll 1$ ). Usually, the  $M_n/3$  value is taken as a threshold. The Mach number is the ratio of gas flow velocity  $v$  and speed of sound  $u_s$  ( $M_n = v/u_s$ ). For example, speed of sound is about  $u_s = 340.4$  m/s in air at a sea level and  $15^\circ\text{C}$ . This value also depends on the temperature and humidity, and thus local gas composition. The Mach

number is named after Czech/Austrian physicist and philosopher Ernst Waldfried Josef Václav Mach. In the viscous laminar regime, a gas flowing in a cylindrical tube can be divided into coaxial gas shells with the thickness of a mean free path. Each gas layer shell is characteristic with its own velocity  $v$ . The considered cylindrical gas shell with thickness  $dr$  accelerates the outer adjacent layer but slows down the interfacing inner layer. Then, these two frictional forces and the force arising from the overpressure determine the gas flow velocity. Indeed a model considering the two frictional forces acting against each other can be found in different publications.<sup>236</sup> However, the gas flow velocity can also be determined using a simplified model that is presented below. Both the models yield the same equation, because each of them is based on simplified conditions but at different deduction stages. As given above, the presented theory lies on the presumption of parallel streamlines along the entire length of a straight tube and small flow velocity to avoid turbulence in the tube. The condition of the parallel streamlines is satisfied in long tubes where the laminar flow is fully developed. The force  $f_0 = Ar(p_1 - p_2)$  exerting on the axial cross section  $A_r$  is induced by pressure difference  $(p_1 - p_2)$ .

Laminar conductance (in SI units) of vacuum components with different geometrical configurations is reviewed in Table 3.4.

Table 3.4 Laminar Conductance of Long Ducts: Analytical Equations for Different Cross-Sectional Shapes— All in SI Units

Vacuum Component	Laminar Conductance
<p>1. Cylindrical tube</p> 	$F_l = \frac{\pi R^4}{8\eta_d l} p_{av} = \frac{\pi D^4}{128\eta_d l} p_{av} \quad [m^3/s]$ <p>For air 20 °C</p> $F_l = 1.35 \times 10^3 \frac{D^4}{l} p_{av} \quad [m^3/s; m; Pa]$
<p>2. Tube with an annular cross section</p> 	$F_l = \frac{\pi}{128\eta_d l} \left[ D_2^4 - D_1^4 - \frac{(D_2^2 - D_1^2)^2}{\ln \frac{D_2}{D_1}} \right] p_{av} \quad [m^3/s]$ <p>For air 20 °C</p> $F_l = \frac{1349}{l} \left[ D_2^4 - D_1^4 - \frac{(D_2^2 - D_1^2)^2}{\ln \frac{D_2}{D_1}} \right] p_{av} \quad [m^3/s]$
<p>3. Tube with an eccentric annular cross section (y - eccentric displacement from the axis)</p> 	$F_l = \frac{\pi D_1 (D_2 - D_1)^3}{96 \eta_d l} \left[ 1 + \frac{6y^2}{(D_2 - D_1)^2} \right] p_{av} \quad [m^3/s]$ <p>For air 20 °C</p> $F_l = 1798 \frac{D_1 (D_2 - D_1)^3}{l} \left[ 1 + \frac{6y^2}{(D_2 - D_1)^2} \right] p_{av} \quad [m^3/s]$
<p>4. Duct with an elliptical cross section</p> 	$F_l = \frac{\pi}{96\eta_d l} \frac{a^3 b^3}{a^2 + b^2} p_{av} \quad [m^3/s]$ <p>For air 20 °C</p> $F_l = \frac{2697}{l} \frac{a^3 b^3}{a^2 + b^2} p_{av} \quad [m^3/s]$

<p>5. Duct with a square cross section</p> 	$F_l = 3.52 \times 10^{-2} \frac{a^4}{\eta_d l} p_{av} \left[ m^3/s \right]$ <p>For air 20 °C</p> $F_l = 1934 \frac{a^4}{l} p_{av} \left[ m^3/s \right]$
<p>6. Duct with a rectangular cross section; for K2 see Figure 3.5</p> 	$F_l = \frac{1}{12\eta_d} K_2 \frac{a^2 b^2}{l} p_{av} \left[ m^3/s \right]$ <p>For air 20 °C</p> $F_l = 4578.75 K_2 \frac{a^2 b^2}{l} p_{av} \left[ m^3/s \right]$
<p>7. Duct with the cross section of an equilateral triangle</p> 	$F_l = \frac{\sqrt{3}}{320} \frac{a^4}{\eta_d l} p_{av} \left[ m^3/s \right]$ <p>For air 20 °C</p> $F_l = 297.4 \frac{a^4}{l} p_{av} \left[ m^3/s \right]$
<p>8. Narrow slit with a rectangular cross section <math>h \ll (100h &lt; b)</math>; insignificant pressure drop</p> 	$F_l = \frac{1}{12\eta_d} \frac{h^3 b}{l} p_{av} \left[ m^3/s \right]$ <p>For air 20 °C</p> $F_l = 4578.75 \frac{h^3 b}{l} p_{av} \left[ m^3/s \right]$
<p>9. Adapted for rectangular tube <math>h \times b</math> where <math>b \geq h</math>; insignificant pressure drop</p> 	$F_l = \frac{1}{12\eta_d} \frac{h^3 b}{l} p_{av} \left[ 1 - \frac{192h}{\pi^5 b} \sum_{n=1,3,\dots}^{\infty} \frac{1}{n^5} \tanh h \left( \frac{\pi n b}{2 h} \right) \right] \left[ m^3/s \right]$ <p>in <math>m^3/s</math> or simplified equation with error ~3%</p> $F_l = \frac{1}{12\eta_d} \frac{h^3 b^3}{l(b^2 + h^2 + 0.371bh)} p_{av} \left[ m^3/s \right]$
<p>10. Narrow slit with rectangular cross section (<math>h \ll b</math>); significant pressure drop</p> 	$F_l = \frac{1}{24\eta_d} \frac{h^3 b}{l} p_{av} \left[ m^3/s \right]$ <p>For air 20 °C</p> $F_l = 2289.38 \frac{h^3 b}{l} p_{av} \left[ m^3/s \right]$
<p>11. Ring slit with radial gas flow <math>(D_2 - D_1)/D_1 \ll 1</math></p> 	$F_l = \frac{\pi}{6} \frac{h^3}{\eta_d \ln \frac{D_2}{D_1}} p_{av} \left[ m^3/s \right]$ <p>For air 20 °C</p> $F_l = 2.88 \times 10^4 \frac{h^3}{\ln \frac{D_2}{D_1}} p_{av} \left[ m^3/s \right]$

Symbols for dimensions are obvious from the attached drawings:  $p_{av} = (p_1 + p_2)/2$  is the

average pressure in Pa; R, radius, D, diameter, l, length of a duct in m, and  $\eta_d$  is the dynamic viscosity at low-vacuum conditions; note for air at 20 °C,  $\eta_d = 1.82 \times 10^{-5} \text{ Pa s}$ .

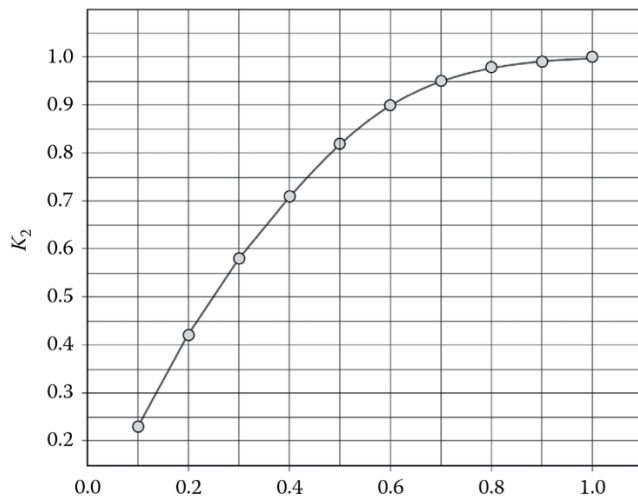


Figure 3.5 Correction factor K2 plotted against the aspect ratio a/b

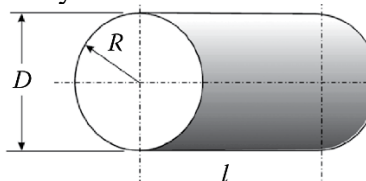
### Molecular Conductance of Long Ducts with Different Shapes by Knudsen Formula

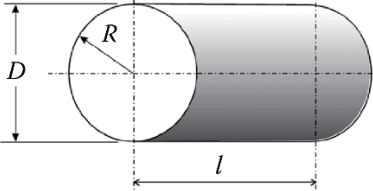
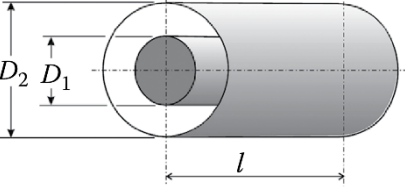
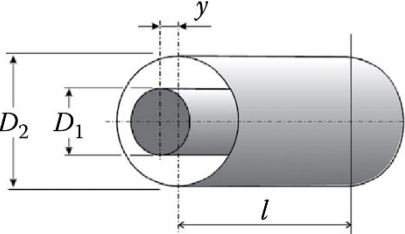
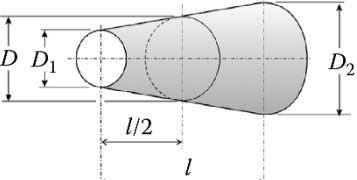
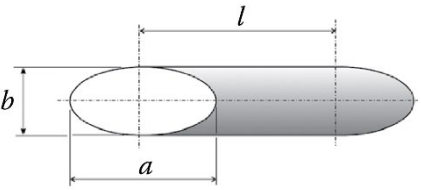
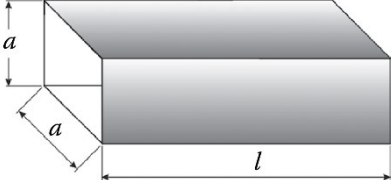
Application of the Knudsen's formula to other geometrical configurations than that of circular tubes gives error data. Thus, many equations for specific geometries have been derived and correlated with experimental data, and introduced in many books related to vacuum technology. We also present such equations but also offer the theory yielding to the Knudsen formula (Equation 7.115), because it leads to (1) Equations 7.118 and 7.119, which are generally accepted for long ducts with circular cross sections; (2) mathematical formats for

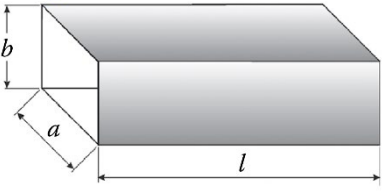
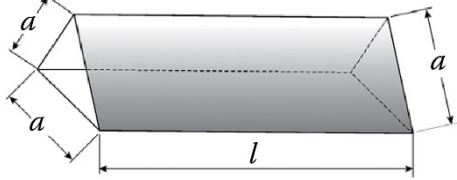
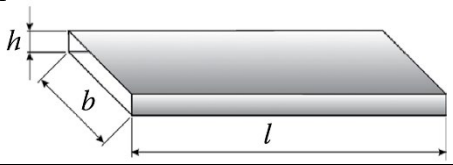
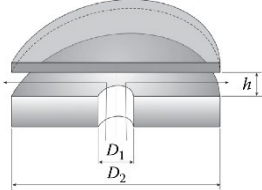
calculation of molecular conductance can be found in different books related to vacuum technology; (3) equations following from Knudsen formula have been used in approximate calculations for long noncircular ducts corrected by shape factors; (4) origin of equations can be documented, and (5) attentiveness of approximation is thus provided.

- Long duct with a rectangular cross section: Despite the knowledge of inaccuracy have been used to estimate molecular conductance of ducts with different cross-sectional geometries. Thus, for a duct with a constant rectangular cross section of  $A = a \times b$  along the tube length and perimeter of  $P_r = 2(a+b)$ , where  $a \geq b$ , we can obtain molecular conductance by simple substitutions of the respective area  $A$  and perimeter  $P_r$  into.
- Long duct with a square cross section: For a duct with square cross section, that is, when the rectangle sides are equal ( $a = b$ )
- Long ducts with elliptical cross sections: The molecular conductance of a duct with a uniform elliptical cross section along its length can also be derived from the fundamental Knudsen formula.
- Long ducts with an annular cross section. The molecular conductance of a tube with an annular cross section formed by two coaxial cylinders with diameters  $D_2 > D_1$  can be deduced from the cross-sectional area  $A = \frac{\pi(D_2^2 - D_1^2)}{4}$ , corresponding to equivalent perimeter  $P_r = \pi(D_2 + D_1)$  of the wetted surfaces  $P_r, l$ , and Knudsen formula.
- Long duct with an eccentric annulus cross section ( $y$  – displacement from the axis of the outer cylinder).

Table 3.5 Molecular Conductance for Long Ducts Based on Knudsen Formula Corrected by Shape Factors

Vacuum Component	Laminar Conductance
1. Cylindrical tube 	$F_m = \frac{\pi}{2} \frac{1}{\epsilon'} \frac{R^3}{l} p_{av} = \frac{\pi}{16} \frac{1}{\epsilon'} \frac{D^3}{l} p_{av} \quad [m^3/s]$ or $F_m = \frac{2\pi v_a R^3}{3} \frac{1}{l} = \left(\frac{8R}{3l}\right) \frac{v_a}{4} \pi R^2 \quad [m^3/s]$ For air 20 °C $F_m = 968.99 \frac{R^3}{l} = 121.12 \frac{D^3}{l} \quad [m^3/s]$
These are correct equations for long ducts though deduced from Knudsen	

formula.	
<p>2. Duct with circular cross section</p>  <p>derived for <math>p_1 \gg p_2</math>.</p>	$F_m = \frac{2\pi v_a R^3}{3} \frac{p_{av}}{l} \frac{p_1}{p_1 - p_2} \ln \frac{p_1}{p_2} \approx \frac{\pi v_a R^3}{3} \frac{p_1}{l} \ln \frac{p_1}{p_2} \quad [m^3/s]$ <p>For air 20 °C <math>v_a = 462.66 \text{ m/s}</math></p> $F_m \approx 484.5 \frac{R^3}{l} \ln \frac{p_1}{p_2} \quad [m^3/s]$
<p>3. Duct with annular cross section; for <math>K_5</math> see Figure 3.6.</p> 	$F_m = K_5 \frac{\pi v_a (D_2 - D_1)^2 (D_2 + D_1)}{12} \frac{p_1}{l} \ln \frac{p_1}{p_2} \quad [m^3/s]$ <p>or</p> $F_m = K_5 \left( \frac{T}{M_a} \right)^{1/2} \frac{(D_2 - D_1)^2 (D_2 + D_1)}{l} \frac{p_1}{p_2} \quad [m^3/s]$ <p>For air 20 °C</p> $F_m = 121.12 K_5 \frac{(D_2 - D_1)^2 (D_2 + D_1)}{l} \frac{p_1}{p_2} \quad [m^3/s]$
<p>4. Duct with eccentrically aligned tubes; for <math>K_6</math> see Figure 3.7.</p> 	$F_m = 14.3 K_6 \frac{D_2^3 \left(1 - \frac{D_1^2}{D_2^2}\right)^2}{l} \left( \frac{T}{M_a} \right)^{1/2} \frac{p_1}{p_2} \quad [m^3/s]$ <p>For air 20 °C</p> $F_m = 45.4 K_6 \frac{D_2^3 \left(1 - \frac{D_1^2}{D_2^2}\right)^2}{l} \frac{p_1}{p_2} \quad [m^3/s]$
<p>5. Tapered duct with circular cross sections.</p> 	$F_m = \frac{\pi v_a D_1^2 D_2^2}{12} \frac{p_1}{Dl} \ln \frac{p_1}{p_2} \quad [m^3/s]$ <p>For air 20 °C</p> $F_m = 121.12 \frac{D_1^2 D_2^2}{Dl} \frac{p_1}{p_2} \ln \frac{p_1}{p_2} \quad [m^3/s]$
<p>6. Duct with an elliptical cross section</p> 	$F_m = \frac{\sqrt{2}\pi}{12} v_a \frac{a^2 b^2}{l(a^2 + b^2)^{1/2}} \frac{p_1}{p_2} \ln \frac{p_1}{p_2} \quad [m^3/s]$ <p>or</p> $F_m = 53.84 \frac{a^2 b^2}{l(a^2 + b^2)^{1/2}} \left( \frac{T}{M_a} \right)^{1/2} \frac{p_1}{p_2} \ln \frac{p_1}{p_2} \quad [m^3/s]$ <p>For air 20 °C</p> $F_m = 171.18 \frac{a^2 b^2}{l(a^2 + b^2)^{1/2}} \frac{p_1}{p_2} \ln \frac{p_1}{p_2} \quad [m^3/s]$
<p>7. Duct with square cross section; correction factor <math>K_2 = 1.115</math>. For <math>K_3</math> see Figure 3.8</p> 	$F_m = K_3 \frac{v_a a^3}{3} \frac{p_1}{l} \ln \frac{p_1}{p_2} = 54.08 K_3 \left( \frac{T}{M_a} \right)^{1/2} \frac{a^3}{l} \frac{p_1}{p_2} \ln \frac{p_1}{p_2} \quad [m^3/s]$ <p>For air 20 °C</p> $F_m = 171.95 \frac{a^3}{l} \frac{p_1}{p_2} \ln \frac{p_1}{p_2} \quad [m^3/s]$

<p>8. Duct with a rectangular cross section for <math>l \gg a</math> and <math>l \gg b</math>;</p> 	$F_m = K_3 \frac{2v_a}{3} \frac{a^2 b^2}{l(a+b)} = 97K_3 \left(\frac{T}{M_a}\right)^{1/2} \frac{a^2 b^2}{l(a+b)} \left[ m^3/s \right]$ <p>For air 20 °C</p> $F_m = 308.44 \frac{a^2 b^2}{l(a+b)} = \left[ m^3/s \right]$
<p>9. Duct with an equilateral triangular cross section;</p> 	$F_m = K_7 \frac{v_a a^3}{12 l} = 15.04 \left(\frac{T}{M_a}\right)^{1/2} \frac{a^3}{l} \left[ m^3/s \right]$ <p style="text-align: center;"><math>K_7 = 1.24</math></p> <p>For air 20 °C</p> $F_m = 47.80 \frac{a^3}{l} = \left[ m^3/s \right]$
<p>10. Narrow slit with rectangular cross section (<math>h \ll b</math>); insignificant pressure drop; for <math>K_4</math> see Figure 3.9.</p> 	$F_m = \frac{2}{3} K_4 v_a \frac{bh^2}{l} = 97K_4 \left(\frac{T}{M_a}\right)^{1/2} \frac{bh^2}{l} \left[ m^3/s \right]$ <p>For air 20 °C</p> $F_m = 308.44 \frac{bh^2}{l} = \left[ m^3/s \right]$
<p>11. Narrow slit with rectangular cross section (<math>h \ll b</math>); significant pressure drop.</p> 	$F_m = \frac{2v_a bh^2}{3 l} \frac{p_{av}}{p_1 - p_2} \ln \frac{p_1}{p_2} \approx \frac{v_a bh^2}{3 l} \ln \frac{p_1}{p_2} \left[ m^3/s \right]$ <p>For air 20 °C</p> $F_m = 154.22 \frac{bh^2}{l} \ln \frac{p_1}{p_2} = \left[ m^3/s \right]$
<p>11. Ring slit with radial gas flow (<math>(D_2 - D_1)/D_1 \ll 1</math>)</p> 	$F_m = 114 \left( \frac{1}{2} + \ln \frac{D_2 - D_1}{2h} \right) \left( \frac{D_2 + D_1}{D_2 - D_1} h^2 \right) \left( \frac{T}{M_a} \right)^{1/2} \left[ m^3/s \right]$ <p>For air 20 °C</p> $F_m = 362.5 \left( \frac{1}{2} + \ln \frac{D_2 - D_1}{2h} \right) \left( \frac{D_2 + D_1}{D_2 - D_1} h^2 \right) \left[ m^3/s \right]$ <p>Accuracy is higher when inequalities <math>\frac{D_2 + D_1}{D_2 - D_1} \gg 1</math> and <math>\frac{D_2 - D_1}{h} \gg 1</math> are greater.</p>

For symbols see the attached drawings:  $p_{av} = (p1 + p2)/2$  is the average pressure (although  $p_{av}$  may be seen in some equations, the molecular conductance is pressure-independent -  $p_{av}$  is eliminated by  $p_{av}$  comprised in  $\epsilon'$ ;  $R$  is the radius,  $D$  is the diameter,  $l$  is the length; all the parameters are in the SI unit system. Although the equations usually overestimate the conductance values of ducts, they can be found in many books related to vacuum technology; see equations recommended for long ducts with arbitrary cross-sectional shapes in Table 3.6.

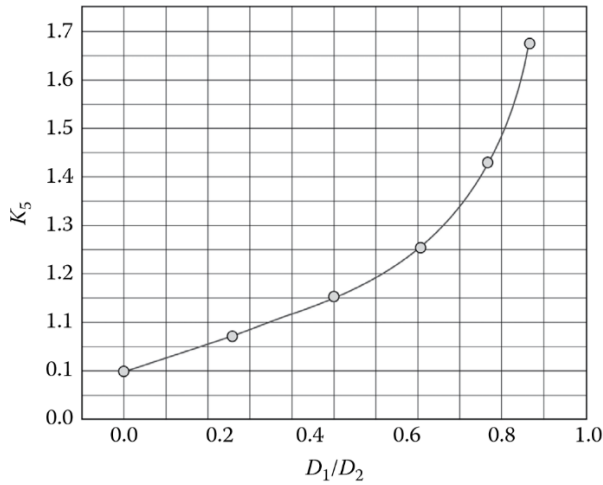


Figure 3.6 Correction factor  $K_6$

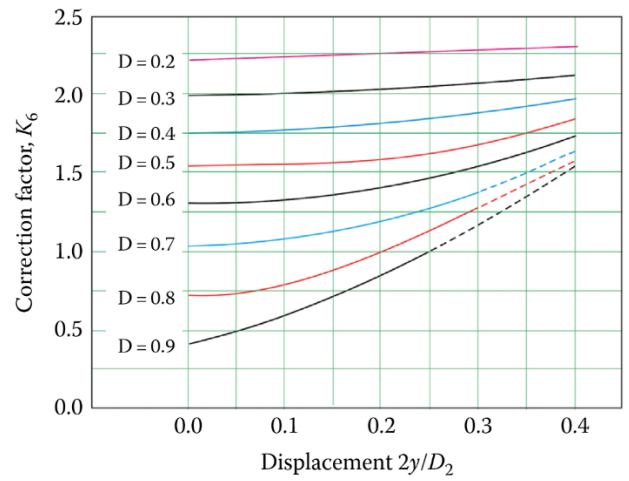


Figure 3.7 Correction factor  $K_5$  plotted against  $D_1/D_2$  for annulus cross section

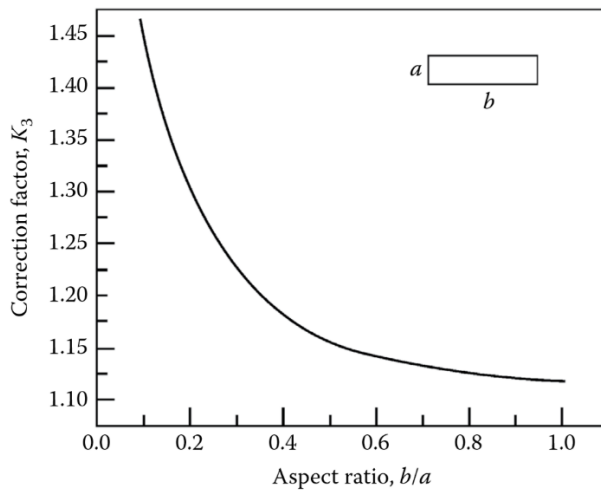


Figure 3.8 Correction factor  $K_3$  plotted against aspect ratio,  $b/a$ , for rectangular cross sections

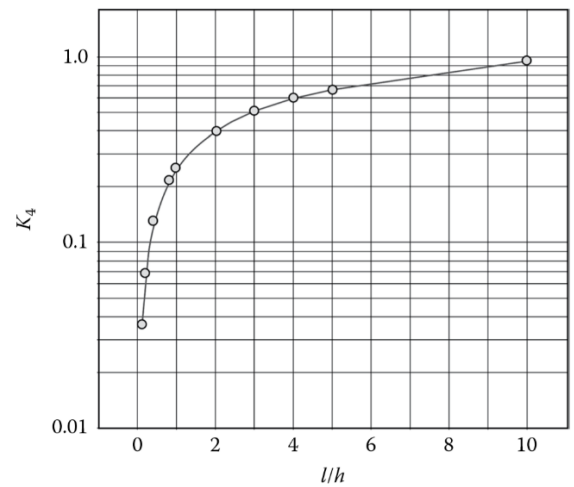
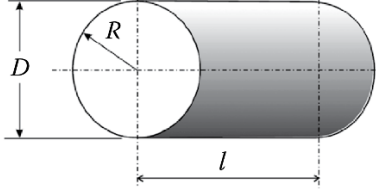
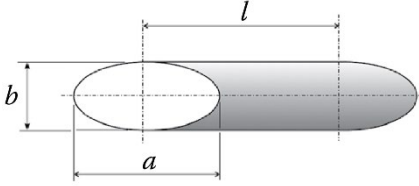
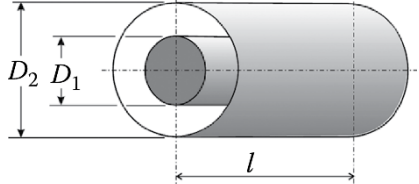
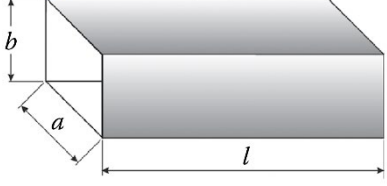
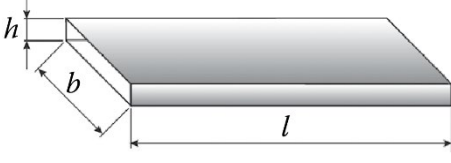


Figure 3.9 Clausing's correction factor  $K_4$ , plotted as a function of  $l/h$  for narrow slits

### Molecular Conductance for Long Ducts by Universal Smoluchowski Formula

At derivations of molecular conductance of long molecular ducts above, Knudsen considered constant flow velocities for the entire cross sections of tubes. Knudsen approach yields analytical equation for the molecular conductivity of the long ducts that is applicable to the tubes with circular cross sections. In other cases, it may lead to significant errors. However, Smoluchowski introduced another approach that leads to an analytical equation applicable to long ducts with arbitrary cross sections. Rigorous treatment of the illustrated problems was also performed by Clausing, who deduced and numerically solved an integral equation for transmission probabilities of vacuum ducts with circular cross sections. Equivalent treatment employing a variation method was applied by DeMarcus (see text and references later). The models based on transmission probability indeed introduce better understanding of the gas flow at molecular flow condition. If a tube bridges two large volume chambers, then molecules randomly enter the tube orifices. As soon as molecules are inside the duct, they are guided by the tube walls. The number of molecules that succeed to pass from one tube end to the other is expressed by transmission probability of the tube, which is affected by the tube geometry. Thus, the tube conductance can be determined from intrinsic conductance of the tube orifice and transmission probability as illustrated on gas flow via apertures and gas flow via short tubes. Based on the intrinsic conductance of a tube orifice  $F_0$  (calculated later as  $F_{ef}$ ) and transmission probability  $\alpha$ .

Table 3.6 Molecular Conductance for Long Ducts for Arbitrary Shapes: Conductance of Long Vacuum Ducts with Constant Circular, Coaxial Annular, Elliptical, Rectangular, and Triangular Cross Sections

<p>1. Circular cross section, long tube</p> <p>Area</p> $A = \pi R^2 = \frac{\pi}{4} D^2$	 <p>Probability</p> $\alpha = \frac{8R}{3l} = \frac{4D}{3l}$ <p>Conductance</p> $F = F_{ef}\alpha = \frac{2\pi}{3} v_a \frac{R^3}{l}$
<p>2. Elliptical cross section, long tube; a and b are the major and minor axes of an ellipse</p> <p>Area</p> $A = \frac{\pi}{4} ab$	 <p>Probability</p> $\alpha = \frac{4b}{3l}$ <p>Conductance</p> $F = \frac{\pi}{12} v_a \frac{ab^2}{l}$
<p>3. Long annulus tube; Diameters <math>D_2 &gt; D_1</math>, <math>l - \text{length}</math>, <math>l \gg D_2</math></p> <p>Area</p> $A = \frac{\pi}{4} (D_2^2 - D_1^2) = \frac{\pi}{4} D_2^2 \left(1 - \frac{D_1^2}{D_2^2}\right)$ <p>For the <math>f(d)</math> values see plot in Figure 3.10</p>	 <p>Probability</p> $\alpha = \frac{D_2}{l} f(d)$ <p>Conductance</p> $F = \frac{v_a \pi D_2^3}{16 l} \left(1 - \frac{D_1^2}{D_2^2}\right) f(d)$ $f(d) = \frac{1}{1-d^2} \left[ \frac{3}{4} - d + d^2 - \frac{2}{3} (1+d^2) E(d) + \frac{2}{3} (1-d^2) K(d) \right]$
<p>4. Rectangular cross section, long tube; <math>l \gg a</math>; <math>l \gg b</math></p> <p>Area</p> $A = ab$	 <p>Probability</p> $\alpha = \frac{a}{l} f(\delta)$ $\delta = \frac{a}{b}$ <p>Conductance</p> $F = v_a \frac{a^2 b}{4l} f(\delta)$ $f(\delta) = \frac{1}{\delta} \ln(\delta + \sqrt{1 + \delta^2}) + \ln\left(\frac{\delta + \sqrt{1 + \delta^2}}{\delta}\right) + \frac{1}{3\delta^2} [1 + \delta^3 - (1 + \delta)^{3/2}]$
<p>5. Narrow slit, long tube; <math>l \gg a</math>, <math>l \gg b</math>; <math>a \gg b</math>, <math>\delta = a/b</math></p> <p>Area</p> $A = hb$	 <p>Probability</p> $\alpha = \frac{h}{2l} \left(1 + 2 \ln 2 \frac{b}{h}\right)$ <p>Conductance</p> $F = \frac{v_a h^2 b}{4 l} \left(1 + 2 \ln 2 \frac{b}{h}\right)$

6. Equilateral triangular cross section, long tube;  $a$  is the length of sides,  $l$  is the duct length,  $l \gg a$

Area

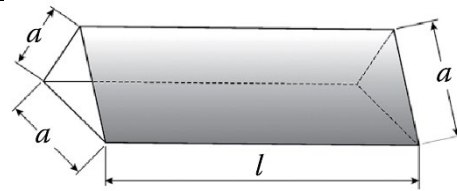
$$A = a^2 \frac{\sqrt{3}}{4} = 0.433a^2$$

Probability

$$\alpha = \sqrt{3} \ln 3 \frac{a}{2l} = 0.952 \frac{a}{l}$$

Conductance

$$F = v_a \frac{3 \ln 3 a^3}{32 l}$$



Equations are constructed on the principle of transmission probabilities and intrinsic orifice conductance; conductance is calculated as the product  $v_a/4$ , area  $A$ , and transmission probability,  $\alpha$ .

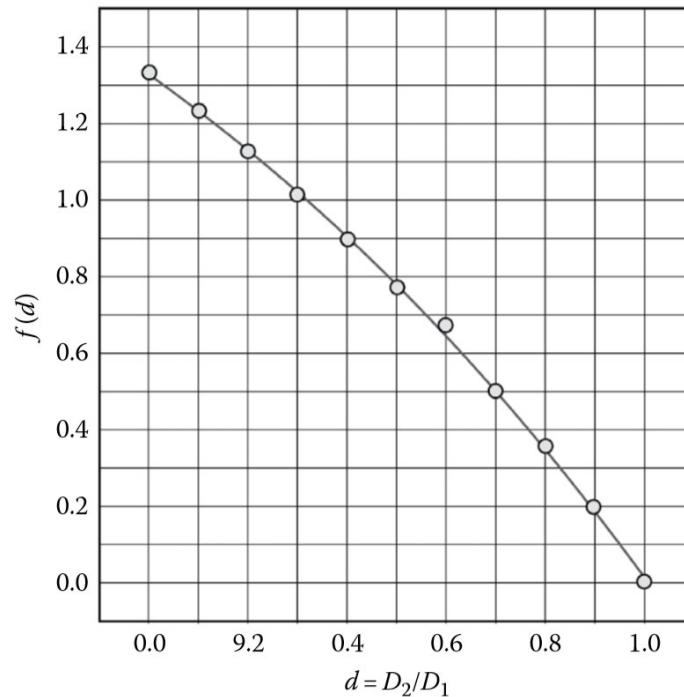


Figure 3.10 Correction factor  $f(d)$

1. R. E. Honig and H. O. Hook, "Vapor Pressure Data For Some Common Gases" RCA Review 21 , 360 (1960).
2. Ishimaru, H. (1990) Developments and applications for all-aluminum ally vacuum systems. MRS Bull., XV (7), 23–31.
3. Mog. D. (1976) Machinable glass-ceramic: a new material for vacuum equipment. Vacuum, 26, 25 ff.
4. Chernatony, L. (1977) Recent advances in elastomer technology for UHV applications. Vacuum, 27, 605-609.
5. Peacock, R.M. (1980) Practical selection of elastomer materials. J. Vac. Sci. Technol., 17, 330-336.

## 4. CLEANING

Experience shows that in order to achieve all but the most modest levels of vacuum it is necessary to clean vacuum vessels and components in some way. This is because as far as vacuum is concerned, the world is a dirty place! In general, vessels and components will have been machined, worked in some way or another, or handled. Such processes may use greases or oils which have high outgassing rates or vapour pressures and which will remain on or in the surface. Marking pens and adhesive tapes leave residues on surfaces which can also enhance outgassing. Water, solvents and other liquids can remain embedded in cracks or pores in a surface and can outgas over long periods. All such contamination can limit the base pressures attainable in a system.

In general terms as far as vacuum is concerned, we define contamination as anything which

- prevents the vacuum system from reaching the desired base pressure
- introduces an unwanted or detrimental species into the residual gas
- modifies the surface properties of all or part of the vacuum system in an undesired way

Thus, for example, a pool of liquid mercury in a vacuum system will, at room temperature, limit the base pressure to about  $2 \times 10^{-3}$  mbar, its vapour pressure. If the system were required to operate at, say, 10<sup>-5</sup> mbar, the mercury would be a contaminant.

In an electron storage ring, the cross section for electrons scattering off a residual gas molecule increases as the square of the atomic number, *Z*, of the scattering species. Thus, for long beam lifetimes (i.e. low electron losses), it is important to minimise the partial pressures of high-*Z* species which are contaminants in the residual atmosphere.

In a system operating at 10<sup>-8</sup> mbar, the partial pressure of hydrocarbons might be 10<sup>-11</sup> mbar.

These hydrocarbon molecules striking a mirror surface can crack or polymerise when irradiated by electrons or photons, leading to maybe graphite-like overlayers or to insulating layers. A complete monolayer might form in about 12 days, assuming that 1 in every 10 molecules impinging on the surface is cracked and sticks. The optical properties of the mirror are therefore altered by the surface becoming contaminated.

Hence there is a necessity to clean to remove actual or potential contaminants. We will define a suitable cleaning process as one which results in the residual vacuum being suitable for the task. This definition is heavily influenced by the observation that most people who use vacuum are not interested in vacuum as such but are interested in an industrial process (semiconductor chip production or metal refining for example) or a scientific experiment (such as studying chemical catalytic reactions on a surface) or operating a machine (maybe a particle accelerator). What they are interested in is having a defined, controlled atmosphere and vacuum is just the simplest way of achieving this.

### Choosing a cleaning process

There is no one cleaning process which is “right” for all vacuum systems, vessels or components.

Some of the things which will need to be taken into account are as follows

- the level of vacuum required (rough, high, UHV, etc)
- if there is a particular performance requirement (e.g. low desorption)
- whether there is a particular contaminant (e.g. hydrocarbons) whose partial pressure must be minimised
- what materials the items are made from
- how the items are constructed
- safety
- cost

Once these have been considered, and we will look at some of these in more detail below, then one can begin to choose a cleaning agent and the necessary processes to achieve the desired result.

It is important to realise that there are very many different “recipes” in the literature and in

the folklore of vacuum. Advocates of a particular process or procedure will defend their choice with an almost religious fervour. Generally, this is because the procedure “works” for them, i.e. it meets their requirements. Often this procedure will not have been tested rigorously against other possible procedures which might be equally good if not better (in some sense) and will therefore in no way have been optimised. This is not necessarily a problem. It often simply means that the processes being used may not be as economical or convenient as they might be. Whether this is important or not depends on the individual situation.

In this article, we will look briefly at both chemical and physical cleaning processes. There are, however, some general points which should be taken into account when deciding what to use. Some of these are as follows.

- Some “cleaning” processes which are often used are applied more for cosmetic purposes to make vacuum chambers look clean by producing mirror finish surfaces and so on. Whether from a vacuum point of view they are actually cleaner is by no means to be taken for granted. Such surfaces could, for example, exhibit enhanced outgassing.
- The minimum chemical cleaning process compatible with the level of vacuum/cleanliness required should always be chosen. The less that needs to be done to a vacuum surface the better.
- Chemical cleaning is a hazardous procedure so must be done safely!
- Processes such as bead or shot blasting, grinding, scraping and mechanical polishing can leave dirt trapped in voids in the surface of materials which can then be very difficult to remove.
- Acid treatments such as pickling, passivation or electropolishing can trap acids in the surface of the material. For demanding UHV applications, a vacuum bake to 450oC is required to remove these completely.

#### **Dependence on the base pressure required**

In general, the lower the base pressure required, the more rigorous the cleaning process will

Table 4.1 Simple cleaning procedures

1 bar	Hot water wash Swab or wash with detergent
1 mbar	Wash in aqueous detergent
10 <sup>-6</sup> mbar	Ultrasonic wash in aqueous detergent Rinse with hot clean (distilled) water
10 <sup>-9</sup> mbar	Ultrasonic wash in hot detergent Vapour wash in solvent vapour Rinse with hot clean (distilled) water Vacuum bake in 250 °C

need to be. (Note that in general it is preferable to use the term “base pressure” rather than “ultimate pressure” which is commonly used. Base pressure refers to the lowest normal pressure attained in a vacuum system in its working condition, whereas ultimate pressure strictly refers to the lowest pressure obtained in a standard defined system measured in a standard way.)

Table 4.1 illustrates in a very schematic fashion some typical common cleaning processes which would be used in sequence. To use this figure, select the approximate pressure required and then apply all the processes in order from the top to the level corresponding to the pressure required.

The user will have to determine what level of contaminants can be tolerated in any given process. It is important to distinguish between the total pressure required in the system and the partial pressures of particular species which can be allowed. As has been said, most processes use vacuum simply because it provides an easily controlled environment for the process and it is really what can and cannot be tolerated in that environment which is important.

For any given process, the user may have to determine by tests what cleaning is necessary to obtain the desired environment.

As has been discussed above, one very common requirement is to reduce hydrocarbon contamination to a minimum. This will often best be achieved by washing in a hot organic solvent such as trichloroethylene or perchloroethylene (where use of these substances, both chlorinated

hydrocarbons, is permitted) followed by washing in hot clean demineralised water and a vacuum bake.

### **How construction affects cleaning**

In order to clean a vacuum component to the highest standards - e.g. capable of working at UHV with very low levels of contaminant species in the residual vacuum - at the design stage careful consideration must be given to how the item is to be cleaned. In particular, crevices, blind holes, cracks, trapped volumes, etc., should be avoided as these will act as dirt and solvent traps. It can be very difficult to remove both dirt and solvent from such areas. Fortunately, good vacuum practice regarding trapped volumes will also result in a component which avoids these problems.

A good design working at lower vacuum levels will also seek to remove any such traps.

One component which must be cleaned with particular care is thin-walled edge-welded bellows often used for motions in vacuum. Care must be taken that the cleaning process does not cause particles to be left in the convolutions, since these can puncture the bellows when it is compressed. Alkaline degreasers can be particularly prone to this as they often throw precipitates. During cleaning, the bellows should be fully extended and a careful final wash with demineralised water and a blow dry with hot compressed air, both inside and out, must be done.

If the process uses chlorinated hydrocarbon solvents then these must be removed completely by heating, as any left behind can corrode the bellows, leading to leaks. This last point is particularly true for accelerators, where the atmosphere in accelerator tunnels can often be warm and humid. The radiation environment also promotes enhanced corrosion, leading to premature failure of the welds.

### **Chemical cleaning agents**

A chemical cleaning agent is simply any substance that might lead to removal of an unwanted contaminant. They will generally be liquids of some sort and will work either by dissolving or by reacting with the contaminant or by removing the surface layers of the substrate and hence liberating the contaminant.

Care has to be exercised that the cleaning agent itself does not introduce contaminants. This will obviously depend on the end use of the item being cleaned. For example, as noted above, hydrocarbons are often a serious contaminant in a vacuum system. However, in mineral oil sealed mechanical vacuum pumps, e.g. rotary pumps, this is not the case as much of the mechanism is of necessity bathed in hydrocarbons. Therefore, a major manufacturer of such pumps uses a hydrocarbon mix to clean the piece parts for his pumps and enjoys the benefit of residual lubrication and corrosion protection on parts not normally lubricated by the pump fluid. In most cases, however, what is desired is an agent that will remove contamination from the item without recontaminating it in some way. The operator has therefore to ensure that the solvent is changed regularly before the buildup of contamination in solution becomes a problem. Examples of some typical cleaning agents are shown in Appendix B. The table should be read with caution and is to be regarded as a starting point only. In all cases, manufacturers data sheets should be consulted and expert technical advice sought before using agents of this type.

The majority of these agents are solvents, which dissolve the contamination present on a surface. Some rely more on a simple washing action, flushing contaminant off the surface, as in a water jet. Others, e.g. detergents, work mainly by reducing the attractive (Van der Waals) force between contaminant and surface atoms. Some work by chemical action e.g. by etching a thin layer off the surface thus releasing the contaminant. The alkaline degreasers and citric acid work this way, as do, to some extent, some detergents. It is important to understand how any particular agent interacts with the materials to be cleaned in order to avoid unexpected side effects.

It should be carefully noted that, in some countries, some of these substances are either banned or their use is strictly controlled under legislation or regulation. It is therefore imperative that the operator consults the relevant authorities before implementing a process involving these agents.

#### **1. Stainless Steel**

The procedure described below for cleaning stainless steel is a very high specification process for the very demanding requirements of an electron storage ring where cleanliness is of paramount importance. For less demanding applications, the procedure could stop at the appropriate point in the

procedure where requirements had been met.

- 1.1 Remove all debris such as swarf by physical means such as blowing out with a high pressure air line, observing normal safety precautions. Remove gross contamination by washing out, swabbing or rinsing with any general purpose solvent. Scrubbing, wire brushing, grinding, filing or other mechanically abrasive methods may not be used.
- 1.2 Wash in a high pressure hot water (approx. 80oC) jet, using a simple mild alkaline detergent. Switch off detergent and continue to rinse thoroughly with water until all visible traces of detergent have been eliminated.
- 1.3 If necessary, remove any scaling or deposited surface films by stripping with alumina or glass beads in a water jet in a slurry blaster.
- 1.4 Wash down with a high pressure hot (approx. 80oC) water jet, with no detergent, ensuring that any residual beads are washed away. Pay particular attention to any trapped areas or crevices.
- 1.5 Dry using an air blower with clean dry air, hot if possible.
- 1.6 Immerse completely in an ultrasonically agitated bath of clean hot stabilised trichloroethylene for at least 15 minutes, or until the item has reached the temperature of the bath, whichever is longer.
- 1.7 Vapour wash in trichloroethylene vapour for at least 15 minutes, or until the item has reached the temperature of the hot vapour, whichever is longer.
- 1.8 Ensure that all solvent residues have been drained off, paying particular attention to any trapped areas, blind holes etc.
- 1.9 Wash down with a high pressure hot (approx. 80oC) water jet, using clean demineralised water. Detergent must not be used at this stage.
- 1.10 Immerse in a bath of hot (60oC) alkaline degreaser (P3 Almeco □ P36) with ultrasonic agitation for 5 min. After removal from the bath carry out the next step of the procedure immediately.
- 1.11 Wash down with a high pressure hot (approx. 80oC) water jet, using clean demineralized water. Detergent must not be used at this stage. Ensure that any particulate deposits from the alkaline bath are washed away.
- 1.12 Dry using an air blower with clean dry air, hot if possible.
- 1.13 Allow to cool in a dry, dust free area. Inspect the item for signs of contamination, faulty cleaning or damage.
- 1.14 Vacuum bake to 250oC for 24 hours using an oil free pumping system.
- 1.15 Reduce the temperature to 200oC and carry out an internal glow discharge using a helium 10% oxygen gas mix.
- 1.16 Raise the temperature to 250oC for a further 24 hours then cool to room temperature.

## 2. Aluminium

2.1 The CERN specification for aluminium chambers is as follows-

- 2.1.1 Spray with high pressure jets at 60°C with a 2% solution of Almeco 29 (an alkaline detergent)
- 2.1.2 Repeat with a 2% solution of Amklene D Forte
- 2.1.3 Rinse thoroughly with a jet of hot demineralised water.
- 2.1.4 Dry with hot air at 80°C.
- 2.2 Another procedure known to give good results is
  - 2.2.1 Immerse in Sodium Hydroxide (45 gm-1 of solution) at 45oC for 1 - 2 min.
  - 2.2.2 Rinse in hot demineralised water.
  - 2.2.3 Immerse in an acid bath containing Nitric acid (50% v/v) and Hydrofluoric acid (3% v/v).
  - 2.2.4 Rinse in hot demineralised water.
  - 2.2.5 Dry in warm air

## 3. Copper

Under most circumstances, copper can be cleaned using the same procedures as for stainless

steel. However, it should be noted that some of the proprietary formulations of alkaline degreasers attack copper and leave surface stains. Organic solvents are usually all right, and cleaners based on citric acid are very good for copper. Indeed, some of these are formulated specifically for this purpose. As always, thorough washing in hot demineralised water and drying in warm, dry air should be undertaken.

Copper is particularly susceptible to surface staining, fingerprints showing up very well! Under some conditions, light surface oxidation takes place which results in a visible blackish film on the surface. As long as this is not a thick, friable or flakey deposit, this will not usually be a problem in vacuum, since it thermally disassociates quite readily.

#### 4. Beryllium

Working with beryllium is subject to stringent safety requirements and the appropriate safety authorities must always be consulted before carrying out any such work. However, provided that care is taken to ensure that no particulates are generated and that suitable precautions are taken, components may be handled safely. Impervious gloves should always be worn when handling beryllium and any skin abrasions or cuts should be covered up.

No stripping, cutting, machining or abrasive operations may be carried out on beryllium except in purpose built facilities.

Otherwise, beryllium may be cleaned in accordance with the procedures for stainless steel.

#### 5. Titanium

Titanium may be successfully cleaned as for stainless steel.

#### 6. Glasses

Simple detergents and hot water washing are effective for cleaning glass.

#### 7. Ceramics

Alumina powder in a water or an isopropanol carrier may be used to remove surface marks from ceramics such as alumina or beryllia. Baking in air to the highest temperature that the material can stand or to 1000°C, whichever is lower, is very effective for removing contamination from the surface pores of the material.

### **Physical cleaning techniques**

#### Blowing

A jet of compressed air or inert gas is a useful technique to remove particulates and liquids, particularly from blind holes, as well as surface dust. A laboratory or site compressed air supply may be used provided that the air supply derives from an oil-free compressor. It should be distributed via cleaned and dried air lines and there should be particulate filtration at or near the point of delivery. Alternatively, bottled gas, e.g. nitrogen, may be used, but again the delivery line should be clean and dry.

#### Bead Blasting

A jet of alumina or silica or some other inert material in the form of small beads is directed onto a surface and physically strips material away. The carrier may be either air or water. The latter is gentler, but both techniques carry the risk of driving contaminants (and beads!) into the surface. Some surface damage may occur. However this is a useful technique for stripping, for example, deposited metal films from the inside of vacuum vessels.

#### “Snow” Cleaning

This technique uses a jet of pellets of solid Carbon Dioxide which is directed onto the surface. This is a non-impact technique which is good for removing particulates and also apparently some hydrocarbon films. It is however, expensive and noisy.

Unlike bead blasting, the technique does not damage the surfaces being cleaned, since the solid CO<sub>2</sub> does not impact the surface. As the particles, usually in the form of small cylindrical pellets, approach the surface at high speed, the shock wave travelling ahead of the particle is reflected from the surface and interacts with the pellets, which sublime. The cleaning action is effected through a cavitation process in the compressed gas as it reflects from the surface.

#### Cutting and Grinding

Cutting and grinding are used to remove surface layers. Both have their place provided they

are done with care. Each technique usually requires a lubricant between tool and workpiece, which for vacuum use is best to be either water or water based, although a good alternative is alcohol. If possible dry cutting is best.

There is a danger of driving contaminants, cutting fluids and swarf into the surface where they can remain trapped.

#### Polishing

Polishing is a gentle form of grinding and carries the same dangers. However fine hand polishing is often required to remove surface blemishes. A useful material for this is ScotchBrite which is essentially fine alumina in a polymeric carrier in the form of a loose weave mat. Diamond powder wetted with alcohol and applied on a lint free pad is also acceptable. Polishing involving pastes and waxes is to be avoided

Small components are often polished in a tumble polisher in which they are immersed in a bath of small wet stones or steel pellets of various shapes which is gently stirred or tumbled.

#### Passivation

As far as cleaning is concerned, passivation techniques are essentially ones which prevent the adsorption of contaminants into the surface of a vacuum system or prevent the permeation of gas from the bulk material into the vacuum system. By and large, these involve the formation of a barrier layer of some sort on the surface.

Some examples are

- oxide films, produced by air baking, glow discharge or other techniques.
- coatings, such as TiN or BN put on the surface by sputtering. These have not been much used except in demonstration systems and will not be discussed further here.
- active films, like getters or NEG. These are discussed in other chapters of these proceedings.

#### Special cleaning techniques

##### Ultrasonic Cleaning

This is essentially a method of enhancing a chemical cleaning process.

The figure shows a two stage cleaning plant. The workpiece is first suspended in the hot liquid (darker shade) in the left hand tank. The ultrasonic transducers set up a pattern of ultrasonic waves in the liquid. As these waves reflect off the surface of the workpiece, interference takes place and a series of cavitation bubbles are generated. Collapse of these bubbles results in contamination particles being dragged off the surface. The contamination then either dissolves in the liquid or, if insoluble, eventually drops to the bottom of the tank as sediment. The result is an enhanced cleaning process. As jobs are cleaned, the liquid in the ultrasonic tank gradually becomes more contaminated and eventually some of this remains on the surface of the workpiece, or indeed may be transferred to it from the liquid. To ensure full cleanliness, the workpiece is withdrawn from the liquid and is suspended in the second (right hand) tank in the solvent vapour (lighter shade). This vapour is generated by the boiling liquid solvent at the bottom of the vapour stage tank. The vapour condenses on the workpiece so that it is washed in the pure liquid solvent condensate which drops back into the boiling liquid, taking the residual (soluble) contamination with it. At the top of both baths are cooling coils which condense the vapour before it can escape from the open top of the tank. These coils are arranged so that the liquid runs back into the ultrasonic stage. This pure liquid solvent tops up the ultrasonic tank and contaminated solvent flows over the dam into the boiler. Thus a distillation process is set up with the contamination gradually being concentrated in the bottom of the vapour stage and the liquid in the ultrasonic tank remaining relatively pure, hence enhancing the life of the solvent charge.

##### Electropolishing

Electropolishing has often been assumed to reduce outgassing by reduction of the surface area presented to a vacuum system. In practice, for any technological metal surface, the real surface area is very much larger (factors of several) than the physical area, because on a macroscopic scale there will be many pits, grooves, cracks, grain boundaries and other defects. Although electropolishing does indeed remove surface asperities and smooths the edges of cracks, the actual benefit achieved is

not very great.

However, electropolishing does remove the amorphous surface layer which is formed when polishing a metal surface (the so-called Beilby layer). It replaces this layer with a relatively well ordered surface oxide layer, which may have barrier properties preventing diffusion (particularly of hydrogen) out from the bulk of the metal into the vacuum.

On the other hand, electropolishing may introduce hydrogen and other contaminants into the surface layers in significant quantities. These can subsequently diffuse out and actually increase the outgassing rate over that of the starting material. Electropolished components require a good bake (preferably at 450°C) to thoroughly outgas the surface in order to see any real benefit.

Despite many studies over a long time, it is only in some recent very careful work on aluminium prepared by various techniques that a correlation between surface roughness and outgassing rate has been demonstrated and even in these results there are some anomalies.

### **Glow discharge**

Glow discharge cleaning is an effective final cleaning process which reduces outgassing and desorption rates. It achieves this essentially by three mechanisms

- The bombardment of a surface by medium energy ions (a few hundred eV) directly desorbs gas adsorbed on the surface and absorbed in the sub-surface region.
- If the discharge gas contains oxygen (or water), oxygen ions ( $O_2^+$  and  $O^+$ ) are created in the discharge. These can react with the adventitious carbon which is always present on a surface to form CO and  $CO_2$  which can be pumped away. Carbon overlayers, usually graphitic or amorphous in character, seem to act as gas reservoirs on a surface.
- A good, well ordered oxide film is generated on the surface which acts as a diffusion barrier.

For accelerators, it is normal to use a simple dc glow discharge, although an ac (rf) discharge may also be used. Fig 4 shows a typical set-up for dc discharges. A gas is admitted to the vessel to be cleaned and a positive dc potential of a few hundred volts is applied to a rod or wire electrode along the axis of the vessel. If the gas pressure is of the order of a few tenths of a mbar (dependent on the actual gas being used and the precise geometry of the vessel) a discharge will be struck and a visible glow seen. The gas molecules are ionised in this discharge and are accelerated to the grounded walls of the vessel which they strike with moderate energies. It is advantageous to stream the gas along the vessel, admitting it at one end and pumping at the other. At these pressures the flow is viscous and this helps to sweep the desorbed gases from the system.

Various gas mixtures have been used. Ar/10%  $O_2$  is the traditional mix and is very efficient; pure  $O_2$ , pure  $N_2$ , pure  $H_2$  and He/10% $O_2$  have also been used effectively. There are a number of criteria which are used in selecting the gas. Of critical importance is whether sputtering of the metal surface is a problem or not. If there are insulators present, then sputtering can cause conducting films to be deposited over their surfaces if they are exposed to the sputtered atoms. Oxygen in the mix seems to help alleviate this by forming thermally unstable metal oxides which are removed from the surface in the discharge. Lighter species sputter less efficiently and so help obviate the problem. Also, heavier gas ions can become buried in the metal surface and can diffuse out over time. This may or

may not be a problem depending on the application. Carrying out the discharge at elevated temperature (e.g. 200°C) helps minimise such accumulation. Thus, the discharge can be conveniently carried out during a bake cycle.

It is helpful to know when to terminate the glow discharge. If, as has been suggested above, the primary benefit is achieved by the removal of adventitious carbon by forming CO and  $CO_2$ , then monitoring the concentration of  $C^{12}$  in the discharge exhaust gas with a residual gas analyser will give a termination point when this concentration ceases to reduce.

For particle accelerators, this procedure is usually carried out as part of the pre-installation processing programme, since in situ glow discharge is difficult in practice.

The benefits of glow discharge cleaning for particle accelerators are by no means fully established. For proton machines fabricated from stainless steel the benefits are well established. For electron machines where the beam space tends to be surrounded by copper, the evidence is not well

in place, although it is believed to be beneficial. A definitive experiment is planned for ANKA in the near future.

#### **Air Baking**

This procedure involves baking vacuum components at normal bake temperatures (250°C) in air. It reduces outgassing rates considerably, particularly for hydrogen. It was thought to work by inducing a barrier oxide layer, but may simply work by depleting the hydrogen from the bulk.

The technique is much favoured in the gravitational wave detector community but its value for accelerators is unproven.

#### **Chemical “Baking”**

An interesting idea originating in Japan is to use a chemical which has a particular affinity for water to react with the water adsorbed on a surface in such a way that the reaction products are gases which may be pumped away.

This technique is claimed (Tatenuma et al, J Vac Sci Technol A16, 1998, 263) to reduce the base pressure in a vacuum system by factors of 80.

However, the technique has to be carried out at a moderate temperature (80°C) so it is unclear what advantages this technique has in practice over a simple bake.

## 5. VACUUM PUMPS

### 5.1. Mechanical pumps

The mechanical rotary pump and the oil diffusion pump are widely used in many kinds of high vacuum systems. The DP system with a mechanical rotary pump is reliable in performance, silent in noise and small in vibration, and cheap in price.

The sputter ion pump (SIP) is suited to ultrahigh vacuum because it can be baked to degas up to about 200 °C. Getter pumps such as the titanium sublimation pump (TSP) and the non-evaporable getter (NEG) pump can also be used for ultrahigh vacuum (UHV) due to the same reason. A well designed SIP indicates accurate pressures in ultrahigh vacuum region.

The SIP and the getter pump need an auxiliary pump. The turbomolecular pump and the dry vacuum pump (DVP) are used as an auxiliary pump in the UHV evacuation system.

Many kinds of dry vacuum pumps (DVPs) are widely used in the film-deposition equipment such as chemical vapor deposition (CVD) systems. Dry vacuum pumps (DVPs), without using any lubricating oil inside the pumps, are resistant to reactive gases used in CVD systems.

The mechanical rotary pump and the mechanical booster pump belong to this category. The rotary vane pump is exclusively used as a backing pump and/or a roughing pump in the oil diffusion pump (DP) system. A mechanical booster pump is often used as a backing pump for the high-pumping-speed DP system in deposition systems.

Harris and Budgen (1976) [2-1] presented an article, "Design and manufacture of modern mechanical vacuum pumps" which covers the design and manufacturing aspects of rotary vane, rotary piston and mechanical booster pumps. Rotary vane pumps are urged by springs to press against the cylindrical stator wall while being carried round the rotor. Figure 5.1(b) shows a rotary piston type of pump where the piston (a hollow cylinder with a hollow tongue attached) is made to process around inside a circular stator by means of the rotating cam within it. Both of these pumps are oil sealed. Figure 5.1(c) shows a mechanical booster pump where the "figure-of-eight" rotors are synchronized by external gears and rotate in the oval stator so as to maintain small clearances between each other and between the stator walls. The rotors run dry of lubricant.

#### **Rotary Pumps**

Although today the rotary vane type is mainly used for pumps of low and medium pumping speed whilst the rotary piston is preferred for higher pumping speeds, clear cut advantages or disadvantages cannot be formulated for either type. One advantage of the rotary vane design is the comparatively small out-of-balance forces consequent upon rotation. The only eccentrically rotating masses are the blades, the center of mass of a blade pair describing an oval path twice per rotor revolution. With the use of various plastic blades, which are somewhat lighter than steel, this imbalance becomes insignificant.

In the two stage operation of a rotary vane pump the gas load is compressed in two stages in series from the inlet vacuum to interstage pressure by the high vacuum or first stage, and then from interstage pressure to discharge (i.e. atmospheric) pressure by the low vacuum or second stage. Oil for lubricating and sealing the first stage is outgassed by the second stage before being passed to the first stage. This together with the sharing of compression between two stages gives very much lower pressure than does a single stage pump.

**Direct Drive Pumps:** The use of direct drive i.e. at 1500 rpm for 50 Hz or 1800 rpm for 60 Hz is made practical by the use of reinforced plastic blades and by further specialized techniques for quieting the operation of the pump shut-down, isolating the pump from the system at the same time admitting air into the pump itself. Oil "suck-back" is thus prevented.

#### **Mechanical Booster Pump**

**General Operation:** Mechanical booster pumps are usually operated at fairly high rotational speeds i.e. 1400–4000 rpm depending on size. This is permissible as there is no mechanical contact of the pumping components. Problems associated with mechanical boosters are:

- 1) Severe heating (particularly rotors) can occur with large gas loads at high compression ratios.

This heating can lead to closure of working clearances and consequent mechanical failure. This problem may be overcome by cooling the rotors with oil passing through their shafts or more conveniently by providing a water-cooled heat exchanger in the gas discharge area close up to the rotors.

- 2) The torque input to the mechanical booster is dependent upon the pressure difference across it. At full rotational speed this becomes unacceptably high above 10–20 Torr inlet pressure, depending on displacement ratio of mechanical booster and backing pump. There are several ways of overcoming this difficulty:
  - (a) by pressure switching such that the pump is only switched on below 10–20 Torr.
  - (b) by providing a pressure relief by-pass such that the maximum pressure differential that the motor can drive is not exceeded.
  - (c) by providing hydrokinetic drive [1, 2] between motor and pump so arranged that motor full load torque is not exceeded. The pump slows down at high pressures maintaining full pressure differential without overheating and without overloading the motor.

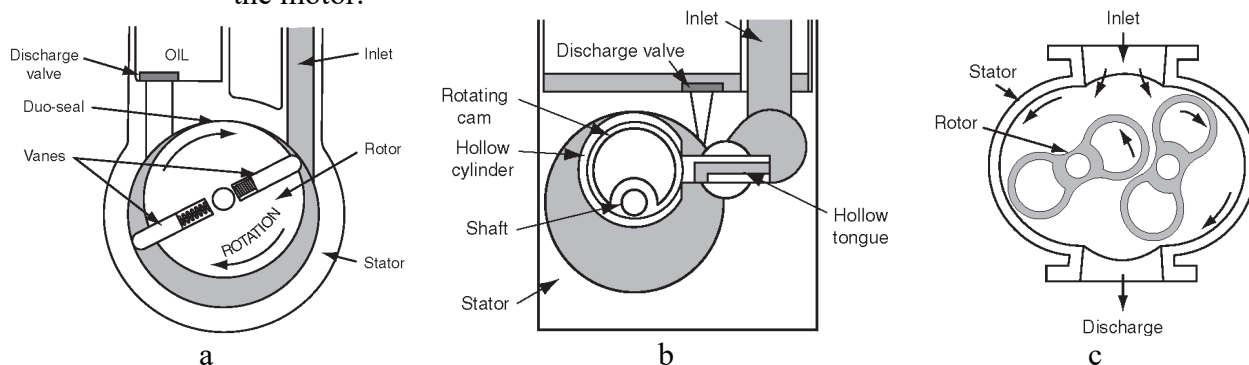


Figure 2.1 (a) Rotary vane pump. (b) Rotary piston pump. (c) Mechanical booster pump

Mechanical boosters fitted with water-cooling and with hydrokinetic drive may be continuously rated at all working pressures and are normally switched on with the backing pump, thus providing a valuable contribution to pumping speed at all pressures.

#### Diaphragm vacuum pumps

Diaphragm vacuum pumps are dry positive-displacement pumps. A crankshaft-driven (Figure 5.2) connecting rod (4) moves the diaphragm (1) that is tensioned between the head cover (2) and the housing (3). The space between the head cover and the diaphragm forms the suction chamber (5). Diaphragm pumps require inlet valves and outlet valves (6) to achieve targeted gas displacement. Pressure-controlled shutter valves made of elastomer materials are used as valves. Since the suction chamber is hermetically sealed off from the drive by the diaphragm, the pump medium can neither be contaminated by oil nor can aggressive media corrode the mechanics. The dead volume between the outlet valve and the suction chamber results in a restricted compression ratio which

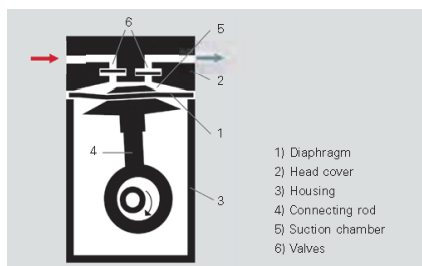


Figure 5.2 Operating principle of a diaphragm vacuum pump

means that with just one pumping stage it is only possible to achieve an ultimate pressure of approximately 70 hPa. Connecting multiple pumping stages in series makes it possible to attain an ultimate pressure of 0.5 hPa. Lower pressures cannot be achieved, as in this case there is no longer sufficient force to open the inlet valve. The principle of the diaphragm pump is particularly well suited for low pumping speeds of up to approximately  $10 \text{ m}^3 \text{ h}^{-1}$ .

Their hydrocarbon-free suction chambers make diaphragm pumps particularly well suited as dry backing pumps for turbomolecular pumps with a Holweck stage. Even two-stage diaphragm pumps that can reach an ultimate pressure of approximately 5 hPa. This is sufficient for backing of pumps for Holweck turbopumps. The clean vacuum is particularly useful for analytical and R&D

applications. Diaphragm pumps, too, do not displace water vapor without gas ballast. Even the low volumes of water vapor that desorb from the walls of high vacuum equipment can allow the ultimate pressure of a diaphragm pump to increase dramatically. However, some diaphragm pumps are equipped with a gas ballast valve that operates in accordance with a patented process. For this purpose, gas is admitted into the connection channel between the first and second stages of two-stage diaphragm pumps, and this is connected with the suction chamber of the first stage via a small hole.

If greater volumes of moisture accumulate and diaphragm pumps without gas ballast are used, suitable separators or cooling traps must be connected upstream to prevent significant condensate formation in the pump. However, the ultimate pressure will nevertheless increase.

Diaphragm pumps differ in terms of their ultimate pressure, pumping speed and their suitability for pumping corrosive gases. The pumping speeds of the pumps are between 3 and 160 l min<sup>-1</sup> (0.25 to 9.6 m<sup>3</sup> h<sup>-1</sup>). Ultimate pressures of less than 4 hPa for two-stage pumps and less than 0.5 hPa for four-stage pumps can be attained. Their pumping speed and the attainable final pressure depend on the mains frequency.

Corrosive gas pump models with coated diaphragms and corrosion-resistant housings are available for pumping corrosive gases.

The designations for the pumps are selected in such a manner as to indicate the pumping speed in l min<sup>-1</sup> and the number of pumping stages. Corrosive gas pumps have the letter C as a suffix to the model designation.

#### Screw vacuum pumps

Two parallel bearing-supported, intermeshing screw rotors (3) having opposite threads synchronously and contactlessly counter-rotate in a cylindrical housing (2) that tightly encloses them, and together form a multi-stage pump. Because of the counter-mesh of the two rotors, the volumes sealed in each thread are advanced along the rotors to the outlet (4). The pump has no valves at either the inlet (1) or the outlet. When a displacement volume reaches the outlet opening, the pressure is equalized with the atmosphere. This means that atmospheric air flows into the displacement volume and is then discharged again as the rotor turns. This pulsing gas flow generates a high level of dissipated energy and heats the pump. The dissipated energy can be minimized by means of internal compression. This internal compression is achieved by reducing the thread pitch in the direction of the outlet. The gaps between the housing and the rotors, as well as between the rotors relative to one another, determine the ultimate pressure which a screw pump can attain. The geometry and the gap configuration which results when the rotors engage with each other also significantly influence the ultimate pressure.

Because the dissipated energy that is generated by the pulsing gas flow heats the pump on the outlet side, cooling is required at precisely this location. The gap between housing and rotors is a function of the temperature differential between the warmer rotors and the cooled housing. The amount of heat produced and the temperature are a function of the inlet pressure range.

Temperatures are lowest at high inlet pressures (nearly atmospheric), as virtually no compression work is performed here and the displaced air transports sufficient heat out of the pump. In addition, the high gas flow also prevents oscillation of the gas in the last stage. During operation at ultimate pressure ( $p < 1$  hPa), the oscillation of the atmospheric air produces higher temperatures at the outlet area, since no gas is passing through the pump and therefore no heat is being transported out of the pump.

HeptaDry pumps are dry screw pumps with internal compression. The screw rotors have a symmetrical geometry with variable pitch. These pumps do not have an end plate with control openings; instead, the gas

is discharged axially against atmospheric pressure. Because of the internal compression, the volume of pulsing gas is low.

This results in lower power consumption, quiet operating, uniform temperature distribution within the pump and low cooling water consumption. This makes these pumps extremely cost-effective, in spite of their robust design.

In recent years, water cooled screw pumps and the multi-stage Roots pumps described in the

following section have been replacing more and more the previously dominating oil-lubricated rotary vane pump in the high pumping speed segment ( $100 - 600 \text{ m}^3 \text{ h}^{-1}$ ).

Advantages of screw pumps include:

- No lubricant in the gas displacement area
- No contamination of the medium to be pumped
- No operating fluid disposal problems
- Higher efficiency due to internal compression
- Virtually constant pumping speed between 1 and 1,000 hPa.
- Good liquid and dust tolerance
- Ideal backing pump for Roots pumps

This makes HeptaDry screw pumps very well suited for chemical applications or processes that generate dust, e. g. for crystal growing or if significant volumes of condensate are produced.

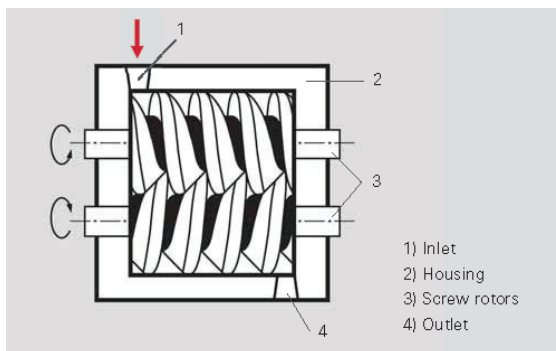


Figure 5.3 Operating principle of a screw pump



Figure 5.4 HeptaDry rotors

In thermostatic cooling, the water flow volume will depend on the following parameters: inlet pressure, gas type, rotation speed and pump size. Due to the waterflow cooling, virtually no heat is dissipated to the atmosphere. This reduce the heat load on any existing air conditioning systems and reduce their energy consumption.

Overview of primary screw pump applications:

- Drying, freeze-drying
- Electron beam welding
- Metallurgy
- Coating
- Load locks
- Chemical applications

HeptaDry pumps are dry screw pumps for applications in the low and medium vacuum ranges where high volume flow rates are required. The pumping speeds of this product line range from  $100$  to  $600 \text{ m}^3 \text{ h}^{-1}$ . Ultimate pressures of under  $0.1 \text{ hPa}$  are attained. Their pumping speed and the attainable final pressure depend on the mains frequency.

Regardless of the model in question, HeptaDry pumps can be continuously operated in their particular operating range. Their effective pumping speed declines in the  $p < 1 \text{ hPa}$  pressure range due to the ever-stronger back-flow between the individual sealed volumes within the pump. There is a similar reason for the decrease in pump-ing speed toward high pressure, as in this case the gas is compressed to pressures in excess of atmospheric pressure through internal compression, and consequently backflow increases significantly due to the high differential pressure.

The standard equipment that comes with the pumps includes: inlet sieve, water-flow cooling with thermostatic valve and thermometer, silencer with non-return valve and frame-mounted design with vibration dampers. The pumps are driven by a three-phase, temperature-monitored asynchronous motor that is suitable for  $50$  and  $60 \text{ Hz}$  ( $3,000$  or  $3,600 \text{ rpm}$ ).

## 5.2. Condensers

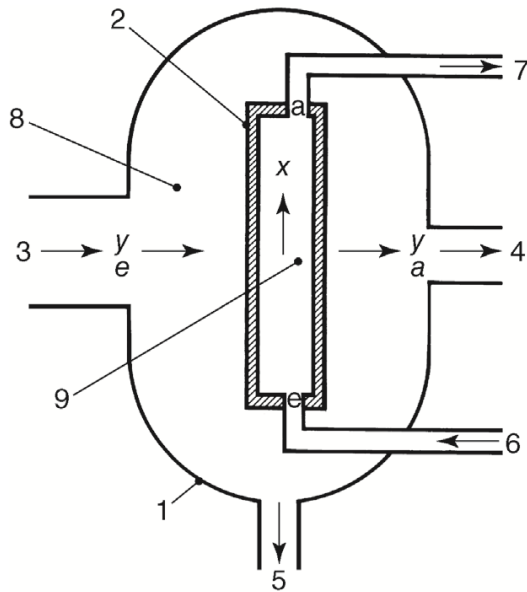


Figure 5.5 Diagram of a condenser. 1: housing; 2: condensation surface = wall of coolant channel; 3(e): incoming vapor/gas mixture; 4(a): discharge of noncondensable components of mixture; 5: condensate drain; 6(e) and 7(a): coolant inlet and outlet, respectively; 8: vapor/gas chamber; 9: coolant channel; x: direction of coolant flow; y: direction of vapor/gas mixture flow.

In drying and condensation processes under vacuum, the main task of the vacuum pumping system is to pump down developing gases and vapors. For vapors, condensers serve as particularly simple and economical vacuum pumps. Pumping with a condenser is limited to vapors. Therefore, a combination with vacuum pumps that initially pump down the air from the process container and, subsequently, pump the process and leakage gases is required. Figure 8.1 illustrates the basic setup: a condensation surface 2, kept at low temperature by means of a coolant flow from in to out in the x direction, is arranged in the condenser housing 1. At the entrance port 3, vapor enters and releases its condensation heat when hitting condenser plate 2 if the temperature of the condenser plate  $T_K$  is considerably below the saturation temperature  $T$  (temperature of dew point, condensation temperature) of the vapor. The coolant absorbs the condensation heat released by the liquefying vapor, and thus heats up and carries off the heat. The condensate drains off through discharge 5. The noncondensed part is removed by a vacuum pump connected to outlet 4.

The vapor pressure curve characterizes the relationship between the saturation temperature  $T_s$  and vapor pressure  $p_s$  of a substance. Figure 5.5 shows vapor pressure curves for water and selected solvents in the range of  $-50\text{ }^\circ\text{C}$  to  $+290\text{ }^\circ\text{C}$ . To the right of the curve, the substance is in gaseous form. To the left of the curve, it is liquid or solid. On the curve, liquid and saturated

vapor coexist in equilibrium. If the temperature of a nonsaturated (superheated) vapor drops, it condenses as soon as it reaches the saturation temperature (temperature of dew point) corresponding to the considered vapor pressure.

Condensation requires removal of the condensation heat, which is equal to the evaporation heat. The specific condensation heat  $r$  is temperature dependent. Water at  $\vartheta = 25\text{ }^\circ\text{C}$ , for example, shows a specific condensation heat approximately 10% higher than at  $\vartheta = 100\text{ }^\circ\text{C}$ .

If, according to the condition given by the vapor pressure curve, a vapor is not saturated but hotter, that is, superheated, removal of the additional superheat is required as well. The superheat can be calculated from the vapor's specific heat capacity.

Precise values of the specific heat capacity and the specific condensation heat at different temperatures can be obtained from steam tables.

## 5.3. Jet and diffusion pumps

### Jet pumps

Jet pumps (or fluid entrainment pumps) are characterized (DIN 28400,1) part 2) by a liquid, gas, or vapor medium (motive fluid) that travels through the pump, thereby transporting the gas to be pumped down. Figure 5.6 shows a general schematic illustration of a jet pump. The jet with velocity  $v_2$  is produced by releasing the motive fluid from pressure  $p_0$  in pressure chamber 1 to pressure  $p_2$  in the jet. In the mixing chamber 3, at suction pressure  $p_s$ , the pumped-down gas mixes with the motive fluid. This causes a transmission of momentum to the pumped-down gas particles that accelerate in

the expanding direction of the motive fluid until they reach the prevacuum chamber 4. Pressure  $p_3$  here is higher than  $p_2$  in the expanding jet so that the gas transported by the motive fluid can be released to the ambient atmosphere either directly from the prevacuum side or by means of an additional vacuum pump (prevacuum pump).

The expanding working fluid in the jet nozzle 5 as well as in the mixing chamber 3, and the pressure increase in the diffuser nozzle 6 follow Bernoulli's equation. Here,  $v$  is the jet velocity,  $p$  is the static pressure in the jet,  $\rho$  is the density of the working fluid in the jet, and  $p_0$  is the pressure in the pressure chamber ( $v_0 = 0$ ):

$$v^2 = 2 \int_p^{p_0} \frac{dp}{\rho} \quad (5.1)$$

Technical designs of fluid entrainment pumps and the detailed functionality vary considerably. A first classification is obtained by considering the physical types of motive fluids:

- liquid jet vacuum pumps;
- gas jet vacuum pumps;
- vapor (steam) jet vacuum pumps.

An additional characteristic is working pressure range. The working pressure influences spreading of the jet in the expansion chamber and the mixing process involving pumped-down gas and motive fluid. Due to fundamentally different operating principles, we differentiate:

- jet vacuum pumps, where intake pressure  $p_{in}$  in the mixing chamber is about equal to the static pressure  $p_2$  in the jet, and
- diffusion pumps with an intake pressure  $p_{in}$  far below the static pressure  $p_2$  in the jet.

In jet pumps, the working fluid and the pumped gas preferably mix in a turbulent boundary layer of the working fluid jet. In diffusion pumps, mixing takes place due to diffusion of the pumped-down gas into the motive fluid jet.

A further important distinctive feature is the mean free path  $\bar{l}$  of gas molecules at the inlet flange to the pump. In jet pumps,  $\bar{l}$  is lower than the annular passage between the jet nozzle and the pump wall (Figure 5.6), and thus, flow is predominantly viscous. For diffusion pumps,  $\bar{l}$  is higher than the opening passage, thus exhibiting molecular flow.

The following considerations focus on the most important pump types for vacuum technology, particularly for high-vacuum applications.

Processes in fluid entrainment pumps are complicated. Therefore, theories that usually are very simplified comply quantitatively with experimental results

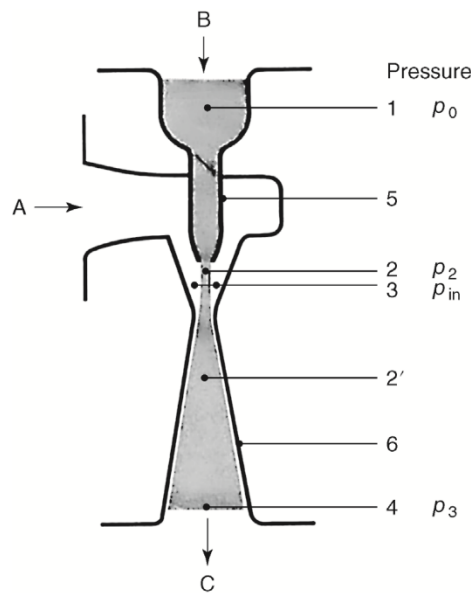


Figure 5.6 Diagram of a jet vacuum pump. 1: pressure chamber (pressure  $p_0$ ); 2 and 2': motive medium jet; 3: mixing chamber (pressure  $p_2$  in the jet); 4: compression chamber (pressure  $p_3$ ); 5: jet nozzle; 6: diffuser nozzle; B: motive medium inlet; A: vacuum connection (intake pressure  $p_{in}$ ); C: fore-vacuum connection (pressure  $p_F$ ).

only in certain individual cases. The most important results that are helpful for practical use are presented.

Many industrial applications use jet pumps with liquid working media for mixing and transporting fluids and even solids. For producing vacuum, these types of jet pumps, such as the most widely known water jet pumps, are used to deliver and compress gases and vapors by means of a liquid working fluid. Here, depending on pressure and temperature conditions, vapors can be condensed partially or completely.

On principle, any liquid can serve as working fluid. However, dimensioning requires thorough knowledge of physical properties such as density, viscosity, and boiling behavior.

In many cases, a closed working fluid cycle is used to prevent wasting working fluid at the outlet of a liquid jet vacuum pump and to recover it for further use. Behind the jet pump, a separator divides the working fluid from the gas, and a circulation pump feeds the liquid back as working fluid. The temperature of the circulating fluid inevitably increases in this operating mode due to the input of pump power and possible condensation of suction stream components. Therefore, a heat exchanger for recooling the liquid is required in the cycle.

The vapor pressure of the working fluid at operating temperature limits the obtainable minimum suction pressures. A water jet vacuum pump with a working fluid temperature of 20 °C, for example, cannot deliver an ultimate suction pressure below 23 hPa. In contrast, ultimate pressures down to 4 hPa can be obtained by using a motive fluid with negligible vapor pressure such as oil.

Counterpressure (outlet pressure) is usually atmospheric pressure although pumping against increased counterpressure is possible. The working fluid's fore pressure essentially determines the tolerable counterpressure and the corresponding motive fluid flow. The higher the motive pressure the lower the motive fluid consumption.

Intense mixing of the liquid jet and the pumped-down gas is necessary in order to obtain optimal pumping speed. This is achieved by integrating a torsion body into the jet nozzle that breaks the liquid jet at the outlet of the jet nozzle. Flow in a water jet pump created in this way is an extremely complex phenomenon. Thus, dimensioning and design until today are based solely on empirical investigations.

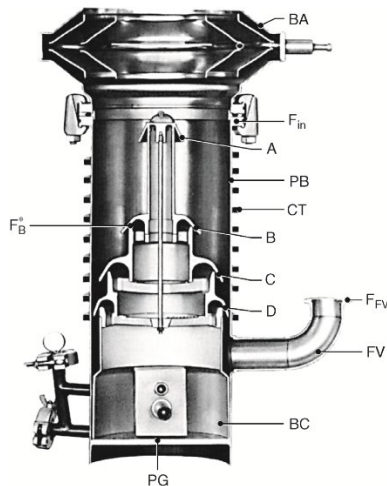


Figure 5.7 Section of a four-stage diffusion pump with attached baffle. A, B, C, D: concentric nozzles; BA: baffle;  $F_{in}$ : high-vacuum flange;  $F_{FV}$ : fore-vacuum flange;  $F_{B^*}$ : narrowest cross section; CT: cooling tube (water cooling); PG: ground plate; PB: pump body; FV: fore-vacuum tube; BC: boiling chamber.

Because pumping speed in a liquid jet vacuum pump is much higher at high suction pressure than at ultimate pressure, this type of pump is particularly useful for startup evacuation of vacuum systems. Typical applications are:

- startup evacuation of suction lines in large centrifugal pumps;
- a variety of vacuum processes in chemical industry;
- evacuation of turbine condensers in power plants.

Liquid jet vacuum pumps are especially suitable for applications where process characteristics require mixing of pumped-down gases and a liquid because the high velocities of flow in the mixing zone of the jet pump present ideal conditions for heat and mass transfer. Due to this property, wastewater technology and drinking water conditioning increasingly utilize water jet pumps for intensively mixing air, oxygen, and ozone with the water to be treated.

Their simple design allows manufacturing jet pumps from a variety of materials. Apart from carbon steel, cast iron, bronze, and stainless steel used in standard designs, other materials such as plastics, porcelain, graphite, or glass are also applicable. Due to this circumstance, jet pumps are utilizable in applications processing aggressive and extremely corrosive media.

Due to relatively low prime costs and easy installation, standard applications use liquid jet vacuum pumps when investment costs are particularly important.

Jet pumps using water vapor as motive fluid (motive steam) are very important for vacuum technology and are applicable down to suction pressures of 1 Pa (0.01 mbar). The typical pressure

range for the motive steam is in the range of 2–20 bar. Due to relatively simple basic geometry of the jet pump and the absence of moving parts, hardly any restrictions arise in terms of materials selection and utilization. Standard materials such as carbon steel, cast iron, bronze, stainless steel, and a variety of plastics already cover a large number of applications. However, using special materials, for example, Hastel-loy, titanium, graphite, porcelain, or even glass, is possible and in fact common in jet pump fabrication.

## Diffusion Pumps

The concept of diffusion pumps can be traced back to an invention by Gaede [3], who was also the first to use this term. Figure 5.7 shows a cross section of a diffusion pump. The cylindrical pump body PB terminates at the top in the high-vacuum inlet flange  $F_{in}$ . A baffle BA is attached to the upper baffle flange. The impact plates of the baffle prevent vapor from entering into the vacuum chamber. At the bottom, the pump body is sealed with a ground plate PG. It forms the heated boiling chamber BC for the pump fluid. The fore-vacuum line FV is attached to the side and contains a small flange FFV for connecting the fore pump. Above the fore-vacuum line, water flows through cooling tubes CT that cool the pump body. Cooling can also be provided by a cooling jacket or, in case of air cooling, by cooling fins. The pump body holds the internal part of the pump including the nozzle system. The image shows a four-stage pump with one high-vacuum stage (A), two medium-vacuum stages (B and C), and one fore-vacuum stage (D). Diffusion pumps with fewer or more stages are also available.

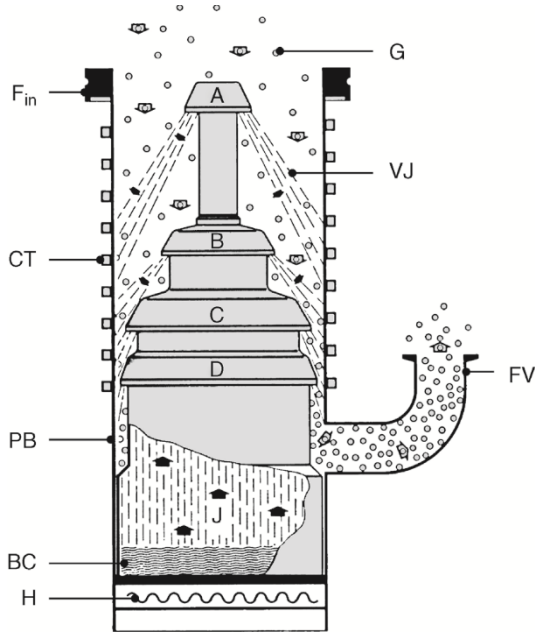


Figure 5.8 Operating principle of a diffusion pump. H: heater; BC: boiling chamber; PB: pump body; CT: cooling tubes;  $F_{in}$ : high-vacuum flange; G: pumped gas particles; VJ: vapor jet; FV: fore-vacuum port; A, B, C, D: nozzles; J: vapor jet.

The operating principle is explained using Figure 5.8. A floor heater H or an immersion heater heats the pump fluid at the bottom of the pump body until a vapor pressure  $p_0 = 0.1 - 1 \text{ kPa}$  develops in the boiling chamber BC. The vapor jet J moves upward inside the vapor tubes of the internal part, enters the annular nozzles A to D (see Figure 5.7) that are formed by the vapor tubes and the nozzle caps, and is deflected downward at this point. Behind the narrowest cross section (e.g.,  $F_b^*$  in Figure 5.7), the vapor jet expands according to gas-dynamic laws and ultimately enters the chamber formed between the nozzle system and the cooled wall of the pump body. Here, expansion and velocity continue to increase.

In the volume below each nozzle cap, an umbrella-shaped vapor jet with annular cross section develops between the nozzle system and the cooled pump body wall. The jet moves downward at high supersonic velocity ( $M \approx 3 - 8$ ). The gas particles G, which are to be pumped, enter the pump from the top through the high-vacuum connection  $F_{in}$  and initially encounter the vapor jet of high-vacuum nozzle A. They diffuse into the jet and accelerate downward due to impacting particles. The vapor condenses when it touches the cooled wall of the pump body PB. The noncondensable gas molecules enter the vapor jet of the intermediate stages B and C where they again accelerate and are transported to the chamber of the fore-vacuum stage D. The gas pressure increases from one stage to the next. The pressure ratio (compression ratio) for a stage can be expressed by the following equation: eject

$$\frac{p_{before}}{p_{after}} = \exp\left(\frac{\rho u d}{D}\right) \quad (5.2)$$

where  $\rho$  is the density of the pump fluid,  $u$  is its velocity, and  $d$  is the width of the jet. The diffusion coefficient  $D$  is approximated by using the molecular weights  $M_G$  and  $M_M$ , and the molecular diameters  $d_G$  and  $d_M$  of the gas and the motive medium, respectively [4]:

$$D = \frac{3}{8\sqrt{2\pi}} \left( RT \frac{M_G + M_M}{M_G M_M} \right)^{0.5} \left( \frac{d_G + d_M}{2} \right)^{-2} \quad (5.3)$$

The compressed gas then enters the fore-vacuum tube FV and is pumped off by the fore-vacuum pump. The condensed motive medium drains down at the inside of the pump body until it reaches the evaporation chamber where it re-evaporates in a cycle.

For constant mass flow, the volume flow rate of the pumped-down gas decreases as it travels from one stage to the next. Therefore, the inside of the pump is designed in such a way that the annular pump surface between the individual nozzle systems and the wall of the pump body decreases from one stage to the next. This has the advantage that the vapor expands less in the stages on the fore-vacuum side and, thus, a higher at-rest (or static) pressure ratio is obtained. This means a higher tolerable pressure on the fore-vacuum side.

Therefore, the first stage of a diffusion pump has the highest pumping speed and the lowest compression ratio. The opposite is the case for the last stage. Smaller diffusion pumps usually have three stages, while larger ones have up to five or six.

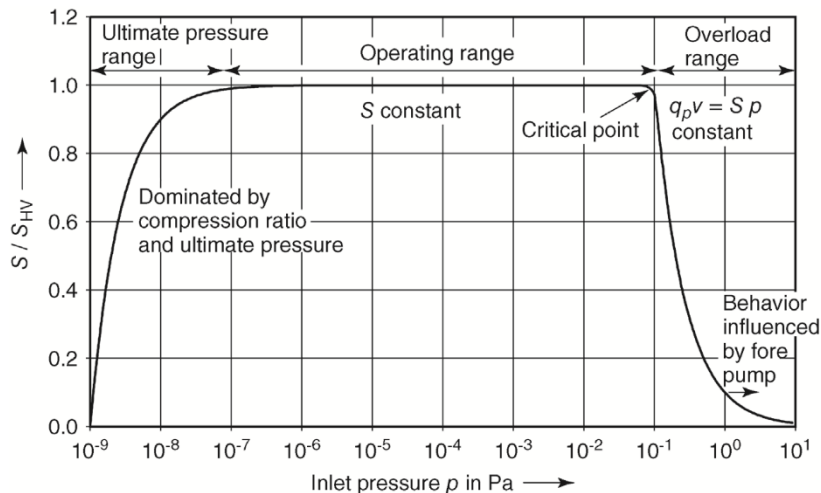


Figure 5.9 Diagram of relative pumping speed (SHV: high-vacuum pumping speed) in a diffusion pump with supposed ultimate pressure of  $10^{-9}$  Pa and the critical point at 0.1 Pa.

Proper cooling of a diffusion pump is crucial for its operation. The highest cooling demand occurs at points where the vapor jet hits the pump wall. If the cooling capacity is too low, the vapor condenses partially and may infiltrate the recipient to be evacuated (backflow). If cooling capacity is too high, the condensate cools too far and flows slower to the evaporation chamber. Thus, the maximum pumping speed of the pump drops and, additionally, unnecessarily high heating power is required for re-evaporation.

Figure 5.9 shows a plot of the pumping speed of a diffusion pump versus inlet pressure. Below a critical pressure, the pumping speed is constant because the probability for gas-molecule impact on the pump flange as well as their pumping probability in the vapor jet is pressure independent. On principle, this pumping speed remains unchanged even for arbitrarily low pressures. However, for very low pressures, the measured or apparent pumping speed drops because the compression ratio, that is, back diffusion from the fore pump, and outgassing of the pump determine the pressure in the pump. The main cause of outgassing in the pump is the backflow of pump fluid and its fugitive fractions.

Beyond the critical point (Figure 5.9) lies the area of constant particle flow: maximum throughput of the pump is reached. In the lower part of this overload area, the size of the fore pump is already very important and can lead to an increase or decrease in  $S(p)$ . In processes with known gas flow rates, the size of the diffusion pump is matched to obtain a pumping speed that is above this rate, and to deliver the desired process pressure.

Several factors may cause undesired pump fluid flow into the recipient (back diffusion):

- Vapor jet molecules from the top first stage accelerate toward the inlet flange due to interactions with gas particles or other motive medium molecules, or due to imperfect nozzle shape.
- Condensed vapor molecules re-evaporate and travel toward the inlet flange. Pump fluid oil creeps to the recipient along the walls.
- Just in front of the heater, oil droplets heat up high enough for them to accelerate toward the recipient as drops (similar to oil splattering in a frying pan).

Appropriate nozzle shapes as well as vapor trap sand baffles mini-mize back diffusion. It should remain below  $1 \times 10^{-10} \text{ g cm}^{-2} \text{ min}^{-1}$ . Corresponding values have in fact been measured [6]. The problem of back diffusion is also covered in [6–9].

## 5.4. Molecular and turbomolecular pumps

Molecular and turbomolecular pumps are connected with each other through their fundamental physical working principles [9]. In both pump types, gas is transported as momentum is transferred to the gas molecules thereby achieving a directed movement.

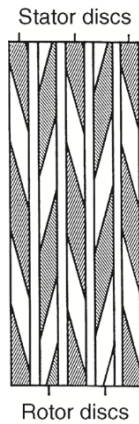


Figure 5.10 Periphery of the rotor/stator stack in Becker's turbomolecular pump. The stator disk at the inlet of the pump increases the compression ratio but reduces the pumping speed.

The momentum transfer takes place through a quickly moving wall or by blades of a quickly turning rotor. Indeed, this principle can only be in the molecular flow range because in this, the mean free path of the gas molecules to be pumped is greater or, better still, substantially greater than the distances within the pump. If one reduces the dimensions accordingly, additional regimes are attainable that usually would be ascribed to the transition range between molecular and viscous flow areas (several hPa). If the dimensions between the walls are decreased accordingly, additional ranges are attainable that usually would be ascribed to the transition range between molecular and viscous flow (several hPa).

Due to this circumstance, a molecular pump is usually not capable of compressing and ejecting against atmospheric pressure but requires a backing pump that compresses from the outlet pressure of the (turbo)molecular pump to ambient pressure. Positive displacement pumps, as described above, that compress to atmospheric pressure are used as backing pumps.

Turbomolecular pumps are built up of fast rotating rotor disks with blades and mirror-symmetrical stator disks lying in between [4] (Figure 5.10). Gas particles are transported through the channels between the blades by an additional momentum transferred by the rotor blades.

Today, turbomolecular pumps are often combined with molecular pump stages, which are designed to exhaust gas at higher pressure. This allows the employment of cheaper, dry positive displacement pumps as backing pumps.

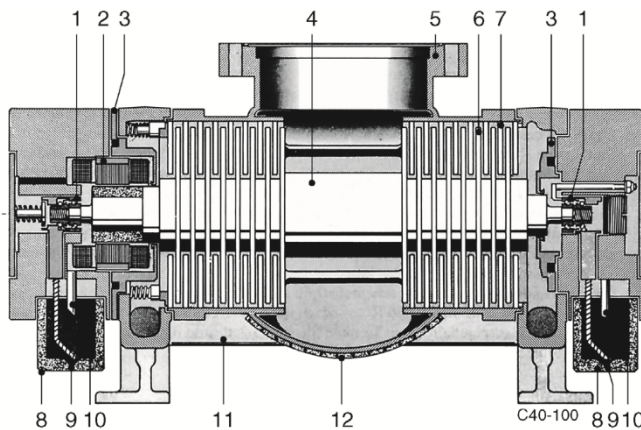


Figure 5.11 Section of Becker's double-flow turbomolecular pump TPU 200. 1: ball bearing; 2: motor; 3: labyrinth box; 4: rotor; 5: high-vacuum flange; 6: rotor disk; 7: stator disk; 8: oil reservoir; 9: oil supply wick to bearing; 10: oil-backflow line; 11: fore-vacuum channel; 12: heating jacket.

In contrast to sorption pumps, which are limited in terms of their gas storage capacity and require regeneration phases, turbomolecular pumps are ready for operation quickly and transport gas through the pump continuously.

Due to the multistage axial pumping principle of the turbomolecular pump, low pressures can be generated at the inlet flange. Desorption of gases, which limits the ultimate pressure, can be reduced by baking. High compression ratios for heavy gases yield ultimate pressures in the area of  $10^{-9}$  Pa. The same pumps can also be used to pump high gas throughputs in the inlet pressure range of  $10^{-1}$ – $1$  Pa. Nowadays, applications of turbomolecular pumps in vacuum process technology with high gas loads (coating, semiconductor production) are economically

far more important than pure vacuum production. The latter was the main field of application at the time such pumps were introduced on a greater scale.

In 1956, W. Becker [4] invented the turbomolecular pump (Figure 5.11). He explained the

basic operating principle of his new molecular pump by the aid of Gaede's theory of the molecular pump. Becker's turbomolecular pump was the so-called double-flow pumps: Two multistage rotor-stator systems with turbine blades (Figure 10.1) pumped the gas from the inlet flange in the center to the fore-vacuum chambers, one of which also contained the drive unit. A common fore-vacuum line is connected to the backing pump. In this way, the ball bearings at both ends of the pump shaft could be housed in the fore-vacuum chambers. Advantages over the previously designed Gaede pump [5] are: high pumping speed, large distances between rotor and stator ( $\approx 1$  mm), and a very high compression ratio due to the multistage design.

Further developments led to single-flow pumps with a smaller, lighter, and more economical design (Figure 5.12). Direct flange mounting to the recipient reduced conductance losses.

### Molecular Pumps



Figure 5.12 Single-flow turbomolecular pump HiPace 700 by Pfeiffer company with attached drive electronics for 48 V DC. 1: high-vacuum flange; 2: fore-vacuum flange; 3: venting valve; 4: purge-gas port; 5: electronic drive unit with remote control socket.

Molecular pumps are also found in the product portfolios of the large manufacturers, but are primarily used in niche applications [6,7]. Generally, the construction methods used follow Gaede, Siegbahn, and Holweck in fore-vacuum-sided pumping stages within turbomolecular pumps to reach higher output pressures. Such types of modified turbomolecular pumps are frequently referred to as compound pumps. Because these turbomolecular pumps are based on historically older molecular pumps and the operating principle of turbomolecular pumps can be well explained by considering this type of pump, we will first discuss the molecular pump.

The type of gas flow is the core difference between the molecular pump stage construction methods: In Gaede stages, it is pumped in a circumferential direction, following Siegbahn, radially along a disk surface, and with Holweck, in a thread-type groove in the surface of a cylinder.

### Turbomolecular Pumps

After the physical fundamentals, the most important technical components and the practical application of the turbomolecular pumps are introduced in the following. Special weight has been given to the description of the rotor and its bearing.

In contrast to the model shown in Figure 5.12, today's turbomolecular pumps are designed as single-flow systems, that is, the first high-vacuum stage is arranged directly below the suction flange in order to reduce conductance losses. A compound pump, that is, a turbomolecular pump with integrated molecular pumping stage, is shown in Figure 5.13. In the housing (1), the bearings (8) and (11) are supporting the rotor (3). The rotor is moved by a motor (13) in quick rotation that is driven by flange drive electronics (28), see also 10.5.5. Between the rotor disks, which mounted on a shaft (4), diametrically split stator disks (2) are inserted. These are held at an axial distance by distance rings. The molecular stage is executed as a Holweck stage, in which a Holweck sleeve (24) attached in at least one Holweck hub (19) rotates within a Holweck stators (12). Particularly with a multistage concentric design, very high compression ratios  $K_0$  of up to 108 are achieved at a low overall length whereby for low gap widths between rotor and stator, exhaust pressure can rise up to approximately 1500 Pa.

The gas enters the pump through the suction flange (16), is compressed by several turbomolecular stages, and is fed to the backing pump via the fore-vacuum port (17). Genuine turbomolecular pumps produce fore-vacuum pressures of approximately 50 Pa under high gas loads.

In compound pumps, the gas compressed by the turbomolecular stages is transported to the Holweck stages with lower pumping speed where it is compressed to a fore-vacuum pressure of 100–1500 Pa. After pumping is completed, the pump can be vented via the vent valve (18). Today two rotor designs are common. The first design is shown in Figure 5.13 and consists of a rotor with disks shrunk onto the shaft. Hence, these are frequently also referred to as "disk rotors". The shaft is

mounted at its two ends: A permanent magnet bearing suited for ultrahigh vacuum (UHV) is found on the suction side and a ball bearing is provided on the fore-vacuum side. The second design is generally referred to as a “bell-shaped rotor”. With this, the blades are milled from the external circumference of a cylindrical base metal. In the center of the base metal, a hollow cavity is created that contains a central shaft and houses the motor and bearing.

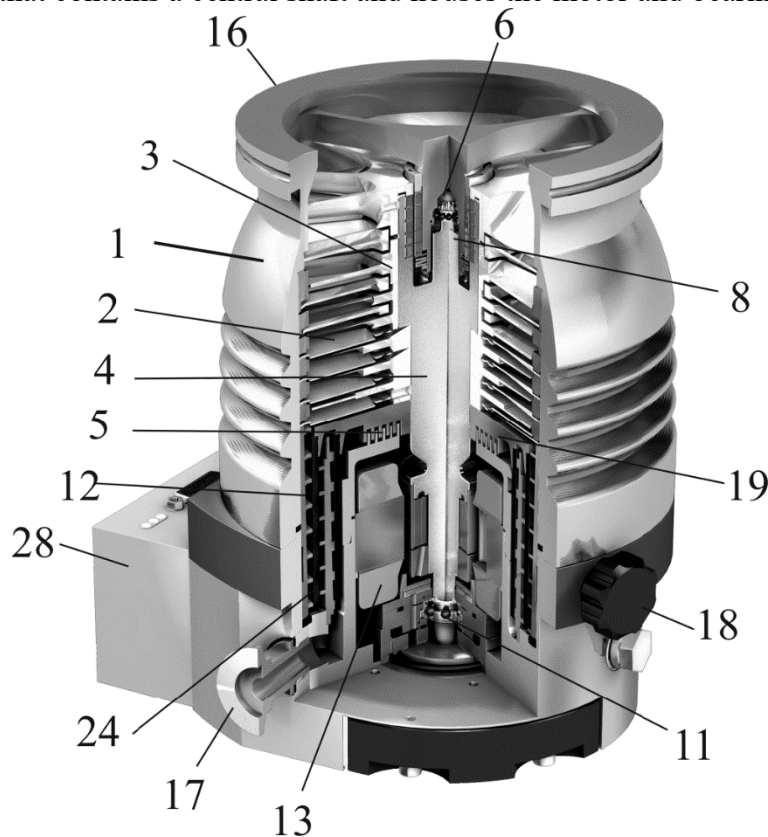


Figure 5.13 Turbomolecular pump with rotor disks shrunk onto the shaft. Bearings at both ends (UHV compatible permanent-magnet bearing on the inlet side and oil-lubricated bearing on the fore-vacuum side) provide favorable dynamic behavior of the rotor. 1: housing; 2: stator; 3: rotor; 4: rotor shaft; 5: labyrinth seal; 6: safety bearing; 8: radial magnetic bearing; 11: lower ball bearing; 12: Holweck stators; 13: motor; 16: suction flange; 17: fore-vacuum port; 18: vent valve; 19: Holweck hub; 24: Holweck sleeves; 28: electronic drive unit.

permitted operating condition. These rotors reach circumferential speeds of up to  $500 \text{ m s}^{-1}$  without exceeding tolerable material stresses.

In bell-shaped rotors, the blades are milled from solid bulk material. The large inside diameter with space for motor and bearings leads to high tangential stresses in the bell. Therefore, the rotational speed is limited. Optimum machining and shaping permits circumferential speeds of  $400 \text{ m s}^{-1}$ .

### Drives and Handling

The high rotary frequencies in turbomolecular pumps are produced by drives using electronic frequency converters. Due to their higher efficiency, brushless direct current (DC) motors with permanent magnets mounted directly on the shaft replaced the formerly used three-phase asynchronous motors. In view of a vibration-optimized operation, brushless, sinusoidally commutated synchronous drives are also used. In brushless DC motors, no current warms up the motor. Therefore, small pumps with  $S = 50\text{--}100 \text{ l s}^{-1}$  are capable of operating on convection cooling and obtain high bearing service life. Motors are available with Hall probes and, also, sensorless variants, where the rotor position is determined by the curve of the coil voltage. Sensorless systems

With both designs, a part of the fore-vacuum-side turbomolecular pump disks can be replaced by one or more concentric Holweck stages (12) in order to produce higher exhaust pressures, whereby diaphragm pumps can be used as backing pumps.

Disk rotors offer the advantage that they can be connected in parallel in order to obtain high gas throughput and fore-vacuum pressures of approximately  $100 \text{ Pa}$ . For this, openings are arranged in the Holweck hub (14) between the two Holweck cylinders, and the thread grooves in the stator are designed accordingly. A part of the Holweck hub can be used to dynamically seal the bearing range and motor range from the pumping space by means of a labyrinth seal (5).

Rotor disks and shafts (Figure 10.18) are made from high-strength aluminum alloys. They comply with special criteria in terms of purity and homogeneity of materials.

Carbon fiber sleeves are used for Holweck rotors. Their low expansion due to thermal load and centrifugal forces guarantees nearly constant inside and outside gap widths in Holweck stages under any

can be more easily used when chemical effects exist or the pumps are exposed to high-energy radiation.

In applications with high-energy radiation (particle accelerators), which can destroy semiconductor components, electronic drive units have to be arranged at a safe location and long cables (up to 100 m) are used to connect them to the pump. Alternatively, asynchronous drives with mechanical frequency converters are used.

Nowadays, advances in miniaturization have promoted designs in which electronic drive units and sometimes the power supply are mounted directly to the pump in order to save an expensive cabling. A DC power supply or mains voltage is used for energy supply (Figure 5.12). Water-cooled pumps require water-protected electronics for directly mounted systems because of water vapor condensation.

Several solutions are available for handling and controlling turbomolecular pumps (see Section 10.7): hand-operated systems, remote control via relays, and computer control through a serial interface (manufacturer-specific) or fieldbus system with standard interface, often combined with a programmable logic controller (PLC).

For operation within a system, inputs and outputs are equipped for controlling the most important functions. Adjustments are made using handheld equipment or a computer. Some manufacturers offer analog inputs with which parameters, particularly the rotary frequency, can be adjusted. Relay outputs signalize nominal speed and possible errors.

A computer over an interface, for example, a serial interface, offers the most comprehensive control possibilities such as with the RS 485. Direct communication is possible only with a manufacturer-specific transmission protocol. Universal control is supplied by a fieldbus system, which can also control other system components. This requires special fieldbus converters (Profibus, DeviceNet). Customer-specific interfaces are provided with the purchase of appropriate quantities.

### **Backing Pump Selection**

The pumping speed of the backing pump shall lie between 1 and 10% of that of the turbopump. Larger backing pumps should be used for larger vacuum chambers and higher gas throughputs. Additionally, manufacturer's guidelines should be respected.

For genuine turbomolecular pumps, two-stage rotary vane pumps or dry fore-pumps should be used with an ultimate pressure  $< 10$  Pa. Compound pumps require less powerful fore-pumps due to their higher fore-vacuum tolerance (critical backing pressure). If the recipient volume is less than 20 l and the pump-down time is irrelevant, a diaphragm pump with  $S = 1 \text{ l s}^{-1}$  is sufficient for a compound pump with a pumping speed of  $500 \text{ l s}^{-1}$ .

To avoid conductance losses, the inlet flange of the turbomolecular pump shall be directly mounted to the recipient. During installation, cleanliness is important. UHV applications call for exclusive use of metal seals. Splinter shields can be mounted into the inlet flange to prevent parts from falling into the pump. However, such measures reduce pumping speed by 5-20%. For vibration-sensitive applications, anti-vibration bellows can be mounted between the pump and the recipient.

Manufacturer's installation instructions should be followed carefully due to the risks involved with possible unpredictable rotor fracture.

### **Startup**

Generally, in case of an oil-sealed backing pump a turbomolecular pump should be started simultaneously with the backing pump to prevent oil-vapor backflow to the recipient, but also in case of a dry backing pump this is an appropriate operation. Delayed starting of the turbomolecular pump is recommended only for pump-down times of the backing pump of more than 10min.

### **Obtaining Base Pressure**

For desired pressures  $< 10^{-6}$  Pa, the turbomolecular pump and the recipient require baking. For this, pumps are equipped with special heating jackets that produce tolerable pump temperatures. If the baking temperature for the recipient is higher than for the pump, the radiation power transmitted to the pump must be calculated. Radiation must be limited in compliance with manufacturer's guidelines. Depending on the temperatures, heating periods of 3-48 h are required to produce base pressures  $< 10^{-8}$  Pa. Residual gas should then only contain masses 2 (hydrogen), 18/16 (water), 28

(CO), and 44 (CO<sub>2</sub>). These constituents desorb continuously from the metal surface of a stainless steel recipient.

### **Operation in Magnetic Fields**

Magnetic fields induce eddy currents in the rotating parts of a pump, which increase the temperature of the rotor. Because heat radiation is the only way of transporting the dissipated energy, magnetic induction must be limited to values between 5 and 10 mT by ferromagnetic shielding.

### **Venting**

Turbomolecular pumps should be vented after shutdown in order to avoid back diffusion of hydrocarbons through the pump from the fore-vacuum side. For gas inlet, special venting ports are arranged between the lowest turbine disks or, in compound pumps, above the Holweck stage. For venting, automatic devices are available that vent for a predefined period only, after the speed drops below an adjustable speed-switch point. This also prevents accidental venting of the vacuum system in the case of short-time power loss. Venting with dry inert gas instead of ambient air avoids water vapor input to the pump. For restart, this measure reduces the time to reach the desired ultimate pressure. Additionally, it prevents chemical reactions between water vapor and possible deposits from the vacuum processes.

Mechanical bearings in turbomolecular pumps are designed to withstand accidental venting through large openings without showing any immediate defect. However, in such situations, the bearings for a short time are overloaded heavily, which reduces their service life. Therefore, for normal operation, certain gradients in pressure rise should not be exceeded during venting.

Axial forces on the bearings rise during venting and generate higher currents in the magnetic bearings (helicopter effect). If the current in the axial bearing of a pump reaches a limit, venting is interrupted, and is not continued before the current drops below a lower limit. Thus, the pump is rapidly vented but without any safety-bearing contact.

### **Maintenance**

Turbomolecular pumps are usually used within very expensive installations (coating systems, semiconductor production, particle accelerators) where down-times produce high costs. Users, therefore, often call for maintenance-free pumps. The minimum request though is that preventive maintenance guarantees reliable operation during a production period.

First, we will focus on pumps with ball bearings. When using hydrocarbon-containing oil, the oil should be replaced according to manufacturers' guidelines. Fluorinated oils do not require replacement under clean operating conditions because they are not subject to any aging. When running processes that produce contamination, special determination of oil-change intervals is advisable. Additionally, if necessary, bearings can also be replaced easily as long as this does not require rebalancing the rotor.

Grease-lubricated bearings have to be replaced after the service life of the lubricant because regreasing is not possible without risking a loss in service life. In pumps with bell-shaped rotors and two ball bearings, parts of the rotor shaft then must be disassembled which might require rebalancing of the rotor.

Safety bearings in pumps with magnetic levitation are subject to wear. They are designed to withstand approximately 20 rotor breakdowns at full speed and 200 gradual run-outs during long-lasting power failures. If such situations arise more often, safety bearings should be replaced preventively. Some manufacturers indicate the wear by monitoring the rotor-running period in the bearings.

In processes with heavy dust generation, the bearing chamber of a pump can be protected by a flow of purge gas in order to prevent contamination. Dust accumulating on rotor blades can cause increasing unbalance and large amounts of dust can clog pump channels. Then, dismounting and cleaning of the pump after certain process-dependent operating periods is necessary.

Turbomolecular pumps used in physical research are often exposed to considerable doses of high-energy radiation. Such radiation can destroy semiconductor components as well as certain plastics. Electronic drive units should, therefore, be arranged at a safe distance and connected to the pumps via long cables. Otherwise, mechanical frequency converters are used.

Ready-for-use pumping units are available for evacuating vacuum chambers for numerous applications. These systems can be equipped with different types of turbomolecular and backing vacuum pumps.

### 5.5. Sorption pumps

Sorption pumps are arrangements in which impacting gas particles are bound to appropriate surfaces due to sorption. This reduces the gas pressure in the container. Thus, sorption pumps act as gas traps without actually transporting the gas through the pump as in the true sense of the word. Sorption pumps are used throughout the entire vacuum pressure range, but chiefly in UHV technology, to produce hydrocarbon-free vacuum.

ISO 3529/2 [11] and DIN 28400, part 2 [9], differentiate between (Figure 5.14) adsorption pumps, getter pumps 11 getter derived from to get, sublimation pumps, and ion getter pumps, the latter divided into evaporation ion pumps and sputter ion pumps, as well as the cryosorption pumps.

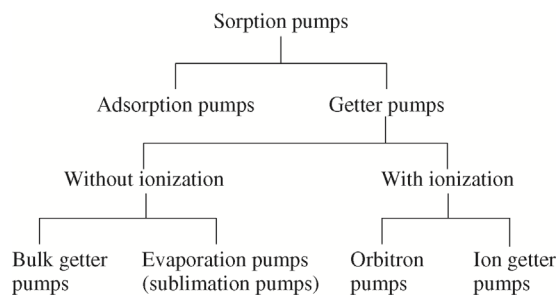


Figure 5.14 Classification of sorption pumps according to sorption principles.

For pumping action, adsorption pumps use the effect that certain solids, particularly at low temperatures, bind considerable amounts of gas. Solids with very large specific surface areas bind gas mostly due to physisorption. The pumps are used in the low and medium-high vacuum range.

A getter pump is a sorption pump in which gas binds to a getter material mainly due to chemisorption. This material is usually a metal or metal alloy, either bulk material or a freshly deposited thin layer.

Pumps that not only adsorb the gas at a surface but also use the effect of gas diffusing into a compact getter material are referred to as bulk getter pumps.

For example, to improve or sustain vacuum in small sealed systems such as CRTs, certain solids are enclosed in the system as getter material that sorbs gases and vapors. Today, NEG pumps represent the predominant type of bulk getter pumps.

In contrast, so-called evaporation getter pumps (sublimation getter pumps) adsorb gas at the surface of continuously or intermittently fresh-deposited thin getter surfaces.

Bulk and evaporation getter pumps are not capable of pumping noble gases and other gases that are relatively passive in their chemical behavior such as methane. Ion getter pumps were developed in order to be able to pump such gases as well.

Ion getter pumps include an additional electrode arrangement that ionizes the gas particles and lets them bombard the getter surface by means of an acceleration voltage. These pumps include so-called orbitron pumps and sputter ion pumps.

Orbitron pumps no longer have any commercial importance and are therefore covered at the end of this chapter. All getter pumps are used to produce high pumping speeds at relatively low pressures (low gas loads), for example, in UHV processing systems, particle accelerators, space simulation chambers, and surface analysis equipment. The latter particularly benefit from the vibration-free operation of this pump type.

Pumping action in ion pumps is produced solely by ionizing, accelerating, and implanting gas particles into solid surfaces by means of electrical fields. Due to low pumping speeds, they are not used in practice. However, the operating principle is used in ion getter pumps and sputter ion pumps, in addition to the getter effect, in order to also pump noble gases and other gases that are difficult to getter.

#### Adsorption Pumps

Certain porous substances, mainly activated carbon and zeolite, show very large specific surface areas (i.e., with respect to mass  $m$  of the porous solid) in the range of  $A_m = A/m \approx 10^6 \text{ m}^2 \text{ kg}^{-1}$ . Thus, the adsorption capacity for gas at the inner surfaces of these

substances is substantial. Monatomic layer of a particles covering a surface corresponds to a particle-number surface density  $\bar{n}_{mono} = 10^{15} \text{ cm}^{-2}$ , that is, approximately  $10^{15}$  particles lie closely packed on each square centimeter. This corresponds to an adsorbed surface-related amount of substance  $v_{mono} = \bar{n}_{mono}/N_A \approx 10^{15} \text{ cm}^{-2}/6 \times 10^{23} \text{ mol}^{-1} = 1.7 \times 10^{-9} \text{ mol} \cdot \text{cm}^{-2}$  ( $N_A$  is Avogadro's constant). The equation of state  $pV = nkT$ , provides the adsorbed surface-related  $pV$ -amount:

$$\tilde{b} = \frac{pV}{A} = \frac{N}{A}kT = \tilde{n}kT \quad (5.4)$$

Multiplying with the specific surface  $A_m$  of the adsorbent yields the adsorbed mass-related  $pV$ -amount:

$$\tilde{\mu} = \frac{pV}{A} \times \frac{A}{m} = \tilde{n}kTA_m \quad (5.5)$$

Equations (5.4) and (5.5) show that the temperature at which  $pV$ -amounts are measured must be stated together with values of these quantities. Therefore, it is useful and usually necessary to relate  $pV$ -amounts to standard temperature  $T_{extrmn} = 273.15 \text{ K}$  in order to obtain definite values. However, the reduction factor for calculating from room temperature to standard temperature  $293/273 = 1.07$  and its reciprocal are often insignificant because the quantities  $p$  (in particular) and  $V$  show a measuring uncertainty of more than 7%. Equations (5.4) and (5.5) thus read

$$\tilde{b}_n = \frac{(pV)_n}{A} = \tilde{n}kT_n \quad (5.6)$$

and

$$\tilde{\mu} = \tilde{n}kT_n A_m \quad (5.5)$$

With

$$\bar{n}_{mono} = 10^{15} \text{ cm}^{-2} \text{ and } A_m = 10^6 \text{ m}^2 \text{ kg}^{-1}, \text{ we find}$$

$$\tilde{b}_{n mono} \approx 38 \text{ Pa l m}^{-2}$$

$$\tilde{\mu}_{n mono} \approx 3.8 \times 10^7 \text{ Pa l kg}^{-1}$$

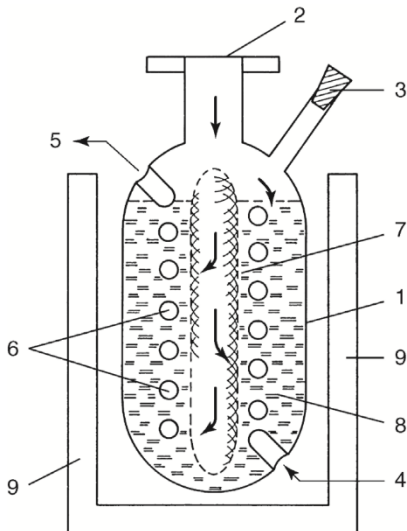


Figure 5.15 Diagram of an adsorption pump. 1 stainless-steel pump chamber, 2 inlet flange (suction port), 3 safety bung, 4 coolant inlet, 5 coolant discharge, 6 cooling coil, 7 tube sieve, 8 adsorbing medium (e.g., zeolite), 9 coolant vessel. Arrows indicate gas flow pumped by adsorption.

At low temperatures, the probability for a gas atom that sticks to the surface to desorb back into the gas volume is lower than that at high temperatures. Therefore, the ability to capture gas is higher at low temperatures than at high temperatures. If the adsorption mass in contact with the recipient volume is cooled, it binds more gas than at normal temperature. Thus, the efficiency of the adsorption pump increases. After the adsorption process has completed, a valve is shut between the adsorption pump and the recipient. On warming of the adsorbent (usually warming to room temperature is sufficient), the gas adsorbed at lower temperature escapes through a venting valve (safety valve 3 in Figure 5.15).

An adsorption pump (Figure 5.15) is basically built up of a vacuum-tight container filled with adsorbing medium (adsorbent). A cutoff valve is placed in the tube connecting to the recipient. Generally, commercial adsorption pumps all use synthetic zeolite. Zeolites are M-aluminum silicates with M denoting sodium, calcium, or lithium. They are produced synthetically in large scale and serve as molecular sieves for separation of mixtures. These utilize the principle of characteristic adsorption for the individual components of the mixtures. Figure 5.16 shows the structure model of a zeolite crystal with cages and pores for gas adsorption. Using activated carbon is dangerous. If a sudden inrush of air occurs, the released heat of adsorption can heat the carbon rapidly so that it may

explode in a reaction with atmospheric oxygen.

For cooling the adsorbent, the container is placed into a Dewar vessel filled with liquid nitrogen. If cooling of the adsorbent is interrupted after pumping and sealing, an automatic safety valve must provide a means for the released gas to escape. The simplest solution is a rubber bung in a tube (Figure 5.15).

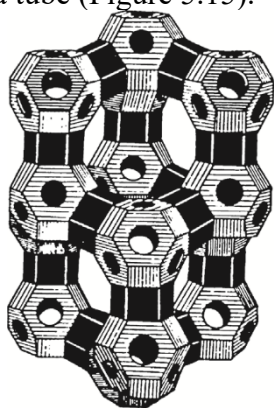


Figure 5.16 Model of an x-type molecular sieve structure [14].

A number of technical improvements are required to optimize the activity of the adsorbent. For rapid cooling and removal of the released adsorption heat during pumping, homogeneous cooling of the adsorbent is necessary [12]. Due to the low thermal conductivity of typical adsorption media, the pump body contains a system of cooling pipes or plates reducing the paths for heat transport. Additionally, an even distribution of gas load onto the complete surface of the adsorbent is mandatory [13]. For this, flow channels made of wire netting increase the surface area available for direct contact between gas and adsorbent. Furthermore, they reduce the flow paths through the closely packed adsorbent (Figure 5.15). Heating equipment regenerates the adsorbent, for example, an electrically heated jacket stretched around the outside of the pump body, which heats the adsorbent to 250-350°C.

### NEG Pumps

#### Requirements on Bulk Getters/NEG

Getter materials in bulk getters bind gas by chemical reaction. Thus, they must be chemically reactive toward residual gases typically occurring in vacuum (CO, CO<sub>2</sub>, N<sub>2</sub>, O<sub>2</sub>, H<sub>2</sub>O, H<sub>2</sub>, etc.). Additionally, however, they should provide easy handling in contact with atmospheric air when being mounted. Metals, in particular, fulfill the former condition. The second property is ascribed to evaporable getter materials because the reactive surface of the getter is produced under vacuum by evaporation. For example, the common barium getters are used to generate elemental barium through a reaction of a mixture of a BaAl<sub>4</sub> alloy and nickel at 800-1250 °C under high vacuum. The barium evaporates from the getter container and condenses as a reactive layer on the opposing surface.

Bulk getters or NEG are used primarily in applications where either evaporation of metal under vacuum is undesired or a surface for depositing a metal film is unavailable.

Bulk getters meet the second requirement by providing a thin protective, for example, passivating layer of oxides and nitrides. It forms spontaneously when the metal surface reacts with air, and protects the underlying metal from further reactions. Under vacuum and higher temperature, this protective layer dissolves due to diffusion into the bulk getter. Therefore, the materials used must also provide appropriate diffusion conditions for those gases to be bound.

#### Activating Bulk Getters/NEG

Getters bind gases at the surface. Thus, large surfaces are desired. After being placed in a vacuum, such surfaces, as any other surface, require decontamination from physically bound gases. This is done by baking.

The oxide/nitride layer on the passivating surface has to be dissolved in order to allow reactions between the getter material and gases. This step involves further heating under vacuum. In contrast to physically bound gases, the chemical bonds between NEG and oxygen as well as nitrogen atoms are too strong to be separated by heating. Therefore, even at temperatures around 1000 K, equilibrium pressures of, for example, oxygen and nitrogen, above their corresponding compounds are in the range of only 10<sup>-15</sup> Pa [15].

However, high temperature increases the diffusion rates of oxide and nitride ions in the getter. Following the concentration gradient, the ions migrate into the bulk getter and the surface returns to its metal state, and thus, regains the ability to bind gases. The temperature required for the diffusion process to take place within a given time depends on the type of getter material. The maximum time frame is usually predefined by the application. It spans from only a few seconds (lamp industry) to days (accelerator applications). In certain cases, partial activation of the getter surface is sufficient

#### Bulk Getter/NEG Stock

A pulverized getter alloy serves as raw material for getter production (the term getter refers

to the ready-made product including getter material as well as holding devices). The particle size is in the range of 50-150  $\mu\text{m}$ . Manufacturers provide getter products as getter strips, getter pellets, getter rings, and sintered bulk getters (known as porous getters).

- Getter strips (Figure 5.17).
- Here, the getter material is rolled on a carrier tape from one or both sides using high force. The carrier is made of a nickel-plated iron sheet or con-stantan (nonmagnetic).
- Getter pellets.
- If the getter material is not too brittle, it can be compressed to pellets.
- Getter rings.
- Getter material is pressed into metal rings with U-shaped cross section. The shape of the ring improves activating when heated with high-frequency excitation.
- Sintered bulk getters (porous getters).

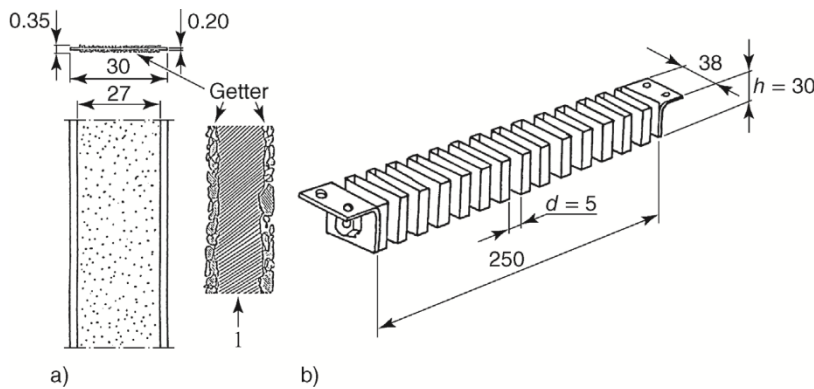


Figure 5.17 Strip getter: (a) standard strip getter 30D, dimensions given in millimeters; (b) strip getter folded to meander shape with a fixing device (getter module). Courtesy of SAES Getters S.p.A.

Mixing getter alloys with suitable metal powders yields sinterable mixtures that are sintered under vacuum to highly porous (up to 50% by volume), self-supporting sintered bodies. For mounting, either these getters are sintered onto metal foil, or carriers and heating elements are sintered into the material. Commercial sintered getters are made, for example, from zirconium (St 171), from zirconium and St 707 (St 172), as well as titanium and vanadium (St 185).

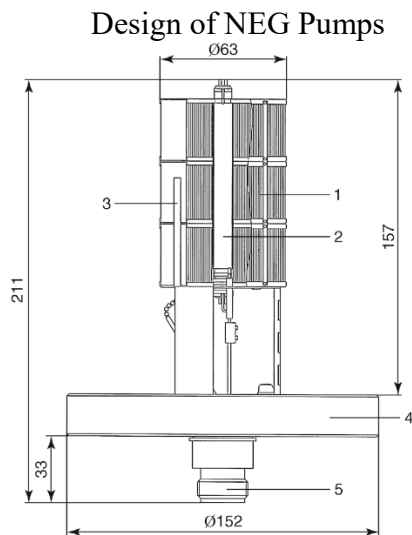


Figure 5.18 Side view with partial section of a bulk getter pump (GP200 MK5 type). Courtesy of SAES Getters S.p.A. 1 Getter cartridge, 2 heating element, 3 thermocouple, 4 base flange (CF), 5 electrical connectors for heater and thermocouple.

Ready to be installed combinations of getters and resistance heaters for activation are referred to as NEG pumps. Generally, the heating element is mounted in the center of a CF flange equipped with lead throughs. Replaceable getter cartridges are fixed to the flange. The getter cartridges are built up either of folded getter strips or sintered getter disks (Figure 11.10). In both cases, the cartridges are designed to provide optimal access and contact between the getter surface and the gases to be bound. Getter strips, for example, are arranged in the cartridge as bellow-type folded rings similar to automobile air filters. The getter cartridge is a cylinder with a central hole for a heating element. The setup in NEG cartridges that contain sintered getter disks is similar. Sintered getter material does not require carriers. Therefore, they usually carry more getter material in a smaller volume.

Special electrical power supplies (NEG pump controllers) are used for activation and are wire-connected to the pump via socket connectors. Larger getter pumps are equipped with temperature probes that allow automatic control of the getter material's temperature. One manufacturer's new series (MK5) features a flange that is bakeable to 400  $^{\circ}\text{C}$  after the socket connector is removed.

NEG-alloys may also directly be applied to the inner

vacuum chamber wall by coating [16]. By this method, which was developed and patented by CERN, the vacuum wall is turned from an outgassing source into a pump. It is helpful in particular where for geometrical reasons conductances to local pumps are small, for example, for insertion devices in high energy accelerators. The coating also reduces the outgassing rate and the secondary electron yield when the walls are exposed to photon (X-ray), electron, and ion bombardment. The getter is activated by a bake-out at 180 °C. The NEG alloy coating of the walls with a depth of about 1 μm is carried out by magnetron sputtering [16].

#### Applications of NEG Pumps

NEG materials are used in many applications that require sealed vacuum with long service life. These include any type of electron tubes [17], lamps, and stainless steel thermos flasks. Additionally, such materials are used for producing gas purifiers that purify process gases for semiconductor fabrication down to the ppt range [18]. Genuine NEG pumps are mainly used in UHV applications because of their high pumping efficiency for hydrogen that limits the ultimate pressure in such applications. Here, they operate together with other pump types, for example, turbomolecular pumps. In addition, ready-for-use combinations of ion getter pumps and NEG pumps are commercially available.

Applications cover surface analytics, very large physical experiments such as particle accelerators, experimental UHV setups, and so on. Furthermore, bulk getters have the ability of purifying noble gases. Such applications include industrial sputter systems (in situ purification) and equipment in geochronology laboratories.

Power consumption of getter pumps is low (after initial activation, further energy supply is often unnecessary). Thus, they are frequently used in mobile analysis equipment (GCM/MS) and space experiments. Bulk getter pumps can also be used to adjust a particular hydrogen partial pressure in a vacuum by setting getter temperature.

#### Evaporation/Sublimation Pumps

Usually, evaporation getters are made from the metals barium, manganese, aluminum, thorium, or titanium. Evaporation getters just as bulk getters are initially degassed using an auxiliary pump, preferably under high vacuum. For this, the getter is heated as far as possible without noticeable evaporation occurring. Analog to subsequent heating for evaporation, heat here is produced either by a high-frequency sleeve coil arranged at the outside of the recipient or by a current-carrying suitable refractory base plate (e.g., tungsten) that holds the getter material. Degassing is finished when the pressure, after rising considerably during heat up, drops close to the initial pressure.

After degassing, the getter material is evaporated using thermal energy. Sufficient evaporation rates are obtained at a vapor pressure of approximately 1 Pa. Evaporated getter material deposits at the walls of the recipient. The produced fresh surface takes up large amounts of gas. The Ba-Al alloy getter material BaAl<sub>4</sub>, designed to produce approximately 200–300 mg of pure barium, is powder-mixed with nickel and pressed into a nickel-coated steel ring. This is mounted at a suitable point in the tube. After evacuating and baking out, the ring heats up to 800 °C due to the action of an outside high-frequency coil. At this temperature, a slightly exothermal reaction occurs in the powder (1.0–1.5 g), the BaAl<sub>4</sub> alloy dissociates, and barium is released and evaporates. The barium vapor condenses at the cold inner surface of the tube walls and produces a thin reflective coating that reaches a temperature of approximately 60 °C during tube operation.

The relatively large amount of barium yields a getter layer with a geometrical surface area of several to many 100 cm<sup>2</sup>. This keeps the residual gas pressure in the tube below 10<sup>-5</sup> Pa throughout its service life: ultrahigh vacuum in your living room!

#### Ion Getter Pumps

Sorption in ion getter pumps relies on (cathodic) sputtering of a getter material inside a gas discharge, and additionally, on bombardment (implantation) of ions from the gas discharge. Utilization of these effects for development and design of vacuum pumps [19] was encouraged by investigations aimed at preventing such processes (gas depletion and erroneous pressure measurement) in ionization vacuum gauges.

Gas discharge in an ion getter pump is of the Penning type [20]. Figure 5.19 illustrates an

electrode arrangement, two parallel cathode plates  $K_1$  and  $K_2$ , and an anode cylinder  $A$  with the  $z$ -axis arranged perpendicularly to the cathode planes. A magnetic field of flux density  $B \approx 0.1 - 0.2 T$  is applied in the  $z$ -direction.

Operating voltage  $U$  between anode and cathodes is approximately 6 kV. Kna-uer [21] and Schuurman [22] thoroughly investigated the Penning discharge in such arrangements.

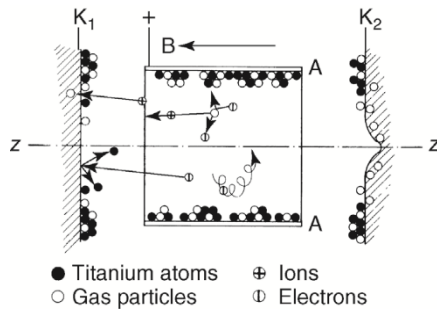


Figure 5.19 Diagram of the pumping action in a Penning cell (diode).  $K_1, K_2$  cathode plates made of getter material (titanium),  $A$  anode cylinder with the  $z$ -axis,  $B$  magnetic field. The getter film with buried gas particles is visible on  $A$  and toward the ends of  $K_1$  and  $K_2$ . Implanted gas particles in the center of  $K_2$  (and  $K_1$  as well, not drawn).

In detail, the pumping effects are as follows: Ion implantation. The applied electrical potential (6 kV) accelerates the ions produced in the discharge to several kV, depending on their point of origin. Acceleration occurs nearly along a straight path toward the cathode because the ions, due to their large mass compared to electrons, are hardly influenced by the magnetic field. The ions penetrate the crystal structure of the cathode by approximately 10 atomic layers (ion implantation). This corresponds to a gas depletion that affects any species of gas ion including atomic and molecular ions of noble gases and other gas species. However, very large molecular ions, such as hydrocarbons, do not penetrate the lattice structure. Of these ions, only the fraction disintegrating during surface impingement is pumped. The penetration depth of such fragments, however, is lower because their kinetic energy is low.

a) Cathode sputtering. The ions hitting the cathode are implanted in part and sputter individual or larger numbers of lattice atoms. These atoms are released and deposit on surrounding surfaces where they form the getter film when the cathode is made from getter material (e.g., titanium). The mass of the sputtered material is roughly proportional to the pressure

in the pump so that the pumping speed adjusts to this pressure. Pumping action, as any getter effect, is strongly influenced by the gas species. Depending on the field configuration caused by the electrons and the volume charge in the discharge, the ions accelerated toward the cathode can become focused to the  $z$ -coordinate. This produces a sputter crater in the center of the cathode (Figure 5.19, cathode  $K_2$ ). In any case, getter action takes place mainly at the edges of the cathodes and at the anode; implantation occurs mostly in the center of the crater because the getter film here is resputtered.

b) Neutral particle implantation. When ions, particularly noble-gas ions, impinge the surface, they can be reflected if they become neutralized in the metal. Indeed, this occurs often in an ion getter pump. Neutralized gas particles then become implanted at other spots because they still carry high kinetic energy.

The getter effect is the predominant effect in an ion getter pump. Nevertheless, the two implantation processes are very important because they represent the cause for noteworthy pumping speed of the ion getter pump for noble gases. For estimating the pumping speed of a Penning cell, we shall consider the following: the number of ionized gas molecules can be expected to be proportional to the pressure and to the number of electrons  $Q_e(p)$  in the volume charge cloud. The latter is slightly pressure dependent. Thus, the discharge current  $I$  amounts to

$$I = K_1 Q_e(p) p \quad (5.6)$$

with the proportionality constant  $K_1$ . The quotient  $I/p$  is also referred to as the sensitivity of the Penning cell.

Furthermore, it can also be expected that the rate of pumped molecules  $q_{pV}$  is proportional to the discharge current:

$$q_{pV} = K_2 I = K_1 K_2 Q_e(p) p \quad (5.7)$$

Because pumping speed  $S = q_{pV}/p$ , it follows that

$$S = K_1 K_2 Q_e(p) p \quad (5.8)$$

Also states that

$$I = Kp^m \text{ with } m = 1 - 1.4 \quad (5.9)$$

Equating Eqs. (5.6) and (5.8) yields

$$Q_e(p) = \frac{K}{K_1} p^{m-1} \text{ with } m = 1 - 1.4 \quad (5.10)$$

so that

$$S = KK_2 p^{m-1} \text{ with } m = 1 - 1.4 \quad (5.11)$$

From this derivation, pumping speed can be expected to drop, even though slightly, with pressure  $p$ .

Equation (5.8) shows that maximizing volume charge  $Q_e$  is beneficial for obtaining high pumping speed. This circumstance has promoted many investigations focusing on the parameters that influence  $Q_e$  (Table 5.1).

Table 5.1 Setting values in commercial ion getter pumps that influence the pumping speed of a Penning cell.

Quantity	Symbol	Variation range
Anode voltage	$U_H$	3.0–7.0kV
Magnetic field strength	$B$	0.1–0.2 T
Cell diameter	$d$	1–3 cm
Cell length	$l$	1–3.2 cm
Distance between anode and cathode	$a$	0.6–1.0 cm
Pressure	$p^m$	m=1–1.4

Under otherwise constant parameters, a minimum field strength  $B_{min}$  ( $\approx 0.03$  T) is required for sustaining the discharge. For  $B > B_{min}$ ;  $S$  initially rises fairly linearly up to a maximum and subsequently drops. In the region rising with  $B$ ;  $S$  also increases linearly with the high-voltage  $U_H$ . Investigations have shown that the distance  $a$  between the anode and cathode should not be too short so that passing of gas particles through the Penning cell is not hindered too much. Similar considerations apply to the length  $l$  of the cell. If  $l$  is too high, conductance for the gas is reduced thus counteracting the benefit of the higher volume charge. For constant  $l/d$ , larger values for  $d$  produce higher pumping speeds but only for pressures below  $10^{-4}$  Pa [23].

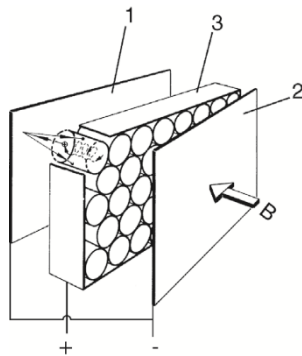


Figure 5.20 In reference to the design of a diode-type ion getter pump. 1, 2 Titanium cathode plates, 3 frame holding cylindrical anode cells. B Magnetic field produced by permanent magnets.

Since the discharge current  $I$  in the Penning discharge is proportional to gas pressure within certain pressure ranges, measurement of  $I$  can be used to determine the pressure in the pump as in a Penning vacuum gauge. However, it was observed often that, for hydrogen in particular [24],  $I$  (and thus  $S$ ) varies considerably in spite of constant pressure, depending on the condition of the pump. Therefore, this pressure reading should be interpreted very carefully. The discharge continues to glow at pressures  $p < 10^{-8}$  Pa. Therefore, baked-out ion getter pumps can be used to produce extremely low gas pressures.

Service life of an ion getter pump is determined mainly by the depletion of getter material. Depletion of the titanium cathode plates by sputtering in the electrode arrangement shown in Figure 5.20 is very inhomogeneous due to the crater formation described above. Thus, more than 90% of the total getter material is not exposed to the discharge and therefore remains unutilized. This efficiency can be increased by arranging the anode system (3) in Figure 5.20 so that it can slide parallel to the cathode plates [25]. Then, areas that have seen less or no exposure are sputtered as well. For working pressure  $p_w$ , approximate values for the service life  $t_s$  of commercial iongetter pumps are given by

$$\frac{t_s p_w}{h \text{ Pa}} \approx 4 \quad (5.12)$$

#### Technical Design (Diode Type)

If a single Penning cell provides a small pumping speed  $S_{P.c.}$ , then  $n$  such cells can be connected in parallel to produce a pumping speed  $nS_{P.c.}$ . Reikhrudel et al. [26] described the first multicell ion getter pump of this kind. Today, anode cells are connected in parallel in a honeycomb design (Figure 5.20). The common cathode plates are arranged at a distance of a few millimeters. The complete electrode system represents a diode and lies in a vacuum-tight, non-magnetic housing that is placed in the gap of a permanent magnet arranged out-side of the vacuum. Pockets in the housing are either included in a pump housing with a flange or placed directly into the wall of the recipient. The com-mon magnet system for all electrode systems has an annular yoke. This keeps stray field losses low and the magnetic flux density in the air gap, that is, in the electrode system, as high as possible. The electrode systems are commonly con-nected to an electrical current feed through in the wall of the pump housing, which is easily detached and replaced. Electrode systems in large pumps are replaceable as well. After the sputtered titanium has become depleted at the cathode, the electrode systems can be replaced by new systems.

A power supply provides high voltage, usually 3–7 kV, for the pump. A current limiter is required to protect the pump from overload as the discharge current rises proportionally to the pressure. For this, a constant-current transformer is often utilized. Voltage and discharge current are measured by monitoring equipment built into the power supply. For electrical current, a loga-rithmic measuring scale is usually available with the reading calibrated in pres-sure units analogous to the design in a Penning ionization vacuum gauge.

#### The Differential Ion Pump

The effect of noble-gas instability described in the previous section can be eliminated by a simple measure that replaces one of the titanium cathodes with a tantalum cathode [27]. Tantalum is a very hard material with high atomic mass that reflects noble gas ions with much higher energy as neutral particles than titanium. The kinetic energy of reflected argon atoms is up to 50 times higher than for titanium [28,29], depending on the reflection angle, and reaches up to 50% of the energy of incidence. This leads to an implantation depth in the anode or opposing cathode high enough for the atoms to be trapped for the rest of the serviceable life of the ion getter pump. This type of an ion getter pump in diode design is referred to as a differential ion pump (DIP). However, the getter effect of tantalum is lower than that of titanium.

This slightly reduces pumping speed compared to a conventional diode pump. However, in addition to noble-gas stabilization, the pumping speed for noble gases is increased to approximately 25% of the pumping speed for nitrogen (compared to approximately 5% in conventional diode pumps). The success of this diode arrangement proved that neutral-particle implantation is in fact an important mechanism, at least when considering noble gases. The inventors of the pump, Tom and James [27], initially tried to explain the higher pumping speed and stability for noble gases with a difference in sputter rates for the two materials, which gave the pump its name. In this case, noble gas atoms would become trapped mainly in the tantalum cathode with the lower sputter rate because here more titanium atoms impinge from the opposing cathode compared to the rate of tantalum atoms being released. How-ever, roughly equal sputter rates were observed soon [29] and the model of the inventors proved wrong. The name, however, prevailed.

Modifications of cathode arrangements were tested using individual pellets for each Penning cell [30], mixtures of titanium and tantalum, or designs with a 1-mm-thick perforated tantalum plate on top of the titanium cathode [31]. Just recently, a commercial pump manufacturer introduced a system with a variable Ti/Ta ratio. However, it should be remembered that each individual Penning cell with Ti cathodes at both ends bares the continuous risk of argon instability.

#### Triode Pumps

Considerably increased pumping speeds for noble gases in ion getter pumps and better constancies are obtained by utilizing a so-called triode arrangement [32-34] as shown in Figure 5.21. Cathodes K here consist not of bulk plates but of mesh. A collector plate F on anode potential is

arranged behind K. Often, the inner wall of the vacuum housing serves for this third electrode, and thus, A and F are at ground potential. The discharge in this setup is restricted to the volume of the anode cylinder and has the same shape as in a diode pump. Between K and F, the discharge is suppressed.

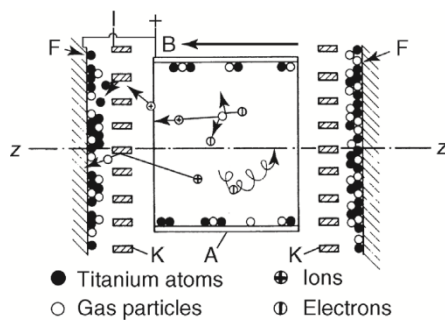


Figure 5.21 Diagram showing pumping action in a triode-assembly discharge cell. K Cathode mesh, A anode, F collector plates, Z anode axis, B magnetic field.

not as intensively due to the loss of kinetic energy experienced during the collisions at K). Therefore, the probability of implanted particles to be released is much lower.

The combination of both effects leads to a pumping speed for noble gases, with respect to nitrogen, of 20-30% in a triode pump compared to 1-10% in a diode pump.

Analogous to diode pumps, several triode cells are combined to compact electrode systems that form pockets, as in diode pumps, with the permanent magnets arranged in between (Figure 5.22). Ion getter pumps following the diode and triode principles look alike from the outside. Figure 5.23 shows a standard ion getter pump with a nominal pumping speed of  $500 \text{ l s}^{-1}$ , always referring to air or nitrogen. The pumping speed of this pump in diode design for argon and helium is 5 and  $50 \text{ l s}^{-1}$ , respectively, and for the triode design 125 and  $150 \text{ l s}^{-1}$ , respectively. In the triode design, starting pressure is 1 Pa and thus 10-fold lower than in diode designs.

Production of triode pumps used to be very time consuming and thus expensive. Each individual Ti cathode strip had to be hand-fixed to the cathode frame. Varian's [37] StarCell triode pump (Figure 5.24) solved this cost problem. Furthermore, it also eliminated an operational problem of triode pumps that often malfunctioned or overheated when pumping hydrogen or water vapor at higher pressure due to short circuits between anode and cathode because they are thermally and electrically isolated from the pump body. The StarCell pump has a considerably larger surface area so that these problems are minimized.

### Operation

Ion getter pumps are used to produce vacuum with low contents of hydrocarbons. Triode pumps indeed are capable of pumping down oil vapor, however, using diode or triode pumps in vacuum systems that contain oil vapors is not profitable. The reason is that the operation of diode pumps can become severely restrained by oil vapor contamination: they start more slowly and show lower pumping speeds.

Ion getter pumps comply with the requirement of very high operational reliability. These pumps form a thoroughly sealed unit together with the vacuum recipient, which prevents air from penetrating even if pump operation stops (e.g., due to power failure). High ambient temperature, radioactive radiation, and strong magnetic stray fields hardly disturb pump operation.

Ion getter pumps require only a single high-voltage wire and no additional supply lines. Via this wire, operation of the pump is monitored, started, or stopped from a remote control site (e.g., remote control in particle accelerators). Due to their vibration-free operation, ion getter pumps are applicable to vibration-sensitive measuring equipment. Compared to other types of UHV pumps

(turbomolecular pumps, cryopumps), they also provide the best ratio of electrical energy consumption and pumping speed.

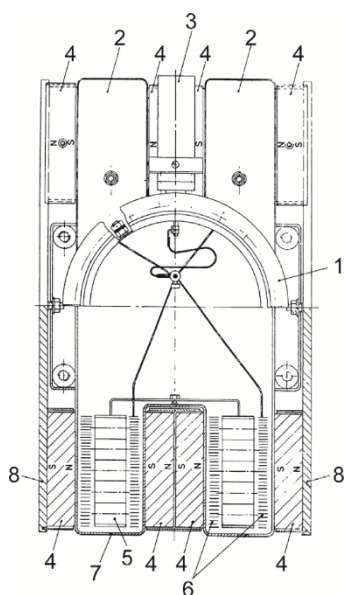


Figure 5.22 Diagram showing the design of an ion getter pump in triode configuration. Upper half of the image: top view. 1 High-vacuum flange, 2 electrode pockets, 3 power supply, 4 permanent magnets. Lower half of image: Section 4. Permanent magnets, 5 anodes A in frame, 6 cathode mesh, 7 collector plate also part of the nonmagnetic pump case, 8 magnet yoke.

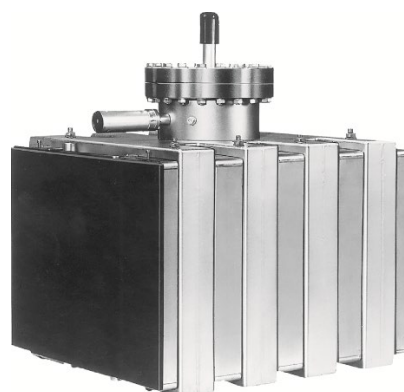


Figure 5.23 Ion getter pump IZ 500/IZ 500D (diode). Main dimensions in mm: width 408, depth 480, height (without sealing flange) 436. Baking temperatures: 350 °C with magnet, 450 °C without magnet. Eight-electrode system. Weight 135 kg.



Figure 5.24 Cathode of the StarCell triode pump by Varian. StarCell is patented and a copy-righted brand name of Varian.

Possible disturbances include the magnetic stray field of the pump as well as the emission of ionized particles, neutral particles (titanium), and soft X-radiation by the gas discharge. The radiation can influence the readings on, for example, mass spectrometers and ionization vacuum gauges. Additional disadvantages are that ion getter pumps are heavy, and most prominently, are hardly applicable to pressures  $> 10^{-2}$  Pa. Indeed, the pumps can cope with short periods of higher pressures, but degassing due to warming of the electrodes prevails after longer operating periods in the pressure range  $> 10^{-2}$  Pa. Thus, the preferred pressure range for continuous operation is  $p < 1$  mPa.

Ion getter pumps should not be started before the pressure drops below a certain starting pressure. For diode pumps, this threshold is 0.1 Pa ( $10^{-3}$  mbar), and for triode pumps, 1 Pa ( $10^{-2}$  mbar). Pumping down the vacuum system to starting pressure is carried out best by using pumps that produce an oil-free vacuum. For containers up to a volume of 300 l, adsorption pumps are appropriate. Sliding vane rotary pumps with preconnected adsorption traps, however, are also suitable if the adsorption medium is regenerated by baking and care is taken that no oil vapor condenses in the connection line on the high-vacuum side. Usually, turbomolecular pumps are used for preevacuation, particularly, when large vacuum chambers are evacuated or if the conductance of pump connections is low for technical design reasons that would require the ion getter pump to operate in the pressure range of  $0.5\text{--}5 \times 10^{-3}$  Pa for longer periods. In this case, the turbomolecular pump evacuates down to approximately  $10^{-2}$  Pa. After the ion getter pump is started, both pumps continue to operate simultaneously for some time.

Starting of an ion getter pump is different for diode and triode pumps. After the high voltage is connected at 1 Pa, a glow discharge is initiated spreading throughout the diode pump and even into the recipient because the complete housing is at ground potential. In the triode pump, however, the

anode completely encapsulates the cathode restricting the discharge to the space between the electrodes right from the start. Therefore, from the beginning, the triode sputters titanium whereas sputtering in the diode is established fully only after the discharge has ceased in the vicinity of the electrons after the pressure drops.

Standard ion getter pumps are available for nominal pumping speeds up to  $500 \text{ l s}^{-1}$ . They are utilized as stand-alone pumps in relatively small vacuum systems (e.g., vacuum deposition systems, zone melting equipment). Large systems use such pumps in situations when vacuum containers, due to their geometry, require multiple small pumps instead of a single large pump (e.g., particle accelerators, storage rings).

#### Orbitron Pumps

An orbitron pump is an ion getter pump utilizing the energy of the electrons both for ionizing molecules and for evaporating getter material. A radial electrical field is established between the cylindrical vacuum housing as cathode (ground potential) and a rod-shaped anode is placed along the center axis of the housing.

In this field, electrons from a glow cathode arranged between the cathodic cylinder and the anode follow multiple orbits along hypocycloid paths around the anode before they hit its surface. This increases the path length of the electrons dramatically, and thus, each electron collides with and ionizes gas particles several times. In the electrical field, the ions travel toward the housing where they become implanted in the getter layer.

An evaporation source is used to produce the getter layer. This source is usually heated with the ionizing electrons; in rare cases, an independent power supply is used. For the former case, the evaporator is combined with the anode of the ionizing equipment: on the rod-shaped anode, a titanium body is placed, heated, and evaporated by the impinging electrons.

### ***5.6. Cryotechnology and cryopumps***

“Cryo” is derived from the Greek word kryos meaning “cold.” Thus, cryotechnology refers to refrigeration technology. Although “cold” is generally understood as temperatures below ambient temperature, it is agreed that only refrigeration in the temperature range  $T < 120 \text{ K}$  is referred to as cryotechnology or cryogenics.

Cryotechnology and vacuum technology are closely interrelated:

- Vacuum is indispensable for thermal insulation in the application of low temperatures in the cryo range: the lower the working temperature, the more important the quality of thermal insulation. In a refrigerated, vacuum insulated system, heat enters from outside through thermal radiation, from thermal conduction by the gas in the vacuum chamber, and from thermal conduction over solid connectors between parts with different temperatures. If the mean free path of the gas molecules is greater than the vessel dimensions, as is the case in the fine vacuum range, the thermal conductivity of the gas decreases linearly with the pressure and is negligible with pressures in the high-vacuum range compared with the other heat transport processes. These vacuum pressures should be reached as a minimum for an effective insulation. Known design principles from high-vacuum and ultrahigh-vacuum technology are applied in order to ensure the necessary low leak rates in cryogenics.
- On the other hand, low temperatures as such can serve for the production of vacuum. At sufficiently low temperatures, all gases transform into a liquid or solid phase with an accordingly low vapor pressure or sublimation pressure. The particles leave the gas phase and the gas pressure decreases accordingly.

This thermal principle is the most direct method of producing vacuum without any moving parts.

Both fields of activity have always promoted each other's development. Only the application of vacuum to the thermal insulation made the liquefaction of hydrogen and helium possible. Later, the condensation trap cooled with liquid nitrogen became an indispensable accessory for the diffusion

pump. Space research required large amounts of liquefied gases for space simulation and as rocket fuel. This led to substantial progress in cryotechnology and broadened the potential range of applications for cryopumps toward other vacuum technological purposes. After a short time, the expansion of the low-temperature research and the introduction of new communication systems that required even lower temperatures triggered the development of reliable refrigeration equipment of varying power levels. Today, they are available to vacuum engineers as refrigeration units for cryopumps.

The technical application of superconductivity for generators, wiring, power generation, energy storage, or in the high-field magnetic technology and nuclear fusion again represents a great challenge to vacuum technology and cryotechnology. The long service life demanded for the superconductivity systems and the high operational safety can only be realized when one also succeeds in keeping the leak rates from the cold seals extremely low and in utilizing the existing cold surfaces in a suitable manner as cryopumps. Thus, a deep understanding of the processes of the condensation and adsorption of gases at low temperatures is essential. The success with high-temperature superconductors is strongly dependent upon the availability of suitable refrigeration [38].

Different refrigeration processes can be applied for the production of low temperatures in the range  $T < 120$  K. Two temperature levels are commonly worked with, namely, 5-20 K for the low-temperature stage and 50-80 K as a temperature of the thermal shield that is required to keep the incidence of thermal radiation on the low-temperature surface sufficiently low.

Today, commercial cryopumps are almost exclusively equipped with their own gas refrigeration machine that is operated with an internal working medium in the cycle, primarily helium. In addition, the pump must only be additionally equipped with a compressor and be supplied with electric power. As a result, the cryopumps are similarly simple to use as other high-vacuum pumps.

In addition, there are direct processes in which the surface to be cooled in special cryostats is brought into immediate contact with the boiling refrigerants. This technology is complicated to use, particularly when it concerns liquid helium. Moreover, a regular and controlled replenishment is necessary to compensate for vaporization losses.

To cool without liquid cryogenes, the cyclic processes are used in which the working gas utilized experiences a periodic change of state. In the cyclic process, work is used to produce cold or, more precisely, to withdraw a specific amount of heat from a cooled object in order that this can be held at a lower temperature  $T$  below the ambient temperature  $T_u$ .

The ratio of the spent work  $W$  and the heat  $Q$  that is taken from the system at a temperature  $T$  indicates the efficiency  $\eta$  of the machine. The theoretical maximum efficiency can be calculated directly from both temperature levels for the case of the completely reversible ideal process that is known as the Carnot cycle:

$$\text{Carnot efficiency } \eta_{\text{Carnot}} = \frac{W}{|Q_{\text{Carnot}}|} = \frac{T_u - T}{T} \quad (5.13)$$

In the Carnot process, the largest possible portion of the supplied work is converted into cold. The formula illustrates the second law of thermodynamics, which states that the working effort strongly increases with the decrease in the desired cryogenic temperature  $T$ . Thus, at least 2.6  $W$  mechanical drive power is required for 1 W of refrigeration power at 80 K, while 1  $W$  at 4 K already requires at least 72  $W$  of mechanical drive power.

Typical efficiencies of real gas refrigerating machines lie at 80 K in the order of magnitude of no more than 10–20% of the Carnot efficiency [39].

The coefficient of performance  $\varepsilon$  for a refrigerating machine refers to the ratio of generated cold to the mechanical work  $W$  utilized for it; this corresponds to the reciprocal value of the machine efficiency  $\eta$ :

$$\varepsilon = \frac{1}{\eta} = \frac{|Q|}{W} \quad (5.14)$$

In contrast to the traditional refrigeration, for example, in the refrigerator where the compression refrigeration cycle with evaporating refrigerant is used for the heat absorption, gas

refrigeration equipment is preferentially used for cryo-vacuum applications and is therefore characterized by the fact that the refrigerant continually exists above the two-phase range.

The cyclic processes used here continuously run between the two temperature levels, ambient temperature and the low temperature, and at two pressure levels. A temperature decrease is achieved when reducing the pressure. The work to be expended serves to compress the expanded gas again. In the simplest case, a throttling valve is used for the expansion of the working gas in which the pressure reduction is not used to extract any technical work and is idealized to happen without thermal exchange with the surroundings. Following the law of conservation of energy (the first law of thermodynamics), the energy content of the system therefore remains constant. Because for real gases the energy content is a function of pressure and temperature, the expansion is connected with a temperature change (Joule–Thomson effect), whereas the temperatures remain constant with ideal gases.

Nevertheless, at a given pressure, there is a dedicated temperature for every gas at which the Joule–Thomson effect disappears. It is called inversion temperature  $T_{inv}$ . Above the inversion temperature, the Joule–Thomson effect is negative; that is, a warming of the gas occurs with the expansion. Below the inversion temperature, the Joule–Thomson effect is positive and the gas cools down. The inversion temperature is dependent upon pressure (inversion curve  $p(T_{inv})$ ). To reach the desired temperature drop by Joule–Thomson expansion, the quantity pair (p, T) upstream the release valve must lie below the inversion curve of the gas concerned.

Nitrogen liquefaction from room temperature is possible through Joule–Thomson expansion alone because the inversion curve includes the temperature of 293 K. Hydrogen and helium gases, on the other hand, must be precooled, for example, through heat transfer at lower temperatures. Helium, the traditional working medium in cryogenic gas refrigeration equipment with a closed cycle, must be precooled to values below the temperature of liquid nitrogen. This occurs within the cyclic process through heat transfer between the colder low-pressure gas and the inflowing warmer high-pressure gas. Either counter flow heat exchangers (recuperators) or regenerators are used for this. While in recuperators the high-pressure gas and the low-pressure gas stand in continuous thermal contact with each other via a thermally well-conducting wall, in regenerators the two gas streams flow successively into the same system. The regenerator alternately absorbs heat and delivers it again. Regenerators also work very efficiently with small driving temperature differences [40]. Through the temporal separation of the release and compression processes, one can manage with only one regenerator and needs no potentially vulnerable changeover devices.

Because no liquefaction of the working gas occurs, only a sliding temperature level can be generated on the refrigeration side of the gas process. If more demanding requirements for the temperature stability exist, of course one can utilize the cryostat technology with boiling refrigerant.

With regard to design details of refrigerating machines, there exists extensive literature [41,42]. In the following, only three of the most frequently used processes for cooling cryopumps are described. All three concern regenerative gas compression refrigeration processes. This refrigeration equipment is also referred to as regenerators.

### **Working Principles of Cryopumps**

It has been known for a long time that gases and vapors bind to cooled surfaces [43]. While this effect has been used for the vacuum improvement practically since its discovery (cooling traps, baffles), the production of a high-level high vacuum or ultrahigh vacuum with the aid of low-temperature cooled surfaces, so with cryopumps, has only found an increasing interest in the last 50 years.

According to DIN 28400, Part 2, “a cryopump is a gas-binding vacuum pump in which gases are condensed on low-temperature cooled surfaces and/or adsorb on low-temperature cooled sorbents (solids or condensate). The condensate and/or adsorbate is held at a temperature where the pressure of the gaseous phase is lower than the desired low pressure in the vacuum chamber.”

Only vacuum pumps operating below 120 K are referred to as cryopumps. The selected temperature depends on the gas species to be pumped out and the desired vacuum level. The condensation pumps that work at higher temperatures are referred to as vapor condensers or simply

condensers.

In contrast to all other pumps, a cryopump is able to achieve the theoretical pumping speed (e.g., for steam) and the pumping surface can be arranged directly inside the recipient, that is, without additional conductance losses through connection flanges. This is why the first cryopumps were used for space simulation chambers. Only here, conventional pumps were not able to achieve the required pumping speeds, so that the high expenditure for cryogenic technology seemed justified. The impressive progress in the technology of the regenerative gas refrigeration equipment has made refrigeration easier in the meantime to the extent that today there are an entire series of applications with which cryopumps with lower pumping speeds successfully compete with conventional pumps or frequently even represent the most advantageous technical solution.

Because the form of the cold surface can be adapted entirely to the available space for installation, the full pumping speed is also available for pumping processes in places that are otherwise barely accessible. As an additional advantage, no working fluid vapors enter the recipient. The capacity of a cryopump is limited because the pumped out gas remains bound to the cold surface. This is not a disadvantage in the high- and ultrahigh-vacuum regime, the primary range of application of the cryopumps, due to the low gas volumes involved. For applications at higher pressures or with processes that require a continuous gas flow being pumped, cryopumps must be regenerated regularly.

The underlying pumping mechanism in cryopumps is the gas binding to the cold surfaces via van der Waals forces [44]. The energetic interaction is strongly dependent upon the type of the binding surface. Accordingly, two cryopump mechanisms are primarily distinguished, the condensation and the (ad-)sorption. In practice, it is often not possible to clearly separate these mechanisms.

### **Gas Condensation**

Condensation describes, in the strict thermodynamic sense, only the gaseous/liquid phase transition. Because it is frequently not relevant to the pumping effect whether the pumped gas is solid or liquid, the name “condensed phase” is used in the linguistic usage for both cases. In the best case, the ultimate pressures achievable at the given temperature of the cold surface through condensation result from the sublimation equilibrium pressure of the solid phase.

Three groups of gases are to be distinguished. While the saturation pressure of water, carbon dioxide, and the higher hydrocarbons already reaches values  $p < 10^{-7}$  Pa at the temperature of the liquid nitrogen ( $T = 77$  K), the saturation pressures of methane, argon, oxygen, and nitrogen drop down to this region only at temperatures in the range  $T \approx 20\text{--}30$  K. Finally, reducing the saturation pressure of neon and hydrogen down to values  $p < 10^{-7}$  Pa requires temperatures in the range of liquid helium, so  $T = 4.2$  K and lower are necessary.

In principle, any gas can be pumped when the selected temperature is sufficiently low. The temperature  $T = 20$  K is sufficient to reach UHV conditions for all gases except neon, hydrogen, and helium. However, hydrogen is particularly interesting for vacuum technology because many materials are able to release it in vacuum. As a result, it is the most relevant residual gas component in the UHV range.

In the use of the vapor or sublimation pressure curves, it has to be considered that these represent the state of the phase equilibrium. In the equilibrium, a net mass flow of zero is reached at the cold surface, that is, no more usable pumping effect appears. Hence, the curves describe the theoretically possible ultimate pressure. In order to achieve a sufficiently high pumping speed in an application with gas flow constantly being pumped in the vacuum, a nonequilibrium must therefore be maintained while the gas to be pumped is thermodynamically over-saturated, usually two decades in pressure. Temperatures of  $T < 3.5$  K are necessary for the binding of hydrogen to a cold surface in UHV if one does not involve the binding mechanisms of cryotrapping and cryosorption that are addressed in the following.

The properties of the formed ice layers depend on the pumping history in a complicated manner and change during growth [44,45].

The capacity of a condensation cryopump is almost infinite provided that the temperature of the cold surface can be maintained. Of course, the growth of a thick layer of ice increases the need

for refrigeration; the finite thermal conductivity of the ice leads to an increase of the temperature on the ice surface that can lead to instabilities [46]. In practice, condensate layers of more than 10 mm in thickness can readily be formed. The efficiency of a condensation pump is close to the theoretical maximum [47].

### Cryosorption

With cryotrapping and cryosorption, the efficiency of a cryopump can be noticeably raised and, hence, the operational temperature range can be moved to higher temperatures. Indeed, the attainable capacities are smaller than those with cryocondensation. The point of the vapor pressure or sublimation pressure curve that refers to the theoretically attainable pressure at a given temperature on the surface of the condensate will be replaced by the sorption phase equilibrium curve. This is described with the aid of the sorption isotherms that describe the dependence of the pressure on the gas amount at the sorbing surface at a given temperature.

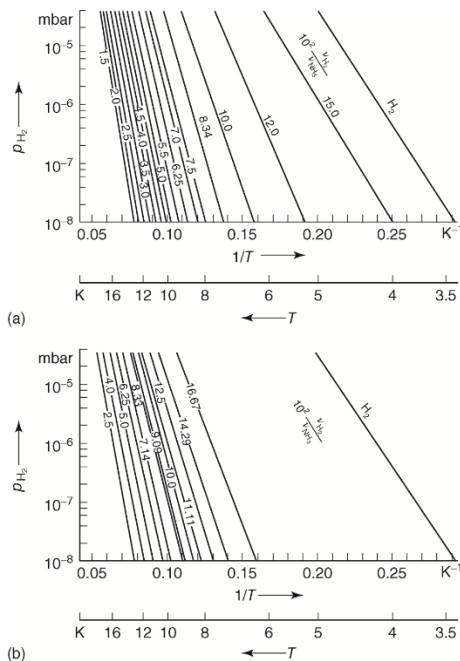


Figure 5.25 (a) Cryosorption of hydrogen to solid ammonia: adsorption equilibrium of  $H_2/NH_3$  condensates for different molar ratios  $v_{H_2} = v_{NH_3}$ ; production of the  $NH_3$  condensates at  $T = 7.99$  K. (b) Cryotrapping of hydrogen with ammonia vapor: hydrogen partial vapor pressure over mixed  $NH_3/H_2$  condensates with different molar ratios  $v_{H_2} = v_{NH_3}$ ; production of the mixing condensates at  $T = 7.99$  K [24].

With cryosorption, the gas binds to the cold surface through physical adsorption forces. The interaction is complex and depends not only on the temperature, but also on the type of the surface. Specific sorbent materials are used for this, such as activated carbon, zeolite, or nanoporous materials that possess an especially high active surface through their porosity. Also, a condensate layer condensed prior to the beginning of the pumping of a higher boiling gas (e.g., argon snow) has a sufficiently high porosity.

At a given temperature, the adsorption phase equilibrium always lies at pressures below the saturation vapor pressure. Hence, through adsorption, gas can also be pumped in the undersaturated range, that is, at considerably higher temperatures than would be necessary for condensation. This is of great significance to the economic pumping for the barely condensable gases such as hydrogen, helium, and neon. By means of cryosorption, at 5 K vacuum in the  $10^{-7}$  Pa range can also be easily achieved for these gases.

Figure 5.25,a illustrates the cryosorption of hydrogen to solid ammonia. In Figure 5.26, the molar adsorption enthalpy  $\Delta H$  of hydrogen to different gas condensates is plotted for various condensation temperatures  $TK$  of the adsorbent. It is shown that carbon dioxide and ammonia are particularly suitable as an adsorbent for hydrogen. Furthermore, it is evident that for all adsorbents, a range of the condensation temperature  $TK$  exists in which layers with particularly strong bindings are formed [48].

The use of gas condensates as a cryosorbent offers certain advantages compared with the use of solid adsorbents. First, the required good thermal contact with the cold surface is provided with condensates. Second, the cryopumps can be regenerated through the evaporation of the condensate and the production of a new layer at relatively

low temperatures in a simple manner. Nevertheless, due to the clearly more complicated process and the need to accept a foreign gas into the system, cryosorption in gas condensates is only used in special cases. All commercial refrigerator cryopumps use solid adsorbents.

### Solid Adsorbents

The main challenge with the application of solid adsorbents (molecular sieves, activated carbon) for pressure reduction in high and ultrahigh vacuum through cryosorption is the heat transfer of the adsorbent to the cold surface. Cooling can only occur through the thermal conductivity in the

adsorbent itself because the heat transfer through the gas to be pumped is negligible under low-pressure conditions. This is why it is essential to establish a high-quality thermally conducting contact, normally by adhesive bonding. The selection of a suitable adhesive must be ensured. Before cooling down the apparatus, the adsorbent must be degassed through bake-out as much as possible.

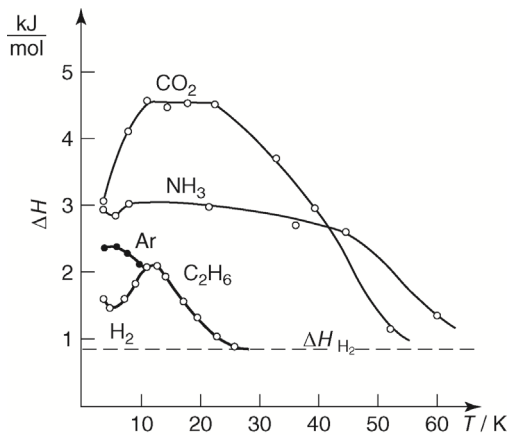


Figure 5.26 Molar sorption enthalpy  $\Delta H$  of hydrogen to selected adsorbents (gas condensates) versus condensation temperature  $T$  of the adsorbent. Dashed line: condensation of  $H_2$ , gas to  $H_{2,solid}$ .

The desorption during the regeneration as well as the total cryosorption pumping process strongly depends on the selected cryosorbents. Due to the great relevance that cryopumps had gained in large nuclear fusion experiments, large-scale qualification programs for a vast number of potential cryosorption materials (sinter metals, porous ceramics and metal meshes, silica gel, molecular sieves, activated carbons) were established in the 1990s. Alongside this, not only the sorbing materials were examined, but an attempt was also made to find an optimum joining technology (resistance to the thermal cycling during regeneration and a good thermal conductivity) on the cooled surfaces (bonding, brazing, plasma coating). These programs were necessary since no experience in usage within the cryogenic temperature range existed with the manufacturers of industrial adsorbents.

In practice (e.g., with all commercial pumps), activated carbon has become the most important sorbent, particularly the nonpolar, microporous variations. The

types that are gained from the carbonization of coconut shells are usually used. The natural source product results in a not too narrow pore size distribution, so that the interaction with the gas particles to be pumped is equally good for all particle types.

As a general rule in commercial pumps, activated carbon material pressed into cylindrical pellets is bonded to the cold surface with an epoxy resin.

Other aspects to be considered in the correct choice of cryosorption materials are the following:

- The cross-sensitivity of the cryosorption materials; that is, a reduction in the nominal pumping speed when the heavily volatile trace gases that require particularly high regeneration temperatures accumulate during the running time.
- The mobility of the sorbed particles; that is, the capacity of the pump can be increased when the particles that are initially pumped on the surface can be transported deeper into the pores through a defined energy input (heating).

In the rough vacuum range, particularly as clean fore pumps for ion getter pumps, liquid nitrogen-cooled cryosorption pumps with zeolite filling have been demonstrated to work very effectively.

### Cryotrapping

The cryotrapping pumping method can be utilized to reach even lower equilibrium pressures. This refers to the pumping of a lower boiling and thus at the same time difficult to condense gas with the aid of a higher boiling gas. In contrast to cryosorption where the gas to be pumped binds on a surface, with cryotrapping it is trapped in mixed condensate snow. Argon, methane, carbon dioxide, ammonia, and higher hydrocarbons have been examined as a condensation partner for hydrogen thus far. At the given temperature of the cold surface, the resulting mixed condensates have a hydrogen partial pressure that is by several orders of

magnitude smaller compared with the vapor pressure  $p_{H_2}$  above the surface of the pure condensate. Figure 5.25, b demonstrates this exemplarily with mixed condensates from ammonia and hydrogen. The comparison with Figure 5.25, a, reveals that with the same molar ratio of ammonia to hydrogen, the drop in vapor pressure is by approximately 30% smaller with cryosorption than with



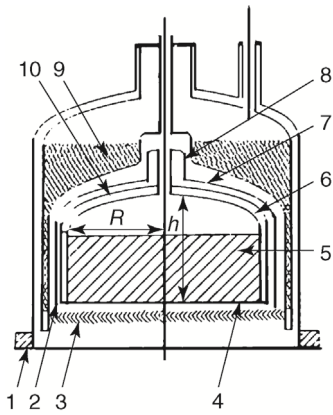


Figure 5.28 CERN - bath cryopump with long operational duration to generate extremely low gas pressures: (1) connection flange; (2) clearance; (3) baffle; (4) pumping surface (condensation surface); (5) liquid helium; (6) Ne filled volume for generating insulating vacuum; (7) radiation shield (Ag plated on interior, exterior blackened); (8) neck, copper-plated; (9) liquid nitrogen; (10) protective housing (silver-plated).

and consists of a force-cooled (water or air) compressor unit and a cold head with two temperature stages that is connected to the compressor unit by flexible pressure pipes (spatially separated). Hence, this pump model is also called cryogen-free.

illustrated in Figure 5.28 with a bath cryopump that has been optimized in any possible way, developed by Benvenuti in the 1970s at CERN. It can be operated at a temperature of the cold surface of 2.3 K and has, in this case for hydrogen, according to pump size, a pumping speed of 4500 and 1100  $\ell \text{ s}^{-1}$ . The accessible ultimate pressure amounts to approximately  $10^{-11}$  Pa. Pumps with this design are equipped with an insulating vacuum; the consumption of liquid helium is, thus, very low, particularly since the radiation shield is also cooled with cold helium gas.

Figure 5.29 shows photographs of a manufactured bath cryopump.

For special applications, cryopumps can be “tailor-made” using standard helium condensers in the refrigerator operation. Such pumps were developed for applications in nuclear fusion.

### Refrigerator Cryopumps

The modern alternative to the bath cryopump is the refrigerator cryopump whose refrigeration supply is produced by a gas refrigerator and generally follows the Gifford–McMahon principle. The refrigerator works with helium gas in a closed cycle

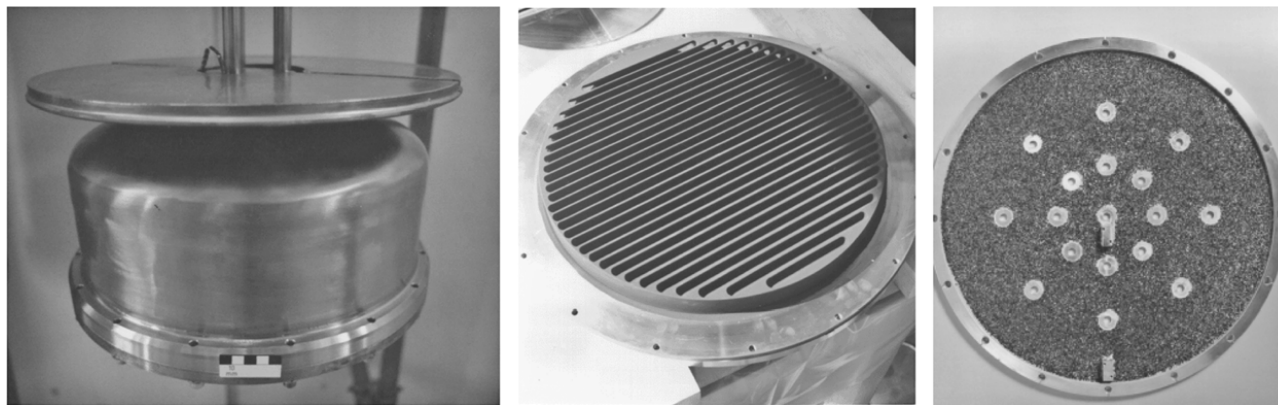


Figure 5.29 Construction elements of a LHe bath cryopump. Left: LHe container made of stainless steel. Middle: baffle made of copper, optically blackened. Below: pumping surface made of aluminum, with activated carbon glued on it.

The cold head of a two-stage Gifford–McMahon refrigerator allows for a refrigerator cryopump (Figure 5.30) to be mounted easily. The radiation shield and baffle of the cryopump are mechanically contacted with the first stage. The cold surfaces are contacted with the second stage. These are designed as plane cranked copper metal sheets that are placed in parallel at a short distance. The interior sides of these sheets that are turned toward each other are coated with activated carbon. At the temperatures given above for the second stage, the geometry of the arrangement and the surface structure of the low-temperature cooled plates (cold surfaces) ensure that any easily condensable gases will primarily condense on the exterior surfaces in the solid phase, while the gases that are difficult to condense (hydrogen, neon, helium) are sorbed on the interior surfaces that have been coated with activated carbon.

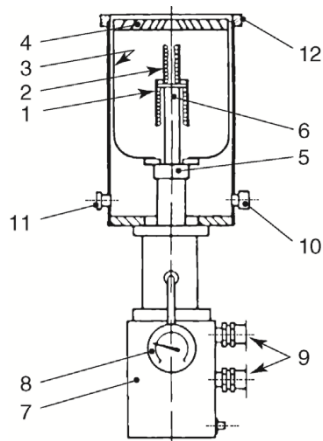


Figure 5.30 Refrigerator cryopump with integrated cold head: (1) cold surface of second stage (pumping surface); (2) adsorbent (interior coating of the cold surface); (3) radiation shield; (4) baffle; (5) cold head, first stage; (6) cold head, second stage; (7) cold head motor with housing and electrical connections; (8) He gauge for hydrogen vapor pressure thermometer; (9) He gas connections to compressor; (10) boiler safety valve; (11) fore-vacuum connecting flange; (12) high-vacuum connecting flange.

The first stage is cooled with a refrigeration capacity between 10 and 80 W – according to refrigerator type and in relation to the load – to a temperature from 50 to maximum 80 K. In the second stage, a refrigeration capacity of 2–5 W at a temperature between 8 and 20 K is available – according to load. These days, GM refrigeration equipment with sufficient refrigeration capacity (several watts) down to 4 K is also available. Together with the use of a sorbent material for the second stage, helium can also be pumped efficiently.

The interactions between the different processes can be very complex. Thus, the buildup of a frost layer at the thermal shield can, on the one hand, lead to a lower transmission probability, for example, in the case of carbon dioxide, and, on the other hand, lead to an additional cryosorption effect in the condensate. If there is an intensified condensation pumping at the sorbent layer, the pumping speed can be reduced for lighter gases. In view of this complexity, it is not easy to predict accurately the pumping of gas mixtures. On the other hand, these effects can also be utilized to separate gas mixtures into individual fractions.

Refrigerator cryopumps of varying sizes whose pumping speeds for air reach from 800 to 60 000  $\ell \text{ s}^{-1}$  are mass produced. Depending on where the connection flange is mounted, the refrigerator cryopump can be directly built into the vacuum vessel or as the appendage pump connected to the vacuum vessel.

Refrigerators with accordingly high refrigeration power are necessary for the operation of large cryopumps with high pumping speed. Nevertheless, there is also the possibility

to use a small refrigerator for the cooling of the cold surfaces and to cool radiation shields and baffle with liquid nitrogen that is taken from a container integrated into the radiation shield. Through the high refrigeration capacity of  $\text{LN}_2$ , such pumps can also pump substantial amounts of water vapor at higher pressures. The losses of liquid nitrogen can be substituted for with an automatically functioning replenishment device that can be connected to the nitrogen container of the cryopumps through a vacuum jacketed pipe.

For the processes with which gas continuously flows in the cryopump or is flushed, for example, when sputtering with Ar, a maximum inlet pressure may not be exceeded. This is dependent upon the refrigeration capacity of the refrigerator and the dimensions of the cold surfaces. As approximate values for the maximum allowed tolerable vessel pressure  $p_{max}$ , the following can be used for normal cryopumps:

$$p_{max} \approx 0.5 \text{ Pa for } N_2, Ar,$$

$$p_{max} \approx 0.15 \text{ Pa for } H_2,$$

For the user, refrigerator cryopumps can be used in the same way as other conventional pumps, that is, the only external interface is the electricity supply (for the helium compression cycle) and the connection flange. As a result, these devices are much easier to use than bath cryopumps and have almost entirely substituted them in the industrial practice. In the United States, cryopumps are traditionally used for semiconductor applications, while in Europe, the turbomolecular pumps are given preference.

#### Development Trends for Cryopumps

Concerning the design and the operating methods, cryopumps demonstrate a far larger variety than any other pump type. This is why the area of cryopumps is continuously evolving. Thus, for example, cryocondensation pumps with possibilities for continuous regeneration were developed. For

this, slowly rotating rotors were incorporated that mechanically scrape off the forming condensate and collect it or thermally evaporate and evacuate it locally. Furthermore, a cryopump with a thermal diffusion stage was developed for applications with an especially high throughput that leads to a viscous flow area within the cryopump.

Cryopumps are unmatched in their flexibility and versatility to be adapted to given conditions and specific requirements. One can return to commercial solutions that are available in the form of versatile standard models or develop individually tailored designs. Moreover, the cryopumps are characterized by a good scalability that allows for the construction of very large units. The demand for high-vacuum pumps with very high pumping speeds is continually rising with the result that the significance of the cryopumps will still increase in the future.

1. H. Wycliffe and A. Salmon, *Vacuum* 21, 223 (1971).
2. B. D. Power, UK Patent No1, 154, 341 (1969).
3. Gaede, W. (1913) German Patent 286404.
4. Jaeckel, R. (1950) *Kleinste Drücke*, Springer, Berlin-Göttingen-Heidelberg, pp. 140 ff.
5. Rettinghaus, G. and Huber, W.K. (1974) Backstreaming in Diffusion Pumps. *Trans. 6th International Vacuum Congress, Kyoto. Vacuum*, 24, 249.
6. Holland, L. (1970) A review of some recent vacuum studies (related to pumps and ion beam sputtering systems). *Vacuum*, 20, 175.
7. Hablanian, M.H. and Maliakal, J.C. (1973) Advances in diffusion pump technology. *J. Vac. Sci. and Technol.*, 10, 58.
8. Meyer, D.E. (1974) Residual gas analysis studies during sputtering of reactive metals. *J. Vac. Sci. and Technol.*, 11, 168.
9. DIN 28400, Teil 2 (1980) *Vakuumentchnik Benennungen und Definitionen*, Beuth Verlag, Berlin.
10. Chew, A.D., Galtry, M., Livesey, R.G., and Stones, I. (2005) Towards the single pump solution: Recent development in high speed machines for dry vacuum pumping. *J. Vac. Sci. Technol.*, A23, 1314.
11. ISO 3529/2 (1981) *Vacuum technology; Vocabulary; Part 2: Vacuum pumps and related terms*. Trilingual edition.
12. Dobrozemsky, R. (1973) *Vakuumentchnik*, 22,41-48.
13. Visser, J. and Scheer, J.J. (1973) *Ned. Tijdschrift. Vac. Technol.*, 11,17-25.
14. Grubner, D.M. et al. (1968) *Molekularsiebe*, VEB Deutscher Verlag der Wissenschaften, Berlin.
15. Ferrario, B. (1998) Getters and Getter pumps, in *Foundations of Vacuum Science and Technology* (ed. J.M. Lafferty), John Wiley & Sons, New York, Chapter 5, pp. 261-315.
16. Benvenuti, C. (2001) *Vacuum*, 60, 57–65.
17. Boffito, C. and Sartorio, E. et al. (1986) An update of non-evaporable getters in electron tubes. *Vakuumentchnik*, 35, 212–217.
18. Jühr, W. (1987) Einsatz von Gettern zur Aufrechterhaltung von Vakua, in *Vakuumentchnik in der industriellen Praxis* (ed. Kerske et al.) Expert, Ehningen, pp. 145-169.
19. Hall, L.D. (1958) *Rev. Sci. Instr.*, 29, 367–370.
20. Penning, F.M. (1937) *Physica IV*, 2,71-75, *Philips Techn. Rundschau* 2 (1937), 201-208.
21. Knauer, W. (1961) *J. Appl. Phys.*, 33, 2093-2099.
22. Schuurman, W. (1966) *Rijnhuizen-Report 66-28*, University of Utrecht.
23. Rutherford, S.L. (1964) Sputter ion pump for low pressure operation, *Proc. 10th Nat. AVS Symposium 1963*, Macmillan Company, New York p. 185.
24. Singleton, J.H. (1969) Hydrogen pumping speed of sputter ion pumps. *J. Vac. Sci. Technol.*, 6, 316.

25. Henning, H. (1980) Proc. 8. Intern. Vac. Congress, Cannes Suppl. Rev., "Le Vide", No. 201 143-146.
26. Reikhrudel, E.M., Smirnitskaya, G.V., and Burnisenica, G.V. (1956) Ion pump with cold electrodes and its characteristics, Radiotekh. Electron, 2, 253.
27. Tom, T. and James, B.D. (1969) Inert gas ion pumping using differential sputter yield cathodes. J. Vac. Sci. Technol., 6, 304. 38
28. Jepsen, R.L. (1968) Proc. 4th Int. Vac. Congr. London 1968, Vol. I 317. 39
29. Welch, K.M. (1991) Capture Pumping Technology, Pergamon Press, Oxford, pp. 103 ff.
30. Baechler, W. and Henning, H. (1968) Proc. 4th Int. Vac. Congr. London 1968, Vol. I 365.
31. Komiya, S. and Yagi, N. (1969) J. Vac. Sci. Technol., 6, 54.
32. Brubaker, W.M. (1959) Transact. of the 6th Nat. Vac. Symp, Pergamon Press, Oxford, pp. 302–306.
33. Vaumoran, J.A. and Biasio, M.P. (1970) Vacuum, 20, 109–111.
34. Singleton, J.H. (1971) Hydrogen pumping by sputter-ion pumps and getter pumps. J. Vac. Sci. Technol., 8, 275–282.
35. Oechsner, H. (1966) Z. Naturf., 21a, 859
36. Bance, U.R. and Craig, R.D. (1966) Vacuum, 16, 647–652.
37. Pierini, M. and Dolieno, L. (1983) A new sputter-ion pump element. J. Vac. Sci. Technol. A, 1, 140.
38. Ruhlich, I. (2002) Gaskaltmaschinen für HTSL-Anwendungen. KI Luft- und Kältetechnik, 8, 361-365.
39. Organ, A.J. (2005) Stirling and Pulse-Tube Cryocoolers, John Wiley & Sons, Inc., New York.
40. Ackermann, R.A. (1997) Cryogenic Regenerative Heat Exchangers, Plenum Press, New York.
41. Frey, H., Haefler, R., and Eder, F.X. (1992) Tieftemperaturtechnologie, VDI-Verlag, Dusseldorf.
42. Flynn, Th. (2004) Cryogenic Engineering, 2. Auflage, CRC Press, Boca Raton, FL.
43. Tait, P.G. and Dewar, J. (1874) Farther researches in very perfect vacuum. Proc. R. Soc. (Edinburgh), 8, 348-628.
44. Maitland, G.C., Rigby, M., Smith, E.B., and Wakeham, W. (1981) Intermolecular Forces, Clarendon Press, Oxford, UK.
45. Haefler, R.A. (1989) Cryopumping, Clarendon Press, Oxford, UK.
46. Anashin, V.V. et al. (1997) Photon induced molecular desorption from condensed gases. Vacuum, 48, 785-788.
47. Syssoev, S.E., Eacobacci, M.E., and Bartlett, A.J. (2010) Controlled formation of condensed frost layers in cryogenic high vacuum pumps. J. Vac. Sci. Technol. A, 28, 925-930.
48. Hirth, J.P. and Pound, G.M. (1963) Condensation and Evaporation, Pergamon Press, Oxford, UK.

## 6. VACUUM MEASUREMENT

### Introduction

Vacuum technology measures pressure  $p$  either directly according to its defining equation, by measuring the force  $F = pA$  exerted to an area  $A$  or indirectly by measuring a physical quantity proportional to the pressure, for example, particle number density  $n$ , particle impingement rate  $\bar{n}c$ , and thermal conductivity, among others.

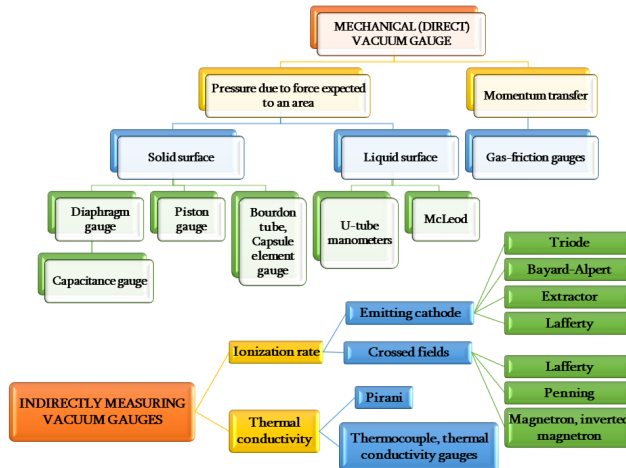


Figure 6.1 Classification of common vacuum gauges according to their physical principles. Crossed fields mean crossed electric and magnetic fields.

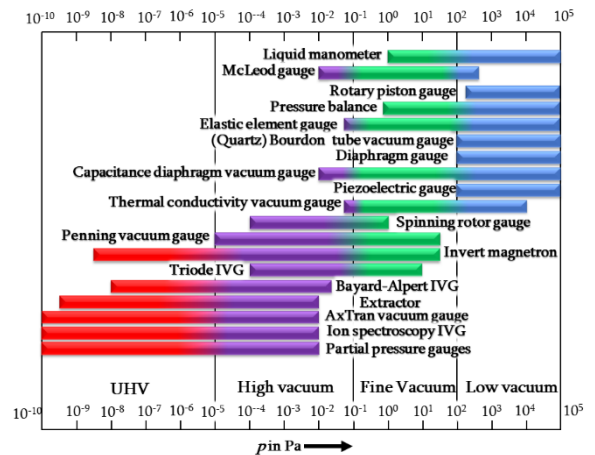


Figure 6.2 Overview of the gauges common to individual pressure ranges.

Measuring pressure directly by assessing the effect of a force is limited to pressures greater than approximately 1 mPa. At this pressure, the force exerted to 1cm<sup>2</sup> amounts to only about 10<sup>-7</sup> N. Measuring such low forces requires an electrically amplified signal.

The pressure range measured in vacuum technology spans across 15 powers of 10. No single gauge type covers the whole range. Figure 6.1 classifies common vacuum gauges according to their physical measuring principles. Figure 6.2 provides an overview of the gauges common to individual pressure ranges.

Calibration of vacuum gauges is usually necessary in order to guarantee correct measurements. Calibration may not be required only in cases where the measuring signal can be traced back to pressure's defining equation. In addition, any physical processes and determining quantities leading to the measuring signal must be sufficiently well known. Particularly, precise knowledge of these data is essential if the measuring signal is used as a primary standard. U-tube manometers and piston manometers are considered suitable for primary standards. However, operating them is elaborate and impractical for everyday measuring tasks, particularly in an industrial environment.

For gas-friction vacuum gauges, physical processes involved are thoroughly investigated and the measuring signal can be traced back directly to particle density and particle impingement rate. However, one parameter, the accommodation coefficient, cannot be given a priori, and thus, calibration is mandatory. Therefore, gas-friction vacuum gauges are covered in this chapter.

### 6.1. Mechanical vacuum gauges

Figure 6.3 schematically illustrates a possible principle of direct mechanical pressure measurement. The diaphragm  $D$  with surface area  $A$  separates two volumes, 1 and 2, with pressures  $p_1$  and  $p_2$ , respectively. The force exerted to the diaphragm toward the right side is given according to Equation. (6.1):

$$F = (p_1 - p_2)A \quad (6.1)$$

and deflects the diaphragm. If the displacement stretch  $x$  is translated into an angular movement  $\phi$ , the gauge directly displays the pressure difference  $(p_1 - p_2)$ . For the principle in Figure 6.3, this is done using a toothed rack  $T$  and pinion  $P$ .

When volume 2 is evacuated down to a reference pressure  $(p_1 - p_2)$ , the vacuum gauge directly registers the absolute pressure  $p_1$  in volume 1.

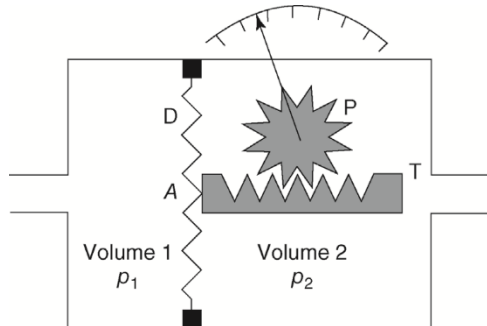


Figure 6.3 Diagram of mechanical pressure measurement using the deflection of a diaphragm.

Mechanical vacuum gauges operating on this principle as well as any liquid manometers generally measure a difference between two pressures. The reference pressure can be negligibly small compared with the measured pressure. The reading on a directly measuring mechanical vacuum gauge is independent of the gas species as long as the temperatures of the measuring instrument and the measured container are equal. If they are not, the reading is gas-species dependent if the measured pressure  $p$  is below the so-called viscous regime ( $p < 50$  Pa).

Common types of mechanical, differentially measuring vacuum gauges are categorized into three groups according to the type of reference pressure and the

location of the sensor.

- Reference pressure is atmospheric pressure. The sensor is placed on the reference-pressure side.
- Reference pressure is zero (i.e., below the resolution of the instrument). The sensor is placed on the measuring side, that is, at a place connected to the volume in which the pressure is measured.
- Reference pressure is zero. The sensor is placed on the reference-pressure side.

### Corrugated-Diaphragm Vacuum Gauges

The diaphragms used here are circular, corrugated membranes. They are mounted in between two flanges, either clamped or welded at their edges. One side of the membrane is exposed to the volume whose pressure is measured. The diaphragm deflection caused by the pressure difference is used as a measure of pressure, and is displayed by a motion work (see principle in Figure 6.3). Diaphragm pressure gauges are of the types (a) and (b) listed above.

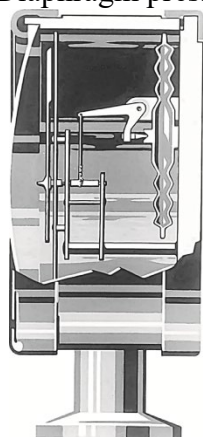


Figure 6.4 Capsule element vacuum gauge

The deflection force for diaphragms is relatively high and their annular fixing makes them comparably insensitive to vibration. A diaphragm can be protected against overload by allowing it to lean against a safety plate or the flange on the low-pressure side. Coating provides a means of protecting the measuring instrument against corrosive gases.

### Capsule Element Vacuum Gauges (Measuring Range 1-100 kPa)

A capsule element is made up of either two circular, corrugated diaphragms or a circular solid wall combined with a circular, corrugated diaphragm, arranged as a cell (Figure 6.4). The cell is evacuated and sealed vacuum-tight. Capsule element vacuum gauges are type (b) mechanical vacuum gauges according to the list.

Thus, the reading of a capsule element vacuum gauge is independent of the ambient pressure. If the test pressure drops, the distance between both walls increases according to their elastic forces or due to an integrated compression spring. This deflection represents the measured quantity, which is translated into a reading by an appropriate sensor. In the instrument shown in Figure 6.4, the measured value is transmitted by a level system. Sensor and display are arranged in the volume where the pressure is monitored. For higher actuating forces, several capsule elements can be mechanically connected in

series. The main advantage of the measuring principle is that the deflection is, to a large extent, proportional to the pressure. A disadvantage is that they are destroyed by gases condensing in the measuring unit or by corrosion in the unit. End-scale deflections of 2 kPa (20 mbar), 10 kPa (100 mbar), and 100 kPa (1000 mbar) are typical in the vacuum range.

Generally, the measuring accuracy of such an instrument can be improved for a certain pressure range by filling the cell with a gas of predefined pressure. This allows measurement accuracies of, for example, 1% in the pressure range between 10 and 11 kPa. However, the disadvantage of this type of operation is that the pressure in the diaphragm cell is temperature dependent. From Equation (6.1), it follows that a rise in temperature  $\Delta T = 3$  K produces a relative change in the pressure reading of 1%.

Slightly modified, the design of capsule element vacuum gauges is used in diaphragm pressure switches as well.

### Bourdon Tube Vacuum Gauges (Measuring Range 1–100 kPa)

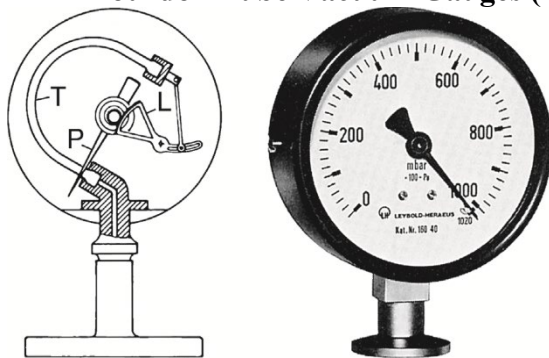


Figure 6.5 Bourdon tube vacuum gauges. Section and front view.

A Bourdon tube vacuum gauge, shown in Figure 6.5, is a typical type of group (a) mechanical vacuum gauge according to list. The inside of a tube (T) curved to a  $270^\circ$  circular arc (usually with oval cross section) is connected to the volume where the pressure is measured. If the pressure drops inside tube T, the bending radius of the arc changes because the force exerted to the (larger) outside surface is higher than the force on the inside of the arc. The ambient pressure reduces the bending radius [1,2]. A level system (L) transfers the resulting deflection directly to a pointer that indicates the reading on a scale

mounted to the gauge. If the surrounding of the tube is at ambient pressure, the reading on instruments of this type depends on the surrounding atmospheric pressure (meteorological conditions, height above sea level). This error can be corrected by rotating the scale around the pointer axis. Bourdon tube vacuum gauges are robust and quite corrosion resistant.

### Quartz Bourdon Tube Vacuum Gauges

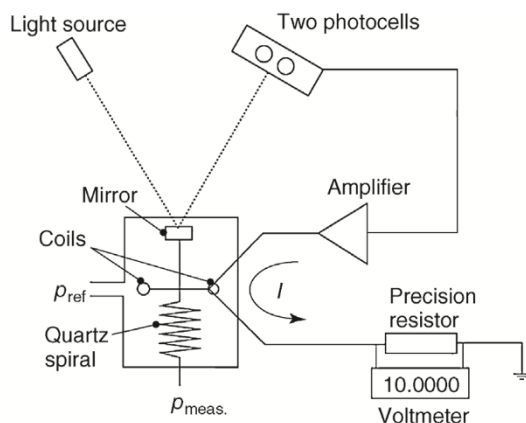


Figure 6.6 Diagram of a quartz Bourdon tube vacuum gauge by Ruska Corporation, Houston, Texas (now GE Sensing). The deflecting force exerted on a quartz spiral due to pressure difference is measured with a beam of light. Electrical coils hold the quartz spiral in the zero position. The coil current is proportional to the pressure.

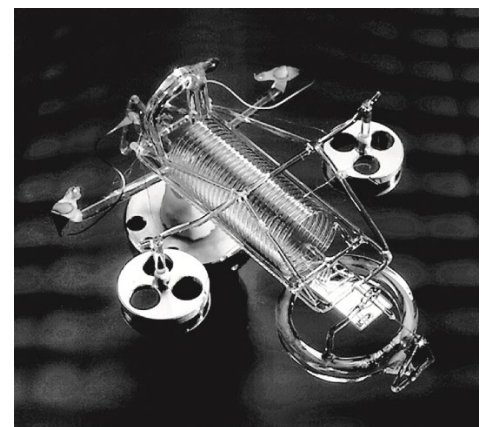


Figure 6.7 Photograph of quartz spiral and balancing coils. (Courtesy of Ruska Corporation, Houston, Texas (now GE Sensing).)

From a measuring technology perspective, quartz Bourdon tube vacuum gauges are a particularly ingenious variant of Bourdon tube vacuum gauges (Figures 6.6 and 6.7). They are type (a) or (c) mechanical vacuum gauges, according to the list.

A helically bent quartz tube is deflected similar to the Bourdon tube vacuum gauge by a pressure difference between the outside and inside. It is repositioned by an electromagnetic coil. The necessary coil current is a measure of the pressure difference. A beam of light optically determines the initial position. A mirror arranged at one end of the spiral reflects the beam and differential balancing of two photodiodes defines the mirror's angle. The reading is simple to linearize and the long-term stability of the instrument is very high because the spiral always returns to its initial position. Typically, readings show relative deviations  $< 2 \times 10^{-4}$  within 1 year of operation and throughout a large measuring range (3–100% of end-scale deflection).

The resolution of the instrument is  $10^{-5}$  of end-scale deflection, and reproducibility is approximately  $2 \times 10^{-5}$ . Instruments are available with end-scale deflections between 7 and 100 kPa.

### Diaphragm (Membrane) Vacuum Gauges

Diaphragm (Membrane) Vacuum Gauges with Mechanical Displays (Measuring Range 0.1–100 kPa).

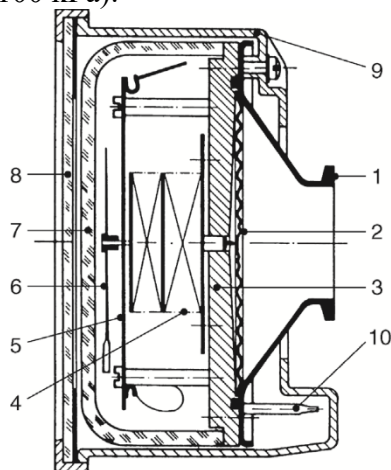


Figure 6.8 Section of a diaphragm vacuum gauge with mechanical display (diagram). (1) Connecting flange and gas inlet, (2) diaphragm, (3) base plate, (4) transfer system for diaphragm deflection, (5) indicating disk, (6) index hand, (7) vacuum-tight glass cap, (8) front plate, part of housing, and (9, 10) evacuating ports.

If we evacuate volume 2 of the system shown in Figure 6.3 down to the pressure  $p = 0$  and subsequently seal it, we obtain a diaphragm vacuum gauge with a reading that is temperature independent (except for temperature-dependent mechanical properties) and independent of atmospheric pressure. Sensor and display are not exposed to the measured gas. Thus, the instrument is a type (c) mechanical vacuum gauge. The system is relatively corrosion resistant because sensitive parts are not exposed to the measured gas. Only the corrugated membrane made from a copper–beryllium alloy might require corrosion protection, for example, by gold plating, in particularly corrosive environments.

As indicated above, deflection of a corrugated diaphragm is largely proportional to the pressure difference. Thus, the scale in such an instrument is linear in the case of a proportional conversion of deflection into reading. However, in many cases it is convenient to use a trick and dilate the reading in the low-pressure range: if the pressures are equal on both sides of the diaphragm, that is, at low pressures, the entire diaphragm surface area is ready to accept the pressure. As the pressure rises into the range of 1–1.5 kPa, the first fold in the membrane comes to rest at the base plate that is manufactured with a corresponding contour (Figure 6.8). The surface area of the membrane thus decreases, the membrane's stiffness increases, and sensitivity drops. In the range 5–6 kPa, the next fold touches the base plate and the membrane's surface area decreases further. This process action repeats a third time in the

range 15–20 kPa. The described trick yields a scale dilated across a wide pressure range.

### Diaphragm (Membrane) Vacuum Gauges with Electrical Converters.

Diaphragm vacuum gauges of the described type are suitable for incorporating electrical sensors as well. Figure 6.9 shows three examples of electrical signal generation. Sensors using wire resistance strain gauges are outdated; however, they are included in the figure to illustrate the measuring concept.

A second principle uses a capacitive displacement sensor. It provides an electrical signal, which can be electronically linearized and teletransmitted.

The inductive displacement sensor in Figure 6.9, a uses a ferromagnetic pin extending more or less far into a differential transformer coil. The produced signal is proportional to the deflection of the diaphragm. Such sensors are available down to an end-scale deflection of 25 Pa but measurement accuracy due to temperature variations is limited to 1 Pa. Inductive sensors show low hysteresis and high reproducibility, and are relatively insensitive against mechanical disturbance (vibration). They are available with electrical current (4–20 mA) as well as voltage outputs (up to 10

V).

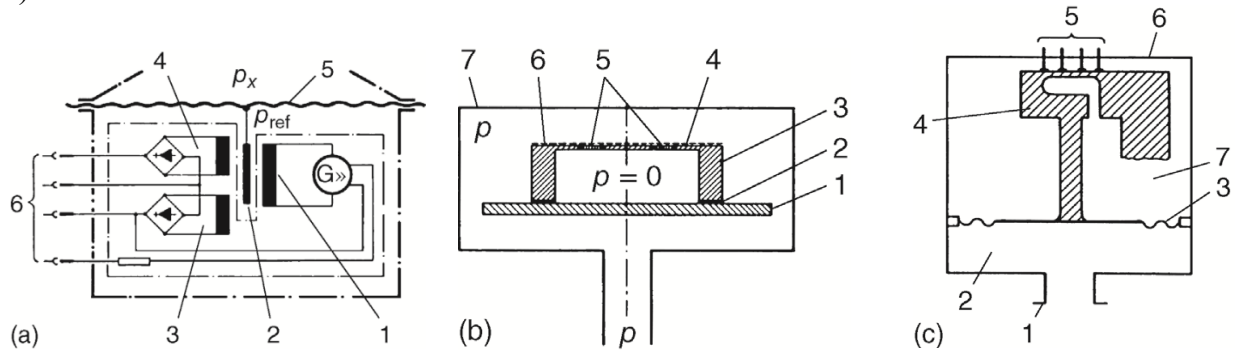


Figure 6.9 (a) Diaphragm vacuum gauge for remote display with inductive displacement transducer.  $p_{ref}$ : reference pressure;  $p_x$ : measured pressure. (1, 3, 4) Differential transformer, (2) ferromagnetic immersion rod, (5) diaphragm, and (6) electrical connectors. (b) Diaphragm vacuum for remote display with piezoresistive sensor. (1) Silicon base plate, (2) vacuum-tight Cu-Si joint, (3) n-silicon cap, (4) diaphragm, (5) resistance bridge of p-silicon integrated into diaphragm by diffusion, with wire connection, (6) flexible protective layer, and (7) housing. (c) Diaphragm vacuum gauge with wire resistance strain gauges. (1) Connecting flange, (2) measuring volume, (3) diaphragm, (4) deflection rod, (5) wire resistance strain gauges, (6) housing, and (7) volume with reference pressure  $p=0$ .

The design in Figure 6.9,c uses a deflecting rod (4) to pick up the diaphragm deflection. Wire resistance strain gauges in a bridge circuit are applied to the rod providing the electrical output signals. The arrangement allows accurate pressure measurements up to 200 kPa.

Diaphragm (Membrane) Vacuum Gauges Using the Piezoresistive Principle.

The piezoresistive effect (Figure 6.9, b), due to which a pressure change causes a change in electrical resistance, is being used increasingly for pressure measurements, even under vacuum. In metals, the change in resistance is determined by the geometrical change of the conductor (cross section, length). Semiconductors additionally show a change in the specific resistance of the material, thereby increasing the piezoresistive effect. Thus, semiconductor materials are preferred for pressure measurements relying on this principle.

Crystalline silicon has extraordinary elastic properties. It can be loaded nearly to the fracture limit, shows hardly any hysteresis, and is very stable. Silicon is thoroughly investigated due to its applications in microelectronics, and processing including doping, thin-film coating, and etching is well under control. Thus, it represents the material of choice.

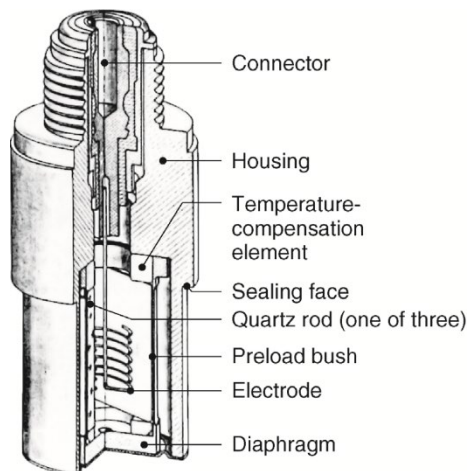


Figure 6.10 Piezoelectric pressure sensor.

For measuring resistance changes, doped low-impedance conductor patterns in radial and tangential directions are applied to one side of the circular diaphragm. The thin silicon disk is etched down to a thin diaphragm from the other side. The resistors are connected in series and are part of a resistance bridge adjusted to  $p < 0.1$  kPa. Changes in gas pressure deform the silicon diaphragm and the following resistance change detunes the bridge. The electronically linearized signal is proportional to the absolute pressure and independent of the ambient atmospheric pressure as well as of the gas species. The measuring head has a very small measuring volume of only 1 cm<sup>3</sup>. The measuring range is 0.1–100 kPa. Integrated circuit technology allows one to integrate amplifiers directly into the sensor element. As in any diaphragm vacuum gauge, absolute pressure is measured if the reference side is evacuated down to below the resolution limit of the measuring instrument, and differential pressure measurement is obtained if the reference side is exposed to any desired pressure value.

However, compensation of the strong temperature dependence of semi-conductor resistors is required.

#### Piezoelectric Vacuum Gauges

If a force is applied to a quartz crystal, the piezoelectric effect produces charges on the crystal surface that are conducted by electrodes and measured with suitable instruments (Figure 6.10). A pressure exerting forces from all sides does not create any charges. Therefore, a piezoelectric pressure sensor uses a diaphragm that transforms the pressure into a force related to the elastic surface of the diaphragm. The force is measured by employing a quartz crystal rod. An electrode conducts the produced charges to a connector plug from where highly isolated connecting wires transfer the charges to the input of a charge amplifier that transforms the charge into a voltage.

#### Resonant Diaphragm Vacuum Gauges

The measuring principle of a resonant diaphragm vacuum gauge [3] is based on the frequency change of a resonator due to changes in a solid. The strain is changed by pressure changes across a diaphragm. Figure 6.11 shows the basic setup of such an instrument, manufactured by micromachining. Two H-shaped resonators are placed onto a thin-etched diaphragm: one in the middle and the other at the edge of the diaphragm. Diaphragm and resonators are made of mono-crystalline silicon with excellent elastic properties. The resonators are 30 $\mu$ m wide, 500  $\mu$ m long, 5 $\mu$ m high, and placed in a specially manufactured vacuum housing with walls made of highly p-doped silicon, just as the resonators.

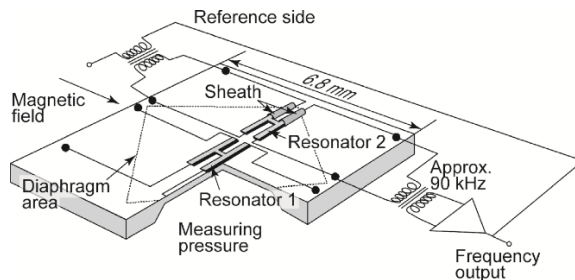


Figure 6.11 Diagram of the sensor chip in a resonant diaphragm vacuum gauge. Image includes electrical coupling for resonator 2.

The two resonators are not exactly equal in size. Thus, their natural frequencies differ slightly and they are excited by self-oscillation. When pressure is applied, resonator 2 at the edge of the diaphragm reduces its resonance frequency  $f_2$  (approximately 90 kHz) and  $f_1$  of resonator 1 in the middle rises. The difference ( $f_1 - f_2$ ) is a measure of the differential pressure. The sum ( $f_1 + f_2$ ) is a measure of the total line pressure to both sides of the diaphragm. Isolation of the resonators and protection against the surrounding pressure by means of the vacuum housing are extremely important for the accuracy of the sensor because

they prevent an impact of ambient pressure on resonator quality (Q factor) and the dependent resonance frequency. The deflection of the diaphragm alone determines the frequency change. If the volume above the diaphragm is evacuated down to pressures below the resolution limit, the sensor can be used as an absolute pressure gauge.

Additional temperature sensors placed on the chip compensate for null drifts and sensitivity changes caused by temperature variations. The frequency change is approximately 20% for a differential pressure of 100 kPa. In this example, the relative strain change in the silicon crystal is  $1 \times 10^{-4}$ .

For the highest accuracy (approximately  $1 \times 10^{-4}$ ), the measuring range of such sensors is 100 Pa to 100 kPa. Long-term and transport stability of these instruments has proven to be very high as well ( $3 \times 10^{-5}$  at 1 kPa) [4]. Unfortunately, these gauges are presently (2015) out of the market.

#### Capacitance Diaphragm Vacuum Gauges.

In capacitive pressure measurement, the measuring diaphragm, deflecting due to pressure, forms one electrode of a capacitor. The change in capacitance of this capacitor caused by the pressure difference from one diaphragm side to the other is measured. The systems are referred to as capacitance diaphragm gauges (CDGs) because the measuring signal relies on a capacitance measurement. The high sensitivity of this pressure measuring technique allows measurements of very small pressure differences, and thus absolute pressures, if the pressure on the reference side is below the resolution limit of the instrument. The resolution limit of these instruments is approximately 1 mPa.

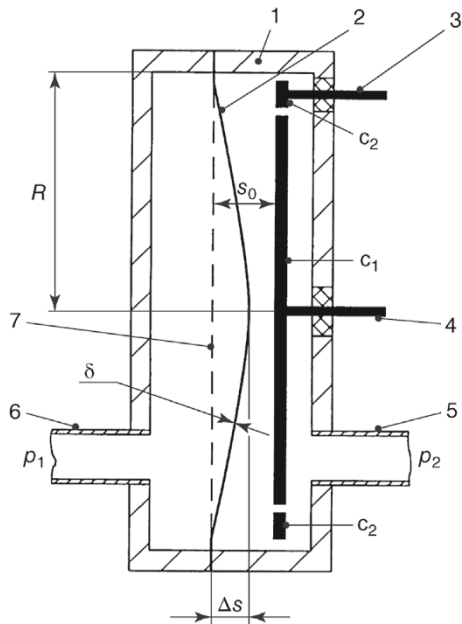


Figure 6.12 Diagram of a capacitance diaphragm vacuum gauge with Invar diaphragm. (1) Housing, (2) diaphragm, (3) leadthrough to capacitor ring  $c_2$ , (4) leadthrough to capacitor ring  $c_1$ , (5) gas inlet (reference pressure  $p_2$ ), (6) connecting port to vacuum vessel with measured pressure  $p_1$ , and (7) diaphragm in zero position ( $p_1 = p_2$ ).  $\delta$ : diaphragm thickness;  $\Delta s$ : deflection of diaphragm;  $s_0$ : distance between diaphragm and capacitor plate  $c_1$ .

Starting in 1949, development of capacitance pressure sensors went through several stages [5] leading to today's designs that show high measuring accuracy, long-term stability, and overload safety. The pressure sensors attached to the instruments are robust and compact. Capacitance vacuum gauges are used in industrial vacuum systems, particularly semiconductor industry, as well as for reference standards for calibration services.

A capacitance vacuum gauge is made up of a transducer and the electronics for processing and displaying the pressure-dependent signal. The latter can be either fully integrated into the transducer or placed inside a separate unit. For separately arranged electronics, the transducer includes a pre-amplifier.

A large variety of transducer designs are commercially available for different applications and measuring ranges. Figure 6.12 shows a schematic illustration of a capacitance vacuum gauge.

The diaphragm (2: deflected; 7: zero position for equal pressure on both sides of the diaphragm) exposed to the measured pressure is a circular disk made of a material with a low coefficient of thermal expansion, for example, Invar or ceramic. Thickness is determined by the desired end-scale deflection and can be as low as 25  $\mu\text{m}$ . It is fixed by welding, cementing, or brazing. For improved zero-point stability, the membrane forms two capacitors with the circular electrode  $c_1$  and the annular electrode  $c_2$ . The difference in capacitance of the two capacitors is used as a measuring signal.

## 6.2. Spinning rotor gauges

Gas friction explains the proportionality between the frictional force of a gas in between a moving and a stationary wall, and gas density  $n$  or pressure  $p$ , for low pressures. More precisely, the frictional force is proportional to the impingement rate  $\bar{n}c/4$  of gas particles. Here, low pressure means that the mean free path  $l$  of gas particles is greater than the distance  $d$  between the walls. If this effect is to be used in a vacuum gauge where wall distances of 1 cm are realistic, Figure 6.2 shows that the pressure must be below 1 Pa.

Meyer [6], Maxwell [7], Kundt and Warburg [8], Sutherland [9], Hogg [10], and Knudsen tried to measure gas friction with disks suspended on thin glass torsion fibers. A disk of the same geometry rotating below accelerates the gas and turns the disk on the fiber until the moment of torsion balances the moment of friction. The torsion angle then is a measure of the pressure. However, in these early experiments, the friction in the disk suspension was too high. Only after 1937, when magnetic suspension allowed frictionless mounting [11], the effect of gas friction was successfully utilized for gas pressure measurements. The first instruments by Beams [12,13] were hard to handle. Later, Fremery [14–17] developed a convincing vacuum gauge.

### Measuring Setup and Measuring Principle

Figure 6.13 shows a schematic illustration of the most important components in a spinning rotor gauge and a section through the measuring head. In a tube (2, length 60 mm, inside diameter 7.5 mm) flange-mounted to the vacuum vessel, a steel (preferably stainless steel) sphere (1, diameter 4–4.76 mm) is freely suspended magnetically. The magnetic field of the permanent magnets (3)

compensates for the main part of the sphere's weight. The superimposed magnetic field of the coils (4) holds the sphere in place.

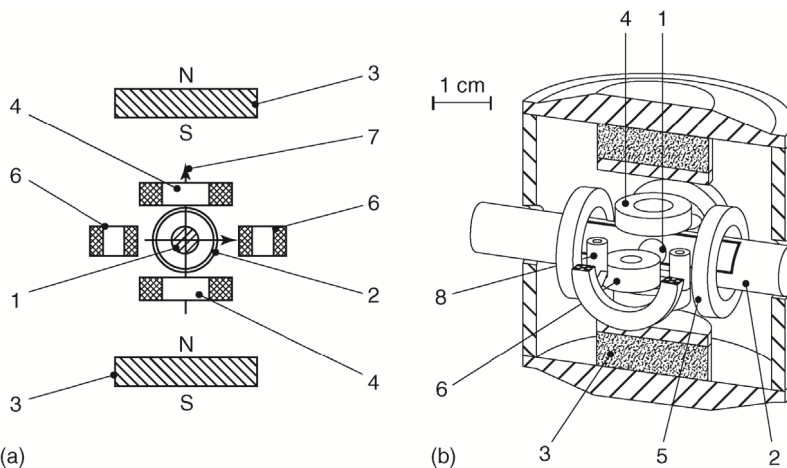


Figure 6.13 (a) Diagram and (b) section of the measuring head in a spinning rotor gauge. (1) Rotor, (2) vacuum tube, (3) permanent magnets, (4) two coils for stabilizing vertically, (5) four driving coils, (6) two signal sensing coils, (7) spin axis, and (8) four coils for stabilizing horizontally.

Two coils (4) hold the sphere vertically; four coils (8) stabilize it horizontally [17]. Four drive coils (5) create a rotating field in the horizontal plane, cycling at a frequency  $\nu_0$  of approximately 415 Hz, that accelerates the sphere around the vertical axis (7) to its initial rotary frequency  $\nu_0$ . After this frequency is obtained, the rotary field is shut off. The rotary frequency of the sphere thus drops according to the retarding moments caused, among other effects, by

impinging gas molecules. The sphere's relative frequency gradient  $\Delta\nu/\nu$  is the measured signal (DCR signal,

deceleration rate). It is picked up by two sensing coils (6) in the horizontal plane. The azimuthally inhomogeneous magnetic field of the sphere, characterized by a magnetic moment, creates an AC voltage with the rotary frequency of the sphere in the sensing coils (6). Retarding effects on the sphere, independent of the number of impinging gas particles, include the current induced in the sensing coils, eddy currents produced by the magnetic moment of the sphere (particularly in vacuum tube 2), and eddy currents produced in the sphere itself by non-homogeneities of the magnetic field. This pressure-independent offset (residual drag) must be subtracted from the measured signal.

### 6.3. Direct electric pressure measuring transducers

At this point, we will list a number of effects that, in principle, can be used for pressure measuring but that have not yet been implemented in widespread applications. These effects include the pressure-dependent natural frequency of oscillator quartz [18,19], pressure-sensitive transistors, pressure-sensitive tunnel diodes, pressure-sensitive photoresistors, and the pressure dependence of the resistance of thin, soft magnetic coatings [20].

### 6.4. Thermal conductivity vacuum gauges

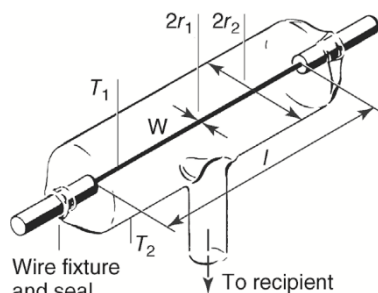


Figure 6.14 Basic setup of a thermal conductivity vacuum gauge.

Thermal conductivity vacuum gauges are pressure measuring instruments for medium and low vacuum that measure the pressure-dependent thermal loss (loss of energy) of a heated element, usually a wire, through the gas.

The measuring principle is based on a 1906 publication by Pirani [21]: a heated wire is part of a Wheatstone bridge that supplies the necessary energy to the wire and measures its resistance or the dissipated power. English literature, in particular, often refers to thermal conductivity vacuum gauges based on a Wheatstone bridge simply as Pirani gauges.

Thermal conductivity vacuum gauges (Pirani gauges) offer several different modes of operation: thermal conductivity vacuum

gauges that maintain constant wire temperature and measure the required heating power, which depends on the pressure, represent the most precise setup and show the largest linear measuring range (0.1 Pa to 10 kPa). However, measuring technology here is the most complex and thus expensive. Alternatively, the heating power or current is kept constant and the compensation current in the bridge can be used as a measure of pressure.

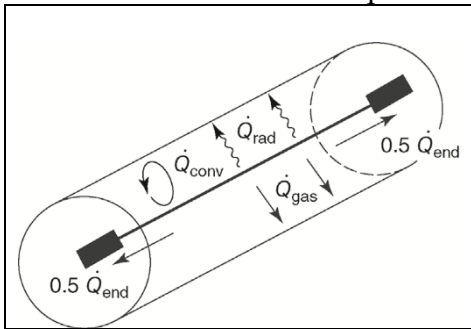


Figure 6.15 Heat fluxes from a heating wire in a thermal conductivity vacuum gauge:  $Q_{gas}$  via the gas,  $Q_{rad}$  due to radiation,  $Q_{conv}$  due to convection, and  $Q_{end}$  due to thermal conduction.

Also, circuits that keep heating power constant and measure the temperature, which depends on the gas pressure, are possible. Usually, a thermocouple is used for this temperature measurement. Here, however, the measuring range is only approximately 0.1 Pa to 1 kPa. Less sophisticated and cheaper versions do without a Wheatstone bridge and use a simple thermocouple for measuring the current that follows the contact voltage in the thermoelement if the heated wire receives constant current. Their measuring range is 0.1-100 Pa.

The principal design of a thermal conductivity vacuum gauge (compare Figure 6.14) usually includes a wire W with a diameter of 5–20  $\mu\text{m}$  and length of 50–100 mm suspended axially in a cylindrical tube of 10–30 mm diameter. When the wire is heated electrically, it approaches an equilibrium temperature  $T_1$  at which the supplied electrical power  $Q = IU$

equals the dissipated thermal power. The latter is made up of four components (Figure 6.15):

1. Thermal conduction  $Q_{gas}$  via the gas between the warm wire ( $T_1 \approx 400 \text{ K}$ ) and the wall at room temperature ( $T_2 \approx 300 \text{ K}$ ). The energy flux rate or dissipated thermal power is proportional to the pressure  $p$ . In the viscous flow regime,  $Q_{gas}$  is independent of pressure. In the transition range, a function of the type  $p/(1 + gp)$  ( $g$ : constant) describes the pressure dependence of  $Q_{gas}$  well, and thus,

$$Q_{gas} = \varepsilon \frac{p}{1 + gp} \quad (6.2)$$

The constant  $\varepsilon$  (sensitivity) includes gas characteristics such as  $C_{molar}$  and  $\bar{c}$ , and  $g$  is a factor determined by the geometry.

2. Thermal conduction  $Q_{end}$  at the wire ends via the wire fixing.
3. Thermal radiation  $Q_{rad}$  emitted by the hot wire (hot with respect to its surrounding).
4. Thermal conduction  $Q_{conv}$  due to convection at pressures  $> 1 \text{ kPa}$ .

$Q_{end}$  and  $Q_{rad}$  are disturbing effects that create the false impression of a gas pressure  $p_0$  in the measuring cell even if the cell does not contain any gas, that is, if pressure is zero. We will set

$$Q_{end} + Q_{rad} = \varepsilon p_0 \quad (6.3)$$

which defines zero pressure. Parameters in the functional dependences of the thermal loss due to radiation include emissivity and geometry of the surface as well as the temperature distribution on the wire. Thus, on the one hand, calculation is difficult and, on the other hand,  $\varepsilon p_0$  might change from one day to the other or even during the course of a single measurement. For simplification, however, constant  $Q_{end}$ ,  $Q_{rad}$ , and thus  $p_0$  are assumed as long as the temperatures of wire and surrounding,  $T_1$  and  $T_2$ , respectively, are kept constant. This is one reason for measurement uncertainty. At pressures low enough for convection to be negligible, the power balance at the wire W reads

$$Q_{el} = Q_{end} + Q_{rad} + Q_{gas} \quad (6.4)$$

or using Equations (6.2) and (6.3)

$$Q_{el} = UI = \frac{U^2}{R} = \varepsilon \left( p_0 + \frac{p}{1 + gp} \right) \quad (6.4)$$

Thus, for pressures at which  $Q_{gas} \propto p$ , measuring the electrical heating power  $Q_{el}$  supplied to the wire in a measuring cell (resistance R) according to Figure 6.14, or a related quantity, with respect to pressure  $p$ , yields a linear proportional signal. At higher pressures where thermal conductance  $Q_{gas}$

is pressure independent, heat dissipation rises only due to convection. At low pressures, thermal radiation, which is also pressure independent, dominates so that the measured signal merges into a constant offset.

#### Thermal Conductivity Vacuum Gauges with Constant Wire Temperature

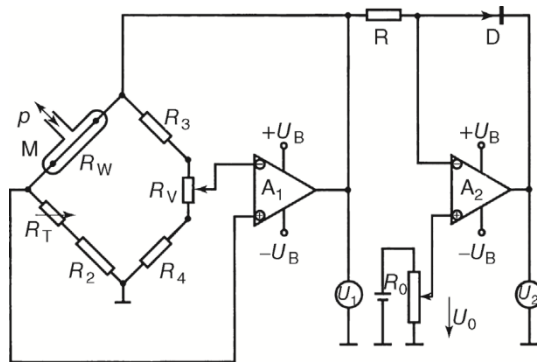


Figure 6.16 Electrical diagram for a thermal conductivity vacuum gauge with constant wire temperature. *M*: measuring cell; *R<sub>w</sub>*: resistance of measuring wire.

Here, a thin wire made of tungsten or nickel with a diameter of 7–10 μm is used for measuring. As Figure 6.16 shows, the wire represents one arm *R<sub>w</sub>* of a Wheatstone bridge including the resistances  $R_2 \approx R_3 \approx R_4 \approx R_w$  and a resistor for temperature compensation *R<sub>T</sub>*. Amplifier *A<sub>1</sub>* controls the voltage *U<sub>1</sub>* at the bridge so that the resistance of the measuring wire, and thus its temperature, is heat flux independent, that is, independent of the pressure. In this case, the bridge is balanced at all times.

Electronics required for displaying the dissipated thermal power *Q<sub>el</sub>*, or the square of heating voltage, are complex. Therefore, the bridge is often not fully balanced; instead, the voltage *U<sub>1</sub>* at the bridge is displayed using an appropriately calibrated voltmeter. In this case, the relation between the shown voltage *U<sub>1</sub>*

and pressure *p* is approximately given by (Equation (6.4)).

$$Q_{el} = 2 \sqrt{R_w \varepsilon \left( p_0 + \frac{p}{1 + gp} \right)} \quad (6.5)$$

Thus, a nonlinear scale is obtained, with zero pressure at approximately 1 Pa so that the pressure range between 0.1 and 1 Pa defies measurement. A more complex circuit (right-hand side in Figure 6.16) allows compensating for zero pressure using a voltage *U<sub>0</sub>* at potentiometer *R<sub>0</sub>*. Taking the logarithm of the voltage *U<sub>1</sub> - U<sub>0</sub>* by means of a diode *D* yields a scale.



Figure 6.17 Section of a measuring tube in a thermal conductivity vacuum gauge (constant wire temperature) with gold-plated tungsten heating wire and a measuring range from 0.1 Pa to 100 kPa. The surrounding cylindrical housing (see heating wires) is temperature controlled to approximately 40 °C for increased measurement accuracy. At higher pressures, heat transport due to convection is used as a measuring signal.

Digital readings often depend on a characteristic curve where a change of 1 V corresponds to a change of one decade in pressure (e.g., the range 1–9 V corresponds to pressure range of 10<sup>-3</sup> to 10<sup>5</sup> Pa). This, on the decades equally distributed curve, however, should not mislead the user that due to the reduction of sensitivity at the limits of the measuring range measurement uncertainties greatly increase. Voltmeters can be used to indicate output voltage of “active” thermal conductivity vacuum gauges, which is then converted to a pressure reading by a formula or table.

At gas temperatures around 300 K and wire temperatures > 400 K, sensitivity  $\varepsilon$  is no longer temperature dependent. A means of calibration is often provided because sensitivity  $\varepsilon$  and zero pressure *p<sub>0</sub>* vary from one measuring setup to the next. Calibration involves the following steps.

At atmospheric pressure, the temperature set point of the heating wire, and thus sensitivity  $\hat{\mu}$ , is adjusted using potentiometer *R<sub>V</sub>* (Figure 6.16) so that the display shows 100 kPa. Next, the measuring tube is evacuated to a pressure that is small compared with the lowest measurable pressure, in this case, approximately 0.01 Pa. Then, compensation voltage *U<sub>0</sub>* is adjusted with *R<sub>0</sub>* until the display indicates that *U<sub>2</sub>* equals zero. In some cases, the

calibration potentiometers  $R_V$  and  $R_\theta$  are integrated into the head of the measuring tube, together with the remaining resistances of the Wheatstone bridge and the resistor for temperature compensation  $R_T$ , as shown in Figure 6.17. Then, the measuring tube can be calibrated prior to delivery so that it can be hooked up to any measuring instrument without requiring any individual adjustment.

This calibration generally prevails as long as the heating wire does not suffer any irreversible changes. There is a possibility of increased blackening on the heating wire due to deposition of contaminants. Such an increase causes a rise in zero pressure, which leads to too high values displayed by the instrument in the low-pressure range, that is, the zero point is never reached. Subsequent calibration using voltage  $U_\theta$  can compensate this deviation throughout a wide range without having any considerable impact on measuring accuracy.

The tungsten wire in the thermal conductivity vacuum gauge shown in Figure 6.17 is gold plated in order to avoid changes in the heating wire.

An additional method of zero-point compensation is given by designing resistor  $R_3$  (Figure 6.16) as a pressure/vacuum-tight encapsulated heating wire element (compensation element), analogous to the measuring-wire cell. If these two cells are thermally short-circuited, temperature changes in both arms of the bridge will have analogous effects: the bridge remains balanced, but only for a certain pressure, namely, the pressure in the compensation element's capsule, because the temperature variation in the heating wire depends on the surrounding pressure. Thus, it is advisable to realize compensation by incorporating variable resistors.

Compared with simple designs (see following sections), sophisticated thermal conductivity vacuum gauges with constant wire temperatures provide wider measuring ranges and have the advantage that they react quicker to pressure changes. This is because their components are not subject to any temperature changes, and thus, no thermal relaxation periods arise, which would delay measuring signal acquisition.

#### Thermal Conductivity Vacuum Gauges with Constant Heating

In addition to the operating mode of a thermal conductivity vacuum gauge using constant wire temperature, the heating wire can also be supplied with constant heating voltage (or constant electrical heating current) (Figure 6.18). Then, the resistance of the wire is acquired as a measure of its pressure-dependent temperature.

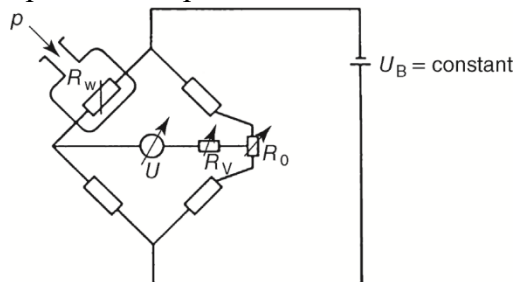


Figure 6.18 Electrical circuit in a thermal conductivity vacuum gauge using constant supply voltage and variable wire temperatures. Top left: measuring cell;  $R_w$ : resistance of measuring wire.

Pirani's [21] antiquated principle uses a heating wire that forms one arm of a Wheatstone bridge operating at constant voltage ( $U_B$ ). If the temperature in the heating wire changes due to pressure variations, resistance  $R_w$  in the wire also changes. This change in resistance detunes the bridge, thus creating a voltage signal  $U$  on the indicating instrument in the bridge's diagonal (Figure 6.18). Using appropriate calibration, the voltage can be translated and displayed as pressure  $p$ . The temperature coefficient of the electrical resistance in the measuring wire's material should be as high as possible. Pure metals or semiconductor resistors (thermistors with positive or negative temperature coefficient) usually meet this condition.

$$U = AU_B \frac{p}{1 + Bd/l} \approx \frac{AU_B}{Bd/l} p = \varepsilon p \quad (6.6)$$

The primary parameter for the measuring range of these thermal conductivity vacuum gauges is the ratio of wire diameter  $d$  and wire length  $l$ .

The upper limit of the measuring range of such instruments is reached when wire temperature  $T_1$  is just above ambient temperature  $T_2$ . Since the balancing current in the bridge's diagonal is proportional to the temperature difference  $T_1 - T_2$ , which drops as the pressure rises, sensitivity  $\varepsilon$  also drops with rising pressure and the scale becomes nonlinear. The linear range for a Pirani gauge with constant heating power is smaller than that in a thermal conductivity vacuum gauge operating at

constant temperature. The lower measuring limit is generally one thousandth of the maximum measurable pressure.

If a thin long wire is used, the factor  $d/l$  in the denominator in Eq. (6.6) is small, and thus, sensitivity  $\epsilon$  is high. However, the highest measurable pressure is fairly low. In contrast, a short wire with larger diameter shifts the measuring range toward higher pressures. Advances in electronics have led to low-priced solutions for measuring small currents. Thus, the reduced sensitivity for lower values of  $d/l$  is no longer significant and the general approach is to use the wider linear measuring range [22].

Possible temperature changes in the gas or in the surrounding have considerable impact on the measuring inaccuracy of a Pirani gauge. For Pirani gauges with constant heating power, in particular, this effect increases as pressure rises because the temperature difference between the wire and the environment drops. At wire temperatures of 400 K ( $p = 0$ ) and a measured pressure of 100 Pa, a temperature change of 1 K produces a deviation in the measured value of approximately 10 Pa. At 600 K wire temperature, the deviation is still between about 1 and 5 Pa [22]. As the ambient temperature changes by 1 K, the zero-point signal changes by approximately 0.1 Pa. The same change is observed when the voltage on the bridge changes by 0.1%.

#### Thermocouple Vacuum Gauges

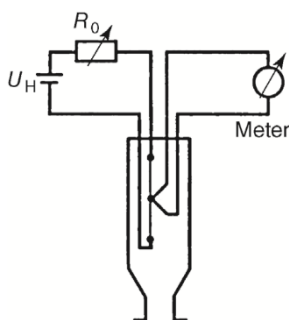


Figure 6.19 Diagram of a thermal conductivity vacuum gauge with thermocouple.

The temperature of the heating wire can also be measured directly using a thermocouple as shown in Figure 6.19. The thermocouple is attached to the heating wire and its thermoelectric voltage is directly monitored. Spot welding or brazing with silver filler metal is used to join the thermocouple, for example, chromel/alumel, and the heating wire. The typical current fed to the heating wire is 150 mA. Here, the wire is considerably shorter than that in a sophisticated Pirani gauge, and thus, sensitivity at low pressures is reduced. Typical measuring ranges lie between 0.1 and several 100 Pa. The system is calibrated at low pressure by adjusting the temperature of the heating wire using a controllable dropping resistor so that the display shows end-scale deflection (highest voltage level). Additional line-up at atmospheric pressure

is often dispensable because then the temperature of the heating wire is just slightly above ambient temperature. Here also, it can be necessary to compensate for changes in the surface condition of the heating wire by readjusting the compensation potentiometer. Above considerations apply likewise to the measuring range and its dependence on wire diameter and wire length.

#### Thermistors

Thermistors are thermal conductivity vacuum gauges in which the heating wire is replaced by oxidic semiconductors usually showing a negative resistance coefficient  $dp/dT$ . Its positive value is considerably above that of tungsten and platinum. Thus, in a bridge circuit, the compensation currents under unbalanced operation are considerably above the currents appearing in glow wires. For improving zero-point stability disturbed by changes in ambient temperature, the same semiconductor material is encapsulated under high vacuum and integrated into the bridge.

### 6.5. Thermal mass flowmeters

Using the effect of heat transport in a gas is not restricted to pressure measurement but can be used for assessing gas flow as well. Whereas pressure measurement utilizes the heat transport from a hot element via thermal self-movement of gas particles, flowmeters utilize the heat transport in a collective flow field of gas particles directed toward low-pressure regions. A thermal mass flowmeter measures the heat transferred from a small, heated tube to a gas flow on its inside.

Gas flowmeters with measuring ranges  $7 \times 10^{-8}$  to  $4 \times 10^{-2} \text{ mol s}^{-1}$  ( $0.1\text{--}5 \times 10^4 \text{ sccm}$ ) are used mainly in semiconductor industry for measuring and controlling gas flows in process reactors. Here, thermal flowmeters based on the introduced principle have prevailed.

A thermal gas flowmeter is made up of a small capillary (usually stainless steel) with an inside diameter of 0.25–1 mm, covered with a coiled heating wire that shows high resistance and a high temperature coefficient of electrical resistance. Such a wire can be used as a heating element and as a temperature sensor. A number of designs are available:

- Two temperature sensors that measure the downstream and upstream capillary temperatures (Figure 6.20) frame a single heating element.
- Two heating elements are integrated into a Wheatstone bridge and react to changes in the temperature profile caused by the gas flow.
- Three heating elements at temperatures  $T_1$ ,  $T_2$ , and  $T_3$  are held at constant temperatures with  $T_2 > T_1 > T_3$ , for a direction of gas flow from 1 to 3. The voltage for the second heating element is the measuring signal.

For the first approximation, the mass flow rate  $\dot{m}$  of the gas can be calculated from

$$\dot{m} = \frac{\dot{Q}}{c_p(T_{lo} - T_h)} \quad (6.7)$$

$\dot{Q}$  is the heat flow from the capillary or the heating element into the gas,  $c_p$  is the molar heat capacity of the gas,  $T_h$  is the upstream temperature of the gas (high-pressure side), and  $T_{lo}$  is the downstream temperature. Either the temperature difference ( $T_{lo} - T_h$ ) is held constant and the required heating power  $\dot{Q}$  is measured, or  $\dot{Q}$  is kept constant and ( $T_{lo} - T_h$ ) is measured.

Nonlinearities (deviations from Equation (6.7)) can have different causes:

- $c_p$  not only depends on the gas species but is also a function of temperature. The gas temperature can be different from the measured wall temperature of the capillary.
- The heat transfer coefficient  $Q_{gas}/Q_{wall}$  can depend on the gas flow.
- As in thermal conductivity vacuum gauges, disturbing effects can be caused by heat transport in the capillary itself, by radiation losses, and by thermal losses due to convection outside of the capillary.

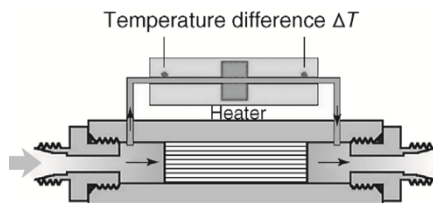


Figure 6.20 Thermal mass flowmeter with a heating element and two temperature sensors measuring the difference between upstream and downstream temperatures,  $\Delta T = (T_h - T_{lo})$ .

The flow is separated in order to increase the measuring range of a thermal mass flowmeter (Figure 6.20): a bypass allows free gas flow, and a branch feeds the gas to the actual sensor. An appropriate flow barrier is arranged in the bypass in order to guarantee laminar flow throughout the entire measuring range.

It is absolutely crucial to encapsulate the flow sensor with a temperature-stabilized housing in order to, on the one hand, precisely define  $T_h$  and, on the other hand, minimize some of the disturbing effects described above as well as provide zero-point stability. Usually, the temperature of the housing is set to 60 °C.

Thermal gas flowmeters are usually calibrated for nitrogen. Manufacturers provide correction factors  $K_{gas}$  for other gas species. However, these factors have to be replaced by correction functions  $K_{gas}(\dot{m})$  if measuring accuracies of less than 20% are required [23,24] because the given correction factors do not consider thermal conduction through the gas.

The bypass can create additional dependences of gas correction factors: for different gas species, viscosity is differently temperature dependent. Thus, for different gas species, gas flows are not distributed among the measuring capillary and the bypass in the same way.

Metrological investigations showed [24] that the orientation of flowmeters with respect to the gravitational field has an influence on the zero point (the temperature distribution of the capillary changes due to variations in convection). However, measured values remain correct if the zero point is corrected. Also, the dependence of sensitivity toward inlet pressure is negligible (0.75% deviation per MPa pressure change). Long-term stability is quite high and the relative measurement deviations remain below  $\pm 1\%$  during an operational period of 1 year [24]. Yet, uncalibrated instruments showed

measuring deviations from correct gas flows of up to 17% [24].

## 6.6. Ionization gauges

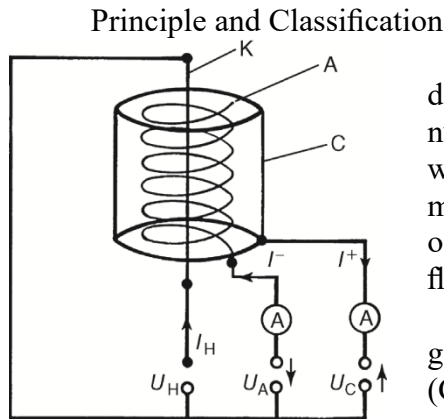


Figure 6.21 Basic design of an ionization gauge with emitting cathode.  $U_H$ : heating voltage;  $I_H$ : electrical heating current in the emitting cathode;  $U_A$ : anode voltage;  $I^-$ : electron current to the anode;  $I^+$ : ion current to the collector; K: cathode; A: anode; C: collector.

Ionization gauges measure pressures indirectly by determining an electrical quantity proportional to the particle number density  $n$ . In order to make this quantity available, the gas whose pressure is to be measured is partially ionized in the measuring head of the ionization gauge. Depending on the method of ionization, the measured electrical quantity is either a pure ion flow or a gas discharge flow.

In the hot-cathode gauge, the electrons used for ionizing the gas are emitted from an emissive cathode, usually a glow cathode (C, Figure 6.21), and accelerated toward a surrounding anode screen. The electrons emitted by cathode C with a current  $I^-$  collide with gas particles that subsequently become ionized with a certain probability. The resulting positive ions reach the ion collector (IC) and are measured as an ion current  $I^+$ .

In ionization gauges with crossed electromagnetic fields, a gas discharge is created by establishing a sufficiently high DC voltage (several kilovolts) between two low pressures also, electron paths are extended considerably by superimposing a magnetic field crosswise over the electrical field. The gas discharge current is pressure dependent and is used as a measure of gas density, that is, gas pressure.

The term cold-cathode ionization gauge should be avoided because it may cause some misunderstanding. Cold cathodes are cathodes that emit electrons not via a glowing wire but by cold field emission. Such cold cathodes may be once capable of replacing the hot cathodes in hot-cathode ionization gauges.

### Emitting-Cathode Ionization Gauges (Hot-Cathode Ionization Gauges)

On their path  $\Delta l$  through a gas of particle number density  $n$ ,  $N^-$  electrons participate in

$$\Delta N^- = N^- n \sigma \Delta l \quad (6.8)$$

collisions and thereby produce the same amount of ions  $\Delta N^+ = \Delta N^-$ . Here,  $\sigma$  is the ionization cross section, which depends on the energy of the colliding electrons and the gas species. The quantity  $n\sigma$ , termed differential ionization  $P_{ion}$ , describes the number of ions produced by each electron per unit length of its path in a gas with particle density  $n$ .  $P_{ion}$  is often given for a pressure of  $p_n = 1$  Torr = 133 Pa and the temperature  $T_n = 273$  K. According to the equation of state of an ideal gas. Figure 6.22 shows the differential ionization  $(P_{ion})_n$  of selected gas species in this state.

Dividing Equation (6.8) by time yields the electrical current. Thus, the electron current  $I_e$  produces the ion current

$$I^+ = I_e n \sigma \Delta l = I_e P_{ion} \Delta l \quad (6.9)$$

with  $P_{ion} = (P_{ion})_n \frac{n}{n_n}$ . Putting the value of  $n$ , into Equation (6.9) yields the relationship between the ion current  $I^+$  to collector C and pressure:

$$I^+ = I_e \frac{\sigma \Delta l}{kT} p = I_e \frac{P_{ion}}{p_n} \Delta l p = I_e S p \quad (6.10)$$

This introduces the gauge sensitivity (ISO 3529:2013), also referred to as sensitivity coefficient,  $S$ :

$$S = \frac{I^+}{I_e p} = \frac{P_{ion} T_n}{p_n T} \Delta l \quad (6.11)$$

which depends on the gas species, the mean free path  $\Delta l$  of the electrons in the measuring head, that is, on system geometry, and so on.  $\Delta l$  defies sufficiently accurate determination. Therefore,

$S$  has to be determined by calibration.

It should be noted that the ion current  $I^+$  has a pressure-independent component. Furthermore,  $S$  is well defined only for a particular gas species. In contrast, the residual gas of pressure  $p_0$  is a mixture of gases with usually unknown composition. Thus,  $S$  is more accurately defined by

$$S = \frac{I^+ - I_0}{I_e(p - p_0)} \quad (6.12)$$

with  $I_0$  denoting the ion current at residual pressure  $p_0$ .

Equation (6.11) also shows that  $S$  depends on temperature  $T$ , a fact worth considering for accurate measurements, particularly in cases where operating temperature differs considerably from calibration temperature.

The gauge sensitivity  $S$  is given, for example, in  $\text{Pa}^{-1}$ .

Another important gauge parameter is the ionization sensitivity  $K$ :

$$K = \frac{\Delta I^+}{\Delta p} \quad (6.13)$$

Here,  $\Delta I^+$  is the current change following the pressure change  $\Delta p$ .

According to Equation (6.10), in emitting-cathode ionization vacuum gauges [25],

$$K = S I_e \quad (6.13)$$

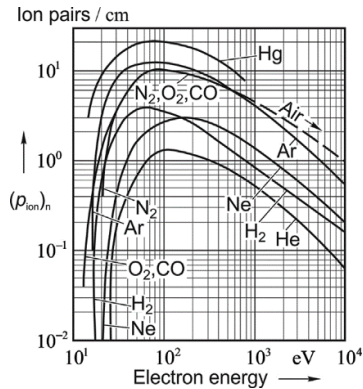


Figure 6.22 Differential ionizations  $(P_{ion})_n$  of electrons versus energy levels in selected gas species at a pressure of 133 Pa and a temperature of 0 °C.

Following Equation (6.10), ion current  $I^+$  is the pressure-dependent measured quantity. The electron current  $I_e$  emitted by the cathode can be subject to a pressure-dependent change at constant heating power due to surface coverage and additional surface effects (work function). Electronic control of the cathode heater keeps the electron current constant at an adjustable level within the range of 10  $\mu\text{A}$  to 10 mA. For a typical value  $I_e = 1 \text{ mA}$  and with a gauge constant  $S = 0.1 \text{ Pa}^{-1}$ , sensitivity  $K = 10^{-4} \text{ A Pa}^{-1}$ , that is, an ion current of  $I^+ = 10^{-8} \text{ A}$  corresponds to a pressure  $p = 10^{-4} \text{ Pa}$ .

#### Design of Emitting-Cathode Ionization Gauges (Hot-Cathode Ionization Gauges)

Based on the principle of an emitting-cathode ionization gauge shown in Figure 6.21, a variety of types have been developed, in particular, when considering measuring range [26] and manufacturing effort. In the following, the four most important designs of measuring systems are introduced, differing mainly in terms of measuring range. Figure 6.23 schematically shows the measuring ranges of the considered types. The lower measuring limit

is reached as soon as the indicated pressure  $p_{ind}$  remains constant in spite of a change in the surrounding pressure  $p_{true}$ . At the upper measuring limit, ion current, that is, indicated pressure, drops as the pressure increases.

#### Concentric Triode

This oldest type of ionization gauge system emerged from an amplifier triode. The central cathode is surrounded by a cylindrical mesh (anode) for electron collection, enclosed by the cylindrical ion collector. The electrons emitted from the cathode accelerate toward the anode and can oscillate around the mesh wires several times before they reach the anode.

Ions produced in the process between the anode and the ion collector by electron collisions approach the ion collector, and thus produce a DC signal that is proportional to the pressure. Figure 6.24 (left) shows such an ionization gauge tube. The lower measuring limit of about  $10^{-5} \text{ Pa}$  is due to the so-called X-ray effect: electrons impinging on the anode release X-ray photons. If these photons hit the collector cylinder, they release secondary electrons that cannot be differentiated from the ion current.

#### Fine-Vacuum Ionization Gauges

Development of burn-out-proof oxide cathodes allowed an increase in service life of

ionization gauge systems and resolved the 1 Pa maximum working pressure limit. However, in the early development stages, the measuring range of triodes could not yet be extended toward higher pressures because gauge coefficients dropped at higher pressures. Calibration curves deviate considerably from linear functions, as shown in Figure 6.23 (triode) [27,28].

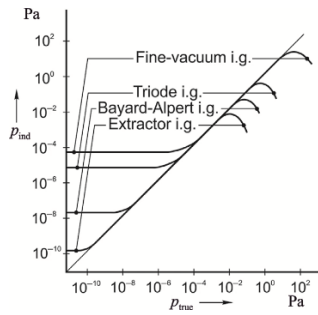


Figure 6.23 Pressure readings  $p_{ind}$  versus true pressure  $p_{true}$  for selected types of ionization gauges.

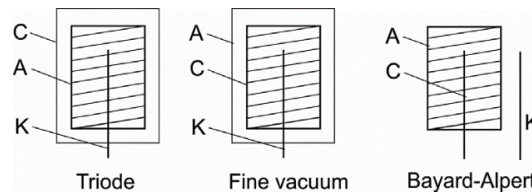


Figure 6.24 Diagram of electrode arrangement of three types of cylindrical ionization gauges with emissive cathode. A: anode; C: collector; K: emissive cathode.

This problem was resolved by switching the functions of the anode and the ion collector and by reducing their distance. The center cathode is surrounded by an ion collecting mesh, at negative potential with respect to the cathode. An electron collector, at positive potential with respect to the cathode, encloses the ion collector. This operating mode extends the measuring range

from 1 to 100 Pa. Figure 6.25 shows such a measuring system as a nude gauge. The cathode is made of an iridium band plated with thorium oxide. Such a cathode is safe from burning out, even at atmospheric pressure. However, it is much more expensive than a cathode manufactured from a thin tungsten wire. For materials used in heating wires.

The slope of the characteristic curve at higher pressures leads to ambiguous pressure readings. In measuring practice, it is often difficult to determine the point at which the system is on the characteristic curve. Experimental investigations help to resolve this issue: in the right part of the characteristic curve, increasing pressure reduces the indicated value.

Schulz and Phleps [29] introduced a historically famous and remarkably simple fine-vacuum ionization gauge, shown in Figure 6.26. Depending on gas species, it provided linear readings up to 130 Pa.

#### Bayard–Alpert Ionization Gauges

Electrons impinging on matter release photons (X-rays). Their number is proportional to the electron current. When these photons hit metal surfaces, they release photoelectrons that leave the surface if an appropriate electrical field is present. In an ionization gauge, such a field exists at the ion collector. The pressure-dependent photoelectron current leaving the collector is proportional to the electron current and adds a constant value to the positive ion current toward the ion collector. Thus, pressure readings are too high. This yields a lower pressure limit between  $10^{-4}$  and  $10^{-5}$  Pa, for the measuring range in the systems introduced above.

For reducing the X-ray effect, Bayard and Alpert [30] suggested building an ionization gauge in which the surface of the ion collector was particularly small (Figure 6.27). The collector is made of a very thin wire (diameter several  $10 \mu\text{m}$ ) and is arranged on the axis of a cylindrical anode mesh, B. The cathode, A, is outside of the anode. Bayard–Alpert ionization gauges show an X-ray limit of  $10^{-8}$  to  $10^{-9}$  Pa.

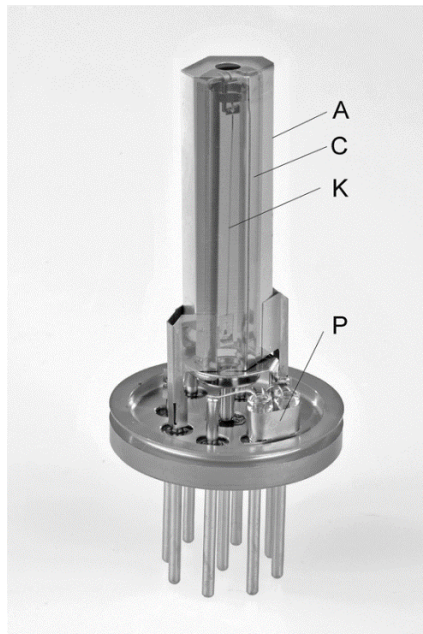


Figure 6.25 Fine-vacuum ionization gauge HPG 400 by INFICON with a measuring range of 1 mPa to 100 Pa, combined with a Pirani gauge. A: anode (+180 V); C: collector (0 V, ground potential); K: cathode (+37 V); P: Pirani gauge.

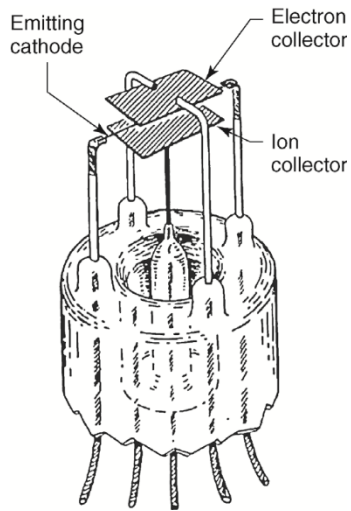


Figure 6.26 Fine-vacuum ionization gauge according to Schulz and Phleps. The emitting cathode is at 60 V, the anode (electron collector) at 120 V, and the ion collector at 0 V.

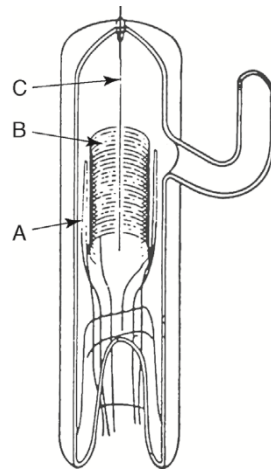


Figure 6.27 Original Bayard-Alpert ionization gauge. A: cathode; B: anode grid; C: collector.

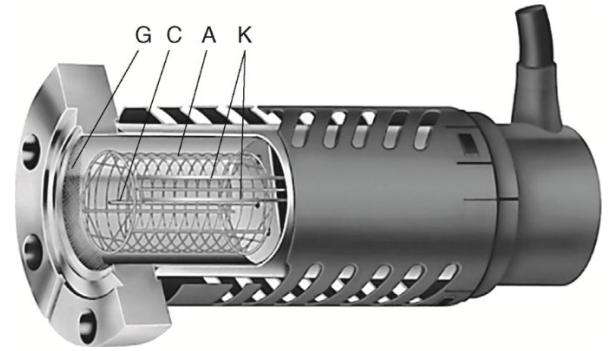


Figure 6.28 Commercially available Bayard-Alpert ionization gauge. K: cathodes (two band cathodes, each fixed at both ends); A: anode; C: central ion collector; G: mesh at ground potential protecting against changes in electrical potential.

Figure 6.28 shows a commercial measuring system of the kind. This sophisticated instrument with its highly stable gauge sensitivity is designed specifically for precise measurements [31,32].

Figure 6.29 shows the block diagram of an ionization gauge. The block denoted with H controls the emission current of cathode C (electron current  $I_e$  can be stepwise adjustable). Block A provides the anode potential and block C amplifies the ion current so it can be displayed on standard current meters. The emission-current control circuit adjusts the heating current of the directly heated cathode in the measuring system such that the electron current is kept precisely constant with a tolerance of 2%.

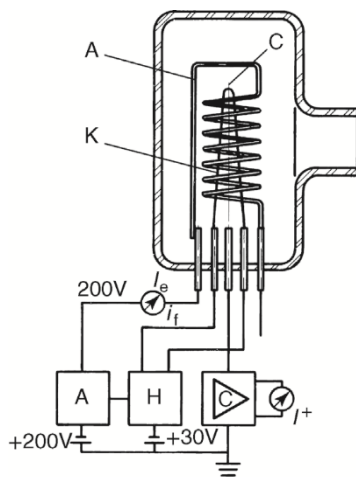


Figure 6.29 Block diagram for operating an emitting-cathode ionization gauge. Electrode system (K, A, C) according to Bayard and Alpert.

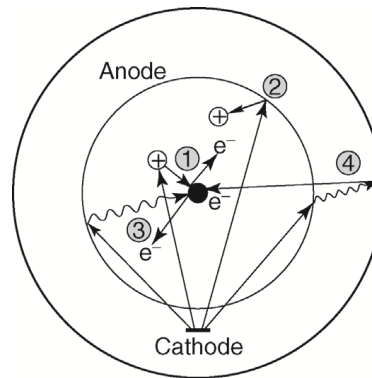


Figure 6.30 Physical effects in a Bayard-Alpert ionization gauge (collector wire in the center). (1) Electron ionizing a gas particle, subsequent release of a secondary electron when the ion impinges on the collector; (2) electron-stimulated ion desorption; (3) X-ray effect, the X-ray photon produced during electron bombardment at the anode releases an electron at the collector; (4) inverse X-ray effect, X-rays release electrons at the wall, which hit the collector (at equal potential as the wall).

A disadvantage of the open cylinder is that ions can escape along the center axis of the cylinder. The electrical field exerts a collector-directed force onto ions produced inside the mesh. In addition, however, the angular momentum must remain constant, and thus, neutral particles with sufficiently high kinetic energy in tangential direction, which turned into ions, can in fact circulate around the collector without impinging on it. If they carry an additional axial velocity component, they thus might exit the anode mesh in the axial direction. Furthermore, escaping is promoted by the lines of the electrical field in the open mesh, which are directed axially, away from the collector.

Thus, the anode mesh is closed in order to increase the gauge sensitivity  $S$ . But then, however, a closed mesh produces nonlinear ion current (with respect to pressure) above approximately 1 mPa, probably due to space-charge effects that are not observed in open cylindrical meshes until pressures reach approximately 10 mPa [33].

Reducing the diameter of the collector wire leads to even smaller pressure values for the lower measuring limit. Van Oostrom [34], for example, used a wire

with a diameter of 4  $\mu\text{m}$ . However, a disadvantage of smaller diameters is that gauge sensitivity drops, again due to the conservation of angular momentum described above.

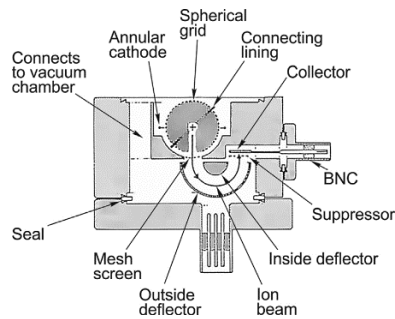


Figure 6.31 Ion spectroscopy tube according to Watanabe [35].

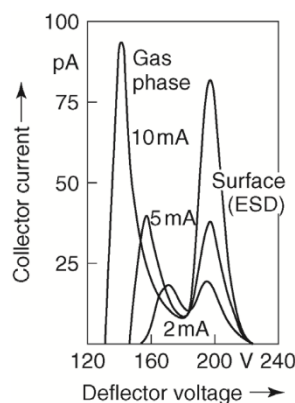


Figure 6.32 Energy spectrum of deflected ions in the ion spectroscopy tube shown in Figure 6.31.

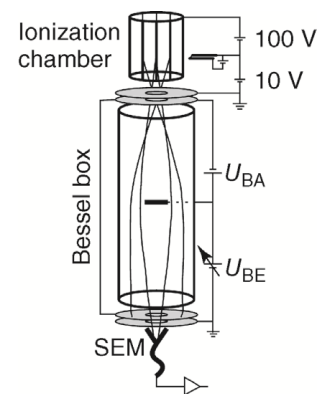


Figure 6.33 Diagram of the AxTRAN gauge, which suppresses ESD ions and X-rays by using a cylindrically symmetric energy analyzer (Bessel box). The image shows the situation at a voltage  $U_{BE}$  that suppresses ESD ions from the anode mesh (see trajectories in the image).

When operating Bayard–Alpert measuring systems, and ionization gauges in general, parasitic errors can cause pressure readings that are too high, particularly under low-pressure conditions. The pressure-independent background current [36–38] usually includes not only the photoelectron current produced by the X-ray effect (Figure 6.30) but also additional inputs from other physical effects and parasitic errors [39–41]. The latter mainly include the so-called ESD (electron-stimulated desorption) [42], that is, desorption of positive ions caused by electrons impinging on a solid surface. In ionization gauges, the electrons hitting the anode release positive ions that reach the ion collector and thus contribute to background current  $I_0$ . Also, negative currents can occur at the collector if the so-called inverse X-ray effect is predominant (Figure 6.30). Furthermore, dissociation of gas particles at hot surfaces and gas released by heated parts of measuring equipment are important issues.

The anode mesh has a surface area of approximately 10  $\text{cm}^2$ . Thus, the number of adsorbed molecules can be considerable ( $10^{16}$  molecules in a single mono-layer). This is why a clean anode is important: after venting or exposure to high pressures, a special degassing procedure activated by the control equipment cleans the anode mesh by means of electron bombardment. In addition, the electron current into the anode should not be too low so that the vacuum gauge is permanently self-cleaning.

Redhead [43] suggested another approach for reducing the lower measuring limit. The so-

called modulator method measures background current  $I_0$  and subtracts it from the measured signal. This requires an additional electrode in the grid space, referred to as modulator, usually a wire parallel to the collector and close to the cylindrical mesh. A modulator at anode potential has little or no effect on a Bayard–Alpert tube.

However, it appeared that  $I_0$  also changes considerably with modulator voltage because the latter influences electron trajectories. Hobson [44] estimated that the corresponding error of measurement would amount to  $3 \times 10^{-10}$  Pa. Thus, the idea had no significant commercial success because the additional effort could not improve the lower measuring limit substantially.

The measuring limit was finally lowered by changing the geometry of the Bayard–Alpert tube. This led to the development of the extractor ionization gauge.

#### Extractor Ionization Gauges

In the extractor principle, the collector is placed in a chamber separate from the volume in which the ions and X-ray photons are released. The aim is to further reduce the X-ray effect. The ions are extracted (hence, extractor ionization gauge) to this separate chamber. The spatial separation considerably reduces the exposure of the collector to X-rays.

Figure 6.31 shows the design of an extractor. An annular cathode envelope the lower part of the cylindrical anode. At the bottom end, the anode is closely opposed to an aperture of a negative extractor cathode at ground potential. The space below the extractor electrode holds a small wire-shaped ion collector shrouded by a reflector electrode at anode potential. In this electrode arrangement, combined with appropriate design, the extraction electrode focuses the ions produced inside the anode grid onto the ion collector. The solid angle under which photons produced at the anode reach the ion collector is far lower than that in Bayard–Alpert systems. The X-ray effect corresponds to a pressure reading of approximately  $1 \times 10^{-10}$  Pa. The upper measuring limit is approximately  $10^{-2}$  Pa.

Benefits of extractor systems are not limited to pressures below  $10^{-8}$  Pa. For the pressure range of less than  $10^{-6}$  Pa, the described parasitic errors for such vacuum gauge systems are extremely low.

Helmer [45,46] further developed the extractor principle by introducing a  $90^\circ$ -deflection unit for ions behind the extraction electrode. In this design, there is no line of sight between the anode and the collector, and thus, the rate of X-rays reaching the collector again drops dramatically.

Watanabe [47] refined Helmer's deflection principle by using the deflection unit as an energy filter. Ions produced at the anode mesh by electron-stimulated desorption carry somewhat higher energy than ions produced in the free space of the anode mesh. This is caused by the space charge of the electrons in the mesh.

In order to increase this effect of space charge, Watanabe used a spherical anode grid (Figure 6.31), which on average provides a higher electron density in the center of the sphere than at the edges. In Watanabe's ion spectroscopy gauge, the deflection unit is a hemispherical deflector with an inner electrode at ground potential and an outer, variable-potential positive electrode.

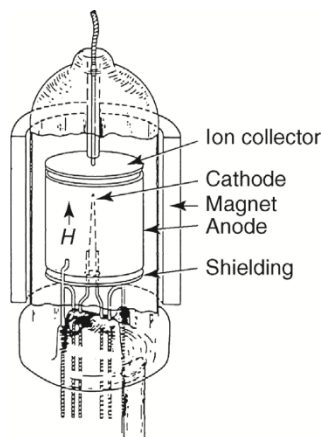


Figure 6.34 Lafferty gauge [50].

Figure 6.32 shows that this vacuum gauge is capable of differentiating between ions from the gas phase and ions produced by electron-stimulated desorption. Those parts of the ion spectroscopy gauge adjacent to the hot cathode are available for degassing by means of direct electrical heating or electron bombardment. The remaining parts of an ion spectroscopy gauge are manufactured from well-thermoconducting materials such as copper or aluminum so that heating and thus outgassing (of hydrogen, in particular) is prevented as far as possible. Watanabe specified a lower measuring limit of  $2 \times 10^{-12}$  Pa.

A simple and commercially available procedure for separating ESD ions from ions produced in the free space uses an energy analyzer referred to as Bessel box [48]. It has the advantage of using a straight, cylindrically symmetric arrangement allowing compact design of ionization gauges (Figure 6.33). The designers of this tube called their system AxTRAN gauge (axial symmetric transmission gauge) [49].

Depending on the voltage UBE, only ions with a particular energy level pass the Bessel analyzer and are detected at the secondary electron multiplier (SEM). ESD ions are thus suppressed by optimizing this voltage. The disk charged to cylinder potential and arranged in the center of the Bessel analyzer prevents direct line-of-sight contact for photons from the anode grid to the SEM, and thus suppresses the X-ray effect. The estimate for the lower measuring limit is  $3 \times 10^{-12}$  Pa (nitrogen equivalent) [51]. Manufacturer's data for the commercially available instrument specify  $5 \times 10^{-11}$  Pa [52].

#### Additional Types of Emitting-Cathode Ionization Gauges

Many other measuring systems in addition to those described in the previous sections have been developed, though, without having found noticeably broad applications.

Lafferty [50] built an ionization gauge with a hot cathode arranged in the axis of an anodic cylinder grid (Figure 6.34). A magnetic field, axial as well, forces the electrons to travel on a circular path, which increases their mean free path compared with a Bayard-Alpert tube by several orders of magnitude. Emission current was limited to 10  $\mu$ A for stable operation. For this ionization gauge, the calculated X-ray limit was  $2 \times 10^{-12}$  Pa.

Further ionization gauges are only listed here in brief: Schuemann suppressor gauge [53], orbitron system (very long electron paths) [54], and Lafferty magnetron gauge with hot cathode [51].

These and other measuring instruments were mainly used for measuring extremely low pressures ( $< 10^{-8}$  Pa).

#### Penning Gauges

The operation principle of these gauges for low pressures uses a gas discharge ignited between two metal electrodes (anode, cathode) by applying sufficiently high DC voltage (in the kilovolt range). The gas discharge current is pressure dependent and thus used as measured quantity. However, if no additional measures are taken, the lower measuring limit is only about 1 Pa. At lower pressures, the number of carriers produced is insufficient for sustaining the gas discharge. The so-called Penning discharge maintains gas discharge even down to very low pressures. For this, it uses a sufficiently powerful magnetic field arranged so that the electron paths from the cathode to the anode are stretched considerably by forcing the electrons onto spiral paths. This leads to higher ion yield. Due to their higher mass, ions are hardly distracted by the magnetic field and travel directly to the cathode. Secondary electrons, produced when the ions impinge on the cathode, nourish the discharge. Within a broad range, discharge current  $I$  is a measure of pressure  $p$ :

$$p = KI^m \quad (6.14)$$

The exponent  $m$  depends on the precise design of the gauge and is in the range  $m = 1-1.4$ .

For a detailed discussion of the operating principle in a Penning gauge, please consider Figures 6.35 and 6.36: a DC voltage of, for example, 3 kV produced in high-voltage generator HV is applied to the annular anode AA of the Penning instrument P via the protective resistor R. The Penning tube has a grounded metal housing H. The two plane walls parallel to the annular anode AA form the cathodes C. The magnetic field  $\rightarrow B$  is applied such that its field lines from one cathode to the other pass through the anode. Ammeter A measures the discharge current  $I$ . Measures must be taken in order to prevent isolation currents between the anode and the cathode because the gauge would indicate these too.

Among other effects, the protective resistor  $R$  (several  $M\Omega$ ) also serves to limit discharge current particularly at high pressures.

Figure 6.37 shows a typical calibration curve for a Penning gauge in the range of  $10^{-8}$  to 1 mbar ( $10^{-6}$  to 100 Pa). As indicated in Figure 6.37, two different discharge mechanisms occur with a transition at about  $10^{-4}$  mbar ( $10^{-2}$  Pa). The discharge is characterized by a negative ring current at lower pressure, and by plasma at higher pressure. In both cases, the magnetic field ( $B=0.1-0.2$ T) predominantly influences discharge because it strongly impedes motion of the electrons perpendicular to the field lines, that is, to the anode (compare Figure 6.35). According to Knauer [84,85], at low pressures, a rotating electron volume charge concentric to the axis of the anode cylinder develops, that is, a ring current of approximately 1 A (shaded area in Figure 6.36). A strong electrical field develops between the anode and this space charge, in which almost the entire voltage applied to the electrodes in the range of 3 kV falls off. The space charge considerably enhances the

radial component of the electrical field (Figure 6.36).

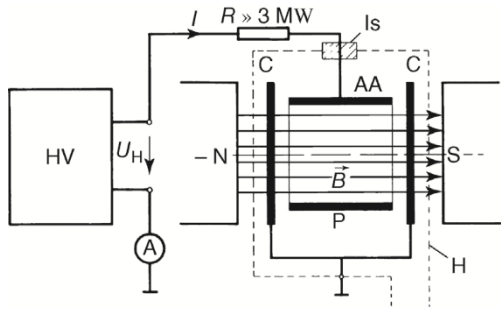


Figure 6.35 Diagram of a Penning gauge. AA: annular anode; C: cathode plates; H: isolating wall of housing; N, S: magnet pole pieces; HV: high-voltage supply;  $U_H=3000\text{V}$ ;  $B=0.1\text{--}0.2\text{T}$ .

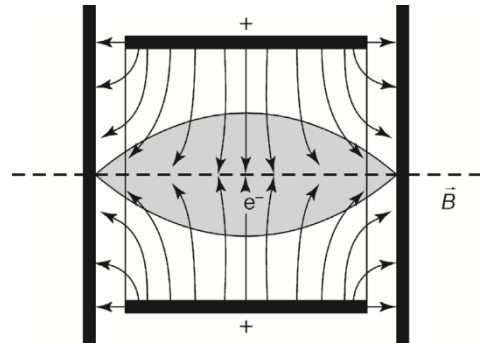


Figure 6.36 Diagram showing the orientations (not the strengths) of the electrical field in a Penning gauge according to Figure 6.35. Shaded area: electron space charge.

Within the space charge ring, a plasma P develops with homogeneously distributed, small number densities of ions and electrons. Its potential is only a few hundred volts above cathode potential; it is of minor importance for the discharge mechanism. Electrons in the ring current, influenced by the crossed fields, follow cycloid paths and approach the anode stepwise only due to collisions with gas atoms.

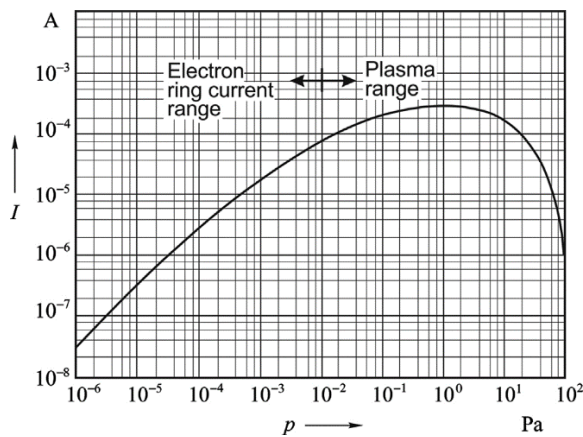


Figure 6.37 Typical calibration curve for a Penning gauge.  $I$ : discharge current;  $p$ : pressure. In the linear range at low pressures, sensitivity  $K \approx 3\text{A mbar}^{-1}$ . Transition between annular electron current and plasma at  $p=10^{-2}\text{ Pa}$  ( $10^{-4}\text{ mbar}$ ).



Figure 6.38 Penning gauge. (Courtesy of INFICON Inc.)

Thus, the magnetic field heavily impedes electron diffusion to the outside. The ring current would persist constantly if the volume were gas-free. Collisions with gas atoms in the volume, apart from causing diffusion as described above, can also cause ionizing. An ionizing collision produces another electron and an ion. The electron merges into the volume charge cloud, that is, the ring current, whereas field  $E$  accelerates the ion toward the inside. In contrast to the electrons with trajectory radii in the area of  $0.1\text{ mm}$  for combined electrical and

magnetic fields, the radius of ion trajectories is higher by a factor determined by the ratio of ion mass to electron mass, and thus in the range of meters. Therefore, ions reach the cathode quickly. Both the number of ions produced per unit time (ionizing rate) and the diffusion coefficient perpendicular to the magnetic field are proportional to gas density  $n$ . Thus, an equilibrium between carrier production (by ionizing) and carrier depletion (by diffusion) can develop in the ring current such that the electron density in the ring current  $I_R$ , and thus  $I_R$  itself, remains constant and nearly independent of  $n$ . Then, the out-side current is proportional to  $n$  throughout the entire pressure range ( $p < 10^{-2}\text{ Pa}$ ), and thus proportional to pressure  $p$ . The fact that the ring current, that is, the axial space charge, indeed slightly follows  $n$  leads to  $m > I$  in Equation (6.14).

The ring current in a Penning system has the same function as the electron current in an emitting-cathode ionization gauge. However, sensitivity is much higher because the electron current is higher. Typical Penning system sensitivities are in the range  $0.02\text{--}0.05\text{ A Pa}^{-1}$ , for pressures below  $0.01\text{ Pa}$ . Penning cells for ion getter pumps can be optimized to  $0.1\text{ eAPa}^{-1}$ .

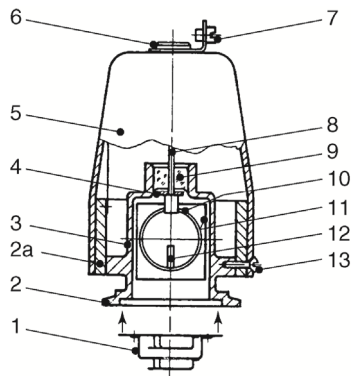


Figure 6.39 Section of a Penning vacuum gauge. (1) Pulled out vapor trap with centering, (2) small flange, vacuum connection, (2a) permanent magnet, (3) housing, (4) protective plate for isolator (9), (5) sealing lid, (6) connector for high-voltage operating power, (7) ground connector, (8) anode connector, (9) compression glass seal, (10) annular anode, (11) cathode plate, (12) ignition pin, and (13) connecting bolt for sealing (5).

readings on such a Penning gauge depend on the condition of the cathode surfaces because electron release during ion collisions is influenced by the state of the cathode surface. Thus, frequent cleaning of the cathodes can be advisable in certain cases. For easier cleaning, cathodes are often made of two thin, replaceable stainless-steel sheets.

As the pressure drops, sensitivity is maintained as long as the ring current continues. Obviously, the ring current depends on an additional supply of electrons released from the cathodes. Otherwise, electrons are depleted from the ring current, which ultimately ceases as the pressure continues to drop. Depending on geometry as well as magnetic and electrical field strengths, such discharges are maintained down to pressures far below  $10^{-9}$  Pa.

Ion getter pumps operate on the same principle. At low pressures, their pumping speed also requires maintaining a continuous discharge.

At pressures  $p > 10^{-2}$  to  $10^{-1}$  Pa, the density of positive carriers in the ring current rises to levels at which the discharge type described above is no longer stable. The entire anode cylinder is filled with more or less equipotential plasma, which now determines the discharge mechanism. Its potential lies between those of cathode and anode. It is separated from both electrodes by space charge layers. In the cathode layer, ions from the plasma accelerate toward the cathode where they release electrons. Thus, the ions resupply electrons, that is, ionizing carriers, to the system, replenishing such electrons that became depleted from the plasma and trapped by the anode due to diffusion perpendicular to the magnetic field. In this mechanism, fluctuations (plasma oscillations) promote such diffusion. Insight into these diffusion-promoting processes is necessary for understanding the high currents observed in such discharges [55]. In the considered pressure range, discharge current and pressure are no longer proportional (Figure 6.37). At higher pressures,

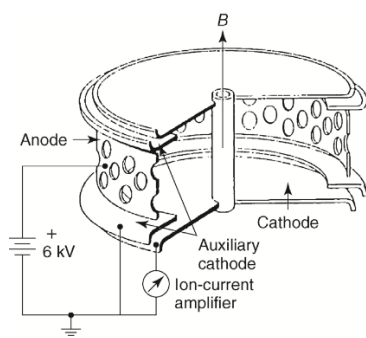


Figure 6.40 Diagram of Redhead's magnetron [56].

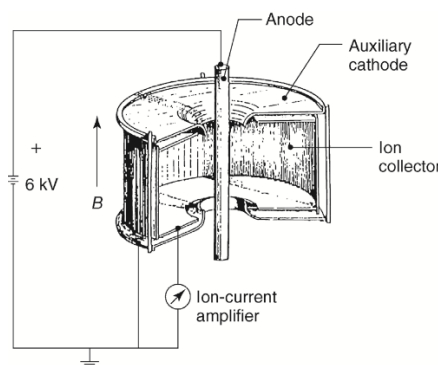


Figure 6.41 Inverted magnetron according to Hobson and Redhead [57].

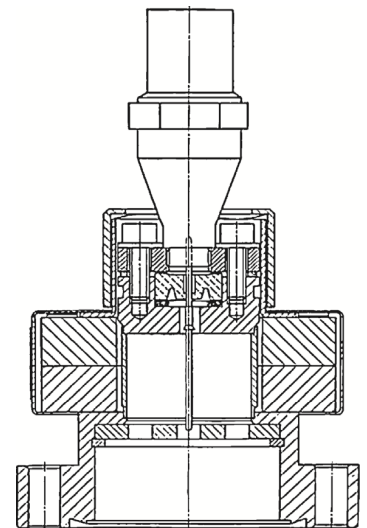


Figure 6.42 IKR020 inverted magnetron by INFICON. (Courtesy of INFICON Inc.)

The main advantage of Penning gauges is that the discharge current in a Penning system is high enough for current measurements, that is, pressure measurements, down to  $10^{-4}$  Pa without using an amplifier if a sensitive ammeter is employed (see also Figure 6.37). Thus, Penning gauges

are cheaper and more trouble-free than emitting-cathode ionization gauges. Utilizing Penning gauges is advisable for simple control tasks if the pressure in a vacuum system is to be checked rather than precisely measured. Figure 6.38 shows a measuring tube. The anode and the cathode plates can be pulled out for cleaning purposes. In order to counteract the contamination issue described above, a baffle as shown in Figure 6.39 should protect the Penning gauge.

The measuring range of a Penning system as shown in Figure 6.37 can be enhanced for measuring lower pressures. For this, an additional amplifier, preferably having logarithmic characteristic, is added to the supply unit.

As a result, the measuring scale is approximately logarithmic throughout a pressure range of  $10^{-7}$  to  $10^{-2}$  Pa. Penning gauges are particularly useful when combined with a thermal conductivity vacuum gauge. The benefit is that the thermal conductivity gauge controls the Penning metering point such that the Penning gauge is activated if the pressure drops below 0.5 Pa, and shut off if the pressure exceeds this threshold value. This yields a continuous pressure scale from  $10^{-4}$  to 100 kPa. Furthermore, the arrangement prevents operator's errors with the Penning gauge. Such errors occur when the Penning system operates at pressures above 1 Pa, as shown in the calibration curve in Figure 6.37, because discharge current drops in this pressure range, and thus, readings are ambiguous.



Figure 6.44 Combined vacuum gauge BCG 450 by INFICON with a range from  $5 \times 10^{-8}$  Pa to 150 kPa.

It is composed of a capacitive diaphragm sensor (left), a Pirani gauge (right), and an ionization gauge of the Bayard-Alpert type (center part). (Courtesy of INFICON AG, Liechtenstein.)

an ionization gauge produces too low pressure readings if the meter uses extrapolation of  $p(I)$  or  $m$  from higher to lower pressures. Thus, at readings of  $10^{-10}$  Pa, an error of one order of magnitude can be expected.

Figure 6.42 shows the design of a modern inverted magnetron.

## 6.7. Combined vacuum gauges

Operators of vacuum systems like to have a compact vacuum gauge that can cover the whole

### Magnetron and Inverted Magnetron

In order to stabilize the discharge and improve starting behavior, Redhead developed the magnetron [56] and Hobson and Redhead designed the inverted magnetron [57].

In a magnetron, the anode is an open cylinder. The cathode forms axis and both end plates of the cylinder (Figure 6.40). In the inverted magnetron (Figure 6.41), the anode is a rod on the axis of a nearly closed cylinder serving as cathode. In the magnetron, two annular rings at cathode potential shield the end disks of the cathode from the high electrical fields. The ion current amplifier does not detect any possible field emission currents produced by the rings.

In inverted magnetrons, guard rings prevent field emission currents between the cathode and the anode. The magnetic field is parallel to the anode. This ionization gauge can be operated at up to 6 kV and 0.2 T.

Both types of gauges with crossed electromagnetic fields trap electrons more efficiently than the Penning type. This improves starting conditions, interrelationships of  $p$ ;  $B$ ; and  $V$  follow theoretical predictions more accurately, and the discharge is stable down to much lower pressures. Redhead and Hobson specified a usable pressure range of  $10^{-11}$  to  $10^{-2}$  Pa for their ionization gauges.

Equation (6.14) applies to these ionization gauges, too. However,  $m$  is pressure dependent, which makes measurements complicated. Generally,  $m$  is higher at high pressures than at low pressures. Therefore, at low pressures,

vacuum range from high vacuum to atmospheric pressure.

For this need, manufacturers developed vacuum gauges that combine different measurement principles in one gauge. Figure 6.44 already gave us an example where a fine vacuum ionization gauge was combined with a Pirani gauge. Common is also the combination of Bayard–Alpert ionization gauge with Pirani gauge. Also, quartz oscillators have been combined with ionization gauges.

A very compact vacuum gauge, where three different measurement principles were combined, is depicted in Figure 6.44. In the range from 150 to 1 kPa, the pressure is measured to be gas species independent by a capacitive diaphragm gauge, from 1 kPa to 2 Pa the pressure is measured by a Pirani gauge, the reading, however, being dependent on the gas species, as this is the case for the third principle, a Bayard–Alpert ionization gauge with a range down to  $10^{-8}$  Pa. In the overlapping ranges of the measurement principles, from 100 Pa to 1 kPa and from 0.5 to 2 Pa, electronic circuits smooth out eventual jumps between the indications obtained from the different measurement principles. These jumps are caused partly by the different gas species dependences of the measurement principles, partly by insufficient calibration, and partly by long-term instabilities of the different gauges. These jumps are a significant problem for combined vacuum gauges, so that their accuracy is rather modest.

1. Wolf, A. (1946) An elementary theory of the Bourdon gage. *J. Appl. Mech.*, 68, 207-210.
2. Jennings, F.B. (1956) Theories on Bourdon tubes. *Trans. ASME*, 78, 55-64.
3. Harada, K. (1999) Various applications of resonant pressure sensor chip based on 3-D micromachining. *Sens. Actuators A*, 73, 261–266. See also Refs. [4,5] herein.
4. Miiller, A. et al. (2002) Final report on key comparison CCM.P-K4 of absolute pressure standards from 1 Pa to 1,000 Pa. *Metrologia*, 39 (Tech. Suppl.), 07001.
5. Redhead, P.A. (1984) The measurement of vacuum pressures. *J. Vac. Sci. Technol. A*, 2, 132-138.
6. Meyer, O.E. (1865) Über die innere Reibung der Gase. *Pogg. Ann.*, 125, 177.
7. Maxwell, J.C. (1866) The Bakerian Lecture: on the viscosity or internal friction of air and other gases. *Philos. Trans. R. Soc.*, 156, 249.
8. Kundt, A. and Warburg, E. (1875) Über Reibung und Wärmeleitung verdünnter Gase. *Pogg. Ann.*, 155, 337.
9. Sutherland, W. (1896) On thermal transpiration and radiometer motion. *Philos. Mag. Ser. 5*, 42, 373.
10. Hogg, J.L. (1906) Friction and force due to transpiration as dependent on pressure in gases. *Proc. Am. Acad. Arts Sci.*, 42, 113.
11. Holmes, F.T. (1937) Axial magnetic suspensions. *Rev. Sci. Instrum.*, 8, 444.
12. Beams, J.W., Young, J.L., and Moore, J.W. (1946) The production of high centrifugal fields. *J. Appl. Phys.*, 17, 886.
13. Beams, J.W., Spitzer, D.M., Jr., and Wade, J.P., Jr. (1962) Spinning rotor pressure gauge. *Rev. Sci. Instrum.*, 33, 151.
14. Fremerey, J.K. (1973) Cavity type permanent magnet suspension. *Rev. Sci. Instrum.*, 44, 1396–1397.
15. Fremerey, J.K. (1983) Gas friction vacuum meter and method of making measuring body US Patent 4395914.
16. Fremerey, J.K. (1982) Spinning rotor vacuum gauges. *Vacuum*, 32, 685–690.
17. Fremerey, J.K. (1985) The spinning rotor gauge. *J. Vac. Sci. Technol. A*, 3, 1715–1720.
18. Ono, M. et al. (1985) Design and performance of a quartz oscillator vacuum gauge with a controller. *J. Vac. Sci. Technol. A*, 3, 1746.
19. Hirata, M., Kokobun, K., Ono, M., and Nakayama, K. (1985) Size effect of a quartz oscillator on its characteristics as a friction vacuum gauge. *J. Vac. Sci. Technol. A*, 3, 1742–1745.
20. Bonfig, K.W. (1988) Technische Druckund Kraftmessung.
21. Pirani, M. (1906) Selbstzeigendes Vakuum-Meßinstrument. *Dtsch. Phys. Ges. Verh.*, 8,

- 686.
22. Leck, J.H. (1989) Total and Partial Pressure Measurement in Vacuum Systems, Blackie, pp. 49 ff.
  23. Hinkle, L.D. and Mariano, C.F. (1991) Toward understanding the fundamental mechanism and properties of the thermal mass flow controller. *J. Vac. Sci. Technol. A*, 9, 2043–2047.
  24. Tison, S.A. (1996) A critical evaluation of thermal mass flow meters. *J. Vac. Sci. Technol. A*, 14, 2582–2591.
  25. Tilford, C.R. (1985) Sensitivity of hot cathode ionization gauges. *J. Vac. Sci. Technol. A*, 3, 546–549.
  26. Edelmann, C. and Engelmann, P. (1982) Möglichkeiten der Messbereichserweiterung bei Glühkathoden-Ionisationsvakuummetern. *Vak.-Tech.*, 31,2–10.
  27. Kno, Z.H. (1981) An approach to the nonlinearity of an ionization vacuum gauge at the upper limit of the measured pressure. *Vacuum*, 31 (7), 303-308.
  28. Wang, Y.-Z. (1984) A fundamental theory of high pressure hot cathode ionization gauges. *Vacuum*, 34, 775–778.
  29. Schulz, G.J. and Phleps, A.V. (1957) Ionization gauges for measuring pressures up to the millimeter range. *Rev. Sci. Instrum.*, 28, 1051.
  30. Bayard, R.T. and Alpert, D. (1950) Extension of the low pressure range of the ionization gauge. *Rev. Sci. Instrum.*, 21, 571.
  31. Arnold, P.C., Bills, D.G., Borenstein, M.D., and Borichevsky, S.C. (1994) Stable and reproducible Bayard–Alpert ionization gauge. *J. Vac. Sci. Technol. A*, 12, 580
  32. Schmidt, K. and Bergner, U. (1996) Stabilität von Hochvakuum-Messrohren. *Vak. Forsch. Prax.*, 8, 177-182.
  33. Peacock, R.N. and Peacock, N.T. (1990) Sensitivity variation of Bayard–Alpert gauges with and without closed grids from 10<sup>-4</sup> to 1 Pa. *J. Vac. Sci. Technol. A*, 8, 3341.
  34. Van Oostrom, A. (1961) *Vacuum Symposium Transactions*, vol. 1, Pergamon Press, New York, 443 pp.
  35. Watanabe, F. (1992) Ion spectroscopy gauge: total pressure measurements down to 10-12 Pa with discrimination against electron-stimulated-desorption ions. *J. Vac. Sci. Technol. A*, 10, 3333-3339.
  36. Repa, P. (1986) The residual current of the modulated BA-gauge. *Vacuum*, 36, 559-560.
  37. Chou, T.S. and Tang, Z.Q. (1986) Investigation on the low pressure limit of the Bayard–Alpert gauge. *J. Vac. Sci. Technol. A*, 4, 2280–2283.
  38. Filipelli, A.R. (1987) Residual currents in several commercial ultra high Bayard-Alpert gauges. *J. Vac. Sci. Technol. A*, 5, 3234-3241.
  39. Berman, A. (1985) *Total Pressure Measurements in Vacuum Technology*, Academic Press.
  40. Grosse, G. et al. (1987) Secondary electrons in ion gauges. *J. Vac. Sci. Technol. A*, 5, 3242.
  41. Harten, U. et al. (1988) Surface effects on the stability of hot cathode ionization gauges. *Vacuum*, 38, 167–169.
  42. Redhead, P.A. (1962) Electron stimulated desorption. *Vacuum*, 12, 267.
  43. Redhead, P.A. (1960) Modulated Bayard–Alpert gauge. *Rev. Sci. Instrum.*, 31, 343.
  44. Hobson, J.P. (1964) Measurements with a modulated Bayard–Alpert gauge in aluminosilicate glass at pressures below 10-12 Torr. *J. Vac. Sci. Technol. A*, 1,1.
  45. Helmer, J.C. and Hayward, W.D. (1966) Ion gauge for vacuum pressure measurements below 1 x 10<sup>-10</sup> torr. *Rev. Sci. Instrum.*, 37, 1652.
  46. Han, S.-W. et al. (1988) Performance of the bent beam ionization gauge in ultrahigh vacuum measurements. *Vacuum*, 38, 1079-1082.
  47. Watanabe, F. (1992) Ion spectroscopy gauge: total pressure measurements down to 10-12 Pa with discrimination against electron-stimulated-desorption ions. *J. Vac. Sci. Technol. A*, 10, 3333–3339.
  48. Craig, J.H. and Hock, J.H. (1980) Construction and performance characteristics of a low cost energy prefilter. *J. Vac. Sci. Technol.*, 17, 1360-1363.

49. Akimichi, H. et al. (1995) Development of a new ionization gauge with Bessel box type energy analyser. *Vacuum*, 46, 749-752.
50. Lafferty, J.M. (1961) Hot-cathode magnetron ionization gauge for the measurement of ultrahigh vacua. *J. Appl. Phys.*, 32, 424.
51. Lafferty, J.M. (1960) Transactions of the American Vacuum Society Symposium, vol. 7, p. 97.
52. ULVAC Cooperation catalog, Japan, January 2006. Available at <http://www.ulvac.co.jp/eng/>.
53. Schuemann, W.C. (1963) Ionization vacuum gauge with photocurrent suppression. *Rev. Sci. Instrum.*, 34, 700.
54. Messer, G. (1980) Long term stability of various reference gauges over a three years period. Proceedings of the 8th International Vacuum Congress, Cannes, Vide Suppl. 201, pp. 191–194.
55. Bohm, D. et al. (1949) Theoretical considerations regarding minimum pressure for stable arc operations. *Natl. Nucl. Energy Ser. 1*, 5, 77ff. and 173 ff.
56. Redhead, P.A. (1958) The townsend discharge in a coaxial diode with axial magnetic field. *Can. J. Phys.*, 36 (3), 255–270.
57. Hobson, J.P. and Redhead, P.A. (1958) Operation of an inverted-magnetron gauge in the pressure range  $10^{-3}$  to  $10^{-12}$  mm Hg. *Can. J. Phys.*, 36 (3), 271–288.

## 7. VACUUM COMPONENTS, SEALS, AND JOINTS

### 7.1. Vacuum hygiene

Vacuum is often applied to run processes under undisturbed or well-defined ambient conditions. To this end, the evacuated system must be protected against penetrating gases (through atmospheric gases or from leaky liquid lines) and be free from or low in contaminations. Penetrating gases and contaminations of the parts exposed to vacuum can disturb the processes running in the vacuum and limit the achievable ultimate pressure. However, the ultimate cleanliness necessary in the vacuum, the vacuum hygiene, always depends on the specific requirements of the respective process.

Figure 3.1 provides an overview of possible disturbing factors from the process surroundings affecting the vacuum.

Table 7.1 Overview of the sources and detection methods for contaminations.

	Particles	Filmic contaminations	Solid-state contaminations
Examples	Turnings Dust Micro- and nanodust	Water/lime Oils Cooling lubricants Proteins Skin oils	Gases bound in solid states (H <sub>2</sub> ) Alloying elements (Si, Pb, Zn, Sn, etc.) Plasticizers Oxide and corrosion layers
Sources	Machining <ul style="list-style-type: none"> <li>▪ Milling, turning, sawing</li> <li>▪ Polishing, grinding, sandblasting</li> </ul> Exposure in atmosphere Floating particles in the cleaning liquid Lint from cloths Particle abrasion during handling Packaging material	Lubricants from machining <ul style="list-style-type: none"> <li>▪ Milling, turning, sawing</li> </ul> Handling of the components without gloves, skin oils, sneezing Minerals and hydro-carbons in the cleaning liquid Residuals from cleaning agents	Welding (annealing colors) Natural affinity of elements of the PSE Contaminations in production process Alloy admixtures
Detection methods	Examination under black light Examination under white light (oblique light and side light)	Residual gas analysis in the vacuum with QMS TDS	Residual gas analysis in the vacuum with QMS
Qualitatively			
Quantitatively	Particle counter (optical) SEM AFM	Residual gas analysis in the vacuum with QMS Fluorescence measurement Outgassing accumulation method	Residual gas analysis in the vacuum with QMS XPS, SIMS, AES, TML

The penetration of atmospheric gases can occur through three possible ways: leakage, permeation, and virtual leakage. Atmospheric leakages primarily originate in junctions while joining or mounting. Other leaks can originate from leakages in liquid cooling lines that are laid in the vacuum. Due to their signature in the residual gas spectrum, the latter can be clearly distinguished from the atmospheric leaks. The permeation of ambient gases through the wall of vacuum recipients can be minimized through the use of suitable materials and the observance of minimum wall

thicknesses (to a negligible level compared with desorption effects). The so-called virtual leaks refer to mistakenly trapped gas volumes in the vacuum. They originate, for example, while mounting a screw in a blind tapped hole under atmospheric pressure. Then, in the vacuum, the trapped gas flows along the thread guide very slowly and continuously into the chamber. Over a (too) long period, the trapped volume generates a continuous gas source with the properties of an atmospheric leak. The gas can be easily evacuated with a ventilation bore or through slots in the screw thread and thus eliminate this apparent leak.

In addition to the penetrating gases, the other disturbance sources can be divided into three classes: particles, molecular contaminations (also referred to as filmic contaminations), and contaminations from the solid-state material. Table 7.1 provides an overview of the type of these contaminations, possible sources, and established detection methods.

Particles prevent the sealing effect of the surfaces to be fitted or mounted and can disturb processes in the vacuum, while, for example, they are deposited on the surface that is to be examined or situated in the process. A particularly great challenge exists in avoiding particle generation during movements in the vacuum or its border areas due to the limited application of lubricants. Thus, under many conditions, grease is suitable as a lubricant for the avoidance of galling (“seizing”) of the screw connections and friction losses. In contrast, low outgassing lubricants are to be used in vacuum or modern materials are to be worked with that show neither galling nor abrasion [1]. Also, traditional materials, such as stainless steels, can be prepared through surface finishing for application without lubricant in vacuum. An example of this is the Kolsterising® of stainless steel surfaces [2].

In addition to particles, we also consider substances as contaminants that are located in or on the surface of solids exposed to vacuum and are found in a solid or liquid phase under atmospheric conditions at room temperature. Then, in vacuum, these are able to desorb into the gas phase with or without a catalytic effect (process-induced outgassing), particularly when the vapor pressure of the substance falls short of the chamber pressure. A process-induced outgassing is present, for example, in particle accelerators where highly energetic particles hit the chamber wall and cause desorption of the atoms or molecules of the surface and/or from the solid state (bulk) into the gas phase.

In contrast to the contaminations that are present on solid-state surfaces or in the solids themselves, molecular contaminations or filmic contaminations refer to such contaminations that additionally arise on the surface, for example, through manufacturing, storage, or handling steps. According to the required vacuum regime or planned process, very different requirements for the material composition and the cleanliness of the components as well as for the use of the components exist. Thus, for example, grease can have a sealing effect in rough vacuum (above the vapor pressure of the substance), but can be disruptive in high vacuum and at lower pressures (below the vapor pressure of the substance) as a result of the then volatile hydrocarbons. Therefore, in HV and UHV and especially XHV, it is essential to work with gloves in order to avoid contamination of the components with skin oils. The semiconductor industry, particularly EUV lithography, has extremely high cleanliness requirements in high vacuum. For these high cleanliness requirements in moderate pressure ranges, the term ultraclean vacuum (UCV) has been established.

The different processes that can be applied for the detection of contaminations are shown in Table 7.1. A series of different qualitative and quantitative valuation and measuring methods can be applied according to component material and component geometry and depending on the contaminations to be examined and the required detection boundaries. From the basic principle, the contaminations are first solved from the surface or from the volume (e.g., upon transition into the gas phase with TML, RGA, and TDS, or by bombardment with highly energetic (charged) particles or radiation with SIMS, XPS, and AES) in order to be analyzed afterward (e.g., through a quadrupole mass spectrometer (QMS) with RGA and SIMS or with an electron detector with XPS and AES). However, the comparability of the results of different processes is only restrict-edly provided due to the type of the extraction and the specific analysis method. For detection of molecular or filmic contaminations (water, hydrocarbons, cooling lubricants, etc.), RGA has been established as a gas chromatographic method [3]. In doing so, the substances outgassing from components and chambers in vacuum are qualitatively and quantitatively examined with QMS. This process is very well suited

to the requirements of different vacuum applications because during the examination the components are exposed to conditions similar to those in the later operation of the vacuum system.

In addition to the detection of contaminations or the examination of the component cleanliness, the cleaning of vacuum components and the preservation of the state of cleanliness through suitable packaging have become an important part of vacuum technology [3]. Chapter 4 provides an overview of the material and surface treatment methods established in vacuum technology. Detailed information regarding the mechanisms of action and the attainable cleaning success of the individual processes can be taken from the literature shown within the table. While plain surfaces of stainless steel are relatively easy to clean, there is an increase in the degree of difficulty and effort of cleaning with the complexity of the geometry (e.g., blind tapped holes, diaphragm bellows, thin bent pipes, spark-eroded slits) and the variety of materials (aluminum, copper, elastomers). Building upon the information presented, appropriate cleanliness requirement profiles and cleaning processes can be determined for specific vacuum applications. Detailed information regarding the established cleaning processes for UHV/XHV components is found, for example, in the publications of the particle accelerators developed by DESY [4], FAIR [5], and CERN [6].

## 7.2. Joining technologies in vacuum technology

Vacuum technology applications need an evacuable and hermetically sealed system that consists of vessels, pipelines, and other components. In addition to the selection of suitable materials and the correct material and surface treatment, the joining technologies applied are crucial for the quality of the generated vacuum.

In mechanical and plant engineering, connections are classified according to different criteria. Static and dynamic connections are classed according to the function, that is, fixed or moveable in different degrees of freedom. If the connections are classed according to manufacturing aspects, a distinction is made between detachable and permanent connections (see Figure 7.1).

In addition to the mechanical stability, a vacuum system requires leak tightness and low outgassing in all junctions that correspond to the targeted ultimate pressure. Restrictions for the possible joining processes arise from this.

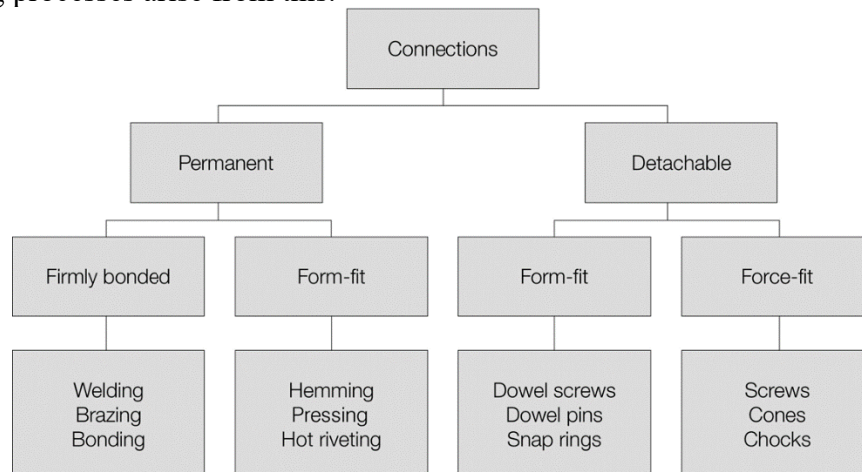


Figure 7.1 System of the most commonly used connections in mechanical and plant engineering.

### Permanent Connections

The German standard DIN 8593-0 defines permanent connection as a “connection made by joining that can only be removed again under acceptance of a damage or destruction of the joined parts” [7].

In vacuum technology, the material-bonded connections that are realized through welding, brazing, or bonding primarily count among the relevant permanent connections.

Application and ultimate pressure determine which joining processes are used for vacuum components. Determining criteria for the selection are

- materials to be joined (Table 7.2);
- outgassing behavior of the joining agents (e.g., adhesive/welding filler/solder);
- gas impermeability of the joining agents (permeation, pore formation, packing density, particle generation);
- temperature resistance of the joining agents (melting ranges, aging);
- mechanical stability of the component (mechanical stress through joining,
- mechanical loads during the operation);
- accessibility of the joint in the joining process;
- particle generation potential of the joining materials.

The joining technologies such as brazing, welding, and bonding have application preferences depending on the materials of the joining partners that should be considered in their selection (see Table 7.2).

Table 7.2 Applicable joining technologies for different material pairings.

Material pairing	Brazing	Welding	Bonding	Examples of use
Fe metals/Fe metals	0	+	0	Components made of corrosion-resistant stainless steel
NF metals/NF metals	+	0	0	Aluminum components, copper tubes in stainless steel flanges
NF metals/Fe metals	+	0	+	Aluminum components with flanges made of corrosion-resistant stainless steel
Metal/glass	+	–	+	Viewports
Metal/ceramic	+	–	+	Insulators, electrical feedthroughs
Glass/ceramic	–	–	+	Optical fiber feedthroughs
Plastic/metal	–	–	+	Insulating constructions, attached elastomer seals

(+) Frequently applied joining process; (0) possible/uncommon joining process; (–) unsuitable/impossible/possible joining method with high technological effort.

### Welding

Welding is a “joining process with which two or more parts are connected and a continuity of the materials of the connecting parts is produced under application of heat or force or both and with or without welding fillers” [8]. In vacuum technology, common welding techniques are tungsten inert gas welding, micro-plasma welding, electron beam welding, laser beam welding, friction welding, explosion welding, and diffusion bonding whose functionality and areas of application in vacuum technology are briefly explained in the following [9,10]:

- Tungsten inert gas welding (briefly, TIG welding or argon arc welding). With this fusion welding technique, an electric arc is used as heat source between the material and the nonmelting tungsten electrode. TIG welding can be used very flexibly and with low technical expenditure by use of a manual torch guidance.
- Microplasma welding. Microplasma welding is used similar to TIG welding; nevertheless, it uses an electric arc of higher energy density with a plasma gas nozzle constricting the electric arc. This also burns stably with low current and allows the welding of low wall thicknesses up to the foil range (0.01–1mm).
- Electron beam welding. With this process, electrons within an evacuated chamber are accelerated through high voltage on the material surface where they convert their kinetic energy with the impact into heat. If the electron beam from the vacuum chamber is led out through pressure stages and directed upon the workpiece under free atmosphere, we talk of

nonvacuum electron beam welding. The quick, complicated pendulum movements that allow the parallel welding of several connections can be generated by deflecting coils.

- Laser beam welding. Laser beam welding uses monochromatic, coherent, and strongly focused light of high energy density as a heat source that enables the welding of electrically conductive and nonconductive materials. Very narrow and deep welded joints (deep weld effect) can be generated without contact. Due to the very local, punctual (concentrated) energy entry, laser beam welding is particularly suitable for components that only admit a low heat input as well as for connections demanding a very low distortion of the component geometry.
- Friction welding. The workpiece surfaces to be joined are moved relative to each other under application of force and are connected through the originating frictional heat and distortion heat without additives. With a fully auto-mated process sequence, short weld times and a high positional accuracy of the joining partners are possible. Friction stir welding is a special method with which the joining partners are plasticized by a rotating tool.
- Explosion welding. The workpieces come into contact with each other and are joined (cladded) under use of an explosion-induced shock wave collision. With explosion welding, no structural changes appear beyond the direct joining zone.
- Diffusion bonding. Diffusion bonding is a special joining technique that is based on the principle of solid diffusion and grain boundary migration. The materials are physically joined with each other under heat and application of pressure without a fusion process. Diffusion bonding can be a recommendable connecting process with new construction materials, intermetallic connections, complex ceramic-based materials, and refractory superalloys.

Certain construction rules are to be followed in the vacuum-compatible welding of components (Figure 7.2) [10]. If the component geometry permits, the seams are always to be welded vacuum-sided to avoid outgassing sources (virtual leaks) and collection points for contaminations. One-ply welded seams are to be preferred over multilayer seams in order to avoid inter-run fusion and decrease the risk of inclusions. Different wall thicknesses and component geometries of the joining partners can complicate welding due to the divergent fusion behavior.

Position of the components				
Non-vacuum compatible				
Vacuum compatible				

Continuous weld seam     
 interrupted weld seams

Figure 7.2 Examples of welded joints compatible with vacuum. (According to Ref. [9].)

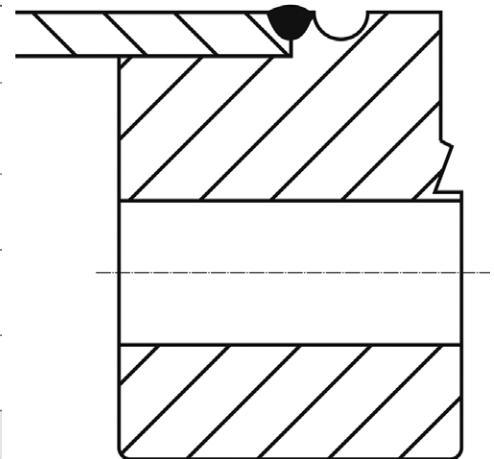


Figure 7.3 Sketch of a flange-to-tube weld with a heat insulating groove.

The heat can be stopped through the insertion of a groove in the joint, and therefore, the heat flux can be controlled (heat insulating groove, Figure 7.3).

The generated bridge can additionally lead to the distortion and thus diminish the stresses of the welding joint. To increase the mechanical loading capacity of the connection, supporting seams on the atmosphere side are used in addition to the vacuum-sided sealing seams. These must be welded with staggering to ensure the accessibility of the seal seam for the test gas.

Also, in vacuum technology, the quality assessment of welded joints is to be questioned after the welding. Special attention is placed on the following criteria.

The tightness of the connection is reached through the absence of fissures, pores, bonding defects, and similar irregularities. Through their corrosive effects, oxidations such as scaling and annealing colors can directly or indirectly negatively influence the outgassing behavior of the connection. The use of welding fillers in vacuum technology is to be critically examined because extremely high cleanliness requirements are made for the weld seams. The application of welding fillers with high cleanliness and without fluxes can counteract against the melting loss of alloy elements and therefore diminish the negative influence on the mechanical stability of the joint. The mechanical stability of a joint is based on its cohesion and is closely linked – alongside the materials used and the seam geometry – with the dimensions of the connection. In addition to this, the originating distortions and stresses must be considered with larger cross sections. Shape and position tolerances are of increased importance in many vacuum applications. Examples of this are the requirements in accelerator technology, the closely tolerated positioning of focus points in the analysis measurement technology, or the need for flat sealing surfaces. Narrow form and position tolerances can require cost-intensive adjustment units, additional construction expenditure (e.g., greater wall thicknesses, heat insulating grooves), or intermediate machining steps (e.g., refacing of flanges and pipe ports).

In some applications of vacuum technology, particularly in accelerator technology, the change of the magnetic permeability during the welding process can have a negative influence on the application. In such cases, the microstructural state of the material as well as the heat influence by the weld process must be considered.

According to the material, welding techniques, and areas of application, different standards are used for the conventional quality assessment of welded joints. For fusion welded joints (except beam welding of steel), DIN EN ISO 5817:2014-06 [10] is frequently applied. Because this standard places the mechanical stability of the connection in the center, adaptations and enlargements must be made that embrace the previously named specific requirements for the respective vacuum application.

Welding techniques are qualified and standardized in order to achieve connections with high quality and reproducibility. In DIN EN ISO 15607:2004-03, instruction can be found for the development of a qualified provisional welding procedure specification (qWPS) up to the qualification for the finished welding procedure specification (WPS) [11].

#### Brazing

The thermal process for a material-bonded joining is referred to as brazing in which the materials are connected with the aid of the liquefaction of an additional component that is called solder. The melt temperature of the base material, the so-called solidus temperature  $T_S$ , is not reached with brazing. The permanent connection originates from wetting the solid base material with the liquid solder and from diffusion of the molten solder into the base material. Solder components form no intermetallic phases with base materials.

Because a fusion of the base materials is not necessary with brazing, materials with different melting ranges can be connected with each other (e.g., steel with copper, ceramics/glass with stainless steel). Brazing is preferentially used in case of formed components with low wall thicknesses or narrow tolerances or hardly accessible joints (Figure 7.4). In vacuum technology, brazing is frequently used to realize metal to ceramic connections (e.g., in electrical feedthroughs), steel–copper connections (e.g., with coolant feeds), or for components made of non-ferrous metals (e.g., titanium and aluminum).

A requirement for a successful brazing is the choice of a solder material suited to the basic materials and operating conditions. The following criteria have to be considered:

- Melting range of the solder material.
- Wettability of the base metals by the liquid solder.
- Solubility of the solder components in the base material.
- Corrosion resistance of the brazing.
- Producibility as solder rod, tape, wire, foil, paste, or powder.

For a successful joining, suitable brazing constructions (narrow gaps, force transmission) and precisely defined brazing processes (defined surfaces, brazing atmosphere, temperatures, hold times) are also necessary with vacuum applications. Figure 7.5 shows an overview of brazing constructions compatible with vacuum.

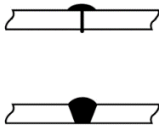
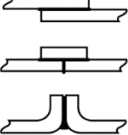
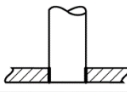
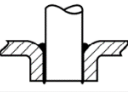
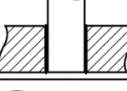
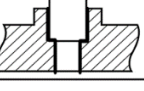
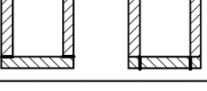
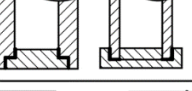
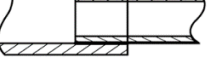
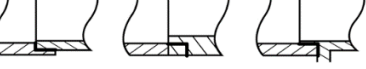
non-vacuum compatible	vacuum compatible
	
	
	
	
	
	

Figure 7.4 Examples of suitable brazing constructions. (Following Ref. [9].)

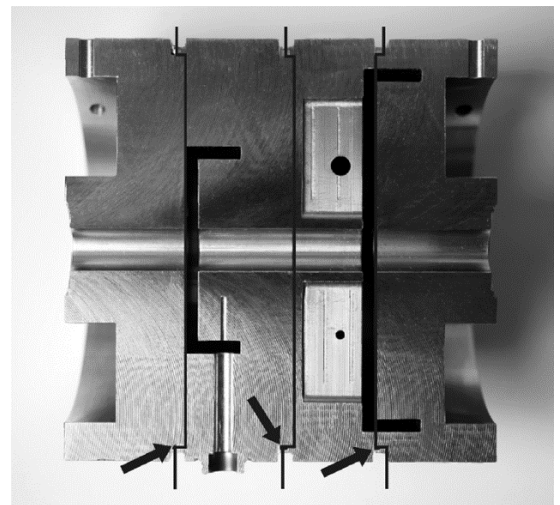


Figure 7.5 Cavity beam position monitor (E-XFEL prototype) in cutaway view, brazed with copper foil 2.0091 DIN EN 1044 CU 104 as an example of a vacuum component with hardly accessible joints. (Courtesy of the Deutsches Elektronen Synchrotron Hamburg.)

Metallic solders are divided according to the temperature of their complete liquefaction, the so-called liquidus temperature  $TL$ , in soft solders ( $TL < 450\text{ }^{\circ}\text{C}$ ), hard solders ( $450\text{ }^{\circ}\text{C} < TL < 900\text{ }^{\circ}\text{C}$ ), and high-temperature solders ( $TL > 900\text{ }^{\circ}\text{C}$ ). High-temperature solders are free of fluxes. The brazing process takes place under inert gas or vacuum atmosphere. The so-called active solders that are used for the brazing of ceramic materials form a special group of metallic solders. Ceramics are generally not sufficiently well wetted by metallic fusions. With the addition of active, reactive (oxygen-affine) elements such as titanium or zircon, the wetting and the brazeability of ceramics are improved through the change in the interfacial chemistry.

Solder materials must comply with additional requirements for the application in vacuum technology:

- Formation of a gas-tight connection.
- Low outgassing of the solder components.
- Low contamination with vacuum-affecting elements.
- Mechanical stability of the connection (stability with pressure differences  $\geq 1\text{ bar}$ ). Heat stability (stability with baking out processes).

Soft solders (primarily based on zinc, lead, or cadmium) are not used in vacuum technology due to the high vapor pressures of the individual solder components and the resulting high outgassing rates as well as the low heat stability.

Hard solders that are suitable for vacuum applications are alloys based on copper, silver, gold, or nickel. For special vacuum requirements, solder materials with very low contaminations in carbon, cadmium, phosphorus, lead, zinc, manganese, and indium are primarily used. The contamination limits are listed in DIN EN ISO 17672:2010-11 “Brazing – Solders” [12]. In this standard, the exact compositions and characteristics of hard solders are also explained.

Different brazing processes are applied according to solder temperature, shape, and material

of the components to be joined. In addition to furnace brazing, flame brazing, resistance brazing, induction brazing, and dip brazing are to be named. These primarily take place with the aid of fluxes for the removal of metal oxide on the surface. Nevertheless, flux residuals can be integrated in the surface and, with this, show a vacuum-affecting or corrosive effect.

Vacuum components are preferentially soldered with high-temperature brazing, that is, in the furnace under vacuum or inert gas atmosphere and without flux. Here, the entire component is fluxed with fitted, applied, or inlaid solder and heated up to solder temperature. Several joints of complex, large components can be soldered at the same time and thus show minimal distortion. Small brazing components can be produced in large quantities in a single batch. The furnace allows constant and defined heating up and cooling down, which is of advantage for the fusion and solidification processes of the brazing alloys. Through an adjustable inert gas atmosphere (CAB - controlled atmosphere brazing) or under vacuum, reactions of the base material and solder with the environment can be eliminated or selectively promoted. The desorption rates of the workpiece surfaces are already lowered during brazing as a result of the high process temperatures. If necessary, a heat treatment can be directly connected to the brazing process in the furnace.

Independent of the brazing process, attention is absolutely to be paid to the fact that while heating up the components the solder temperature is reached not only at the heat source or at the temperature measuring thermocouple, but also truly on the surfaces to be soldered. At too low temperatures, insufficient wetting or flowing of the solder will entail incomplete gap filling. The results are leaky brazing joints or considerable strength losses. A too quick cooling down leads to segregations (local decompositions) of the molten solder that favor the formation of undesirable microstructures with brittle phases, microcracks, and significant concentration fluctuations. Poor or unpredictable mechanical properties of the soldered joint are the result.

#### Adhesive Bonding

Adhesive bonding is a nonthermal, material-bonded joining process in which an additional component (adhesive) wets the surfaces of the base material. In particular, adhesive bonding finds application:

- if the materials and material combinations to be joined are difficult or not weldable (e.g., titanium, tantalum with stainless steel),
- with nonbrazable materials with low temperature resistance (e.g., plastic, aluminum),
- if a low-distortion and low-stress joining is necessary,
- when joining materials are sensitive to temperature.

The base material is not modified with bonding – unlike with brazing and welding. Because no diffusion processes take place between the materials used, a vast number of material combinations can be joined.

A distinction is made between physically and chemically bonding adhesives. For vacuum applications, bonding is only used with chemically curing adhesives because physically bonding adhesives reach adhesion through the evaporation of solvents or dispersion media. Chemically reacting adhesives produce their adhesive properties through chemical reactions, for example, through cross-linking [13]. Therefore, a distinction is made between two- (or more) component systems and one-component systems.

With two-component adhesives (2C-adhesives), two spatially separated preparations are used. One of the preparations contains resinous monomers (binders), while the other contains hardeners. The chemical reaction of the adhesive polymer begins with the contact between the binder and the hardener. Therefore, 2C-adhesives can only be processed within a defined period of time. After insertion of the adhesive in the joint, the curing time in which the final strength of the bonding is built follows. This curing time is influenced by temperature and electromagnetic waves (e.g., UV light).

With one-component adhesives (1C-adhesives), the ready-for-use adhesive is inserted directly into the adhesive joint. The adhesive hardens with the change in the ambient conditions. This can happen, for example, through a temperature rise, admission of air humidity, exclusion of air oxygen, or contact with the substrate surface. Also with the chemically hardening 1C-adhesives, chemical

reactions between the binder and hardener are responsible for the formation of the polymer. As opposed to the 2C-adhesives, the binder and hardener of 1C-adhesives cannot or only extremely slowly react under the storage conditions recommended by the manufacturer. In the databases of the NASA [14] and the European Space Agency ESA [15], approximately 2500 adhesives are listed and characterized with regard to the mass loss in vacuum. A low TML value indicates a good vacuum suitability by a low outgassing rate.

Adherence has extremely high requirements for the cleanliness and freedom from grease of the surfaces to be joined. Contact with the hands alone is sufficient to diminish the adhesive effect and render the bonding useless. The bonding strength can be increased by machining, such as, for example, by grinding, brushing, or blasting. Through roughening and the enlargement of the surface associated with it, the adhesive is additionally form-fitted in the surface. Chemical (e.g., pickling) or physical pretreatments (e.g., corona and plasma processes, flame treatments) can also increase the bonding strength. For the after-treatment of the adhesive seam, for example, the use of primers (preservation of the adhesive bond) is available. The use of primers improves the adhesion quality and protects the bonding against humidity and corrosion. In this process, the primer must always be adapted to the adhesive.

Bondings are always subject to aging and their durability is determined by mechanical (static and dynamic forces), chemical (humidity, solvents), and physical (heat, UV, and other radiation) influences. In the selection of the adhesive, the possible temperature load must also be considered alongside the ambient conditions. The adhesive will become brittle and crack at too low temperatures. At too high temperatures, the adhesive will soften and can melt/degrade.

#### Detachable Connections

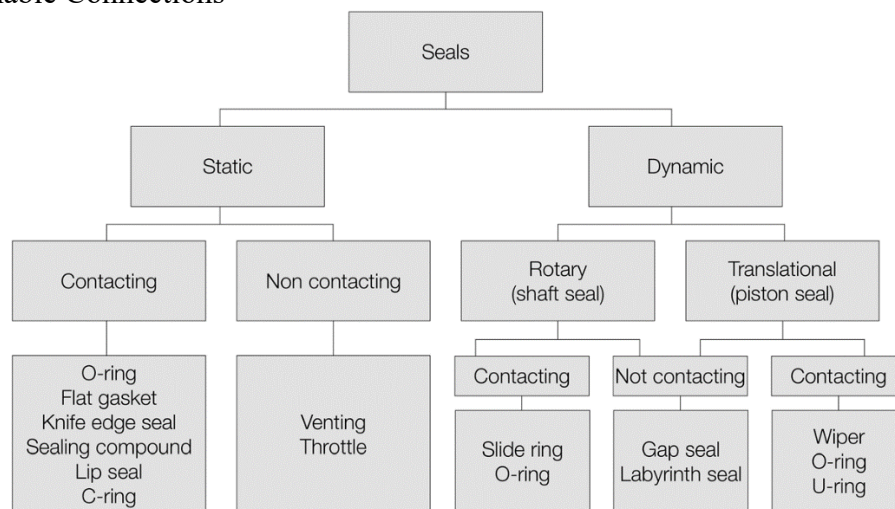


Figure 7.6 Classification of seals in mechanical and plant engineering.

For reasons of flexibility and a simple maintenance, the individual components of a vacuum facility should be detachably connected with each other. Form-fit and force-fit connections must be suitable for the many application-specific aspects in vacuum technology. The connections must comply with the different process-related requirements:

- pressure range,
- outgassing behavior,
- leak tightness,
- temperature resistance,
- chemical resistance,
- magnetizability,
- particle generation.

All detachable connecting systems in vacuum technology need a sealing medium, generally referred to as seal, to ensure the necessary leak tightness.

Seals count among the design elements in mechanical and plant engineering and are divided

into static and dynamic elements (see Figure 7.6). In both cases, contacting seals are common in vacuum technology; dynamic, noncontact gap seals are known for special applications [16]. Static seals for vacuum applications are O-ring seals, flat seals, knife edge seals, and lip seals; sealing compounds are used in special cases. O-ring seals and lip seals are only activated through a pressure difference between the spaces to be sealed, whereas flat and knife edge seals require an external pressing force for the sealing effect. Differently from that common in mechanical engineering, in vacuum technology, such seals that are loosened or connected during the operation of a vacuum system are considered as dynamic seals, for example, valve plate seals. Although this classification is systematically not quite exact, a valve plate seal also has its fundamental function in the static sealing and thus must never seal and allow a relative movement of the seal partners at the same time. Nevertheless, this widespread classification should be used here (Figure 7.6).

The detachable connections that are widespread in vacuum technology can be most suitably classed according to their permeation (leak) rates and therefore according to the pressure range in which they can be used. Table 7.3 provides an overview of the most common connecting systems and elements.

The division of the different connecting systems according to the pressure range reveals that varying values of leak rates of the connections limit the application.

Table 7.3 Detachable connections of vacuum technology and their areas of application.

Area of application	Connecting system	Seal partner	Seal	Typical application	Typical He permeation leak rate $Pa\ l\ s^{-1}$
Fine vacuum	Conical ground glass joint	Glass cone surface	Grease	Glass apparatuses for chemistry/ biology	Not specified
High vacuum		Flat sealing surface	Metal C-ring coted	Special applications, large nominal diameters	$10^{-5}$
	Lip seal	Flat sealing surface	Elastomer lip seal	Vacuum vessel doors	$10^{-6}$
	ISO/KF flange system	Flat sealing surface		Vacuum systems in high vacuum	$10^{-6\ a)}$ ( $10^{-7}$ )
	Swagelok Ultra-Torr	Metal cone surfaces	Elastomer O-ring	Pipe screw connections	$4 \times 10^{-7}$
	Swagelok VCR	Metal seal lips	Metal flat seal	All metal fittings	$4 \times 10^{-9}$
Ultra-high vacuum		Flat sealing surface	Metal O-ring concave, gas-filled, coated	Special applications, large nominal diameters	$10^{-7}$
	KF flanges system	Flat sealing surface	Metal edge seal		$< 4 \times 10^{-7}$
	Bostec H-seal	Knife edge	Metal profile seal	Special applications	Not specified
	Helicoflex	Flat sealing surface	Covered metal spiral ring	Special applications, large nominal diameters	$< 10^{-8}$
	VATSEAL	Flat sealing surface	Metal profile seal		$< 10^{-8}$
	COF flange system	Conical sealing surface	Metal round wire	All-metal seals, Nominal large diameters	$< 10^{-8}$
Extreme ultra-high vacuum	CF/QCF flange system	Knife edge	Metal flat seal	Vacuum systems in ultra-high vacuum XHV	$< 10^{-9}$

a) Leak rate with ISO and KF flange systems depending on the flange material.

### 7.3. Components

#### Standard Components and Chambers

The design of a vacuum chamber decisively influences the success and the repeatability of processes or experiments and at the same time is an essential expense factor. With the materials and manufacturing methods available today, a large part of the requirements in chamber building can be realized with standard components. Various components are required for the construction of vacuum systems (Figure 7.7). Leak-tight connections are primarily achieved through standardized flanges. The functional components are joined through connecting and manifold pieces, such as, for example, crosspieces or elbows.

In addition to the design of vacuum chambers applicable to vacuum, the principle of important functional components such as valves and electrical, mechanical, and optic feedthroughs is described. Furthermore, the possibilities of the heat supply and dissipation to ensure the process stability are explained.

#### Vacuum-Applicable Designing and Joining

Before and also during the planning and design of a vacuum recipient, the user should also consider the potentially appearing mechanical loads, process-related mechanical stresses, the material choice, the necessary wall thicknesses, the stability of the joints, and necessary tolerances of the interfaces (flange outlets). The clarification of these questions enables the optimal design of the vacuum chamber for the subsequent application.



Figure 7.7 Vacuum components.

Undesirable outgassing can be minimized through the use of materials with low inherent vapor pressure and nonporous surfaces. In addition to the required mechanical stability against atmospheric pressure as well as corrosion resistance, the surfaces should be easy to clean. Depending on the application, stainless steel, aluminum, copper, glass, special elastomers (FKM,

e.g., Viton®; PTFE, e.g., Teflon®), and ceramics are commonly used in vacuum technology. From a manufacturing point of view, the vacuum chambers can be divided into three groups:

- Cylindrical chambers. The simplest design is the cylindrical chamber. It is characterized by a very stable geometry. The resulting advantage with cylindrical chambers is that relatively low wall thicknesses can be realized. Cylindrical chambers can be closed through weld flanges, specially produced “lids,” “dished heads,” or domed disks. For the construction of cylindrical chambers, the industry offers standard elements in terms of tube diameters and wall thicknesses as well as for the closure of the chamber.
- Spherical chambers. The spherical chamber is a commonly used variation. Spheres dispose of an especially stable geometry against external and internal loads (pressure). In spite of the manufacturing-related larger tolerance of the spheres or hemispheres, exact focus points are realizable with modern technologies.
- With the cylindrical as well as the spherical chambers, the manufacturing expenditure disproportionately increases with the reduction of the tolerances. In the concept phase, it should always be checked whether the necessary high accuracy can be achieved more cost effectively with adjustment possibilities for the components to be assembled.
- Rectangular chambers. Rectangular chambers are the third variation. With rectangular

chambers, significantly more attention must be placed on the mechanical stability depending on the application. Due to their geometry, rectangular chambers are vulnerable to buckling during the pumping out. For the mechanical layout of rectangular chambers, the application of FEM software for the calculation of the deflection of the side walls is recommended.

- Double-walled chambers. For various processes, it is necessary to heat chambers or also to dissipate heat. This can be realized through the welding of cooling channels or with double-walled chambers. In order to prevent turbulences and to achieve an efficient temperature exchange, suitable guide plates that provide a forced direction to the medium are to be installed between the walls.
- Design of vacuum vessels. In view of the occurring stresses and pressure differences, vacuum vessels must be configured safely and reliably. In contrast to overpressure vessels, there are no mandatory regulations for vacuum vessels. Independent of this, the material choice, calculation, configuration, production, checking, and commissioning occur according to approved rules of engineering. For the orientation, for example, large-scale research institutes such as CERN, DESY, BESSY, or ESRF define their requirements for materials, production, and testing very specifically.

For the design of the chambers, the leaflets of the “Arbeitsgemeinschaft Druckbehälter” (Pressure Vessels Working Committee) in the “AD 2000 Code for Pressure Vessels” [17] that specify all essential safety standards according to the European Pressure Equipment Directive can be referred to. The calculation fundamentals are also clearly summarized therein:

B0 – Design of pressure vessels (general part).

B3 – Domed ends subjected to internal and external overpressure.

B4 – Dished heads.

B6 – Cylindrical shells subjected to external overpressure.

The pages B3, B4, and B6 also contain equations for the calculation and examination of wall thicknesses with external overpressure that can be used for the configuration of vacuum chambers.

#### Mechanical Feedthroughs

Mechanical feedthroughs are required to transfer the movements that are generated outside a vacuum chamber into the vacuum. The air-sided drive can occur manually, electrically, or also pneumatically. Already ensuring that the movement in the vacuum is low in loss and low in wear – without or with low outgassing lubricants – is quite a special challenge. At the same time, there is the additional requirement for a leak rate of the feedthrough that has to be as low as possible.

A mechanical feedthrough basically consists of a force-transferring element (shaft), a seal, and a flange. Mechanical feedthroughs are divided into three groups according to their operating principles:

- feedthroughs with dynamic seals,
- feedthroughs with flexible elements,
- feedthroughs with magnetic force coupling.

#### Valves

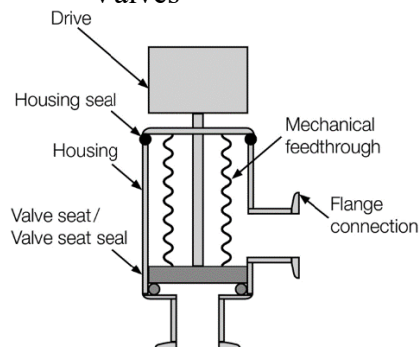


Figure 7.8 Schematic presentation of a right-angle valve.

Valves are feedthroughs for gases that, according to demand, can admit, regulate, throttle, or interrupt the gas flow between two volumes. They are placed between two or more systems with different pressures. Conductance, leak rate, number of the guaranteed load cycles, and media-exposed materials characterize the valves in vacuum technology. A valve consists of a valve case, valve seal, mechanical movement feedthrough, and an external drive (mechanically, electrically, or pneumatically). The basic construction of a valve is shown in Figure 7.8.

Many valve types are used in vacuum technology. Valves can be used either for opening and closing or for regulating. The actual conductance of valves has a decisive

influence on processes and on process times, which is why knowledge of them is of great importance. With the application of an angle valve, the effective pumping speed of a pump can be reduced by up to 50% in comparison with the application of an in-line valve of comparable geometrical dimensions.

#### Pressure Regulation

The pressure in a vacuum system results from the equilibrium between the inflowing gas and the pumping speed of the pump. Vacuum valves can influence the amount of the inflowing gas as well as the outflowing gas and, with this, the equilibrium pressure. This occurs in combination with pumps and sensors.

When the gas inflow is regulated in the chamber, we speak of an upstream regulation, while in contrast when the pumping speed of the pump is changed through a valve a downstream regulation exists. Different systems find application depending on the response time and sensitivity. With these regulations, the process gas composition and decomposition phenomena as well as the gas type-dependent pumping speed of pumps are to be considered.

A change of the effective pumping speed through a conductance change to the pump serves the rather rough regulation. Gate valves are ideal for the throttling of pumps because in open position the pumping speed is barely influenced by the high conductance.

According to the size of the system, pressure range, and pumping speed, needle valves, that is, valves with small variable apertures or conductances as well as with capillaries, come into use for upstream regulation.

Dosing valves are suitable for very sensitive applications due to their smooth actuation and low conductance. The regulation through valves is no longer sufficient for an extremely high accuracy and a stable process gas composition. Mass flow controllers (MFCs) are used for this. The mass flow rate of the gas is measured directly in the device through a thermal measuring system. It is to be noted that the MFCs mostly cannot close completely, and therefore, an additional closing valve is necessary.

#### Electrical Feedthroughs

Electrical feedthroughs provide the transfer of electric energy into the vacuum or out of it.

They consist of one or several conductors, a dielectric, and a metal housing. These components must be joined with each other through a hermetic seal so that a leak rate that is sufficiently low for the respective application is ensured.

An electrical feedthrough is hermetically connected with its metal housing to a vacuum flange or the vacuum chamber wall through a welded joint, but some-times also by means of a bulk head fitting or a screw-in thread. The dielectric serves as an electric insulation of the contacts of the ideally grounded vacuum chamber. Paschen's law is to be followed in the selection of a suitable electrical feed-through. It describes the dependence of the breakdown voltage in a gas atmosphere in relation to the gas type, the pressure, and the electrode gap. For a typical conducting feedthrough distance in the order of magnitude of 1 mm, a minimal breakdown is shown for air in the pressure range of 100-1000 Pa, so that a voltage breakdown can already occur with a few hundred volts. With higher pressures, the breakdown voltage rises again linearly, and with lower pressures, even exponentially. The maximum voltage load specified by manufacturers for an electrical feedthrough is primarily only valid for a residual gas pressure of  $p < 10^{-2}$  Pa.

#### Optical Feedthroughs [18]

Electromagnetic radiation, from the infrared (IR) through the visible (VIS) and up to the ultraviolet and extreme ultraviolet (UV/EUV) range, is taking on greater importance in vacuum. With optical feedthroughs (viewports, and optical fiber feedthroughs,), the transfer of electromagnetic radiation from the atmosphere into the vacuum and vice versa is being realized in different optical qualities.

In practice, it is about processes that are induced by electromagnetic radiation as well as about the processes in which electromagnetic radiation is generated. In addition, the detection of electromagnetic radiation is an important means for the process observation and process control.

An optical feedthrough basically consists of the optical material (window or fiber) and a frame that is usually metallic. These materials with very different material properties (e.g., thermal expansion coefficient) must be hermetically joined with suitable connecting materials. The optical

materials have the properties that are necessary to lead the electromagnetic radiation into a vacuum chamber or out of it as undisturbed as possible and in the optically required quality. Therefore, values for attenuation, absorption, dispersion, and plane parallelism, among others, are defined. The defined optical properties can be changed in their quality during the joining process.

The technical characterization of a viewport usually occurs according to the intended purpose. Viewports that only serve the visual observation are specified with the type of the optical material (ordinarily borosilicate glass), the view diameter, the helium leak rate, and the operating temperature/heating rate.

The properties/quality of the optical material for viewports that meet higher optical requirements are further specified. Common parameters are

- transmission range,
- refractive index,
- surface flatness,
- surface defects,
- parallelism.

These parameters describe, among others, effects such as reflection, absorption, dispersion, and image defects.

Viewports for optical applications are often provided with a coating in order to optimize the reflection or the transmission according to the use. With coated viewports, the coated diameter also matters alongside the view diameter.

A viewport normally consists of three components: the flange (installation of the viewport into the chamber), the optical material (transfer of the radiation), and the connecting element. The connection between the optical material and the flange has to be vacuum-tight, mechanically stable (pressure difference  $>1$  bar), and low in outgassing. In addition, it must provide for the equilibrium of the mechanical stresses, for example, through thermal expansion. It can be

- elastomer sealed,
- bonded,
- soldered, or
- fused.

#### Optical Fiber Feedthroughs

Optical signals can also be transported through fiber-optic cables (also called optical fiber) into a vacuum chamber. Monochromatic as well as polychromatic light can be guided precisely and flexibly.

Alongside the standard demands of vacuum technology, an optical fiber feedthrough (OFF) for vacuum applications must meet the optical demands, which is why the feedthroughs are additionally characterized by insertion loss, reflection loss, and intrinsic loss per fiber length. The type of the fiber can be characterized by the core or expanded beam diameter or the mode field diameter. The fiber type must correspond with the feedthrough and with the connecting cable so that greater losses are prevented.

A fiber can be joined into a flange in complete length, which, however, is problematic for a failure-free operation due to the high rupture susceptibility of unprotected fibers. On the other hand, feedthroughs with plug connectors stand out due to a high flexibility and operational reliability. In addition to the optical fiber feedthrough, protected fibers are used as a cable on both the air side and the vacuum side. According to application, high requirements are made on the vacuum side for the low outgassing of the protective sleeve of the fiber. The overall balance of the attenuation is determined by the plug type as well as the quality of the plugs.

#### Heat Supply and Dissipation

The transmission of heat occurs through thermal conduction, convection, and heat radiation. Because heat radiation is independent of substance, it is the only heat transport possible in pressure ranges  $<1$  mPa. Thermal conduction and convection are dependent upon a substance and gas type, respectively. In the pressure range  $>1$  mPa, the pressure dependence on thermal conduction and heat convection follows complex interrelationships. Because specific heat supply and dissipation are often

relevant to the process in the vacuum, this dependence must be considered and also be controlled, which can be realized through separate operation devices or the entire process control system. In addition, baking out processes play a crucial role for the cleanliness in the vacuum, the avoidance of contaminations through decomposition, and the achievement of the HV, UHV, and XHV ranges. Heat supply and dissipation can only be specifically controlled if a measurement of temperature is possible at the points relevant to the process.

#### Temperature Measurement in the Vacuum

Temperatures in the vacuum are primarily measured by a thermocouple or pyrometer. The use of thermocouples is based on the Seebeck effect [19] with which an electric voltage originates in a closed circuit with different conductors at the contact points with different temperatures.

When choosing conducting materials for the suitable temperature range, attention is to be paid to the fact that the thermotension changes nearly linearly. Electrical as well as thermal insulation has an influence on the measuring accuracy and reproducibility.

In order to outwardly transport the thermovoltage of the measuring point in the vacuum, a suitable thermocouple feedthrough is required for the type used. Here, the suitable conductors are externally connected to the fitting legs, whereas on the external side a regular cable is sufficient to determine the voltage in the measuring device. As described above, here, analog conditions are valid for the vacuum suitability of the feedthrough.

Pyrometers work on the fact that each body that has a temperature  $>0$  K emits heat radiation. The intensity, the spectral distribution, and the position of the emission maximum are dependent upon the temperature of the material to be measured and the material itself. Based on the Stefan–Boltzmann law, the total radiation power is proportional to the fourth power of the absolute temperature. A pyrometer can directly measure the external temperatures of vacuum chambers and vacuum systems. In order to be able to carry out pyrometric measurements in the vacuum, optical feedthroughs such as viewports or optical fiber feedthroughs for the respected wavelength range are required. While with viewports a direct view contact must exist between the measured object and the pyrometer, with fiber optical feedthroughs the emitted heat radiation is coupled into the fiber by a collimator lens and guided to the pyrometer in a flexible path.

#### Heat Dissipation from the Vacuum

Process heat can be dissipated either integrally through the chamber wall or directly at the place of the origin.

The integral heat dissipation through the external chamber wall can be achieved either by cooling lines with a good thermal connection to the wall or by the use of double-walled chambers (Section 17.4.1). The temperature range and the dissipated heat quantity determine the construction design, the cooling liquid, and the flow velocity.

For the local heat dissipation, cooling liquids are commonly used and, if necessary, supported by Peltier elements [20]. A liquid feedthrough is required for cooling with cooling liquids. While with refrigerant temperatures at  $>0$  °C, a simple pipe in the flange is sufficient, refrigerant temperatures at  $<0$  °C with icing effects near the flange seal are to be avoided through the use of an insulating vacuum.

#### Baking Out Processes and Heat Supply

The heat supply into a vacuum system can occur through heat generation inside and outside the vacuum.

With heat generation outside the vacuum, three proven possibilities are distinguished

- heating tapes,
- heating tents or heating boxes
- heating collars.

Heating tapes are flexibly applicable for various geometries. The rated powers usually lie between 20 and 250 Wm<sup>-1</sup> and, according to implementation, they are suitable for temperatures of up to 900 °C. However, it is to be noted that heating tapes overheat themselves above decomposition temperature if they are not regulated. For the secure and failure-free operation of heating tapes, the minimum bending radius may not be undercut while, at the same time, the correct laying distance and the thermal insulation toward the air side are to be ensured. With the application of various

heating tapes, different temperature ranges can be generated at several zones and temperature-sensitive components can be omitted.

Heating tents and heating boxes dispose of inside heating surfaces with good external insulation and generate a constant temperature of the air around the chambers and equipment whose homogeneous distribution can be supported by internal ventilating fans. They allow no specific differences in temperature in various areas and require the temperature resistance of all included components.

Heating collars for chambers and components are tailor-made heating devices that heat directly on the surface and are thermally well insulated on the outside. They allow for different heating zones as well as the omission of temperature-sensitive components. The typically used materials are, for example, glass silk, silicone, PTFE, and aluminum-coated or silicone-coated materials. For the application in the clean room, there are silicone-free and low in particle solutions for temperatures up to 200 °C.

#### ***7.4. Vacuum sealing technology***

The individual components of a vacuum system, e.g. vacuum chambers, pumps, valves, measurement instruments, etc., are connected with one another either directly or by means of pipe components or resilient elements. The detachable interfaces between the components must be vacuum-tight. In configuring a vacuum system, however, as few detachable joints as possible should be used, as they represent a significantly more frequent source of potential leakage than non-detachable joints.

Flange components from stainless steel, aluminum and steel can be used as connection elements. Metal hoses made of stainless steel are preferable to thick-walled rubber or thermoplastics for flexible joints. They are a strict necessity from the lower medium vacuum range onward.

From low to high vacuum ranges, ISO-KF flange connections with nominal widths of DN 10 to DN 50 are used for detachable connections, for larger nominal sizes of DN 63 to DN 1000 ISO-K and ISO-F flanges are used. Ultra-high vacuum compatible releasable connection, are in nominal widths DN 16 to DN 400 as a CF flange connection, respectively for larger nominal diameters of DN 400 to DN 800 flanges as a COF flange.

##### **O-ring seals and grooves**

When vacuum technology components are detachably joined, seals must be used to prevent ambient air from flowing into the vacuum. To prevent this, there are, depending on the application and pressure range different types of seals.

O-rings are the most frequently used of all seals. They are available in different materials, usually elastomers with a hardness in the range of 65 to 80 Shore A. The unit Shore A is used for soft elastomers as a measure of malleability. The higher the number, the lower the deformation with the same applied force. The suitability of O-rings as good vacuum seals stems from their ability to adapt to the minute unevenness of the mating surfaces. The surface of the O-ring must be free of releasing grease or talcum, smooth and crack-free and scratch-free. The rings should be seamlessly pressed, the parting of the pressing tool should be on the level of the ring diameter and can be removed by grinding.

The O-ring can be coated with a thin film of a low vapor pressure grease (silicon grease, mineral oil-based or perfluoropolyether-based grease), depending upon the application in question. The vacuum grease smooths out small irregularities on the sealing surfaces and the surface of the O-ring and thereby improves, particularly at low degrees of deformation, the sealing effect. Here, the vapor pressure of the grease should be noted increases greatly with the temperature and should be well below the desired operating pressure. In addition, it must be examined whether components of the grease or low amounts of hydrocarbons are compatible with the application. In the case of dry installation, particular attention must be paid to surface quality, the cleanliness of the mating surfaces as well as to the sealing material. In addition, the degree of deformation should not be too small, to ensure good contact between the O-ring and sealing surfaces.

The cord diameter of the O-rings is usually 2 to 12 mm. The diameter for many connections is 5 mm resp. 5.33 mm in the area of the inch dimension. Generally speaking, O-rings are used as static seals. If dynamic stress is involved, precision O-rings that are manufactured especially for this purpose or alternatively mechanical seals or radial shaft seal rings, should be used.

O-rings can also be used in axial or radial grooves (Figure 7.9), in addition to being employed in conjunction with centering rings or sealing washers. In most cases, O-rings are placed in grooves and pressed between flanges, by generally using a combination of one flat flange and one grooved flange. The grooves must be carefully dimensioned. There are no generally accepted dimensions for this. The dimensions listed in the tables of O-ring suppliers are only reference values and are used for orientation. They must be checked by the user on each specific application and suitability (e.g. through tests). Elastomers swell, shrink, harden or can even crack, due to external influences, such as temperature, pressure or reactions with the fluids used. This must be considered when selecting the elastomer and the groove. In addition, the sealing effect must be sufficient during each operating condition to ensure that the O-ring is not excessively compressed. If due to an increase in volume of the

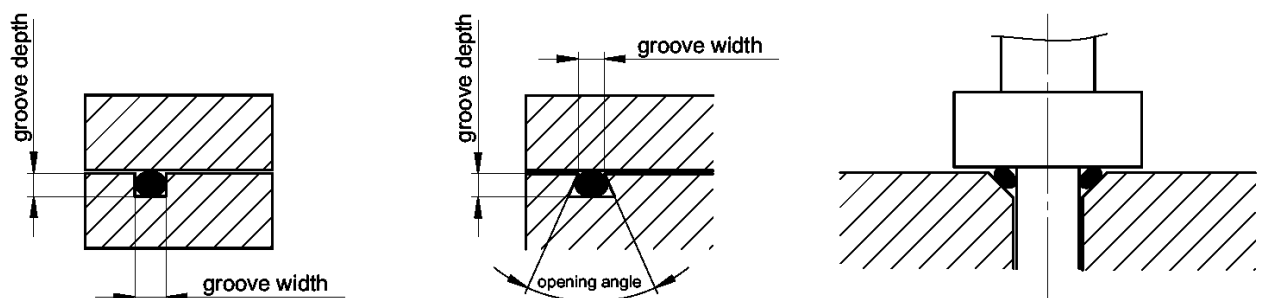


Figure 7.9 O-ring seals in rectangular groove, trapezoidal-groove and in an angular position

O-ring the groove is overfilled, it can damage the O-ring or even distort the flange.

For static sealing the maximum compression for a cord thickness of 5 mm should be about 25%. Smaller diameters can be compressed more, larger diameters less. In practice, a compression of less than 15 %, in particular for dry mounting, can cause an insufficient sealing effect. The deformation force is mainly determined by the cord thickness and the hardness of the elastomer. To compress an O-ring of 5.33 mm thickness by 20 %, approx. 5 N per mm of sealing length is required for a hardness of 70 Shore A resp. 7 N/mm for 80 Shore A.

To facilitate assembly, the diameter of the O-ring groove is usually selected somewhat larger than the diameter of the O-ring. This keeps the O-ring in the groove during assembly. Elastomer rings can safely be stretched in length by 5 %. The maximum stretch is dependent on the material and the operating conditions.

Elastomeric seals with trapezoidal or similar cross-sections can be used, for example, for valve seats and for lids and doors of vacuum chambers. The trapezoidal opening should be dimensioned such that the O-ring is not damaged when inserted and on the other hand is not pulled out when the valve plate is lifted or when you open the chamber door. In addition, with large contact forces, as they occur e.g. for large chamber doors, the trapezoidal-groove must allow enough room for the deformed O-ring, so that its deformation is kept within limits.

To seal screws, e. g. oil filler screws or oil drain plugs, the O-ring is installed in an angular position. The thread has a chamfer of  $45^\circ$  at the upper end, into which the O-ring is inserted and then compressed by the surface of the screw. The seal should be lubricated, so it is not damaged during tightening. In addition, the installation space must be greater than the volume of the O-ring.

Flat gaskets in combination with planar sealing surfaces are to be avoided in vacuum technology as much as possible. For this, a hard to reach high contact force is required, so that the sealing material fills any surface irregularities. If flat gaskets are used, this usually happens with circulating locally raised sealing surfaces, for example, with the combination of CF flange with a FKM flat gasket.

### ISO-KF flange

ISO-KF small flange components are described in DIN 28403 and ISO 2861 in nominal diameters DN 10 to DN 50. The connections suitable for pressures up to  $1 \cdot 10^{-8}$  hPa and can be used for overpressures up to 1,500 hPa. With metal seals, the pressure range can be extended to less than  $1 \cdot 10^{-9}$  hPa. The significantly higher contact pressures required for this are created with special clamps for metal seals.



Figure 7.10 ISO-KF connection with centering ring and clamping ring

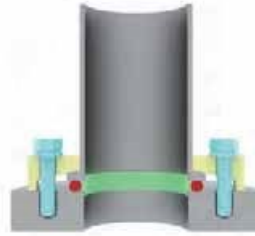


Figure 7.11 ISO-KF flange mounted on base plate with centering ring and claw clamps

An ISO-KF connection consists of two symmetrical flanges and one O-ring seal, which is positioned and supported with an internal or external centering ring (Figure 7.10). The necessary pressing force for the sealing is created by a clamping ring, which is placed over the conical tightening area and is tightened with a wing screw. This allows for a fast, efficient assembly and disassembly without any tools.

The flanges can be aligned around its main axis in any direction.

For mounting a KF flange on a base plate, (Figure 7.11) claw clamps or bulkhead clamps are used as clamping elements. The dimensions of the bores in the base plate can be found in the product description of the claws and bulkhead clamps.

#### ISO-K/ISO-F flange

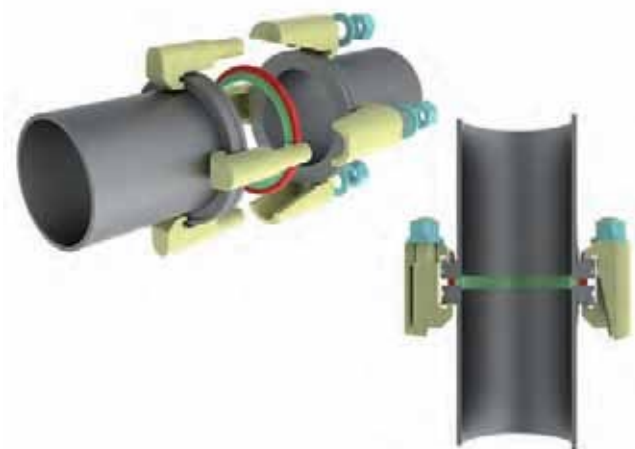


Figure 7.12 ISO-K connection with centering ring and double claw clamps

ISO-K clamping flange components and ISO-F fixed flange components are described in DIN 28404 and ISO 1609 in nominal diameters DN 10 to DN 630 for ISO-K flanges and to DN 1000 for ISO-F flanges. The connections are suitable for pressures up to  $1 \times 10^{-8}$  hPa and can be used for overpressures up to 1,500 hPa. With metal seals, the pressure range can be extended to less than  $1 \times 10^{-9}$  hPa. Metal seals require significantly higher contact forces. Screwed flange connections provide that. If clamp screws are used, their number must be increased if necessary.

An ISO-K and ISO-F compound consists of two symmetrical flanges and one O-ring seal, which is positioned and supported with an inner centering ring and also supported by an outer ring. The required contact pressure for sealing, is created with double claw clamps (Figure 7.12) or screws (Figure 7.16).

With ISO-K flanges, a circumferential outer ridge on the back of the flanges prevents slippage by the clamp screws. The flanges can be aligned around the main axis in any direction. Claw clamps are used for mounting an ISO K flange on a base plate. Depending on whether a centering ring is resting on the base plate (Figure 7.13) or an O-ring lies in base plate (Figure 7.14), claw clamps of different heights are used. Alternatively, the ISO-K flange can be screwed with a bolt ring onto the base plate (Figure 7.15).

The ISO-F flange has a fixed bolt hole circle that is dependent on the nominal diameter. The flanges can be aligned with a hole spacing around the main hole axis.

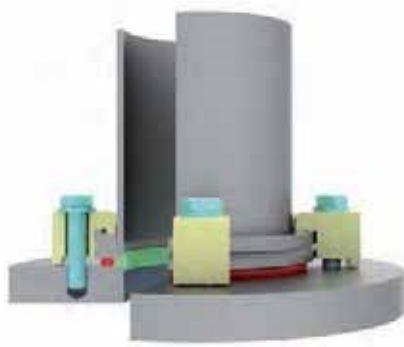


Figure 7.13 ISO-K flange mounted on base plate with centering ring and claw clamps



Figure 7.14 ISO-K flange mounted on base plate with O-ring nut and claw clamps for base plate with sealing groove

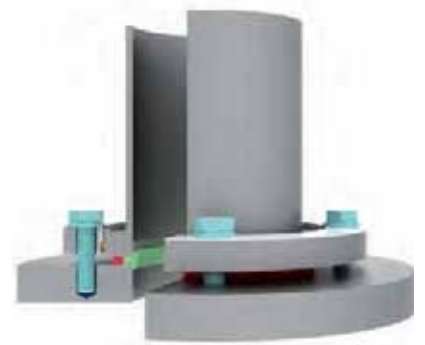


Figure 7.15 ISO-K flange mounted on base plate with centering ring, bolt ring and screws

An ISO-F flange can be bolted onto a base plate. As a seal, a centering ring can be used or an O-ring with a sealing groove in the base plate.

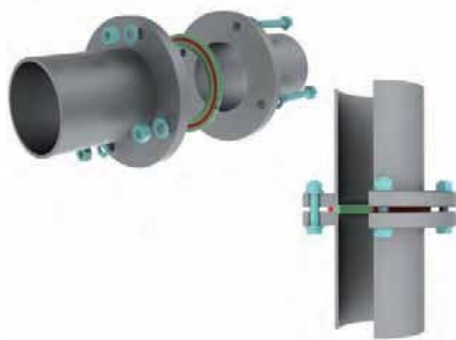


Figure 7.16 ISO-F connection with centering ring and screws



Figure 7.17 ISO-K flange with bolt ring mounted on ISO-F flange with centering ring and screws

Mounting an ISO-K flange on to an ISO-F flange can be done with a bolt ring (Figure 7.17). To install the bolt ring, it is slipped over the ISO-K flange and then a circlip is put into the outer circumferential groove of the ISO-K flange. The flanges can be aligned around the main axis in any direction.

#### CF flange

CF flanges are described in ISO 3669 in nominal diameters DN 16 to DN 250 and detailed in ISO/TS 3669-2 in nominal diameters DN 10 to DN 400. In addition to these standards, there are additional variants by manufacturers or users available on the vacuum market. For nominal diameters up to DN 250, they can often be combined.

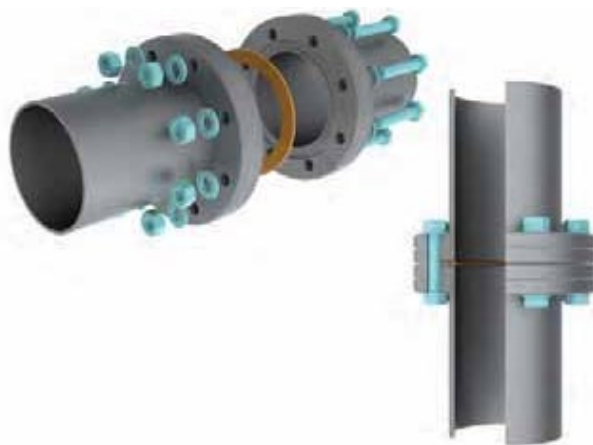


Figure 7.18 CF connection with copper flat gasket and screws

The larger nominal diameters are less common and differ considerably from each other. If there are doubts regarding the compatibility, the dimensions should be compared with each other.

CF flanges were designed for UHV applications, are bakeable up to 450°C and suitable for pressures less than  $1 \times 10^{-12}$  hPa. The demands on the materials are relatively high. CF flanges are made almost entirely of stainless steel, generally with a low carbon content. The material 1.4307 is sufficient for many applications. For higher demands, for example, regarding the strength or a low magnetizability, the premium stainless steel 1.4429 ESR is

recommended. For use on aluminum chambers, special bimetal flanges were developed, consisting of an aluminum base and a stainless steel surface or aluminum flanges that are equipped with hardened surface seal areas. In practice, however, their use often fails due to the relatively high price, the critical processability or the limited bakeability.

### COF flanges

COF flanges are used for large nominal diameters for ultra-high vacuum-compatible connections. They are bakeable, suitable for pressures up to approx.

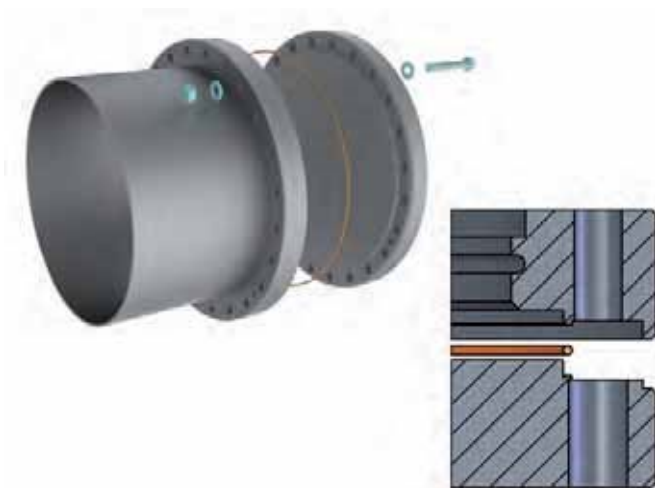


Figure 7.19 COF connection with copper wire seal and screws

During assembly, the seal is tightly inserted on the cutting edge of the “male” side. The sealing surfaces of the two profiles enclose the copper ring. An extrusion takes place on the cutting edges. The cold flow is limited by the vertical inner wall of the “male” flange, so that very high pressures are created in the boundary layer. Under the high pressure, the copper of the microstructure adjusts to the cutting edges and to fills small surface defects, which creates a metallic ultra-high vacuum-tight connection.

Previously used copper wires cannot be reused. For pressures up to approx.  $1 \times 10^{-8}$  hPa, seals made of FKM can be used. They are usually not reusable, but allow faster assembly, for example, if flanges are mounted frequently, e.g. when leveling the system.

During assembly, it is important that the screws are initially tightened uniformly diametrically, to avoid any tension. Subsequently, the screws should be tightened in sequence, in several passes, step-by-step until the copper is connected to the sealing surfaces in an ultra-high vacuum-tight manner. When baking out, it must be ensured that the heating and cooling are smooth and not done too fast. Temperature differences on the flange connection lead to tensions, which may cause leaks.

In the UHV and XHV ranges, seals made of a metallic base material are used whereby the metallic seals must be plastically deformed for the achievement of the necessary sealing effect. The plastic deformation provides for the fact that the production-related unevenness and waviness of the sealing surfaces are compensated and roughness

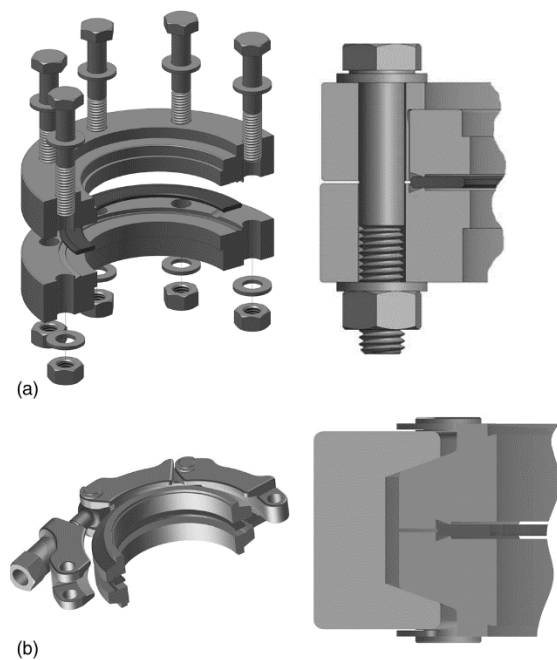


Figure 7.20 Schematic drawings of the CF flange system (a) and the QCF flange system for the simple, quick, and space-saving implementation of CF flanged joints (b).

valleys are closed. As seal materials for CF and QCF connections, oxygen-free, high-purity copper (99.99%, OFHC quality, CU-OFE, material number CW009A) is primarily used; pure aluminum (99.5%, EN AW 1050) is more rarely used. In special applications, other metal materials are also used. If the connections are baked out at more than 200 °C, silver-plated copper seals should be used to protect the seal against oxidation.

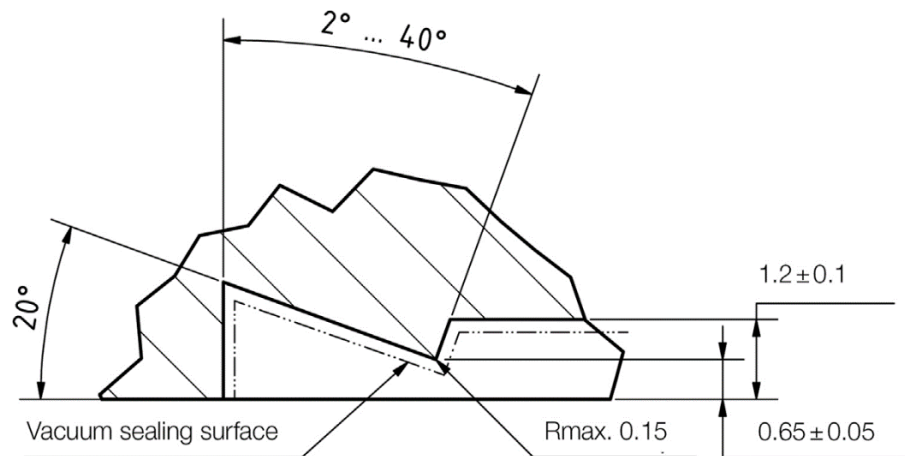


Figure 7.21 CF flange system: cross-section drawing of the knife edge.

The most widespread metal seal in vacuum technology is the combination of a flat seal and sealing surfaces with a knife edge (CF flange system, Figure 7.20a). In the ISO 3669 standard “Vacuum technology – Bakeable flanges – Dimensions,” the external flange dimensions and the number and position of the screws are defined depending on the flange diameter [21]. The sealing forces to be applied in reality and the resulting contact pressure are dependent upon the hardness of the flange and sealing materials as well as upon the knife edge geometry. From 2007 and in supplement to the previously named standard, there is ISO/TS 3669-2 - Vacuum technology “Bakeable flanges - Part 2: Dimension of knife-edge flanges” that is used worldwide as technical specification (TS) [22]. In addition to the external dimensions of the flanges, it also defines the geometry of the knife edge that is shown in Figure 7.21. For the generation of the sealing force, the use of stainless steel screws grade A2 strength class 70 with a tensile yield strength of 640 MPa is common. If flanges as well as bolts and nuts are made of stainless steel, suitable measures are to be taken to avoid galling (seizure) of the threads. Galling describes the formation of a connection between components on the basis of adhesion. Due to their adhesive properties and the lower hardness of Cr-Ni steels, they are especially vulnerable to galling in comparison with most other steels. The application of lubricants that are suitable to vacuum technology or Kolsterising® [23] of the connecting elements reduces the danger of the galling [24].

The QCF connection demonstrates the further advancement of the existing CF flange system (Figure 7.21). This flange system unites the simple assembly principle of the KF connections with the sealing principle of the CF connections. With this flange system, the sealing force is applied through a VaCFix® clamp chain on conically shaped flanges. The seal and sealing surface or knife edge of the flanges correspond to ISO/TS 3669-2. The use of the VaCFix® clamp chain, which ensures the same tightness and operational safety, enables a substantially easier, quicker, and more space-saving assembly of the flanged joint than the conventional CF flanges to be connected with screwing.

In addition to flat seals, profiles and concave rings with an open (C-ring) or round cross section as well as diamond-shaped (rhombic) cross sections (e.g., VATSEAL) are used. A great advantage of this seal form is the applicability for any flange geometry.

To achieve a better sealing effect with hollow ring seals, they are often provided with soft metallic coatings on the exterior side, for example, silver or aluminum. A variation of the metal C-rings are referred to as Helicoflex® seals in which an additional spiral spring is brought into the ring cross section. The spring causes an enlargement and a steadier distribution of the reset force.

### Other flange standards

In addition to the listed vacuum flanges there are numerous other flange standards which are used, for example, in industrial and process engineering, but are not as widespread in vacuum technology. Often, their surfaces are rough and designed for flat seals. For systems that operate under vacuum and overpressure, vacuum flanges can only be used to a very limited extent. For this purpose, flanges according to EN 1092-1 are used, for example. To design flanges that are suitable for vacuum, the sealing surfaces must be reworked; for example, a flange with an O-ring groove and a flange with a smooth sealing surface are paired. Therefore, the relevant statutory regulations for pressure vessels and piping must be observed.

### Screws

The importance of screws in the design of metal-sealed connections, cannot be underestimated. Screws also have application limits before they break. Improperly installed screws are potential sources of risk for leaks, especially with cyclic thermal stresses.

Two important mechanical factors must be considered when mounting screws: tensile strength  $R_m$ , which describes from which tensile stress upwards it results in screw breakage, and the yield point  $R_{p0,2}$ , which indicates from which stress upwards the tension force remains the same for the first time or becomes less, despite increasing elongation of the screw. This represents the transition between the elastic and plastic range. Screws should not be subjected to stresses that are higher than the 0.2 % yield point  $R_{p0,2}$ . The reference values for the tightening torque of screws are therefore values that take a 90 % utilization of the 0.2 % yield point into account.

The tensile strength and yield strength of steel screws (Table 7.4) at room temperature can be found in the specification under their strength classes, i. e. a two-digit number combination. The first number 1/100  $[N/mm^2]$  indicates the tensile strength. The multiplication of both numbers results in 1/10  $[N/mm^2]$  of the yield point. Example: strength class 8.8,  $R_m=8 \cdot 100 N/mm^2 = 800 N/mm^2$ ,  $R_{p0,2}=8 \cdot 8 10N/mm^2 = 640 N/mm^2$ .

Table 7.4: Mechanical characteristics and material of screws at room temperature

Type of screw	0.2%yield point $R_{p0,2} [N/mm^2]$	Tensile strength $R_m [N/mm^2]$	Material
Stainless steel A2-70	450	700	Stainless steel 1.4301 1.4303 1.4307
Stainless steel A4-80	600	800	Stainless steel 1.4401
Steel, strength class 8.8	640	800	Carbon steel, quenched and tempered

In the designation of stainless steel screws, the material quality and the tensile strength are indicated. These are: A for austenitic, 1 to 5 for the alloy type, and the strength class: -70 for strain hardened or -80 for high strength. The strength class equals 1/10  $N/mm^2$  of the tensile strength. Example: specification A2-70, A2 equals austenitic, alloy type 2, 70 equals  $R_m=70 10 N/mm^2 = 700 N/mm^2$ .

The nuts used, should have at least the same strength as the screws. For steel nuts, a number is indicated which equals 1/100  $[N/mm^2]$  of the test tension. Example: the number 8 equals  $R_m = 800 N/mm^2$ . For stainless steel screws, a nut with either the same or a higher material quality and property class must be used.

To determine the tightening torque and the preload stress, it is necessary to know the friction coefficient  $\mu_{total}$  of the screw connection. Due to the variety of surfaces and lubrication conditions, it is impossible to provide reliable values. The scattering is too large.

For this reason, only scattering ranges for the friction coefficient can be provided. To determine the correct torque, a test under operating conditions is recommended.

The friction coefficients (Table 7.5) can be reduced by the use of lubricants, however, the large scattering range remains the same. It should be noted that a smaller friction coefficient leads to a lower maximum torque. Hence:

Use of lubricants → friction coefficient  $\mu_{total}$  drops → less torque is necessary or may be applied.

Table 7.4: Friction coefficient for stainless steel and zinc-plated steel screws

Screw	Nut	$\mu_{total}$ without lubrication	$\mu_{total}$ with MoS <sub>2</sub> paste	$\mu_{total}$ greased
A2 or A4	A2 or A4	<b>0.23-0.50</b>	<b>0.1-0.20</b>	–
Steel electrolytically galvanized	Steel electrolytically galvanized	<b>0.12-0.20</b>	–	<b>0.10-0.18</b>

For stainless steel screws, the friction values in the thread and on the supporting surfaces are substantially greater than with tempered steel screws. The scattering ranges of the friction values is also much larger (up to above 100 %). Due to the high edge pressure, they also tend to get stuck. A lubricant can generally help in this case. Alternatively, silver plated screws or nuts can be used.

#### Properties of screws at elevated temperatures

When using screws at elevated temperatures (Table 7.5), it must be noted that the tensile strength and yield point are reduced. In addition, the creep strain or heat resistance must be considered as a basis for assessing the mechanical strength. Therefore, information on yield strength serves only as a guide. For critical or safety-related applications and other mechanical parameters and all influencing factors must be considered.

Table 7.5 Temperature dependence of the 0.2% yield point for stainless steel and steel screws with diameters ≤ M24

Type of screw	0.2% yield point R <sub>p0.2</sub> [N/mm <sup>2</sup> ] at				
	20 °C	100 °C	200 °C	300 °C	400 °C
Stainless steel A2-70	<b>450</b>	<b>380</b>	<b>360</b>	<b>335</b>	<b>315</b>
Stainless steel A4-80	<b>600</b>	<b>510</b>	<b>480</b>	<b>450</b>	<b>420</b>
Steel, strength class 8.8	<b>640</b>	<b>590</b>	<b>540</b>	<b>480</b>	–

If a through-hole screw connection is tightened by the rotation of the nut, a tensile force is created in the threaded bolt and an equal compressive force between the plates. As a result, the screw is elongated and the component compressed. Through the elongation of the screw, the preload stress is created. The clamping force is produced by the compression of the parts, and without any additional force on the connection is the same size as the preload force.

During tightening of the screw, friction between the contact surfaces is created. With a growing preload force, the friction moments in the thread and the nut contact area increase. The maximum preload force represents the sum of the friction moments the majority of the total tightening torques. With lubricated screws (small friction coefficients) the friction proportion is lower, so that the screws produce a higher preload stress with the same tightening torque. It should be noted that the maximum permissible tightening torque with lubricated screws is lower than with non-lubricated screws.

Preload force and torque cause tensile and torsional stresses in the screw. Both influences must be simultaneously considered during the calculation of the screw load. An alternative for the calculation is tables, as they appear in the VDI guideline 2230. If a 90 % utilization of the 0.2 % yield point is considered acceptable, the maximum permissible tightening torque and the associated preload stresses for the different friction coefficients can be found there. However, the information only represents non-binding values for guidance. For critical or safety-related applications, all influencing factors that may be required for a screws calculation must be considered. Excerpts from the tables for stainless steel and steel screws are listed below.

If screws are screwed into blind holes, an enclosed hollow space is created at the end of the threaded hole. Such dead volume is drained under vacuum only very slowly and leads to prolonged outgassing, which manifests itself in the same way as a leak. It is therefore also called a virtual leak. Under high vacuum and particularly UHV conditions, dead volume of this type should be constructively avoided or if that is not possible, it must be vented.

An alternative are vacuum screws which offer a comfortable means of venting. Their core has drilled holes (degassing bores). The screw head area has also a radial milling groove (degassing reduction), through which the area of the feedthrough hole of the screw connection is vented. The mechanical parameters for screws are not applicable to vacuum screws, as the vent hole leads to mechanical weakening.

Tightening technology.

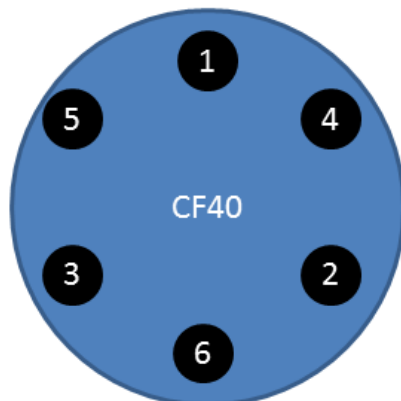


Figure 7.22 CF-40 flange nut tightening sequence

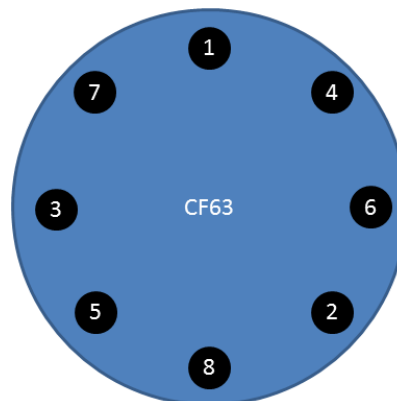


Figure 7.23 CF-63 flange nut tightening sequence

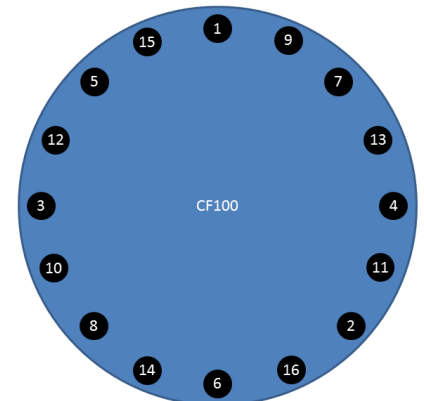


Figure 7.24 CF-100 flange nut tightening sequence

The implied but unvoiced condition being: and ensure that the Cu gasket is evenly clamped thus creating a leak-free seal. In regard to the order to tighten the nuts, however realised it that when taken literally one would only ever tighten 3 of the 6 nuts. The more correct but slightly longer adage would seem to be: “Do one miss one, until you land back where you started when you do, do not do that one but instead the next one, then do one miss one in the opposite direction and try to ensure even loading by only increasing the tightness by  $\frac{1}{4}$  a turn on each nut” Needless to say this is expressed more simply in a diagram, and so I direct you attention to figure 7.22. Once you reach nut 6, restart again from nut 1 and continue until the copper of the gasket is just visible between the flanges ( $\sim 1.5$  mm) or for those of you with a torque wrench set it to 20 Nm.

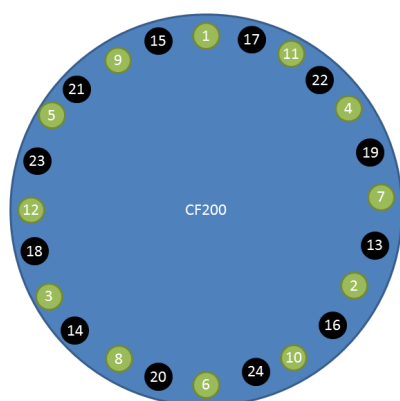


Figure 7.25 CF-200 flange nut tightening sequence

However, that made me think: what is the correct sequence to use on other flanges? Well both a CF-16 and CF-40 flanges have 6 nuts so the sequence for both is shown in figure 7.22. Generalising the sequence you would come up with a do one miss ( $\frac{n}{3}$ ) - 1, where n is the total number of nuts on the flange. Or put a different way, tighten every ( $\frac{n}{3}$ )th nut. Great, but what about when the number of nuts is not divisible by 3? Like on a CF-63, 100 or 160 flanges? Well the whole point of the sequence is to evenly bite the gasket. So, for any flange the “triangular-reverse-direction” loading would seem logical. Hence for a CF-63 flange you would use the sequence in figure 7.23 and for a CF-100 the sequence in figure 7.24. This same selection rules can be applied to CF-160 flanges.

Once you reach CF-200 you have 24 holes ( $\frac{n}{3} = 8$ ) and the sequence is a multi-pass version of the original CF-40 flange shown in figure 7.25.

1. CEROBEAR GmbH, CERABEAR ceramic bearing technology, Herzogenrath 2014, [http://www.cerobear.de/fileadmin/images3/Prospekte/CEROBEAR\\_company\\_brochure.Pdf](http://www.cerobear.de/fileadmin/images3/Prospekte/CEROBEAR_company_brochure.Pdf)
2. BODYCOTE WÄRMEBEHANDLUNG GMBG, Kolsterising Corrosion resistant surface hardening of austenitic stainless steel, Nürnberg 2005, [internet.bodycote.org/kolsterising/brochures/147-302\\_body\\_kolst\\_rd\\_gb\\_finr.pdf](http://internet.bodycote.org/kolsterising/brochures/147-302_body_kolst_rd_gb_finr.pdf)
3. Posth, O., Wunderlich, H., Flämmich, M., and Bergner, U. (2012) Reinigung von Vakuumbauteilen für UHV- und UCV-Anwendungen. Vak. Forsch. Prax., 24 (6), 18-25.
4. U. Hahn and K. Zapfe: Richtlinien für UHV-Komponenten bei DESY, Technische Spezifikationen Nr.: Vakuum 005/2008 Version 1.6/ 22.09.2010 [https://mhf-e-wiki.desy.de/images/c/c6/Vakuum\\_005\\_DESY\\_UHV\\_Richtlinien\\_1-5\\_final\\_tamp\\_eng.pdf](https://mhf-e-wiki.desy.de/images/c/c6/Vakuum_005_DESY_UHV_Richtlinien_1-5_final_tamp_eng.pdf)
5. GSI (2011) Testing the Cleanliness of Cryostat Insulation Vacuum Components. Technical Guideline. Available at <http://indico.gsi.de/getFile.py/access?resId=20&materialId=0&confId=1420>.
6. Taborelli, M. (2007) Cleaning and Surface Properties. CERN. Available at <http://cds.cern.ch/record/1047073/files/p321.pdf>.
7. DIN 8593-0:2003-09 (2003) Fertigungsverfahren Fügen - Teil 0: Allgemeines; Einordnung, Unterteilung, Begriffe, Beuth Verlag, Berlin.
8. DIN 1910-100:2008-02 (2008) Schweißen und verwandte Prozesse – Begriffe – Teil 100: Metallschweißprozesse mit Ergänzungen zu DIN EN 14610:2005, Beuth Verlag, Berlin.
9. Dorn, L. (2007) Hartlöten und Hochtemperaturlöten, Expert Verlag, Renningen.
10. DIN EN ISO 5817:2014-06 (2014) Schweißen – Schmelzschweißverbindungen an Stahl, Nickel, Titan und deren Legierungen (ohne Strahlschweißen) – Bewertungsgruppen von Unregelmäßigkeiten, Beuth Verlag, Berlin.
11. DIN EN ISO 15607:2004-03 (2004) Anforderung und Qualifizierung von Schweißverfahren für metallische Werkstoffe – Allgemeine Regeln (ISO 15607:2003), Beuth Verlag, Berlin.
12. DIN EN ISO 17672:2010-11 (2010) Hartloten - Lote, Beuth Verlag, Berlin.
13. DIN 8593-8:2003-9 (2003) Fertigungsverfahren Fügen - Teil 8: Kleben; Einordnung, Unterteilung, Begriffe, Beuth Verlag, Berlin.
14. NASA: MAPTIS Materials and Processes Technical Information System NASA's Authorized Guide to Materials. <http://maptis.nasa.gov/>
15. ESA/ESTEC/TOS-QM, Materials and Processes Division: SME INITIATIVE COURSE MATERIALS, SME1-Intro.ppt. <http://esmat.esa.int/SME/sme.html> Class 10 Materials Group Adhesives, Coatings, Varnishes: [http://esmat.esa.int/Services/Preferred\\_Lists/Materials\\_Lists/materials\\_lists\\_9.html](http://esmat.esa.int/Services/Preferred_Lists/Materials_Lists/materials_lists_9.html)
16. Patentschrift DE 10 2008 019 681 B4. Schenk, C.; Risse, S.; Harnisch, G.; Peschel, T.; Bauer, R. Mittels aerostatischer Lagerelemente geführter Tisch für Vakuumanwendungen
17. TÜV e.V. (2011) AD 2000-Regelwerk, TÜV e.V., Berlin.
18. Rietmann, T., Gottschall, S., Sahib, Ch., Flämmich, M., and Bergner, U. (2013) Optik braucht Vakuum. Vak. Forsch. Prax., 25 (1), 18–26.
19. Bergmann, L. and Schäfer, C. (1971) Lehrbuch der Experimentalphysik, Bd. 2, Elektrizitätslehre und Elektromagnetismus, 6th edn, Gruyter, Berlin, Chapter III 29.
20. Apertet, Y., Ourdane, H., Glavatskaya, O., Goupil, C., and Lecoeur, P. (2012) Optimal working conditions for thermoelectric generators with realistic thermal coupling. Europhys. Lett., 97, 28001.
21. ISO 3669:1986 (1986) Vacuum technology – Bakable flanges – Dimensions. Withdrawn. Available at [http://www.iso.org/iso/catalogue\\_detail.htm?csnumber=9124](http://www.iso.org/iso/catalogue_detail.htm?csnumber=9124)
22. ISO/TS 3669-2:2007-09 (2007) Vacuum technology - Bakable flanges - Part 2: Dimensions of knife-edge flanges, Beuth Verlag, Berlin.
23. Bach, F.-W., Laarmann, A., Mählwald, K., and Wenz, T. (2004) Moderne Beschichtungsverfahren, 2. Auflage, Wiley-VCH Verlag GmbH.
24. Wiegand, H., Kloos, K.-H., and Thomala, W. (2007) Schraubenverbindungen (Untertitel: Grundlagen, Berechnung, Eigenschaften, Handhabung), 4. Auflage, Springer.

## 8. LEAK DETECTION

### 8.1. Basic principals

Not only in research but also increasingly in the industry, tightness of vessels, tubing, components, and packaging are a key issue. Driving forces include environmental protection and the associated legislation as well as competition for ambitious customers calling for highly sophisticated, reliable products. Companies seek to certify their quality management systems, and thus, demand objective measuring methods with testing equipment calibrated traceable (to national standards).

Therefore, rather than developing more and more sensitive leak detectors for smaller and smaller leaks, progress seeks to provide quicker and certifiable procedures for economic survival in the competitive industrial environment. This also explains why tracer-gas leak detection using leak detectors is gaining in importance while historical procedures such as bubble emission techniques or pressure rise/drop are becoming less common. Employing leak detectors correctly and selecting tailored, application-oriented leak testing methods requires thorough knowledge of the fundamental physical principles involved. These shall be covered in the following sections, with a focus on practical applications.

If a vacuum system has a leak and is evacuated via a pumping system with the pumping speed  $S$  down to pressure  $p$ , small compared to ambient pressure  $p_0$ , then a constant leakage flow penetrates through the leak channel. Given as  $pV$  flow  $q_{pV}$ , it is referred to as leak rate. For stationary pumping action,  $q_{pV}$ ;  $p$ , and  $S$  are:

$$p = \frac{q_{pV}}{S} \quad (8.1)$$

For leak detection and leak measurements, a vacuum system can be immersed in tracer gas (or test gas, subscript "T," tracer gas acts as "search gas"), or the tracer gas is sprayed onto the system. Then, the partial pressure

$$p_T = \frac{q_{pV,T}}{S_T} \quad (8.2)$$

is detected or measured with a tracer-gas-specific detector namely a leak detector.

During operation of a vacuum system, air continuously passes through the

leaks. Therefore, the leak rate  $q_{pV,T}$  measured with the tracer gas has to be converted to the leak rate of air  $q_{pV,air}$ . In the first step, this calculation requires an assumption regarding the type of flow, based on the pressure conditions and the order of the leak rate. Then, the leak rate can be calculated from specific properties (relative molecular mass, viscosity) of the tracer gas and air.

Since every vacuum system includes a pump with defined pumping speed, leak detection can be carried out for a system equipped with a partial-pressure gauge for measuring tracer-gas pressures. The latter is true in many cases, particularly for ultrahigh vacuum (UHV) systems. Other cases however, especially when testing individual components, utilize a separate high-vacuum pumping system with an integrated mass-spectrometer partial-pressure gauge.

Leaks and leak detection

In non-destructive testing, a leak is defined as a hole, a porous area, a permeable area for gases or a different structure in the wall of a test specimen through which a gas can escape from one side of the wall to the other due to a difference in pressure or concentration [1]. Expressed in simpler terms, leaks are small holes through which gases or liquids flow from the side of higher pressure to the side of lower pressure. The geometry of the holes is not known. This means that the tester does not know whether the leak is a smooth-walled round pipe or occurs in the form of a crack or gap, for instance. Assumptions and calculations can only be made for ideal geometries. Since the real geometry of a leak channel is usually unknown, only calculated values can be assumed as an upper limit for a leakage rate. NOTE: The European standard DIN 1330-8 referred to previously uses the term "leakage rate". In the interests of readability, we will continue to use the more common term "leak rate".

A leak can be a harmless leak such as a dripping water faucet. Leaks involving the escape of aggressive media or toxic substances can have more serious consequences. The accident suffered by

the US space shuttle Challenger in 1986 was also due to the failure of an O-ring on the solid fuel rocket and the leakage of hot combustion gases.

Any number of technical products will not function, or will not function for an adequate period of time, if they have leaks.

Examples include:

- The refrigerant circulation system in refrigerators
- Air conditioning systems in cars
- Automobile tires
- Automotive fuel tanks or heating oil tanks
- Processing systems in the chemical or pharmaceutical industries.

In many cases, the leak-tightness of machines and systems in the production process is an indispensable prerequisite for the quality of the manufactured products.

Returning to the original definition of a leak, we thus find that it is impossible to completely prevent substances from flowing through a wall. The term "tight" therefore refers to the requirements of the respective machine, plant or vessel, and must be quantified accordingly.

Leakage rate

Let us consider a bicycle tube having a volume of 4 liters. It has been inflated to a pressure of three bar (3,000 hPa), and without any additional inflation should have a maximum pressure loss of 1 bar (1,000 hPa) after a period of 30 days.

The leakage rate

$$Q_L = \frac{\Delta p \cdot V}{\Delta t} \quad (8.3)$$

$Q_L$  - Leakage rate [ $Pa \cdot m^3 \cdot s^{-1}$ ]

$\Delta p$  - Pressure change during measurement period [ $Pa$ ]

$V$  - Volume [ $m^3$ ]

$\Delta t$  - Measurement period [ $s$ ]

Or to illustrate: The leakage rate of a vessel having a volume of 1 cubic meter is 1 [ $Pa \cdot m^3 \cdot s^{-1}$ ], if the interior pressure increases or decreases by 1 Pa within 1 second. Please refer to Table 8.1 for conversion to other customary units.

Table 8.1 Conversion table for units leak rate

	$Pa \cdot m^3/s = W$	$mbar \cdot l/s$	$Torr \cdot l/s$	$atm \cdot cm^3/s$	$lusec$	$sccm$	$slm$	$mol/s$
$Pa \cdot m^3/s$	1	10	7.5	9.87	$7.5 \times 10^3$	592	0.592	$4.41 \times 10^{-4}$
$mbar \cdot l/s$	0.1	1	0.75	0.987	750	59.2	$5.92 \times 10^{-2}$	$4.41 \times 10^{-5}$
$Torr \cdot l/s$	0.133	1.33	1	1.32	1000	78.9	$7.89 \times 10^{-2}$	$5.85 \times 10^{-5}$
$atm \cdot cm^3/s$	0.101	1.01	0.76	1	760	59.8	$5.98 \times 10^{-2}$	$4.45 \times 10^{-5}$
$lusec$	$1.33 \times 10^{-4}$	$1.33 \times 10^{-3}$	$10^{-3}$	$1.32 \times 10^{-3}$	1	$7.89 \times 10^{-2}$	$7.89 \times 10^{-5}$	$5.86 \times 10^{-8}$
$sccm$	$1.69 \times 10^{-3}$	$1.69 \times 10^{-2}$	$1.27 \times 10^{-2}$	$1.67 \times 10^{-2}$	12.7	1	$10^{-3}$	$7.45 \times 10^{-7}$
$slm$	1.69	16.9	12.7	16.7	$1.27 \times 10^4$	1000	1	$7.45 \times 10^{-4}$
$mol/s$	$2.27 \times 10^3$	$2.27 \times 10^4$	$1.7 \times 10^4$	$2.24 \times 10^4$	$1.7 \times 10^7$	$1.34 \times 10^6$	$1.34 \times 10^3$	1

racer gases

The test gases that are used for leak detection (also called tracer gases) should satisfy the following conditions: They should

- Be non-toxic for humans, animals and the environment
- Not displace air, as hazardous situations, such as suffocation, could otherwise occur
- Be inert, i. e. slow to react, and should neither react chemically nor be flammable
- If possible, not be present in air. Only with a gas that is present in the smallest possible concentration in the ambient air is it possible to detect even the smallest leaks
- Not be mistakable for other gases
- Be quantifiable through test leaks.

The tracer gas helium satisfies all of these requirements. As a noble gas, it is not capable of chemically reacting. Only 5 ppm of it is present in atmospheric air, thus enabling even the smallest leakage to be detected. Since it is lighter than air, it does not pose a health hazard. Specific detection is possible using mass spectrometry, a highly sensitive and very selective analytical process. There are many commercially available test leaks that are designed either as a diffusion leak or a flow leak.

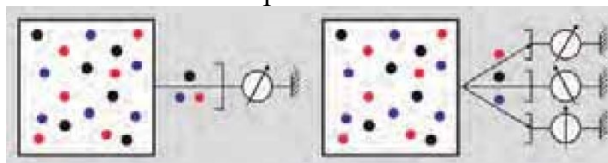
The criteria described above are met by hardly any other test gas, an exception being forming gas 95/5 which is a mixture of 95 % nitrogen and 5 % hydrogen. The combustible hydrogen which is explosive in a wide mix range with air, is diluted to a degree where the mixture is neither explosive or combustible and is therefore safe for use as a test gas. The same mass spectrometry detectors can also be used as a sensitive test for hydro-gen. Due to the higher background signal of hydrogen in the analytical technology used, it does not attain the same detection sensitivity as with the test gas helium, but it by far exceeds the detection sensitivity of the pressure decay method.

## 8.2. Mass spectrometers and residual gas analysis

Mass spectrometry is one of the most popular analysis methods. A mass spectrometer analyzes the composition of chemical substances by means of partial pressure measurement under vacuum.

Mass and charge (Figure 8.1)

- Total pressure is the sum of all partial pressures in a given gas mixture
- In order to determine the partial pressure of a certain component of a gas, it must be measured in isolation from the mixture
- This necessitates prior separation of the mixture
- This is accomplished on the basis of the mass-to-charge ratio  $m / e$



No separation: Total pressure

Separation as a function of time or space: Individual partial pressures

Figure 8.1: Total and partial pressure measurement

Analyses are typically performed in the field of research & development and in the production of products that are used in daily life:

- ❖ Research & Development
  - Catalysis research
  - Drug development
  - Development of new materials
- ❖ Monitoring production processes
  - in metallurgy
  - in chemical synthesis
  - in semiconductor production
- in surface technology
- ❖ Trace and environmental analysis
  - Aerosol and pollutant monitoring
  - Doping tests
  - Forensic analysis
  - Isotope analysis to identify the origin
- ❖ Analysis of products in
  - the chemical industry
  - high purity gas production pharmaceuticals
  - the automotive (supply) industry (leak detection) \
  - Quality assurance of food products

Mass spectrometers are used to analyze gases. Solid or liquid substances can also be analyzed if they are vaporized in an upstream inlet system. The gas is diluted by pumping it down to a low pressure (molecular flow range) in a vacuum chamber and ionizing it through electron bombardment. The ions thus generated are separated in a mass filter according to their charge-to-mass ratio.

Figure 8.2 shows the typical components of a mass spectrometer system.

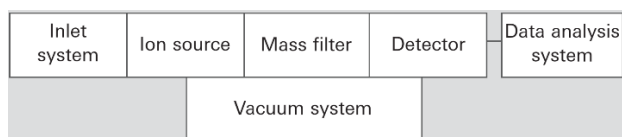


Figure 8.2: Components of a mass spectrometer

- The substances to be analyzed are admitted to a vacuum chamber through the inlet system via a capillary or metering valve, for example, and then are
- pumped down with the vacuum system

to the system's working pressure.

The actual analyzer is located in the vacuum and consists of the following components:

- The ion source ionizes neutral gas particles, which are then
- separated in the mass filter on the basis of their mass-to-charge ratio  $m/e$ .
- The ion current is measured using a Faraday detector or a secondary electron multiplier (SEM) after the ions have left the separating system. The current is a measure of the partial pressure of the respective gas molecules or a measure of fragments that may have been generated in the ion source.
- A data analysis system processes the ion currents measured with the aid of the detector and presents these currents in various forms. Today, data analysis software programs are capable of supporting the user in interpreting mass spectra.

Mass spectrometers differ as a result of the wide variety of available versions. The main difference consists of the separating systems. The following four types of mass filters are in widespread use today:

- Sector field devices use the deflection effect of a magnetic field on moving charge carriers.
- Time-of-flight mass (TOF) spectrometers utilize the differing velocities of molecules of equal energy for the purpose of separation.
- In ion traps, the trajectories of the ions are influenced by a high-frequency field.
- Quadrupole mass spectrometers utilize the resonance of moving ions in a high-frequency field (similar to ion traps).

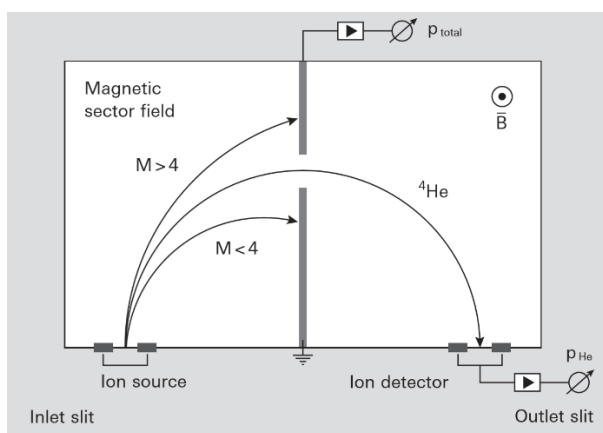


Figure 8.3: Operating principle of the 180° sector mass spectrometer

Our discussion will be confined to sector field mass spectrometers and quadrupole mass spectrometers, as these are the mass spectrometers that are most widely used in the field of vacuum technology.

#### Sector field mass spectrometers

Because of their simple, robust design, sector field mass spectrometers are used for helium leak detectors. Their mass range is restricted to masses of between 2 u (hydrogen molecule) and 4 u (helium atom). This makes it possible to build small, compact but very powerful mass spectrometers.

Operating principle The operating principle of sector mass spectrometers is shown

in Figure 8.3.

Neutral gas particles are ionized in an ion source through electron bombardment (Figure 8.4 a). The electrons thus generated with mass  $m$  with a load  $q$  pass through a potential gradient  $U$  towards the magnetic sector field and at the same time take up the kinetic energy,

$$E_{kin} = qU = \frac{mv^2}{2} \quad (8.4)$$

i.e. they pass through the sector field at a speed  $v = \sqrt{\frac{2qU}{m}}$ . Where the charge is identical, the speed and thus the time required to pass a given distance depends on the mass. This is exploited directly by time-of-flight mass spectrometers for the purpose of separating masses. In sector field mass spectrometers, the ions describe a circular path in the homogeneous magnetic field caused by

the Lorentz force which acts on the moving ions perpendicularly to the speed and perpendicularly to the magnetic field.

$$F = qvB \quad (8.5)$$

On a circular path with a radius  $r$  the Lorentz force is equal to the centripetal force.

$$qvB = \frac{mv^2}{r} \quad (8.6)$$

This is used to calculate the radius of the path

$$r = \frac{mv}{qB} \text{ with formula 8.4 } r = \sqrt{\frac{2mU}{qB^2}} \quad (8.7)$$

The sector field mass spectrometers used for leak detectors are equipped with a permanent magnet which supplies a constant magnetic field and in Figure 6.3 is positioned perpendicular to the image plane. The spectrometers are adjusted in such a way that the trajectory of singly charged helium ions first passes through an orifice and then through the outlet slit and finally strikes the detector. All other molecules are unable to pass through the slit and are re-neutralized. The ion current measured for helium is proportional to the helium partial pressure. As can be seen from Equation 8.7, the radius of the path can be varied through the accelerating voltage  $U$ . In practice, use is restricted to deflecting not just  $^4\text{He}$  but also ions with an  $m/e$  ratio of 2 and 3 towards the outlet slit and so detect the gases hydrogen and  $^3\text{He}$ .

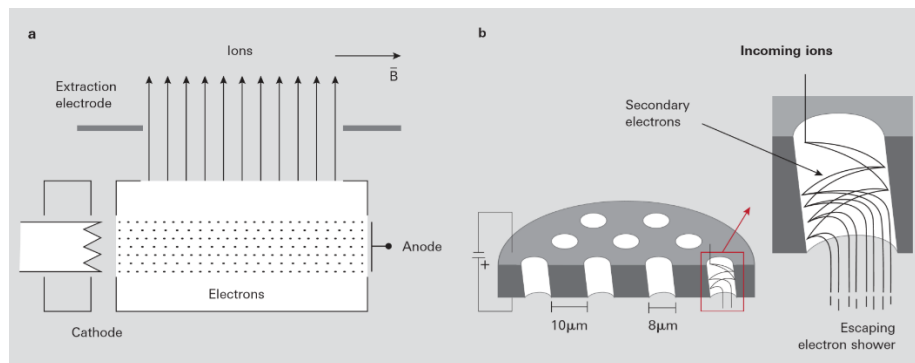


Figure 8.4: Sector field mass spectrometers: (a) Ion source, (b) Detector

To obtain a high detection sensitivity of the helium test gas during leak detection, the sector field mass spectrometer is fitted with a sensitive detector.

A straightforward metal collector (Faraday cup) no longer meets today's requirements, so modern leak testers

incorporate micro channel plates which are extremely compact and have high gain and low noise. These glass micro channel plates that are metal-coated on both sides have a large number of fine channels which run at a slight angle to the end faces (Figure 8.4 b) and whose interior surfaces are coated. If an ion strikes this surface, an avalanche of secondary electrons is triggered and this is accelerated towards the detector by the voltage applied to the plate.

According to Equation 8.7 the radius of the trajectory is inversely proportional to the magnetic field. The materials available for permanent magnets place restrictions on the magnetic field strength. This results in a typical radius of the order of 10 cm for helium spectrometers. To ensure that the trajectories of the ions are not interrupted by collisions, the mean path length must be approximately of the same magnitude. The maximum continuous operating pressure for helium sector field mass spectrometers is therefore approximately  $10^{-5}$  hPa.

Application notes Sector field mass spectrometers for detecting helium are today integrated in leak testers with an automatically controlled vacuum system. As a result the operator does not have to worry about the functional capability of the spectrometer. We would draw your attention at this point to the importance of the cleanliness of the interior surfaces for maintaining a high detection sensitivity.

- Deposits can result in local space charges when bombarded with scattered ions. These charges deflect the path of the helium ions and reduce the number of ions reaching the detector.
- Deposits on the micro channel plate reduce the yield of secondary electrons and so lower the amplification factor.

While it is possible to simply clean the interior walls of the spectrometer, contaminated micro channel plates must be replaced. It is extremely important for objects and equipment to be clean so as to maintain the high detection sensitivity of the instruments.

### Quadrupole mass spectrometers (QMS)

**Quadrupole mass filter** The filter system of a quadrupole mass spectrometer consists of four parallel rods arranged in the form of a square. Each pair of opposite rods in Figure 8.5, designated (+) or (-), is connected to each other. Between the two pairs of rods, an electrical voltage consisting of a DC portion  $U$  and an AC portion with amplitude  $V$  and frequency  $f = \omega/2\pi$  is applied:

$$U_{quad} = U + V \cdot \cos \omega t \quad (8.8)$$

At this point, only a brief phenomenological description of the operating principle will be provided. For a more detailed description, please refer to the special literature [2, 3, 4].

Ideal quadrupole fields require rods that have a hyperbolic profile. In actual practice, however, cylindrical rods are used, with the rod radius being equal to 1.144 times the field radius  $r_0$  (refer to Figure 8.5 for a definition of the field radius). An electrical quadrupole field is formed between the rods. Ions of varying mass are injected axially into the rod system at approximately equal energy and move through the rod system at uniform velocity. The applied quadrupole field deflects the ions in the X and Y directions, causing them to describe helical trajectories around the Z axis through the mass filter. If the amplitude of the trajectory oscillation is smaller than field radius  $r_0$ , the ions reach the detector; if the amplitude exceeds this the ions will discharge on the rods or the surrounding surfaces and will not pass through the filter.

To solve the equations of motion, two dimensionless variables  $a$  and  $q$  are introduced which combine the parameters of the quadrupole (DC voltage  $U$ , AC amplitude  $V$ , field radius  $r_0$ , angular frequency  $\omega = 2\pi f$ ) and that of the ion (charge  $Q = z \cdot e$ , mass  $m = M \cdot m_u$ ).

$$a = \frac{8QU}{mr_0^2\omega^2} \quad (8.9)$$

and

$$q = \frac{4QU}{mr_0^2\omega^2} \quad (8.10)$$

With this simplification, Mathieu's differential equations are obtained, the solutions for which

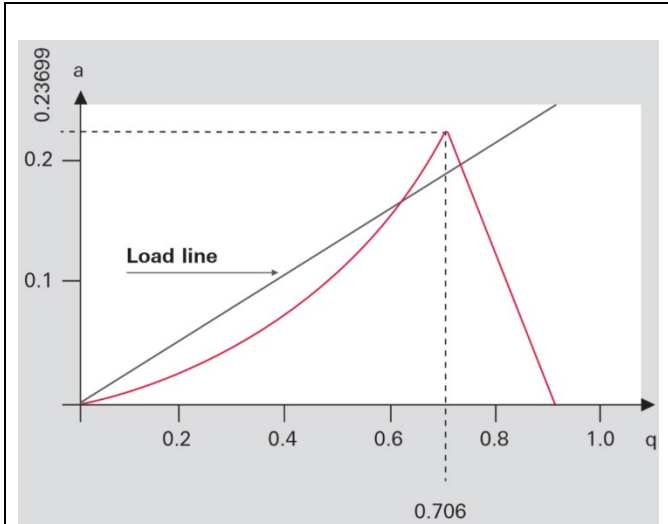


Figure 8.6: Stability diagram of a quadrupole filter

are well-known in mathematics; they can be used to calculate the range of stable trajectories with oscillation amplitudes  $r_{max} < r_0$  for pairings of stability parameters  $a$  and  $q$  located under the triangle formed by the two limiting curves in Figure 8.6. All solutions outside this range result in increasing oscillation amplitudes and thus in neutralization of the ions on the quadrupole filter rods. Dividing the two equations by one another gives:  $a/q = 2U/V$ . This is the slope of the so-called load line of the mass filter.

At the limit the load line intersects the peak with the values:  $a_p = 0.237$  and  $q_p = 0.706$ .

The quadrupole filter is transparent only for voltage ratios  $\frac{U}{V} = \frac{a_p}{2q_p} < 0.1678$ , i. e. where the load line intersects the stability range. All ions whose parameters  $a$  and  $q$  are located in the triangle above the load lines will reach the detector.

Introducing the ratio  $m_u/e$  between the atomic mass unit  $m_u = 1.6605 \cdot 10^{-27} \text{ kg}$  and the elementary charge  $e = 1.6022 \cdot 10^{-19} \text{ A} \cdot \text{s}$  ( $m_u/e = 1.0365 \cdot 10^{-8} \text{ kg A}^{-1} \text{ s}^{-1}$ ) and multiplying this by the dimensionless mass number  $M$  of the corresponding ion obtains the following conditions for voltages  $U_p$  and  $V_p$  for the apex of the stability triangle (with the constants  $k_u = 1.2122 \cdot$

$10^{-8} \text{ kg A}^{-1} \text{ s}^{-1}$  and  $k_u = 7.2226 \cdot 10^{-8} \text{ kg A}^{-1} \text{ s}^{-1}$ ):

$$U_p = k_u M r_0^2 f^2 \quad (8.11)$$

$$V_p = k_v M r_0^2 f^2 \quad (8.12)$$

The stability conditions show that at a fixed frequency, there is a direct proportionality between the voltages and the masses at the quadrupole filter and that a linear mass scale is obtained with varying voltage amplitudes.

With the DC voltage shut off  $U = 0$ , all trajectories of the ions where  $q < 0.905$  will be stable; according to Formula 8.6 these will be all masses where

$$M > \frac{k_H V}{r_0^2 f^2} \quad (8.13)$$

Where  $k_H = 1.0801 \cdot 10^7 \text{ kg}^{-1} \text{ s}$  is a constant. The filter thus acts as a high pass in this operating mode. As the RF amplitude  $V$  increases, ever-heavier types of ions become unstable, starting with the light masses, and are thus separated out. This operating mode produces an integral spectrum and allows a total pressure measurement to be carried out.

The ion injection conditions are crucial for transmission of ions through the filter. Ions must enter the quadrupole in an area as close as possible to the center of the rod system and ideally move parallel to the axis of the rod.

The greater the field diameter (distance between rods) and the longer the quadrupole (rod length), the easier it is to fulfill these conditions. In addition, the geometric accuracy (production tolerances) is easier to achieve the greater the rod dimensions.

In practical operation, the ratio  $U/V$  is activated as a function of the mass number in such a manner that the actual resolution  $M/\Delta M$ , does not remain constant, but that instead the line width  $\Delta M$  remains constant. This means that resolution increases proportionally to the mass number. Due to Equation 8.12 ( $V$  is proportional to  $M$ ), the quadrupole (as opposed to the sector field mass spectrometer) produces a linear mass scale.

One point of major significance for a QMS is the required RF power. If  $C$  is used to designate the overall capacity of the system and  $Q$  to designate the quality factor of the power circuit, the required RF power will increase

$$N_{RF} = \frac{C}{Q} M^2 r_0^4 f^5 \quad (8.14)$$

with high powers of  $f$  and  $r_0$ . An enlargement of field radius  $r_0$  will lessen the relative mechanical tolerances that occur, thus resulting in improved behavior. Essentially, it is advantageous to select  $f_0$  and  $r_0$  as large as possible. However, there are limits to this due to the associated increase in RF power according to Equation 8.14. While extending the rod system permits a lower operating frequency, the size of a production unit should not exceed certain practical dimensions.

The required mass range and desired resolution are governed by the dimensions of the filter and the operating frequency selected. Devices with 6, 8 and 16 mm rod diameters and appropriately matched electronics are available to satisfy the satisfy most requirements.

What follows is a brief digression on the relationship between resolution and mechanical precision. Let us consider a quadrupole mass filter that works at the apex of the stability diagram; i.e. with high resolution. The following equation applies Equation 8.11:

$$U = 1.2122 \cdot 10^{-8} \frac{\text{kg}}{\text{A} \cdot \text{s}} M r_0^2 f^2 \quad (8.14)$$

for the DC amplitude and Equation 8.11

$$U = 7.2226 \cdot 10^{-8} \frac{\text{kg}}{\text{A} \cdot \text{s}} M r_0^2 f^2 \quad (8.15)$$

for the AC amplitude. Here,  $M$  designates the mass of the ion,  $r_0$  the field radius and  $f$  the frequency at which the filter is operated. We are making the idealized assumption that both voltages  $U$  and  $V$ , as well as frequency  $f$ , can be set and maintained "as precisely as desired."

It follows from this that:  $M = c_k \frac{1}{r_0^2}$  ( $c_k$  is a constant) and following differentiation, division by  $M$  and determination of the value, the filter scatter caused by  $r_0$  is:

$$\frac{dM}{M} = \frac{2 \cdot \Delta r_0}{r_0} \quad (8.16)$$

Let us assume that the field radius  $r_0$  changes by  $dr_0 = 0.03$  mm over the length of the mass filter. Now let us consider the effect of this change on the scatter for two mass filters of different sizes. For optimal transmission, the resolution set on the spectrometer (we select:  $M/M = 1/100$ ), must be greater than the scatter generated by the fluctuation of  $r_0$ . For a filter with a field radius of 3 mm, this results in  $dM/M = 2 \cdot 0.03\text{mm}/3\text{mm} = 0.02$ , i. e. the scatter due to the imperfect geometry hinders the desired resolution. For a different filter with a larger field radius of 12 mm, this results in  $dM/M = 2 \cdot 0.03\text{mm}/12\text{mm} = 0.005$ , the geometry does not hinder the desired resolution. In other words: if a resolution of  $\Delta M/M$  has been set for both filters, then in the first case most of the ions will not be able to pass through the filter. In the case of the large filter for the second quadrupole, all ions will be able to pass through the filter.

Although this simplified error calculation by no means takes into account all of the effects that can contribute to transmission, it does demonstrate several fundamental relationships:

- The field radius must be maintained significantly higher than 1 % over the entire length of the filter, depending on the mass range selected. Fluctuations in the field radius will result in transmission losses.
- The larger the dimensions of the rod system are selected, the lower the influence of the absolute mechanical tolerances will be.
- The higher the mass range within which adjacent masses should be differentiated, the stricter will be the requirements relating to the relative accuracy of the mass filter.

Summary. A quadrupole mass filter is a dynamic mass filter for positive and negative ions. The mass scale is linear to the applied amplitude of the RF voltage. Mass resolution can be conveniently and electrically set by means of the ratio between the DC voltage  $U$  and the high-frequency voltage amplitude  $V$ . Due to their compact dimensions and light weight, quadrupole mass spectrometers are suitable both as pure residual gas analyzers and, in higher quality design, as sensors for gas analysis.

### 8.3. Leak detection with tracer gases

Many companies use leak detectors based upon mass spectrometers and quartz window sensors to detect the presence of tracer gases. Mass spectrometers ionize a gas mixture and isolate the desired tracer gas on the basis of their mass-to-charge ratio. Quartz window sensors are based on the selective permeation of light gases through a quartz membrane.

Design of a leak detector with a mass spectrometer

The operating principle of quadrupole mass spectrometers is shown in chapter 8.2 These units are used both purely as residual gas analyzers or process gas analyzers as well as for leak detection. Inlet systems for analyzing gas mixtures at higher pressures, including for leak detection, are described in chapter 8.2 Gas analysis systems on the basis of quadrupole mass spectrometers can be used as multi-gas leak detectors.

The operating principle of sector mass spectrometers is shown in chapter 8.2

The spectrometer cell of a leak detector shown in Figure 8.7 also only works at pressures under  $10^{-4}$  hPa. In leak detectors, this pressure is generated and maintained by the pumping system of the leak detector. This does not require any operator intervention.

Leak detectors with mass spectrometric analyzers are designed as shown in the diagram in Figure 8.8.

A mass spectrometer (spectrometer cell (8)) for masses 2, 3 and 4 (corresponding to test gases H<sub>2</sub>, 3He and 4He) is attached to the inlet flange of a turbopump (high vacuum pump (7)). A backing pump evacuates the turbopump through the exhaust valve (6). A test specimen (in DIN EN 1330-8 also referred to as “test object”) is evacuated through the inlet with the valve (3) open. Valves (6) and (3) are connected in such a manner that the required backing vacuum pressure of the turbopump always takes priority over evacuation of the test specimen. Once the test specimen has been

evacuated, it can be connected to the backing vacuum or to the interstage pump of the turbopump via valve (4), depending on the pressure range concerned. Test gas is now sprayed onto the test specimen from the outside and together with the ambient air penetrates into the test specimen through leaks. The test gas present in the residual gas flows counter to the pumping direction through the turbopump via valves (3) and (6) to the spectrometer cell, where it is detected. The different compression ratios of the turbopump for air and the light test gas helium, which differ by multiple powers of ten, are utilized for this purpose.

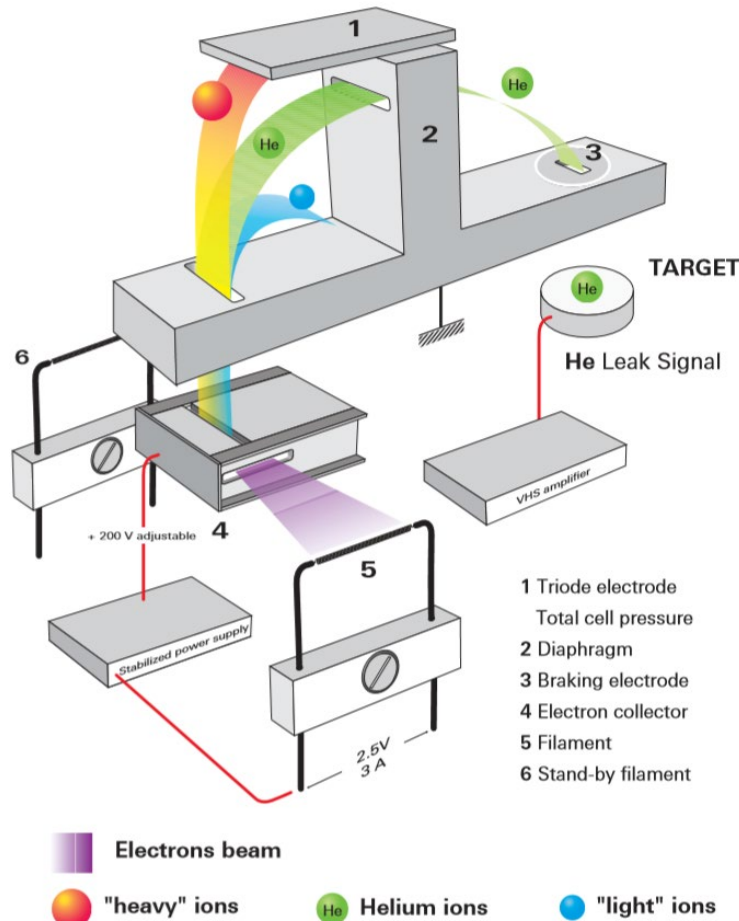


Figure 8.7 Working principle of a sector mass spectrometer

While the high compression ratio of the turbopump keeps air away from the mass spectrometer, light gases arrive there at a relatively high partial pressure. The turbopump thus acts as a selective filter for helium and hydrogen. This is why a mass spectrometer enables helium and hydrogen to be detected in the test specimen even at pressures  $< 10$  hPa (higher for some devices). Several powers of ten of the helium partial pressure, and thus a leakage rate range in the counterflow of between 1 and  $10^{-9}$  Pa m<sup>3</sup> s<sup>-1</sup> can be covered by means of various interstage pumps in the high vacuum pump (4), as well as by operating it at different speeds that exponentially influence the compression ratio. A pressure in the range of several powers of  $10^{-2}$  hPa must be attained in the test specimen and leak detector in the main flow for the highest sensitivity stage of the leak detector (intake via valve (4)).

Due to the upstream turbopump, the mass spectrometer always operates at an extremely low total pressure, and is thus well

protected against contamination and failure.

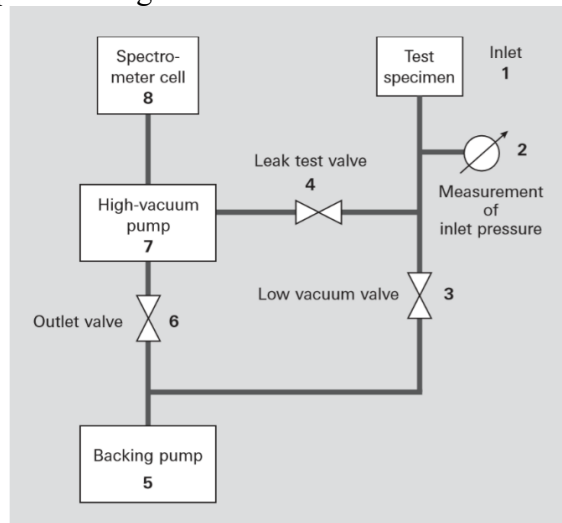


Figure 8.8 General leak detector flow chart

Design of a leak detector with a quartz window detector (Figure 8.9).

While mass spectrometric detectors separate a gas mix by ionization followed by separation in a magnetic or electrical field, quartz window detectors make use of the different permeation properties of gases.

The tracer gas mix is conveyed to the quartz surface of a heated diaphragm. The carrier layer for the quartz diaphragm consists of a silicon wafer with several thousand holes through which all incoming gas atoms and molecules can reach the quartz diaphragm. The separation itself takes place at the quartz diaphragm which allows helium, but not other gases, to pass through it. The thickness and

temperature of the diaphragm are influencing factors for the permeation of the helium test gas. After the gases have passed through the diaphragm, the tracer gas that has entered is ionized and the ion current is a measure of the leak rate.

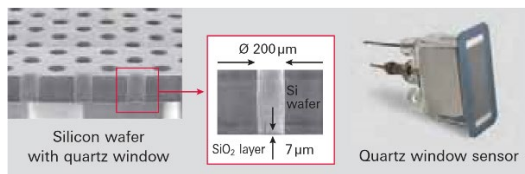


Figure 8.10 Operating principle of quartz window sensor

the response time of the sensor at higher system pressures.

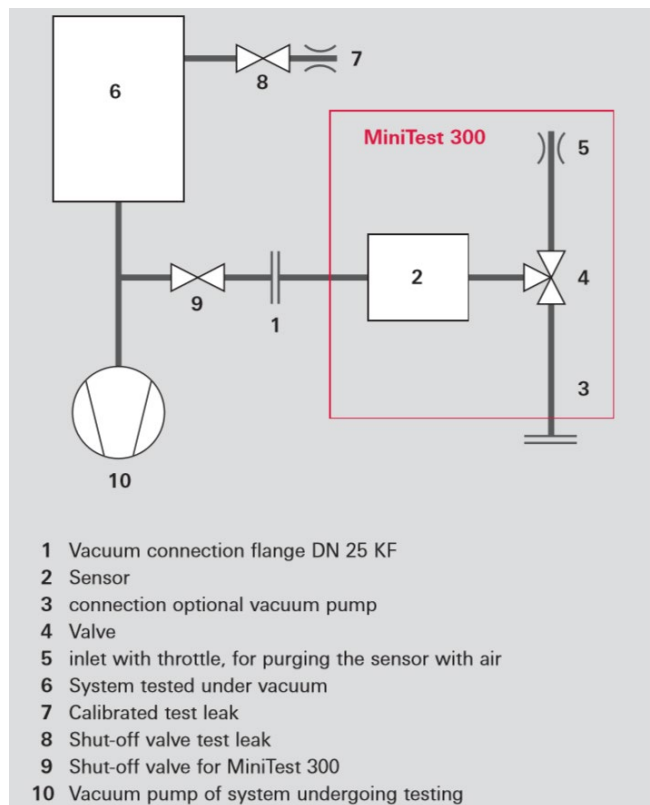


Figure 8.11 Vacuum diagram of the MiniTest quartz window leak detector on a system

of test specimens is typically determined for quality assurance purposes, be performed?

Leak detectors are equipped for two operating methods:

- The vacuum method, in which the test specimen is evacuated and helium exerts its effect from the outside.
- The sniffer method, in which the workpiece is filled with test gas overpressure  $\Delta p > 100$  hPa and the escaping test gas is sucked into the leak detector via a sniffer valve and detected.

Calibrating the leak detector.

The leak detector must be calibrated in order to determine leakage rates. This is done using a commercial test leak, which generates a known and reproducible test gas rate under defined conditions. Commercial test leaks are available in the form of a permeation leak or a capillary leak with or without a test gas reservoir. Leak detectors are usually equipped with permeation leaks with a helium reservoir. For calibration, an appropriate working cycle is often built in that automatically performs the calibration.

To obtain precise measurements, the unit should be calibrated before each use. To test large

The unit is connected to the system (Figure 8.11) to be tested (6) with a vacuum connection flange (1). The connection (3) can optionally be connected to an additional vacuum pump. To prepare the leak test, this pump can evacuate the vacuum system of the unit while the shut-off valve (9) is still closed.

The shut-off valve (9) is opened for the test. The optional pump can generate a gas flow which reduces

The sensor (2) measures the partial pressure of helium in the vacuum. A test leak (7) on the system is used to determine the response time and calibrate the unit.

To protect the sensor and to purge the unit after a strong signal, automatic purging can be carried out. The valve (4) opens the inlet with the throttle (5) and the sensor is purged briefly with atmospheric air.

Test methods

The test procedure used to detect leaks depends upon the type of test specimen and the required test results. The following criteria are formulated in the standard DIN EN 1779 [5]:

- Will the test specimen be tested at overpressure or in a vacuum? In selecting the test method, if possible a method should be chosen that takes into account the pressure gradient encountered when the test specimen is actually used.
- Is only a partial area or the whole area of the test specimen to be tested?
- Should local leak detection, which is used to find leaks, be carried out or should integral leak detection, where the leakage rate

test specimens for which additional vacuum pumps are in use, it is advantageous to use an external test leak. The measurement accuracy can depend on where the test leak is attached. Consequently, it is necessary to take flow conditions within the vacuum area into consideration. The use of external test leaks is also useful for determining the maximum response time.

Local leak detection.

Local leak detection is used to identify leakage in a test specimen.

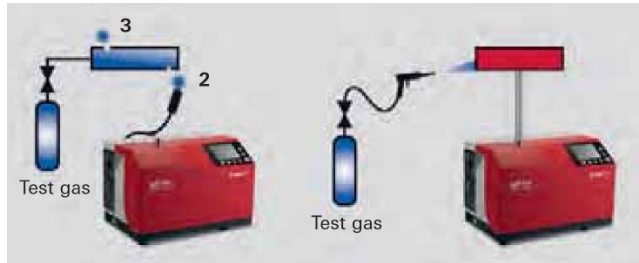


Figure 8.12 Local leak detection with sniffing and vacuum methods

In the vacuum method, the test specimen (vessel) is connected to the leak detector, and helium is briefly sprayed onto a suspected area using a spray gun. If the pressure in the test specimen is in the molecular flow range, i. e.  $< 10^{-3}$  hPa, the test speed will be dependent on the volume of the test specimen and the effective pumping speed of the test setup for helium. The smaller the test specimen or the greater the pumping speed of the leak detector or auxiliary pump used,

the quicker the result is obtained. At higher pressures, particularly in the laminar flow range greater than 1 hPa, the display speed will be much slower and will be governed by the pumping speed of the leak detector's backing pump.

In the sniffer method according to Figure 8.12 the test specimen (3) is filled with test gas overpressure. A sniffer probe (2) is connected to the test gas connection of the leak detector. The test gas that escapes through leaks in the test specimen can be detected by sniffing with the probe.

Individual leaks can be identified using local leak detection. However, the sum of all leakage cannot be determined. That is why this process offers only limited suitability for providing a GO / NO GO indication for quality assurance purposes.

Table 8.2 Local leak detection by sniffer and vacuum methods

	Sniffing Leak Detection	Vacuum Leak Detection
Method	Sniffing the test gas-filled test object	Spraying with helium
Mechanical strength	Against overpressure	Against atmospheric pressure from the outside against the vacuum (pressure difference 1000 hPa)
Detection limit	$< 1 \cdot 10^{-8} Pa \cdot m^3 \cdot s^{-1}$	$< 5 \cdot 10^{-13} Pa \cdot m^3 \cdot s^{-1}$

Integral leak detection.

Integral leak detection is used to determine the total leak rate, i. e. the total leak rate of all leaks in the test specimen. Here, too, the vacuum method and the sniffer method can be used.

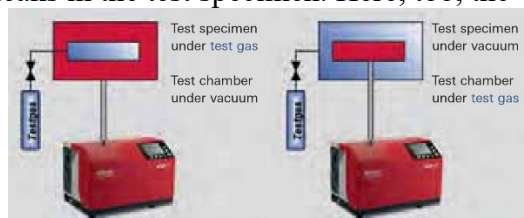


Figure 8.13 Integral leak detection with the vacuum method



Figure 8.14 Integral leak detection of enclosed objects with the sniffer method

In the integral vacuum method (method A1 in accordance with DIN EN 1779, Figure 8.13 right-hand side), the test specimen (e. g. a vacuum system) is evacuated and the surrounding space is filled with a defined quantity of test gas. The surrounding enclosure can be a plastic film or a rigid vessel. It is important that the test specimen is exposed to a defined

quantity of the test gas to enable conclusions to be made about the test gas concentration at the leak and

a reliable quantitative conclusion to be reached.

When testing enclosed test objects (method B6 in accordance with DIN EN 1779, Figure 8.13 left-hand side) the test specimen is filled with helium and placed in an encasing vacuum vessel. The escaping test gas is identified and quantified by the leak detector.

In the sniffer method, the test specimen is filled with the test gas (method B3 in accordance with DIN EN 1779, Figure 8.14) and placed in an enclosing vessel. Contrary to the method described previously, this vessel does not require to be evacuated and can remain at atmospheric pressure. This means that less stringent requirements are placed on the apparatus as in the previously described method. The escaping gas is collected in the enclosing shell and needs to be mixed well during the test (using a fan, for instance) to ensure that a uniform concentration of test gas is present in the analytical chamber. The sniffer probe of the leak detector is used to determine the increase in the concentration of the test gas escaping from the test specimen which collects in the enclosing shell. The detection limit for this method is determined by the concentration of the test gas in the dead volume of the enclosing shell and the additional increase in the test gas concentration. This means that this method is considerably slower than the integral method under vacuum and its use is normally restricted to small test specimens with limited part throughput.

Table 8.3: Integral leak detection by means of the sniffer and vacuum methods

	Sniffing Leak Detection	Vacuum Leak Detection	
Method	Accumulation test, collection of escaping test gas in an enclosing shell or chamber	Test specimen under overpressure, measurement of escaping test gas in a vacuum chamber	Test specimen under vacuum, measurement of test gas escaping from an enclosing shell into the test specimen
Mechanical strength	Against overpressure of the test gas	Against overpressure of the test gas	Against atmospheric pressure from outside against vacuum (pressure differential 1000 hPa)
Speed	Slow	Fast	Fast
Limit of detection	Use mainly $< 1 \cdot 10^{-5} Pa \cdot m^3 \cdot s^{-1}$	$< 5 \cdot 10^{-13} Pa \cdot m^3 \cdot s^{-1}$	$< 5 \cdot 10^{-13} Pa \cdot m^3 \cdot s^{-1}$

#### 8.4. Application notes

Prior to beginning any leak detection process with helium, the user must clarify several fundamental questions:

- How pressure-resistant is the test specimen?
- Is there a preferred direction for pressure resistance and can the pressure gradient encountered by the test specimen in actual use be simulated?
- Is only the location of the leakage to be determined or should it be quantified?
- Should the integral leak rate of the test specimen be determined? If so, what is the maximum acceptable leak rate?
- What fluid reference applies for the leak rate indicated?
- What test pressures does this apply for?
- Are there any safety aspects to be considered?

On the basis of these answers an appropriate test method can be selected from among the methods indicated in previous chapters.

##### Leak detection with helium

The leak detector must be calibrated prior to conducting a localizing leak detection or integral leakage test. A helium test leak integrated in the Pfeiffer Vacuum leak detector is used for this purpose. The calibration routine is started either when the leak detector starts up, at the touch of a button or automatically and runs according to a fixed software protocol. Following calibration, the

leak detector is ready for use.

The user is kept constantly informed about the status of the unit and the leak rate measured through visual displays and acoustic signals. With the audible signal, the frequency of the signal tone rises as the leakage rate changes. The time at which the acoustic signal is given can be determined by the user by programming a threshold value. Visual signals can be read either on the control panel on the unit concerned or on a wired or wireless remote control unit. This allows leak detection to be carried out by just one person.

The following must always be observed when using helium as the test gas:

- Helium is lighter than air. So when helium is used in the atmosphere, the leak detection process should always begin at the highest point of the test specimen. This prevents a false signal being emitted due to helium rising at a leak above where the current test is being conducted. The upward flow of helium can be interrupted however by air currents. In cleanrooms with laminar gas flow from the ceiling to the floor the working direction is reversed.
- Excessive amounts of the test gas should not be sprayed, as this can increase the concentration of helium in the ambient air. This results in an increased background signal in the leak detector and growing insensitivity during the test.
- If the backing pump of the leak detector used or an auxiliary pump are oil-lubricated, then helium accumulates in the exhaust space in the backing pump and dissolves in the oil, and can diffuse back to the high vacuum area from this point. After detecting high leak rates, the use of gas ballast in the backing pump can help to discharge accumulated helium from the pump system and reduce the background signal that is indicated.

In the vacuum method, it is necessary to generate a sufficiently low vacuum to allow the leak detector to be operated at maximum sensitivity. Otherwise the leak detector will still indicate residual helium from the pumped-down ambient air.

Additional vacuum pumps (auxiliary pumps) with high pumping speeds must therefore often be used for large test specimens. In this case, the leak detector should be connected directly to the recipient pump ports for the large vacuum pump, i.e. parallel to the auxiliary pump.

When the auxiliary pump is running, the partial flow ratio of the system must be defined by measuring with a test leak in order to determine the leakage rate. Only through measuring is it possible to reliably indicate what proportion of the escaping test gas is pumped down by the auxiliary pump and what proportion can be detected in the leak detector.

When working with the sniffer probe, the pressure in the vessel must be at least 100 hPa higher than the ambient pressure. Due to the natural helium content of the air, the sensitivity of the sniffer method is lower than that of the vacuum method. Moreover, the delayed reaction of the leak detector to the inflowing helium must also be taken into consideration. The response time is also dependent on the length of the sniffer probe used.

Leak testing with helium or another test gas does not necessarily have to be carried out with the parameters that are decisive for the specification. Conversions are possible, for example, for various gases, gases and fluids, different pressure conditions, mass leak rates and volume leak rates, etc.

Comparison of test results with leak detector and quadrupole mass spectrometer.

Quadrupole mass spectrometers are primarily used to analyze the composition of gas mixtures. They require test pressures in the high vacuum range. Mass spectrometers can be used with almost any tracer gas, as their use does not necessarily depend on the classic tracer gas helium. Residual gas analyzers can detect leaks in a vacuum system without any special test gas. They analyze the mass of the gases in the air.

Leak detectors for the tracer gas helium are not currently designed on the basis of quadrupole mass spectrometers. Their greater robustness and long-term stability as well as the easier quantification of results and data interpretation have resulted in the fact that above all mass spectrometric detectors on the basis of magnetic sector mass spectrometer are mainly used for this purpose.

Units with detectors based on a quartz window sensor are used too for applications which do

not require the superior sensitivity of mass spectrometric detectors. Units with quartz window sensors make it possible to work at very high test pressures and high water vapor exposure.

Table 8.4 Comparison of leak detector and quadrupole mass spectrometer

	Leak Detectors	RGA/QMS
Leak, localization	Yes	Yes
Leak, quantitative	Yes	No
Leak, virtual	No	Yes
Permeation	Rough indication possible, no differentiation between permeation and desorption	Yes, data interpretation possible
Desorption		Yes, conclusion about desorbing gases
Test pressure	high	low
Detection limit	$< 5 \cdot 10^{-13} \text{Pa} \cdot \text{m}^3 \cdot \text{s}^{-1}$ (sector field MS) $< 5 \cdot 10^{-13} \text{Pa} \cdot \text{m}^3 \cdot \text{s}^{-1}$ (quartz window detector)	Ion current dependent on rod system and detector
General	Quantitative leak rate measurement possible	Qualitative instrument, quantification complex, requires more expertise, provides more information

1. DIN EN 1330-8:1998-7 Zerstörungsfreie Prüfung – Terminologie – Teil 8: Begriffe der Dichtheitsprüfung
2. Dawson, Peter H., Quadrupole Mass Spectrometry and Its Applications, American Institute of Physics (1997)
3. Gross, Jürgen H., Mass Spectrometry: A Textbook, Springer (2011)
4. Fachbericht Balzers BG 800003, Das Funktionsprinzip des Quadrupol-Massenspektrometers (1990)
5. DIN EN 1779:1999-10: Zerstörungsfreie Prüfung – Dichtheits- prüfung – Kriterien zur Auswahl von Prüfmethode n und -verfahren

## 9. VACUUM SYSTEM OPERATING

### 9.1. Electronic integration of vacuum system

Control by Means of Process Sensors and Automated Data Processing Requirements and Applications.

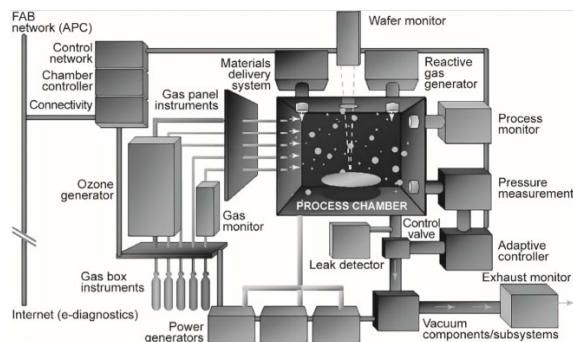


Figure 9.1 Possible components of a vacuum process chamber. Processes operated determine installed components.

Vacuum process systems and their components such as gas flow regulators, vacuum pumps, vacuum monitoring equipment, plasma generators, and evaporator units provide large amounts of data for monitoring and controlling processes in vacuum technology. A number of special monitoring solutions are also available for reliable supervision of processes. For electronic monitoring, the main components of a vacuum process chamber are integrated into a bus system. It is necessary to monitor every process critical parameter. Integrated sensors should transmit the required information not only to the system's control but also to higher level systems (Figure 9.1).

There is a continuous demand for more productive, more economical, and more energy efficient electronic devices. This requires a continuous reduction of the pattern size on wafers of larger size and challenges the vacuum systems for continuous improvement.

For economic reasons, chip manufacturers must reduce times to mature yield (85% in processors, 90% in memory components). This requires continuous process monitoring and automated control. Considering approximately 40 mask steps per wafer, the complete production process can take several weeks. A leading processor manufacturer in Dresden, Germany, has therefore developed automated processes for production and material handling in his production site, coming close to an autonomous factory. Apart from appropriate software, this approach requires sophisticated procedures for process monitoring as well as sensors.

In other areas as well, sophisticated process monitoring is a prerequisite, for example, for constant coating thicknesses across the entire surface in large-area glass coating and solar panel manufacturing. Sensor and measuring principles that have prevailed for the various tasks in practical applications are listed in Table 9.1.

Table 9.1 Process sensors/measurement principles and applications.

Process sensors/ measurement principles	Processes	Applications
Mass spectrometer/RGA	PVD/sputtering, ion implantation	Monitoring of vacuum conditions Residual and process gas composition End-point determination Outgassing behavior of substrates
Plasma emission spectrometer	PECVD	End-point determination
	Plasma etching	Plasma analysis
Infrared (FTIR/NDIR) spectrometer	Plasma etching	End-point determination Process residual-gas monitoring
VI probe/RF probe	Plasma processes	Plasma characterization via electrical parameters
Particle detectors	Vacuum processes	Monitoring of process vessel contamination

Very complex processes require high levels of sensor integration into the automated system. Stand-alone sensor units with additional operator attention are inappropriate for such production environments. Effective process monitoring should therefore respect and continuously optimize the criteria shown in Figure 9.2 in order to improve error analysis and product quality.

## Integrated Solutions

As mentioned, sensor integration is important due to two main reasons:

- Process monitoring and systems control must be capable of being automated.
- Data transfer to production controls or external systems such as APC (advanced process control), SPC (statistical process control), or MES (manufacturing executing system).

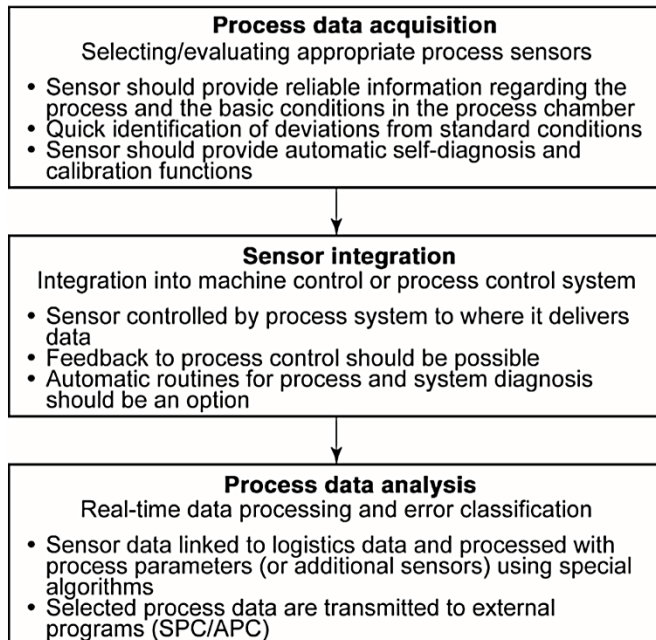


Figure 9.2 Criteria for efficiently implementing and optimizing process control.

This strategy allows reliable monitoring and control of processes and systems as well as further data handling for thorough data analysis and quality control in production. In the past, sensors often provided simple analog or digital signals only (e.g., for identifying end-points or deviations from set point values). Today, digital interfaces and protocols provide bidirectional data transfer between sensors and system controllers. Many sensor manufacturers provide convenient software solutions for data handling, however, often involving manufacturer-specific protocols. In spite of ongoing standardization, particularly in semiconductor industry, protocols for process sensors have not yet been standardized. The following sections describe available concepts of integration in brief.

### ASCII Protocols

Some of today's process-monitoring systems such as mass spectrometers (residual gas analyzers—RGA) are equipped with an embedded processor including system software. The process sensor can thus operate without any additional computer or software required. This applies to both the acquisition of measurement data such as partial pressures as well as to measurement configuration data including mass range, ionization, and further parameters. Comprehensive electronic control of an RGA also features an integrated web server, easily controllable from remote locations via a standard web browser. The ASCII protocol contains sensor-specific functions and is thus published by the manufacturer. Optional tools provide integration into programming environments such as Java or C++ . Accompanying TCP/IP Ethernet protocol implementation integrates the system into the local network, thus resolving common limitations of serial interfaces.

### Standardized Bus

Systems Initially, sensor networks were developed for transmitting digital information such as “on” or “off” to machines or facilities. The most common bus type, especially in Europe, is the ASI system [1], providing solutions for simple and lowcost system controls. In addition to such simple signals, the next higher grade fieldbus is capable of transmitting more complex information, for example, set points or actual values, and it allows regulation loops. Typical examples of fieldbus systems [2] developed for industrial automation about 20 years ago include DeviceNet [3], Interbus, and Profibus [4]. New developments focus on TCP/IP and real-time processing. Due to its standardized protocols, Ethernet TCP/IP provides universal networking between office computers, higher level enterprise networks, and down to the individual sensor. The successor to Profibus (data transfer rate 16 megabits per second) is called Profinet (data transfer rate 100 megabits per second) and is based on the Industrial Fast Ethernet with TCP/IP. Utilizing a special chip (switch), Profinet guarantees cycle times of one millisecond at a jitter of one microsecond even when many sensors and actuators are connected [5]. SEMI (Semiconductor Equipment and Materials Institute) already accepted Profibus/Profinet in its SEMI E54.8/ E54.14 standard for applications in semiconductor

industry in April 2005. A disadvantage is the limited length of a message. Integrating a larger number of complex process sensors is limited. Thus, these bus systems are restricted to integration of simple sensors with just few measurement values and simple components such as gas flow regulators.

#### Sensor Integration According to SECS and HSMS Standards

In semiconductor industry, processes predominantly define necessary protocols. Thus, for historical reasons, protocols based on the serial interface RS232 [6] such as GEM (generic equipment model) and SECS (semiconductor equipment communication standard) have established. Many suppliers of semiconductor manufacturing equipment have adapted these standards and provide corresponding software for process integration. For example, the SECS standard enables a host computer to start measurement cycles and allows transfer of measured values. SECS-I is based on RS232 and has a limited message length of 8 megabyte. SECS-II messages pass through the network as structured binary data without wasting bandwidth. If the HSMS standard (high-speed message services) is used on a TCP/IP network, the maximum message size is upgraded to 16 megabytes. The GEM standard defines a sequence of SECS-II messages for certain scenarios predefinable by the manufacturer of the equipment.

A disadvantage of serial-interface communication protocols is that the number of simultaneously communicating peers is limited to two. Furthermore, integration of process sensors is constrained because usually only two serial-interface ports are present. One of them maintains communication to the external manufacturing execution system (MES) whereas the other handles the process. Primarily, MES is responsible for the entire process control. It transfers logistics data (product IDs, recipes), and collects and prepares systems' process data. The HSMS protocol, introduced several years ago, was not able to resolve these limitations [7]. Some commercial products overcome the restrictions by utilizing software multiplexers that allow multiple accesses to the protocol. Figure 18.4 shows an example of how the interface limitations can be resolved using the MKS® Blue Box®.

#### Process-Data Analysis

Performing process-data analyses is suggested if many process parameters are monitored. Data volumes and information complexity from process sensors (e.g., mass spectra, adsorption spectra) often call for real-time data processing so that these data are utilizable for process monitoring and control. For this, sensor- and process-specific algorithms consider raw data of sensors and other measured quantities or information. Higher level systems for process monitoring and optimization make use of a set of procedures, specialized on the complexity of semiconductor manufacturing, and providing control throughout several process steps. Some of these techniques are listed below:

SPC (Statistical Process Control). Error frequencies are correlated with machine and sensor data to localize and resolve long-term influences on final product quality. Process-wide statistical analyses check whether process tolerances are met and which impact on quality is to be expected from deviations in individual process steps.

AEC (Advanced Equipment Control). Monitoring of process chambers or processing systems using active sensors that are capable of taking corrective actions. If variations from set point values occur, running processes are terminated or warnings or alerts are raised.

APC (Advanced Process Control). Networked systems process data in a higher level system and dynamically adjust preceding and succeeding processes. A combination of all involved sensors identifies trends and drifts, and correlates them to machine, system, and production data of the entire cycle.

FDC (Fault Detection and Classification). Sensors control product quality during production in real time, and by using process-specific models, identify negative trends that could lead to quality loss even in succeeding processes. Machine and sensor data help to predict characteristics such as coating properties and to determine whether a product is still within a tolerable process window.

## ***9.2. Pressure control***

Pressure in a vacuum system can be controlled in two ways [8]:

- by the gas injected into the system,
- by the effective pump speed.

Control by the gas inlet has the advantage that the time constant  $\tau = V/S_{eff}$  of the system remains unchanged. Such an additional change places high demands on a controller. A constant effective pumping speed also has the advantage that composition and total pressure of the residual gas remain constant. This is particularly important, if the residual pressure may disturb the process. For surface processes (e.g., evaporation), however, where the gas flow cannot be changed, pressure control via the effective pump speed is the only choice. Also in coating processes, where the total gas flow as well as its composition (carrier gas, active gas) must remain constant, the effective pump speed is controlled. To control the gas flow in, dosing valves and mass flow controllers are used. The latter are composed of a flowmeter and a control valve. We mention that the linearity of a flowmeter is rather limited. With digital technique and look-up tables nonlinearities cannot be completely compensated. For the purpose of calibration, repair, or replacement mass, flow controllers can be easily replaced. Control of effective pump speed may be performed by the pump itself or a variable conductance between process chamber and vacuum pump, for example, via a dosing valve. The pump speed of only a few pumps and only in a few pressure ranges can be controlled. The pump speed of membrane pumps, turbomolecular pumps, and in particular Roots pumps can be changed by controlling their frequency. The times for adjustment are normally relatively slow so that this type of pressure control is limited to processes where time constants are not critical. When control or dosing valves are being used, one needs to consider that the effective pump speed consists of three contributions: the conductance of the control valve  $C_{CV}$ , the conductance of the connection tubes to the pumps  $C_{tube}$ , and the intrinsic pump speed  $S_0$

$\frac{1}{S_{eff}} = \frac{1}{S_0} + \frac{1}{C_{tube}} + \frac{1}{C_{CV}}$	(9.1)
-----------------------------------------------------------------------------	-------

For given  $q_{pV,process}$ , the lower limit of the controllable pressure range is given by  $p_{min} = q_{pV,process}/S_{eff}$  with  $C_{CV}$  in maximum value. The upper limit is determined by the smallest conductance  $C_{CV}$  of the control valve close to its vacuum tight position (if applicable). Suitable control valves are iris diaphragms (these are not vacuum tight), butterfly valves, gate valves, and Chevron baffles with adjustable blade angles. The linearization of the conductance is difficult and depends on the valve type. It is achieved by an appropriate gear between driving motor and valve mechanics.

### 9.3. Technic for operating low-vacuum system

Many, particularly industrial vacuum processes are carried out under low vacuum. Typical examples are clamping, holding, handling, and sorting of small and larger flat workpieces, pouring of liquids, deep-drawing of plastic components, drying, impregnating, evaporating, and condensing, packaging of foodstuff and luxury foods such as meat, fruits, coffee, and so on. Even LCL (Less than Container Load) packaging increasingly relies on low-vacuum equipment. Many of these processes utilize the pressure of atmospheric air for the process by establishing a pressure difference  $\Delta p$ . Other processes require reduced amounts of oxygen and/or humidity in the air without calling for extreme vacuum. However, in any case, mechanical stresses on the vacuum vessels (chambers) must be considered. Regardless of how intense a vessel is evacuated, the load on containers never exceeds the ambient atmospheric pressure of approximately 1bar.

#### Assembly of Low-Vacuum Systems

From a vacuum-technological view, requirements concerning tightness and gas emissions in a low-vacuum system are comparably low. Therefore, components meeting just these low requirements are utilizable. Joining and sealing such components often involves screwed joints, sealed with Teflon tape. Shut-off elements are standard valves as used for gas lines. However, to avoid unpleasant surprises and the delays they produce, it is advisable to use vacuum flanges and elastomer seals for any joints in the low vacuum as well, and to seal rotary leadthroughs with rotary shaft seals or cup leather shaft seals.

## Pumps: Types and Pumping Speeds

Table 18.3 Pumping-speed ranges of commercial vacuum pumps for producing rough vacuum.

Pump types	Pumping-speed ranges
Diaphragm pump	1 – 20 $m^3h^{-1}$
Liquid ring vacuum pump	10 – 20000 $m^3h^{-1}$
Multiple vane pump	1 – 5000 $m^3h^{-1}$
Sliding vane rotary pump	1 – 600 $m^3h^{-1}$
Rotary plunger pump	100 – 500 $m^3h^{-1}$
Screw-type pump	70 – 2500 $m^3h^{-1}$
Vapor jet pump	20 – 100000 $m^3h^{-1}$

vane pumps are used mostly for  $p_w \geq 50$  mbar, whereas oil-sealed sliding vane rotary pumps and rotary plunger pumps are common to applications with  $p_w < 50$  mbar. Screw-type pumps and vapor jet pumps are used in both pressure ranges. Roots pumps (usually combined with oil-sealed rotary vacuum pumps) are rarely employed in low-vacuum technology (only, for example, if considerable amounts of process gases develop at low working pressures of approximately 10 mbar). The pumping speed applied to a vacuum apparatus or system is determined by the desired working pressure, pump-down times, amounts of gases and vapors released, and the leakage gas flow. If the amount of gas or vapor produced in a process is unknown, it is often appropriate to select pumping speed from Figure 9.3. Note, however, that Figure 9.3 is based on empirical values and can only provide a rough guideline. Particularly for vessel volumes  $V < 100$  l and in the low-vacuum range, lower pumping speeds than obtained from Figure 9.3 are often sufficient. In pump assembly, appropriate dimensioning of tubing diameters is mandatory.

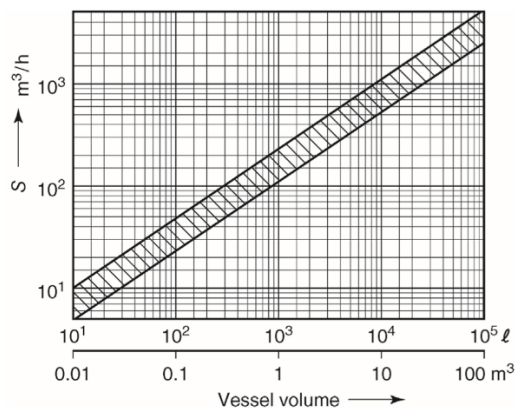


Figure 9.3 Suggested effective pumping speeds  $S_{eff}$  (guidance values) at vacuum vessels for rough-vacuum (and fine-vacuum) operation.

Manufacturers protect their brand-new metal components against corrosion either with an airtight packaging or with a grease film. Before greased components are mounted in a vacuum system, they should be degreased and subsequently dried thoroughly.

### Assembly of Fine-Vacuum Systems

Due to higher tightness demands of fine vacuum, every component must remain below the maximum tolerable leakage rate  $q_L = 10^{-3}$  mbar $\ell s^{-1}$ . If this threshold value is not met, lower working pressures are producible only with disproportionately high pumping speeds, that is, with uneconomic pumps. In addition, systems must be kept dry (free of water vapor) and clean. Surfaces exposed to vacuum have to be free of corrosion and must be prepared appropriately, for example, by sandblasting. Each detachable joint is sealed with elastomer seals, and parts moved mechanically

Numerous pump types as listed in Table 9.2 are available for producing low vacuum. The specific operating functionalities, conditions, and economic considerations determine designs and utilization of pumps (Table 9.2). As a rough, but not compulsory guideline for pump selection, we can differentiate between working pressures  $p_w < 50$  mbar and  $p_w > 50$  mbar. Liquid (water) ring vacuum pumps and dry-running multiple

### Low-Vacuum Pressure Measurement

Most measuring instruments available for low vacuum are different types of mechanical gauges, for example, diaphragm vacuum gauges. In the low-vacuum range, pressure readings of mechanical vacuum gauges are independent of the gas or vapor species.

### 9.4. Technic for operating fine-vacuum system

Most industrial vacuum processes operate in the fine (medium) vacuum range, that is, at pressures between 1 and 103 mbar. As long as working pressures in the vacuum systems remain above  $p_w \approx 1 \times 10^{-2}$  mbar, outgassing flows are w mostly irrelevant. However, they can be disturbing in the deeper fine-vacuum range, that is, at working pressures between  $1 \times 10^{-2}$  and  $1 \times 10^{-3}$  mbar.

must be free of grease when they are inserted into the evacuated volume.

#### Pumps: Types and Pumping Speeds

Usually, two-stage rotary pumps, dry-running screw-type pumps, Roots pumps, and vapor jet pumps are used for producing medium vacuum. While those two stage, oil-sealed rotary pumps and screw-type pumps available feature relatively low pumping speeds (max. approximately  $S_n = 2 \times 10^{-3} \text{ m}^3 \text{ h}^{-1}$ ), combinations of Roots pumps and multistage vapor jet pumps offer pumping speeds up to  $S \approx 10^5 \text{ m}^3(\text{Tn.p}) \text{ h}^{-1}$ , or  $S \approx 0.044M_r \text{ kgh}^{-1}$  gas (or vapor). Technical and n economic considerations determine whether an individual application should employ a Roots pump combination or rather a multistage unit of vapor jet pumps. No general suggestions can be given here. However, the following list of factors should simplify decision making:

- 1) medium or media to be pumped (gases, vapors, or gas–vapor mixtures: composition, and particularly, water vapor contents);
- 2) amounts of these pumped media, available time;
- 3) type and amount of possibly appearing corrosive media;
- 4) temperature of pumped medium;
- 5) starting pressure (usually ambient atmospheric pressure);
- 6) desired working pressure of the pump unit;
- 7) ambient temperature of the pump unit;
- 8) dimensions and weight of the pump unit (including motor), distance between the pump unit and the vacuum system;
- 9) inner volume of the vacuum system;
- 10) leakage rate;
- 11) type and size of connecting flanges on the system;
- 12) power supply voltage and kind of current (three-phase current or DC), tolerable peak (switch-on) current;
- 13) electrical power consumption of the pump unit;
- 14) available motive media (water vapor or oil), vapor costs.

#### Pressure Measurement

Vacuum gauges for technical fine-vacuum systems mainly include capacitance vacuum gauges, thermal conductivity vacuum gauges, and (fine-vacuum) ionization vacuum gauges.

### ***9.5. Technic for operating high-vacuum system***

When operating HV systems, outgassing of the inner surfaces of the apparatus or system is of much more concern than the free gas and vapor in the volume. To achieve the necessary evacuation time and base pressure, it is necessary to consider the criteria for selection of materials as well as the manufacturing methods and cleaning procedures described above.

#### Pumps: Types and Pumping Speeds

The HV range is the domain of turbomolecular and still diffusion pumps. Since outgassing fluxes in high vacuum are made up of hydrogen mainly, pumping times are reduced by adding cryopumps, cooled with liquid nitrogen only.

Setups of pump units in terms of pump types and sizes are determined by

- working pressure;
- pump-down time until working pressure is obtained;
- system volume;
- amount of process gas flow;
- amount of total leakage rate in the system;
- amount of outgassing fluxes.

If the values of these quantities are mostly unknown, the pumping speed to be installed for a given vessel volume can be approximated using Figure 9.4. The diagram is based on experience values that can only provide a rough guideline. It is applicable to the high and ultrahigh vacuum. With time, nearly all surfaces in HV applications are subject to increased contamination. This leads to

higher outgassing rates, and thus, prolonged pump-down times. Thus, when in doubt, HV pumps with higher pumping speeds are selected. As experience shows, such an approach ultimately saves on time and costs.

#### Cleaning of Vacuum Gauges

Contaminants and layer of contaminants affect the accuracy, the correctness of measurement, of all vacuum gauges. The sensitivity is changed, the zero stability and the residual reading (offset) are worsened. When in ionization gauges contaminants cover the electrical insulators of feedthrough, leakage current develop and sparkovers may occur.

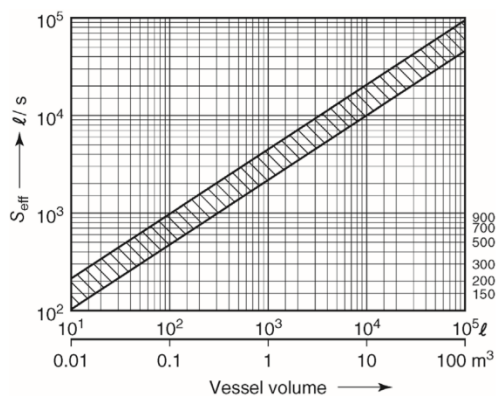


Figure 9.4 Suggested effective pumping speeds (guidance values!) at vacuum vessels for high- and ultrahigh-vacuum operation versus vessel volume.

used with caution to clean the connection tube and filter of a membrane gauge. You can expect success of the cleaning procedure only, if the contaminants can be easily removed. Finally, the vacuum gauge is dried in a dry box at moderate temperature (consider manufacturer's manual) or in a simple vacuum system.

The same described procedure may be applied for a thermal conductivity gauge (Pirani gauge), except that one should abstain from shaking the solvent due to the sensitive, thin heating element (wire).

Ionization gauges with crossed electric and magnetic fields ("cold cathode gauges") are relatively robust and easy to dismantle, so that the parts are well accessible for cleaning. This can be done mechanically by a nonwoven fabric (carded web) with successive application of isopropanol. In some cases (see gauge manual), dilute acids may be used for cleaning.

Ionization gauge with emissive cathodes cannot be efficiently cleaned, except by running the "degas" option or exchange of the cathode.

### 9.6. Technic for operating ultrahigh-vacuum system

The very low gas pressures (i.e., gas densities) in UHV are obtained and maintained only if

- total leakage rates are extremely low;
- outgassing rates are very low;
- negative pump feedback, for example, motive medium backflow (diffusion pumps), is practically zero;
- re-emissions of previously pumped gas (ion getter pumps, cryopumps) are practically zero.

The low outgassing rates are met only if the UHV part of the system, including connected and accompanying components, are bakeable at high temperature ( $\vartheta > 100^\circ\text{C}$ ). Thus, UHV technology relies predominantly on stainless steel components (vacuum vessels, valves, tube seals), specially designed gauges, Viton- or metal (Cu, Al, In)-sealed flange connections, ceramic feedthroughs for electrical energy, and special windows. The following components for producing and maintaining

UHV are fully or partially bakeable:

- turbomolecular pumps;
- ion getter pumps;
- titanium evaporation pumps (sublimation pumps);
- bulk getter pumps (Non evaporable getter pumps);
- cryopumps;
- adsorption pumps and dry-running positive displacement pumps (as fore pumps).

As well as combinations of these pumps. However, utilizing such components is not the only prerequisite for successfully operating at extremely low gas pressures. In fact, many rules and procedures, as covered in this section, should be followed during assembly of a UHV system. For the pump types listed above, leakage rates and pump feedback can be kept sufficiently low when employing carefully completed permanent and detachable joints. After one or two hours of baking at approximately 450 °C, and subsequent cooling, outgassing rates of metals drop to approximately  $10^{-8}$ – $10^{-9}$  mbar  $\ell$  s<sup>-1</sup> m<sup>-2</sup>. However, baking at  $\vartheta \approx 300$  °C, but for longer periods of time, generally also yields outgassing rates in the range of 10<sup>-8</sup> mbar  $\ell$  s m<sup>2</sup>. Glasses even provide outgassing rates of only approximately  $10^{-10}$  mbar  $10^{-8}$  s<sup>-1</sup> m<sup>-2</sup> after baking for longer periods at 450°C. As a general guideline, we may summarize: Outgassing rates drop by an order of 10 per 100K increase in baking temperature.

#### Operating Guidelines for UHV Pumps

Rapid production and maintaining of extremely low pressures are not the only aims of UHV technology. In many cases, residual gases must also be free of hydrocarbons. For this reason, UHV production relies nearly completely on oilfree pumping systems.

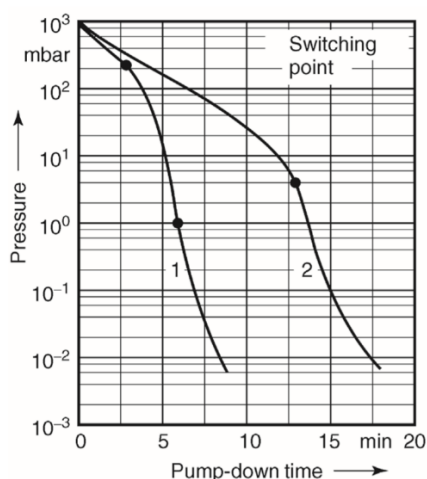


Figure 9.5 Pump-down times for a 180 $\ell$  vessel using adsorption pumps (ASP) and dry runner (DR, pump with oil-free pumping volume). Pumping intervals for curve 1: 1000mbar – 200mbar DR, 200mbar – 1mbar ASP 1, 1mbar – 10<sup>-2</sup> mbar ASP 2, precooling time of ASP approximately 10min. Pumping intervals for curve 2: 1000mbar – 4mbar ASP 1, 4mbar – 10<sup>-2</sup> mbar ASP 2, precooling time of ASP approximately 25min.

**Adsorption Pumps** For large vessels, several adsorption pumps (ASP) should be utilized so that at least one ASP DN 20 per 30 $\ell$  vessel volume initially reduces vessel pressure from atmospheric pressure down to several mbar. After these saturated ASPs have been shut off from the vessel, a formerly closed valve is opened, connecting to an additional ASP carrying clean adsorbent. With this procedure, pressures below 10<sup>-2</sup> mbar are produced easily. Pumping times can be reduced considerably when a dry-running rotary pump is added to the adsorption pumps. This setup is shown in Figure 9.5. The ultimate pressure producible with ASPs is determined chiefly by those gas species that are present in the vessel when pumping starts (usually atmospheric air) and are difficult or impossible to adsorb such as He and Ne.

#### Ion Getter Pumps

Ion getter pumps are used frequently in UHV systems. In these applications, they are equipped with metal-seal flanges and are bakeable at higher temperatures for reduced self-emissions of gases. Baking temperatures with attached magnet range up to  $\vartheta = 350$  °C, with detached magnet up to  $\vartheta = 450$  °C. Ion getter pumps are often combined with an (integrated) titanium evaporation pump featuring high pumping speed for hydrogen.

Depending on operating conditions, ion getter pumps require cleaning from time to time, and regeneration when getter capability (pumping speed) changes. Hydrocarbons disturb smooth operation of ion getter pumps. Crack products develop in the gas discharge and on the titanium surface, thus contaminating cathode surfaces and impeding titanium sputtering. Therefore, vacuum systems including ion getter pumps should at least be cleaned with

grease-free organic solvents, or preferably, be steam-degreased. Grease-sealed joints (ground-in connections) are disadvantageous as well.

Ion getter pumps contaminated with hydrocarbons (oil vapors, vacuum grease) can be cleaned by baking at  $\theta=300^{\circ}\text{C}$ . Then, released hydrocarbons have to be pumped off with an additional pump while the ion getter pump is not in operation. For subsequent, thorough cleaning of the electrodes, oxygen or air is fed to the system at  $p=1 \times 10^{-6}$  mbar, followed by argon. If baking does not reestablish the initial pumping speed and ultimate pressure in an ion getter pump, the pump housing, and if cathode mesh is not too worn, the anodes of the electrode system require cleaning. Electrode systems with depleted cathode mesh should be replaced. When pump housings and electrodes are cleaned, the high-voltage electrical feedthrough should also be checked in terms of insulation. This electrical feedthrough is easily demountable and thus replaceable if necessary.

#### Titanium Evaporation Pumps

Titanium evaporation pumps are used mainly in combinations with ion getter pumps and turbomolecular pumps. The pumps are usually operated intermittently due to their limited titanium reservoir. Evaporation and idle times are adjusted with the supply unit. Evaporation time (typically between 5s and 5min) is adjusted prior to conducting the experimental procedure. Idle times depend on pressure and gas load. Too short interruptions of operation may prevent sufficient cooling of the getter screen after vapor deposition. The screen gradually heats, leading to increased gas emissions. Too long interruptions can lead to saturation of the getter layer, and thus, to a loss in pumping action. For low gas loads, the following reference values are suggested:

Pressure in mbar	Operating interruption
$1 \times 10^{-5}$	Several minutes
$1 \times 10^{-7}$	Several minutes
$1 \times 10^{-9}$	10-30 min
$1 \times 10^{-10}$	Several hours

The heating current of the evaporator determines the rate of evaporation. It can be adjusted in several ways. New evaporator coils release large amounts of gas during first use. Therefore, the electrical current should be raised very gradually during initial operation of an evaporator coil. If the pressure rises too high, the fore pump should be engaged. If several new evaporator coils are employed, they should be

degassed back-to-back. If the producible ultimate pressure rises after longer operating periods, deposited titanium layers have to be removed, involving disassembly of the screen plates. The getter screen and the plates are best cleaned with a wire brush (preferably stainless steel) or via sandblasting.

#### Turbomolecular Pumps

For UHV production, turbomolecular pumps are utilized with metal-seal connecting flanges and detachable baking equipment. In particular, note that heavy oil outgassing develops and potentially lasts for several hours during initial pump-down with a fresh-oil filled turbomolecular pump. Therefore, a turbomolecular pump should not be started before the necessary fore-vacuum pressure is obtained. After this, gas bubbles escaping from the oil reservoir no longer influence the UHV.

#### Cryopumps

All three types of cryopumps, bath cryopumps, evaporator cryopumps, and refrigerator cryopumps, are used for producing UHV. Ultimate pressures  $p < 10^{-4}$  mbar are obtainable even when pumping hydrogen, and even if the temperature of the cold surface  $T > 4.2\text{K}$ , as long as the cold surface is covered with a carbon layer working as absorbent. When utilizing bath and evaporator cryopumps, attention must be paid to helium consumption, liquid nitrogen consumption (if used), and particularly to the gas-species-dependent capacity of the pump. UHV cryopumps are either equipped with ConFlat flanges or welded directly onto the recipient.

#### Bulk Getter (NEG)

Pumps Bulk getter (NEG) pumps are used as the so-called flat getters in research facilities and industrial applications, for example, electron microscopes. The following example [9] illustrates application of NE flat getters.

#### Pressure Measurement

Ionization vacuum gauges are applicable to pressure measurements in the UHV range [10,11]. Bayard-Alpert gauges are used frequently.

## Venting

If an apparatus contains cryopumps or other cooled surfaces, before venting, they have to be heated at least to room temperature. In order to reduce water vapor uptake, UHV systems should be vented with dried air or pure nitrogen.

## Ultrahigh-Vacuum Systems

Such systems include low-cost, simple UHV systems used mainly in industrial applications. High-cost UHV systems are employed in accelerators for major elementaryparticle research, featuring one thousand or even more vacuum pumps of various types and the corresponding components used for monitoring and control. Most of the pumps, measuring equipment, and components used here are covered in the previous sections. Thus, the following section provides a brief roundup with additional comments. Additionally, references listed above contain special information providing in-depth coverage of the continuously developing state of the art in UHV technology.

### Ultrahigh-Vacuum (UHV) Components

UHV components include

- CF flanges;
- tube pieces, bends, T-, and crosspieces equipped with flanges;
- flexible elements;
- valves;
- windows;
- feedthroughs.

### Ultrahigh-Vacuum (UHV) Pump Stands

Preferred pump combinations for evacuating UHV vessels are listed in Table 9.4. Here, the most important steps in a pump-down procedure are covered considering the UHV pump stand. Pumping times apply to evacuation of a clean and empty vessel with open intermediate valve and should be treated as guideline values. For repeated evacuation (charge changes), the intermediate valve is shut first, thereby reducing the volume and yielding shorter rough-pumping times. These

Table 9.4 Common pump combinations for producing ultrahigh vacuum.

UHV pumps	Fore pump
Ion getter pump plus (integrated) titanium evaporation pump	Adsorption pump(s) and oil-free rotary vacuum pumps
Turbomolecular pump (and titanium evaporation pump)	Two-stage sliding vane rotary pump and adsorption trap
Turbo-drag pump (turbomolecular pump with Holweck stage) plus Ti evaporation pump	Diaphragm pump
Bath, evaporator, or refrigerator cryopump	Two-stage sliding vane rotary pump or adsorption pump(s) or dry positive displacement pump

should be acquired from manufacturers' manuals. For baking the apparatus, heating jackets are arranged at appropriate positions. It should be taken care that tolerable temperatures are not exceeded at certain points such as elastomer seals of the intermediate valve and the permanent magnet of the ion getter pump, in the example. In continuous operation, temperatures of elastomer seals and permanent magnets should be limited to 150°C and 380°C, respectively. Further critical points in UHV apparatuses are vacuum measuring tubes made of glass. The vessel is equipped with a water cooling system for preventing excessive heating of the bell, particularly the usually integrated window, and for reduced gas emissions. High or very high temperatures

develop, for example, in annealing furnaces. For venting a UHV pump stand and UHV systems in general, UHV measuring equipment and ion getter pumps have to be cut off from the recipient prior to venting using an intermediate valve. If a system does not include an intermediate valve, measuring equipment and ion getter pumps must be turned off prior to venting. Any surfaces that are at low temperature when operating (getter screens, cryosurfaces) should reach room temperature before the system is vented in order to prevent water vapor from condensing (formation of ice!). A common

approach for warming the cold surfaces is to replace the coolants (water, liquid nitrogen) with pressurized air at ambient temperature. Actual flooding should employ dry nitrogen, if available, fed to the system via a gradually opened vent valve. Any vacuum-side surfaces should be exposed to atmospheric air only as shortly as possible.

1. AS-International Association, [www.asinterface.net](http://www.asinterface.net).
2. Wellenreuther, G. and Zastrow, D. (2002) *Automatisieren mit SPS, Theorie und Praxis*, Vieweg, Braunschweig/Wiesbaden, 2002, ISBN 978-3-528-13910-0.
3. Moyne, J.R., Najafi, N., Judd, D., and Stock, A. *Analysis of Sensor/Actuator Bus Interoperability Standard Alternatives for Semiconductor Manufacturing*, Sensors expo conference proceedings, Celveland, OH, September 1994.
4. Profibus International (2002) *Profibus Technology and Application, System Description*. [www.profibus.com](http://www.profibus.com).
5. Profibus International (2002) *ProfiNet Technology and Application, System Description*. [www.profibus.com/libraries.html](http://www.profibus.com/libraries.html).
6. SEMI Standards SEMI E30 *Generic Model for Communications and Control of Manufacturing Equipment (GEM)*, 2007, <http://ams.semi.org/ebusiness/standards>
7. SEMI Standards SEMI E37 *High-Speed Message Services (HSMS) Generic Services*, 2008, <http://ams.semi.org/ebusiness/standards>.
8. Pöcheim, N. (1995) *Druckregelung in vakuumsystemen*. *Vakuum in Forschung und Praxis*, 1, 39–46.
9. Briesacher, J. et al. (1990) *Non-evaporable getter pumps for semiconductor equipment*. *Ultra Clean Technol.*, 1, 49–57.
10. Tilford, C.R. (1983) *Reliability of high vacuum measurements*. *J. Vac. Sci. Technol.*, A1 (2), S. 152–162.
11. Weston, G.F. (1979) *Measurement of ultra-high vacuum*. *Vacuum*, 29 (8/9), 277–292 and 30 (2) (1980), pp. 49–69.

## REFERENCES

1. Scientific Foundations of Vacuum Technique, Second Edition. By Saul Dushman, Late Assistant Director, Research Laboratory, General Electric Company, Schenectady, New York. Revised by Members of the Research Staff, General Electric Research Laboratory. J. M. Lafferty, Editor. John Wiley and Sons, Inc., 440 Park Avenue South, New York 16, N. Y. 1962. xviii + 806 pp.
2. A. Roth Vacuum Sealing Techniques, Pergamon Press, Oxford, 1966. Hardcover. Condition: Good. First Edition. Octavo. Hardcover Cloth. First Edition. 1966. Ex-Library with the usual treatments. Text in English 845 pp
3. Edited by Karl Jousten, Handbook of Vacuum Technology, Second, Completely Revised and Updated Edition 2016 Wiley-VCH Verlag GmbH & Co. KGaA. Published 2016 by Wiley-VCH Verlag GmbH & Co. KGaA. 1040 pp.
4. Nagamitsu Yoshimura, Vacuum Technology. Practice for Scientific Instruments. Springer; 2008 edition (January 28, 2008) 353 pp.
5. Igor Bello. Vacuum and Ultravacuum Physics and Technology, 2018 by Taylor & Francis Group, LLC CRC Press is an imprint of Taylor & Francis Group, an Informa business 1063 pp.
6. E.A. Deulin, V.P. Mikhailov. Yu.V. Panfilov, R.A. Nevshupa (Mechanics and Physics of Precise Vacuum Mechanisms 2 vols.), Moscow, NPK "Intelva", 2000, 2001. 234 pp.
7. Richard W. Roberts, Thomas A. Vanderslice, ULTRAHIGH VACUUM AND ITS APPLICATIONS, Catalog Card No. 63-18110 Printed in the United States of America, C 93565, March, 1964, 199 pp.
8. Donald M. Mattox The Foundations of Vacuum Coating Technology. Second Edition. 2018 Elsevier Inc, 361 pp.
9. David Garton "Vacuum Technology and Vacuum Design Handbook for Accelerator Technicians" ISBN number, 192126814X , ISSN number: 10307745, Nov,2011
10. Dorothy M. Hoffman, John H. Thomas, Bawa Singh. Handbook of Vacuum Science and Technology ISBN: 0123520657 · Publisher: Elsevier Science & Technology Books Pub. Date: October 1997, 835 pp.
11. Helge S. Kragh • James M. Overduin The Weight of the Vacuum A Scientific History of Dark Energy ISSN 2191-5423 ISSN 2191-5431 (electronic) ISBN 978-3-642-55089-8 ISBN 978-3-642-55090-4 (eBook) DOI 10.1007/978-3-642-55090-4 Springer Heidelberg New York Dordrecht London, 113 pp.